CVEN 489-501: Special Topics in Mixing and Transport Processes in the Environment

Engineering – Lectures

By
Scott A. Socolofsky &
Gerhard H. Jirka

5th Edition, 2005

Coastal and Ocean Engineering Division
Texas A&M University
M.S. 3136
College Station, TX 77843-3136

Recommended Reading

Journal Articles

Journals are a major source of information on Environmental Fluid Mechanics. Major journals include *Environmental Fluid Mechanics*, published by Kluwer, the *Journal of Hydraulic Engineering* published by the American Society of Civil Engineers (ASCE), the *Journal of Hydraulic Research* published by the International Association of Hydraulic Engineering and Research (IAHR), *Limnology and Oceanography* published by the American Society of Limnology and Oceanography (ASLO), *Physics of Fluids*, published by the American Physics Society (APS), and the *Journal of Fluid Mechanics* published by Cambridge University Press, among many others. These are all available through the Texas A&M University library: newer articles are available through on-line subscriptions, and older articles (usually before 1995) are available in bound volumes in the library stacks.

Supplemental Textbooks

The material for this course is also treated in a number of other books; in particular, the following supplementary texts are recommended:

Fischer, H. B., List, E. G., Koh, R. C. Y., Imberger, J. & Brooks, N. H. (1979), *Mixing in Inland and Coastal Waters*, Academic Press, New York, NY.

Hemond, H. F. & Fechner-Levy, E. J. (2000), '*Chemical Fate and Transport in the Environment*, Academic Press, San Diego, CA.

Condensed Bibliography

The following books are also recommended for in-depth study of individual topics:

Acheson, D. J. (1990), *Elementary Fluid Dynamics*, Oxford Applied Mathematics and Computing Science Series, Clarendon Press, Oxford, England.

Csanady, G. T. (1973), *Turbulent Diffusion in the Environment*, D. Reidel Publishing Company, Dordrecht, Holland.

Kundu, P. K. & Cohen, I. M. (2002), *Fluid Mechanics*, 2nd Edition, Academic Press, San Diego, CA.

Mei, C. C. (1997), *Mathematical Analysis in Engineering*, Cambridge University Press, Cambridge, England.

Rutherford, J. C. (1994), *River Mixing*, John Wiley & Sons, Chichester, England.

van Dyke, M. (1982), *An Album of Fluid Motion*, The Parabolic Press, Stanford, CA.

Wetzel, R. G. (1983), *Limnology*, Saunders Press, Philadelphia, PA.

Preface

Environmental Fluid Mechanics (EFM) is the study of motions and transport processes in earth's hydrosphere and atmosphere on a local or regional scale (up to 100 km). At larger scales, the Coriolis force due to earth's rotation must be considered, and this is the topic of Geophysical Fluid Dynamics. Sticking purely to EFM in this book, we will be concerned with the interaction of flow, mass and heat with man-made facilities and with the local environment.

This text is the first Part in a two-part book to accompany a two-semester course in Environmental Fluid Mechanics. In this Part, Mixing and Transport Processes in the Environment, passive diffusion is treated by introducing the transport equation and its application in a range of unstratified water bodies. Passive diffusion refers to mixing processes that occur due to random motions and that have no direct feedback on the dynamics of the fluid motion. The second Part, Stratified Flow and Buoyant Mixing, covers the dynamics of stratified fluids and transport under active diffusion. Active diffusion relates to mixing processes that have a direct feedback on the equations of motion due to changes in the density of the carrier fluid. This first Part is appropriate for senior level undergraduate students; whereas, the second Part is more appropriate for first-year graduate students.

The text is designed to compliment existing text books in water quality, air quality, and transport. A unique feature of this text is that most of the mathematics is written out in sufficient detail that all of the equations should be derivable (and checkable!) by the reader. This fifth edition adds more homework problems to each chapter and expands the text and explanations in each chapter.

The chapters are all organized in a similar fashion. Following the chapter heading, the first two paragraphs orient the chapter in the context of the other chapters and outline the material to be covered. In the first section of the chapter, general, background information is covered that is needed to fully understand the contents of the chapter. The middle sections develop the appropriate theory and present the mathematical derivations. The final section in each chapter presents applications of the material to engineering practice. At the end of each chapter, a summary section highlights the key points and a set of exercises are presented as possible homework problems. The book contains a single references section and index.

This book was compiled from several sources, including the lecture notes developed by Gerhard H. Jirka for courses offered at Cornell University and the University of Karlsruhe, lecture notes developed by Scott A. Socolofsky for courses taught at the University of Karlsruhe and Texas A&M University, and notes taken by Scott A. Socolofsky in various fluid mechanics courses offered at the Massachusetts Institute of Technology (MIT), the University of Colorado, and the

University of Stuttgart, including courses taught by E. Eric Adams, Helmut Kobus, Ole S. Madsen, Chiang C. Mei, Heidi M. Nepf, Harihar Rajaram, Joe Ryan, and Ain Sonin. Many thanks goes to these mentors who have taught this enjoyable subject.

Comments, questions, and corrections on this script can always be addressed per E-Mail to the address: `socolofs@tamu.edu`.

College Station, *Scott A. Socolofsky*
January 2005 *Gerhard H. Jirka*

Contents

1. Concepts, Definitions, and the Diffusion Equation

Environmental fluid mechanics is the study of fluid mechanical processes that affect the fate and transport of substances through the hydrosphere and atmosphere at the local or regional scale[1] (up to 100 km). In more layman's terms, environmental fluid mechanics studies how fluids move substances through the natural environment as they are also transformed. In general, the substances we may be interested in are mass, momentum or heat. More specifically, mass can represent any of a wide variety of passive and reactive tracers, such as dissolved oxygen, salinity, heavy metals, nutrients, and many others. This course and textbook discusses passive processes affecting the transport of species in a homogeneous natural environment. That is, as the substance is transported, its presence does not cause a change in the dynamics of the fluid motion. The book for part 2 of this course, "Stratified Flow and Buoyant Mixing," incorporates the effects of buoyancy and stratification to deal with active mixing problems where the fluid dynamics change in response to the transported substance.

This chapter introduces the concept of mass transfer (transport) and focuses on the physics of diffusion. Because the concept of diffusion is fundamental to this part of the course, we single it out here and derive its mathematical representation from first principles through to an important solution of the governing partial differential equation. The mathematical rigor of this section is deemed necessary so that the student gains a fundamental and complete understanding of diffusion and the diffusion equation. This foundation will make the complicated processes discussed in the remaining chapters tractable and will start to build the engineering intuition needed to solve problems in environmental fluid mechanics.

1.1 Concepts, Significance and Definitions

Stated simply, environmental fluid mechanics is the study of natural processes that change concentrations.[2]

These processes can be categorized into two broad groups: transport and transformation. Transport refers to those processes which move substances through the hydrosphere and atmosphere by physical means. As an analogy to the postal service, transport is the process by which a letter goes from one location to another. The postal truck is the analogy for our fluid, and

[1] At larger scales we must account for the Earth's rotation through the Coriolis effect, and this is the subject of geophysical fluid dynamics.

[2] A glossary at the end of this text provides a list of important terms and their definitions in environmental fluid mechanics (with the associated German term) to help orient the reader to a wealth of new terminology.

the letter itself is the analogy for our chemical species. The two primary modes of transport in environmental fluid mechanics are advection (transport associated with the flow of a fluid) and diffusion (transport associated with random motions within a fluid). The second process, transformation, refers to those processes that change a substance of interest into another substance. Keeping with our analogy, transformation is the paper recycling factory that turns our letter into a shoe box. The two primary modes of transformation are physical (transformations caused by physical laws, such as radioactive decay) and chemical (transformations caused by chemical or biological reactions, such as dissolution and respiration).

In engineering practice, environmental fluid mechanics provides the tools to (1) assess the flow of nutrients and chemicals vital to life through the ecosystem, (2) limit toxicity, and (3) minimize man's impact on global climate.

1. **Ecosystem Dynamics.** Nutrients are food sources used by organisms to generate energy. Engineers need to know the levels of nutrients and their transformation pathways in order to predict species populations in freshwater ecosystems, such as the growth and decay of algal blooms in response to phytoplankton and zooplankton dynamics. Some common nutrients and vital chemicals are oxygen, carbon dioxide, phosphorus, nitrogen, and an array of heavy metals, among others.
2. **Toxicity.** For toxic chemicals, engineers need to understand natural transport and transformation processes to design projects that minimize the probability of occurrence of toxic concentrations while maintaining an affordable budget. Some common toxic chemicals are heavy metals (such as iron, zinc, and cadmium), radioactive substances (such as uranium and plutonium), and poisons and carcinogenic substances (such as PCBs, MTBE, carbon monoxide, arsenic, and strong acids).
3. **Global Climate Change.** Some chemical species are also of interest due to their effects on the global climate system. Some notable substances are the chlorofluorocarbons (CFCs) which deplete the ozone layer, the greenhouse gases, in particular, carbon dioxide and methane, which maintain a warm planet, and other substances, such as sulfate aerosols that affect the Earth's reflectivity through cloud formation.

It is important to remember that all chemicals are necessary at appropriate levels to sustain life and that anthropogenic input of chemicals into the hydrosphere is a necessary characteristic of industrialization. Engineers use environmental fluid mechanics, therefore, to avoid adverse impacts and optimize the designs of engineering projects and to mitigate the effects of accidents.

1.1.1 Example Problems

Although environmental fluid mechanics addresses basic processes that we are all familiar with through our natural interaction with the environment (e.g. sensing smoke in a crowded bar), its application in engineering is not frequently taught and students may find a steep learning curve in mastering its concepts, terminology, and significance. This problem is compounded by the fact that a whole new set of equations must be mastered before meaningful design problems can be addressed. Here, we pause to introduce several typical problems and their relationship

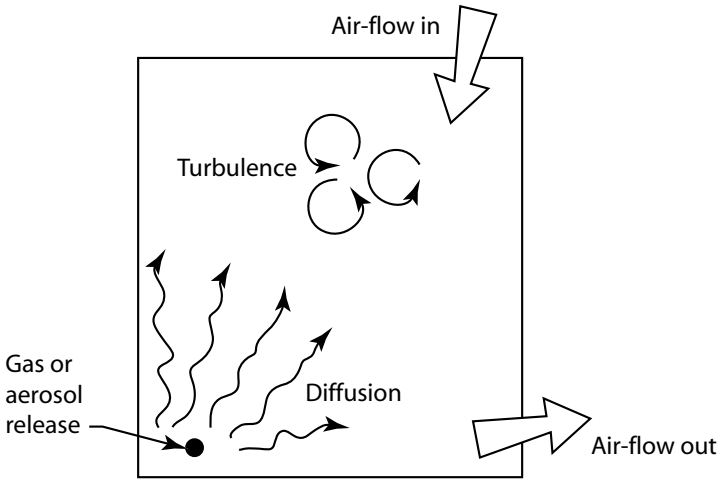

Fig. 1.1. Schematic of the mixing processes in an enclosed space. A point source of substance is released in the lower left corner of a room. Mixing is caused by flow into and out or the room through the ventilation system and by random motions in the circulating air.

to environmental fluid mechanics to whet the appetite for more detailed study and to give a context for the derivations that follow.

Indoor air pollution. Chemicals that we come in contact with the most readily are transported through the air we breath. The two important transport processes are advection (movement with the air currents generated by wind or by air distribution systems) and diffusion (gradual spreading of the substance by random motions in the air). This is depicted schematically in Figure 1.1.

When the anthrax problems in the U.S. Postal Service surfaced shortly after 9/11, there was a lot of discussion about "weapons grade" anthrax which could be dispersed by the air. Typical anthrax spores are too heavy to be carried very far by air. However, if anthrax can be transported by aerosol particles (particles small enough that they have no appreciable settling velocity), then the threat is much greater. Diffusion, especially turbulent diffusion, as we will see in Chapter 3, is very efficient at distributing aerosols throughout an enclosed space. In fact, diffusion is primarily what allows you to smell wet paint, smoke, or a pleasant perfume. If anthrax could be dispersed through the air, then it could diffuse efficiently throughout enclosed spaces, greatly increasing the risk that anyone entering the space would be infected.

When engineers design indoor air systems, one thing they are concerned with is the ability of the system to keep the space well mixed (that is, free of deadzones were contaminants could get concentrated) and frequently refreshed (new air replacing old). Environmental fluid mechanics provides the tools to estimate mixing rates and to design better systems. New designs might be quieter, or use less energy, or rely on natural ventilation generated by temperature differences between the indoors and outside. The first topics we will cover, diffusion followed by advection, are directly related to these problems and design issues.

River discharges. Because rivers are readily accessible and efficiently transport chemicals downstream, they are the primary receiving waters for a whole host of industrial and public

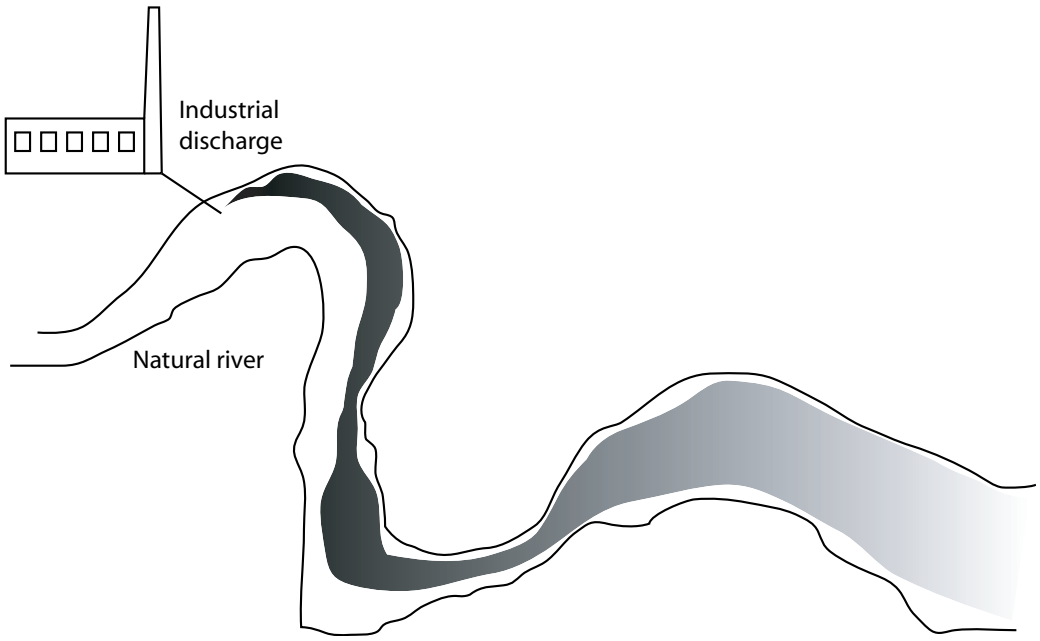

Fig. 1.2. Schematic of a point-source discharge of an industrial byproduct into a natural stream. As the source moves downstream, it spreads laterally due to diffusion and advection.

wastes (see example illustrated in Figure 1.2). Moreover, it is very likely that your community wastewater treatment plant discharges its treated water into a local river or reservoir. Although the water is well treated, it still likely contains nutrients that will promote algae and bacteria growth downstream, which in turn affect dissolved oxygen levels and promote eutrophication (rapid aging) in lakes. Before passage of the Clean Water Act in the United States, pollution in rivers was a major problem. Now, every point discharge must be evaluated by a government agency and approved based on an assessment of its likely impact on the natural system. Water quality standards are an example of the types of data that the impact assessment may be based upon. Today, most people agree that direct discharges are not the major cause of the remaining environmental problems in our lakes and rivers. Instead, nonpoint sources (sources that do not originate from a pipe, but rather from a large, sometimes hard to define area) are the primary source of contaminants.

To keep the impact of point discharges low, engineers must evaluate the impacts in the near field (effects near the source) and the far field (downstream impact that is not affected by the specific dynamics of the discharge mechanism). The near-field is dominated by diffusion processes that cause the contaminant to rapidly mix with its environment. The far field is dominated by advection, dispersion (stretching due to non-uniform velocity profiles in rivers) and transformation processes that may eliminate the contaminant by natural biodegradation. Each of these topics will be discussed in detail in this course.

Oxygen exchange. Not all substances that are of interest in environmental fluid mechanics are harmful. One important chemical we will study is oxygen, a necessary input to respiration. Oxygen levels can be depleted in water by biodegradation of wastes. This is primarily possible

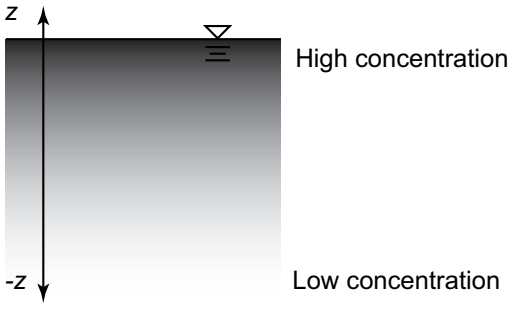

Diffusion of oxygen through
air-water interface

Fig. 1.3. Schematic of the diffusion of oxygen into a water body through the air-water interface. The dark area represents regions of high oxygen concentration, and the lighter area represents a region of lower oxygen concentration.

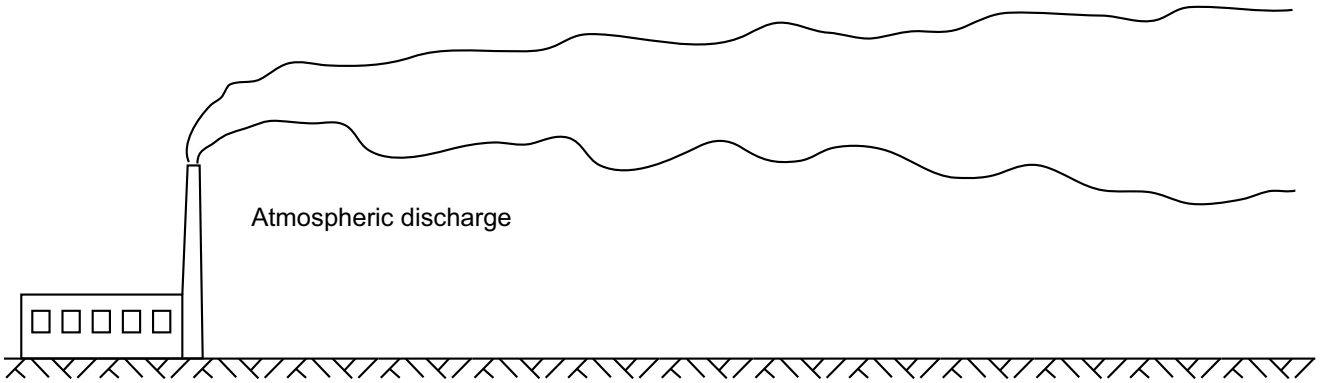

Fig. 1.4. Schematic of the release of an industrial byproduct into the atmosphere through a chimney stack. The plume moves downstream due to an average wind field.

because of the relatively slow rate of exchange of oxygen between the water and the atmosphere. When the water becomes depleted, oxygen will dissolve out of the atmosphere and into the water and then diffuse downward into the water body. This is depicted in Figure 1.3.

This is an important characteristic of diffusion, that it transports chemicals from regions of high concentration to regions of low concentration. If this were not the case, then a strong odor would just get stronger and stronger in the location of the source and never be noticed away from the source. Instead, diffusion reduces the magnitude of the odor at the source and causes the odor to spread into the clean surroundings.

Atmospheric mixing. Probably the most noticeable release of chemicals into the environment is through smoke stacks at industrial and power plants (see schematic in Figure 1.4). Because of condensation in the waste stream, the expelled gas is made visible by a trail of smoke or clouds. This is also visible in automobile exhaust on a cold winter's day. In the summer, when auto exhaust is not visible, we rarely think about all the chemicals that surround our car; however, when cold air makes the exhaust visible, it can be surprising. The tools of environmental fluid mechanics are used to predict the concentrations of gases both in summer and winter and to

help design exhaust systems, both for your car and for factories, that do not result in toxic levels. Again, the primary mechanisms we must address are transport (advection and diffusion) and transformation (reactions).

1.1.2 Expressing Concentration

In order to evaluate how much of a chemical is present in any region of a fluid, we require a means to measure chemical intensity or presence. This fundamental quantity in environmental fluid mechanics is called concentration. In common usage, the term concentration expresses a measure of the amount of a substance within a mixture.

Mathematically, the concentration C is the ratio of the mass of a substance M_i to the total volume of a mixture V expressed

$$C = \frac{M_i}{V}. \tag{1.1}$$

The units of concentration are [M/L^3], commonly reported in mg/l, kg/m^3, lb/gal, etc. For one- and two-dimensional problems, concentration can also be expressed as the mass per unit segment length [M/L] or per unit area, [M/L^2].

A related quantity, the mass fraction χ, is the ratio of the mass of a substance M_i to the total mass of a mixture M, written

$$\chi = \frac{M_i}{M}. \tag{1.2}$$

Mass fraction is unitless, but is often expressed using mixed units, such as mg/kg, parts per million (ppm), or parts per billion (ppb).

A popular concentration measure used by chemists is the molar concentration θ. Molar concentration is defined as the ratio of the number of moles of a substance N_i to the total volume of the mixture

$$\theta = \frac{N_i}{V}. \tag{1.3}$$

The units of molar concentration are [number of molecules/L^3]; typical examples are mol/l and μmol/l. To work with molar concentration, recall that the atomic weight of an atom is reported in the Periodic Table in units of g/mol and that a mole is $6.022 \cdot 10^{23}$ molecules.

The measure chosen to express concentration is essentially a matter of taste. Always use caution and confirm that the units chosen for concentration are consistent with the equations used to predict fate and transport. A common source of confusion arises from the fact that mass fraction and concentration are often used interchangeably in dilute aqueous systems. This comes about because the density of pure water at 4°C is 1 g/cm^3, making values for concentration in mg/l and mass fraction in ppm identical. Extreme caution should be used in other solutions, as in seawater or the atmosphere, where ppm and mg/l are *not* identical. The conclusion to be drawn is: always check your units.

1.1.3 Dimensional analysis

A very powerful analytical technique that we will use throughout this course is dimensional analysis. The concept behind dimensional analysis is that if we can define the parameters that a process depends on, then we should be able to use these parameters, usually in the form of dimensionless variables, to describe that process at all scales (not just the scales we measure in the laboratory or the field).

Dimensional analysis as a method is based on the Buckingham π-theorem (see e.g. Fischer et al. 1979). Consider a process that can be described by m dimensional variables. This full set of variables contains n different physical dimensions (length, time, mass, temperature, etc.). The Buckingham π-theorem states that there are, then, $m - n$ independent non-dimensional groups that can be formed from these governing variables (Fischer et al. 1979). When forming the dimensionless groups, we try to keep the dependent variable (the one we want to predict) in only one of the dimensionless groups (i.e. try not to repeat the use of the dependent variable).

Once we have the $m - n$ dimensionless variables, the Buckingham π-theorem further tells us that the variables can be related according to

$$\pi_1 = f(\pi_2, \pi_i, ..., \pi_{m-n}) \tag{1.4}$$

where π_i is the ith dimensionless variable. As we will see, this method is a powerful way to find engineering solutions to very complex physical problems.

Example: Reynolds number. As an example, consider a problem from your first course in fluid mechanics where we want to predict when a fluid flow becomes turbulent. Here, our dependent variable is a quality (turbulent or laminar) and does not have a dimension. The variables it depends on are the velocity u, the flow disturbances, characterized by a typical length scale L, and the fluid properties, as described by its density ρ, temperature T, and viscosity μ. First, we must recognize that ρ and μ are functions of T; thus, all three of these variables cannot be treated as independent. The most compact and traditional approach is to retain ρ and μ in the form of the kinematic viscosity $\nu = \mu/\rho$. Thus, we have $m = 3$ dimensional variables (u, L, and ν) in $n = 2$ physical dimensions (length and time).

The next step is to form the dimensionless group $\pi_1 = f(u, L, \nu)$. This can be done by assuming each variable has a different exponent and writing separate equations for each dimension. That is

$$\pi_1 = u^a L^b \nu^c, \tag{1.5}$$

and we want each dimension to cancel out, giving us two equations

$$\begin{aligned} t \text{ gives:} \quad & 0 = -a - c \\ L \text{ gives:} \quad & 0 = a + b + 2c. \end{aligned}$$

From the t-equation, we have $a = -c$, and from the L-equation we get $b = -c$. Since the system is under-defined, we are free to choose the value of c. To get the most simplified form, choose $c = 1$, leaving us with $a = b = -1$. Thus, we have

$$\pi_1 = \frac{\nu}{uL}. \tag{1.6}$$

This non-dimensional combination is just the inverse of the well-known Reynolds number Re; thus, we have shown through dimensional analysis, that the turbulent state of the fluid should depend on the Reynolds number

$$Re = \frac{uL}{\nu}, \tag{1.7}$$

which is a classical result in fluid mechanics.

Example: mixing scales. In environmental fluid mechanics we often want to know how long it will take for a chemical to mix through a space or how far downstream a chemical will go before it mixes to a certain size. In this problem we have three parameters: L is the distance over which the chemical spreads, D is a measure of the rate of diffusion, and t is the time. Although we have not formally introduced D, it is sufficient now to know that its dimensions are $[L^2/t]$ and that large D give rapid mixing and small D give slow mixing. Thus, we have three variables and two dimensions (L and t), yielding one non-dimensional number

$$\pi_1 = \frac{Dt}{L^2}. \tag{1.8}$$

Later, we will see that this number is called the Peclet number.

If we want to know over how large a distance diffusion will spread a chemical in a time t, we can rearrange the non-dimensional number to solve for length, giving

$$L \propto \sqrt{Dt}. \tag{1.9}$$

This is a classical scaling law in environmental fluid mechanics, and one that we will use frequently. The proportionality constant will change for different geometries, but the scaling relationship will remain. Hence, $\sqrt{Dt}$ will be called the diffusion length scale. With this background, we are now prepared to introduce the important concept of diffusion in more mathematical detail.

1.2 Diffusion

As we have seen, a fundamental transport process in environmental fluid mechanics is diffusion. Diffusion differs from advection in that it is random in nature (does not necessarily follow a fluid particle). A well-known example is the diffusion of perfume in an empty room. If a bottle of perfume is opened and allowed to evaporate into the air, soon the whole room will be scented. We also know from experience that the scent will be stronger near the source and weaker as we move away, but fragrance molecules will have wondered throughout the room due to random molecular and turbulent motions. Thus, diffusion has two primary properties: it is random in nature, and transport is from regions of high concentration to low concentration, with an equilibrium state of uniform concentration.

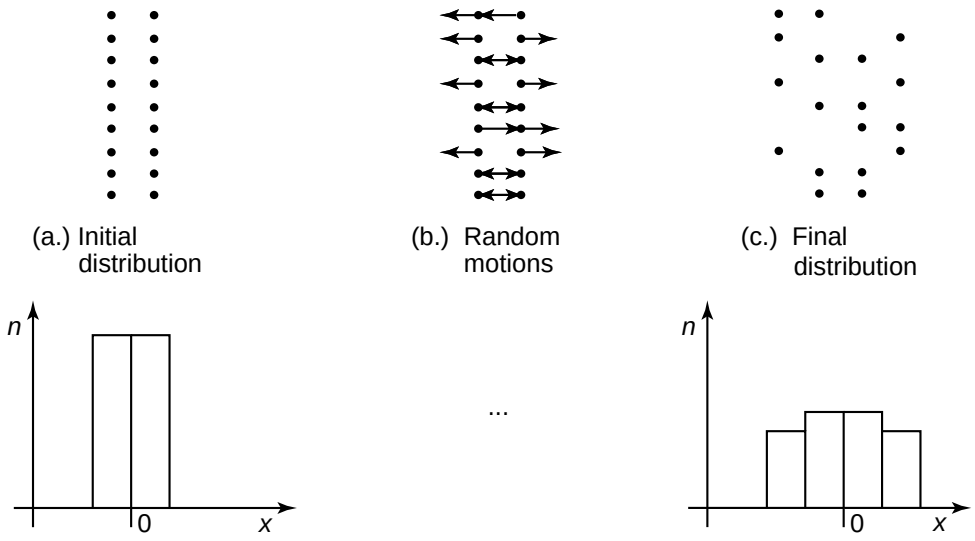

Fig. 1.5. Schematic of the one-dimensional molecular (Brownian) motion of a group of molecules illustrating the Fickian diffusion model. The upper part of the figure shows the particles themselves; the lower part of the figure gives the corresponding histogram of particle location, which is analogous to concentration.

1.2.1 Fickian diffusion

We just observed in our perfume example that regions of high concentration tend to spread into regions of low concentration under the action of diffusion. Here, we want to derive a mathematical expression that predicts this spreading-out process, and we will follow an argument presented in Fischer et al. (1979).

To derive a diffusive flux equation, consider two rows of molecules side-by-side and centered at $x = 0$, as shown in Figure 1.5(a.). Each of these molecules moves about randomly in response to the temperature (in a random process called Brownian motion). Here, for didactic purposes, we will consider only one component of their three-dimensional motion: motion right or left along the x-axis. We further define the mass of particles on the left as M_l, the mass of particles on the right as M_r, and the probability (transfer rate per time) that a particles moves across $x = 0$ as k, with units $[\mathrm{T}^{-1}]$.

After some time δt an *average* of half of the particles have taken steps to the right and half have taken steps to the left, as depicted through Figure 1.5(b.) and (c.). Looking at the particle histograms also in Figure 1.5, we see that in this random process, maximum concentrations decrease, while the total region containing particles increases (the cloud spreads out).

Mathematically, the average flux of particles from the left-hand column to the right is kM_l, and the average flux of particles from the right-hand column to the left is $-kM_r$, where the minus sign is used to distinguish direction. Thus, the net flux of particles q_x is

$$q_x = k(M_l - M_r). \tag{1.10}$$

For the one-dimensional case we can write (1.10) in terms of concentrations using

$$C_l = M_l/(\delta x \delta y \delta z) \tag{1.11}$$

$$C_r = M_r/(\delta x \delta y \delta z) \tag{1.12}$$

where δx is the width, δy is the breadth, and δz is the height of each column. Physically, δx is the average step along the x-axis taken by a molecule in the time δt. For the one-dimensional case, we want q_x to represent the flux in the x-direction per unit area perpendicular to x; hence, we will take $\delta y \delta z = 1$. Next, we note that a finite difference approximation for dC/dx is

$$\begin{aligned} \frac{dC}{dx} &= \frac{C_r - C_l}{x_r - x_l} \\ &= \frac{M_r - M_l}{\delta x (x_r - x_l)}, \end{aligned} \tag{1.13}$$

which gives us a second expression for $(M_l - M_r)$, namely,

$$(M_l - M_r) = -\delta x (x_r - x_l) \frac{dC}{dx}. \tag{1.14}$$

Taking $\delta x = (x_r - x_l)$ and substituting (1.14) into (1.10) yields

$$q_x = -k(\delta x)^2 \frac{dC}{dx}. \tag{1.15}$$

(1.15) contains two unknowns, k and δx. Fischer et al. (1979) argue that since q cannot depend on an arbitrary δx, we must assume that $k(\delta x)^2$ is a constant, which we will call the diffusion coefficient, D. Substituting, we obtain the one-dimensional diffusive flux equation

$$q_x = -D \frac{dC}{dx}. \tag{1.16}$$

It is important to note that diffusive flux is a vector quantity and, since concentration is expressed in units of $[\mathrm{M/L^3}]$, it has units of $[\mathrm{M/(L^2T)}]$. To compute the total mass flux rate $\dot{m}$, in units $[\mathrm{M/T}]$, the diffusive flux must be integrated over a surface area. For the one-dimensional case we would have $\dot{m} = A q_x$, where $A = \delta y \delta z$.

Generalizing to three dimensions, we can write the diffusive flux vector at a point by adding the other two dimensions, yielding (in various types of notation)

$$\begin{aligned} \boldsymbol{q} &= -D \left(\frac{\partial C}{\partial x}, \frac{\partial C}{\partial y}, \frac{\partial C}{\partial z} \right) \\ &= -D \nabla C \\ &= -D \frac{\partial C}{\partial x_i}. \end{aligned} \tag{1.17}$$

Diffusion processes that obey this relationship are called Fickian diffusion, and (1.17) is called Fick's law. To obtain the total mass flux rate we must integrate the normal component of $\boldsymbol{q}$ over a surface area, as in

$$\dot{m} = \iint_A \boldsymbol{q} \cdot \boldsymbol{n} dA \tag{1.18}$$

where $\boldsymbol{n}$ is the unit vector normal to the surface A.

Example Box 1.1:
Diffusive flux at the air-water interface.

The time-average oxygen profile $C(z)$ in the laminar sub-layer at the surface of a lake is

$$C(z) = C_{sat} - (C_{sat} - C_l)\text{erf}\left(\frac{z}{\delta\sqrt{2}}\right)$$

where C_{sat} is the saturation oxygen concentration in the water, C_l is the oxygen concentration in the body of the lake, δ is the concentration boundary layer thickness, and z is defined positive downward. Turbulence in the body of the lake is responsible for keeping δ constant. Find an expression for the total rate of mass flux of oxygen into the lake.

Fick's law tells us that the concentration gradient in the oxygen profile will result in a diffusive flux of oxygen into the lake. Since the concentration is uniform in x and y, we have from (1.16) the diffusive flux

$$q_z = -D\frac{dC}{dz}.$$

The derivative of the concentration gradient is

$$\begin{aligned}\frac{dC}{dz} &= -(C_{sat} - C_l)\frac{d}{dz}\left[\text{erf}\left(\frac{z}{\delta\sqrt{2}}\right)\right] \\ &= -\frac{2}{\sqrt{\pi}}\cdot\frac{(C_{sat} - C_l)}{\delta\sqrt{2}}e^{-\left(\frac{z}{\delta\sqrt{2}}\right)^2}\end{aligned}$$

At the surface of the lake, z is zero and the diffusive flux is

$$q_z = (C_{sat} - C_l)\frac{D\sqrt{2}}{\delta\sqrt{\pi}}.$$

The units of q_z are in [M/(L^2·T)]. To get the total mass flux rate, we must multiply by a surface area, in this case the surface of the lake A_l. Thus, the total rate of mass flux of oxygen into the lake is

$$\dot{m} = A_l(C_{sat} - C_l)\frac{D\sqrt{2}}{\delta\sqrt{\pi}}.$$

For $C_l < C_{sat}$ the mass flux is positive, indicating flux down, into the lake. More sophisticated models for gas transfer that develop predictive expressions for δ are discussed later in Chapter 5.

1.2.2 Diffusion coefficients

From the definition $D = k(\delta x)^2$, we see that D has units L^2/T. Since we derived Fick's law for molecules moving in Brownian motion, D is a molecular diffusion coefficient, which we will sometimes call D_m to be specific. The intensity (energy and freedom of motion) of these Brownian motions controls the value of D. Thus, D depends on the phase (solid, liquid or gas), temperature, and molecule size. For dilute solutes in water, D is generally of order $2{\cdot}10^{-9}$ m^2/s; whereas, for dispersed gases in air, D is of order $2 \cdot 10^{-5}$ m^2/s, a difference in magnitude of 10^4.

Table 1.1 gives a detailed accounting of D for a range of solutes in water with low salinity (0.5 ppt). We see from the table that for a given temperature, D can range over about $\pm 10^1$ in response to molecular size (large molecules have smaller D). The table also shows the sensitivity of D to temperature; for a 10°C change in water temperature, D can change by a factor of ± 2. These observations can be summarized by the insight that faster and less confined motions result in higher diffusion coefficients.

1.2.3 Diffusion equation

Although Fick's law gives us an expression for the flux of mass due to the process of diffusion, we still require an equation that predicts the change in concentration of the diffusing mass over time at a point. In this section we will see that such an equation can be derived using the law of conservation of mass.

Table 1.1. Molecular diffusion coefficients for typical solutes in water at standard pressure and at two temperatures (20°C and 10°C).[a]

Solute name	Chemical symbol	Diffusion coefficient[b] (10^{-4} cm^2/s)	Diffusion coefficient[c] (10^{-4} cm^2/s)
hydrogen ion	H^+	0.85	0.70
hydroxide ion	OH^-	0.48	0.37
oxygen	O_2	0.20	0.15
carbon dioxide	CO_2	0.17	0.12
bicarbonate	HCO_3^-	0.11	0.08
carbonate	CO_3^{2-}	0.08	0.06
methane	CH_4	0.16	0.12
ammonium	NH_4^+	0.18	0.14
ammonia	NH_3	0.20	0.15
nitrate	NO_3^-	0.17	0.13
phosphoric acid	H_3PO_4	0.08	0.06
dihydrogen phosphate	$H_2PO_4^-$	0.08	0.06
hydrogen phosphate	HPO_4^{2-}	0.07	0.05
phosphate	PO_4^{3-}	0.05	0.04
hydrogen sulfide	H_2S	0.17	0.13
hydrogen sulfide ion	HS^-	0.16	0.13
sulfate	SO_4^{2-}	0.10	0.07
silica	H_4SiO_4	0.10	0.07
calcium ion	Ca^{2+}	0.07	0.05
magnesium ion	Mg^{2+}	0.06	0.05
iron ion	Fe^{2+}	0.06	0.05
manganese ion	Mn^{2+}	0.06	0.05

[a] Taken from `http://www.talknet.de/~alke.spreckelsen/roger/thermo/difcoef.html`

[b] for water at 20°C with salinity of 0.5 ppt.

[c] for water at 10°C with salinity of 0.5 ppt.

To derive the diffusion equation, consider the control volume (CV) depicted in Figure 1.6. The change in mass M of dissolved tracer in this CV over time is given by the mass conservation law

$$\frac{\partial M}{\partial t} = \sum \dot{m}_{in} - \sum \dot{m}_{out}. \tag{1.19}$$

To compute the diffusive mass fluxes in and out of the CV, we use Fick's law, which for the x-direction gives

$$q_{x,in} = -D \left.\frac{\partial C}{\partial x}\right|_1 \tag{1.20}$$

$$q_{x,out} = -D \left.\frac{\partial C}{\partial x}\right|_2 \tag{1.21}$$

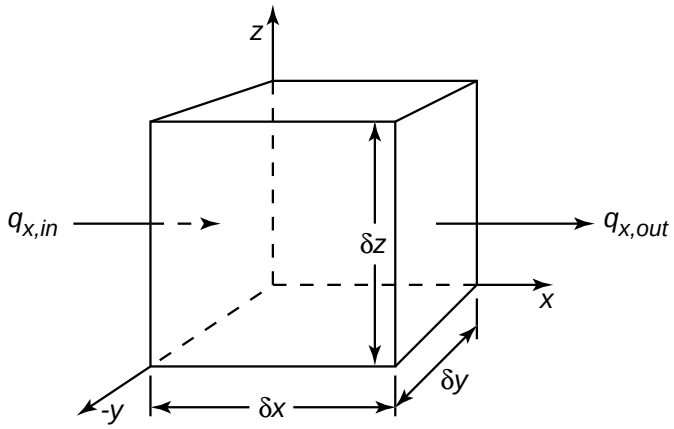

Fig. 1.6. Differential control volume for derivation of the diffusion equation.

where the locations 1 and 2 are the inflow and outflow faces in the figure. To obtain total mass flux $\dot{m}$ we multiply q_x by the CV surface area $A = \delta y \delta z$. Thus, we can write the net flux in the x-direction as

$$\delta \dot{m}|_x = -D\delta y \delta z \left(\left.\frac{\partial C}{\partial x}\right|_1 - \left.\frac{\partial C}{\partial x}\right|_2 \right) \tag{1.22}$$

which is the x-direction contribution to the right-hand-side of (1.19).

To continue we must find a method to evaluate $\partial C/\partial x$ at point 2. For this, we use linear Taylor series expansion, an important tool for linearly approximating functions. The general form of Taylor series expansion is

$$f(x) = f(x_0) + \left.\frac{\partial f}{\partial x}\right|_{x_0} \delta x + \text{HOTs}, \tag{1.23}$$

where HOTs stands for "higher order terms." Substituting $\partial C/\partial x$ for $f(x)$ in the Taylor series expansion yields

$$\left.\frac{\partial C}{\partial x}\right|_2 = \left.\frac{\partial C}{\partial x}\right|_1 + \frac{\partial}{\partial x}\left(\left.\frac{\partial C}{\partial x}\right|_1 \right) \delta x + \text{HOTs}. \tag{1.24}$$

For linear Taylor series expansion, we ignore the HOTs. Substituting this expression into the net flux equation (1.22) and dropping the subscript 1, gives

$$\delta \dot{m}|_x = D\delta y \delta z \frac{\partial^2 C}{\partial x^2} \delta x. \tag{1.25}$$

Similarly, in the y- and z-directions, the net fluxes through the control volume are

$$\delta \dot{m}|_y = D\delta x \delta z \frac{\partial^2 C}{\partial y^2} \delta y \tag{1.26}$$

$$\delta \dot{m}|_z = D\delta x \delta y \frac{\partial^2 C}{\partial z^2} \delta z. \tag{1.27}$$

Before substituting these results into (1.19), we also convert M to concentration by recognizing $M = C\delta x \delta y \delta z$. After substitution of the concentration C and net fluxes $\delta \dot{m}$ into (1.19), we obtain the three-dimensional diffusion equation (in various types of notation)

$$\begin{aligned}\frac{\partial C}{\partial t} &= D\left(\frac{\partial^2 C}{\partial x^2}+\frac{\partial^2 C}{\partial y^2}+\frac{\partial^2 C}{\partial z^2}\right)\\ &= D\nabla^2 C\\ &= D\frac{\partial C}{\partial x_i^2},\end{aligned} \tag{1.28}$$

which is a fundamental equation in environmental fluid mechanics. For the last line in (1.28), we have used the Einsteinian notation of repeated indices as a short-hand for the ∇^2 operator.

1.2.4 One-dimensional diffusion equation

In the one-dimensional case, concentration gradients in the y- and z-direction are zero, and we have the one-dimensional diffusion equation

$$\frac{\partial C}{\partial t} = D\frac{\partial^2 C}{\partial x^2}. \tag{1.29}$$

We pause here to consider (1.29) and to point out a few key observations. First, (1.29) is first-order in time. Thus, we must supply and impose one initial condition for its solution, and its solutions will be unsteady, or transient, meaning they will vary with time. To solve for the steady, time-invariant solution of (1.29), we must set $\partial C/\partial t = 0$ and we no longer require an initial condition; the steady form of (1.29) is the well-known Laplace equation. Second, (1.29) is second-order in space. Thus, we must impose two boundary conditions, and its solution will vary in space. Third, the form of (1.29) is exactly the same as the heat equation, where D is replaced by the heat transfer coefficient κ. This observation agrees well with our intuition since we know that heat conducts (diffuses) away from hot sources toward cold regions (just as concentration diffuses from high concentration toward low concentration). This observation is also useful since many solutions to the heat equation are already known.

1.3 Similarity solution to the one-dimensional diffusion equation

Because (1.28) is of such fundamental importance in environmental fluid mechanics, we demonstrate here one of its solutions for the one-dimensional case in detail. There are multiple methods that can be used to solve (1.28), but we will follow the methodology of Fischer et al. (1979) and choose the so-called similarity method in order to demonstrate the usefulness of dimensional analysis as presented in Section 1.1.3.

Consider the one-dimensional problem of a narrow, infinite pipe (radius a) as depicted in Figure 1.7. A mass of tracer M is injected uniformly across the cross-section of area $A = \pi a^2$ at the point $x = 0$ at time $t = 0$. The initial width of the tracer is infinitesimally small. We seek a solution for the spread of the tracer in the x-direction over time due to molecular diffusion alone.

As this is a one-dimensional ($\partial C/\partial y = 0$ and $\partial C/\partial z = 0$) unsteady diffusion problem, (1.29) is the governing equation, and we require two boundary conditions and an initial condition. As boundary conditions, we impose that the concentration at $\pm\infty$ remain zero

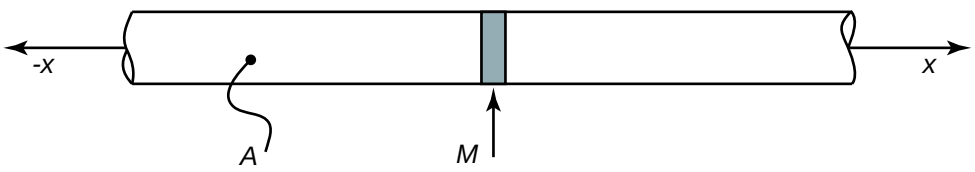

Fig. 1.7. Definitions sketch for one-dimensional pure diffusion in an infinite pipe.

Table 1.2. Dimensional variables for one-dimensional pipe diffusion.

	Variable	Dimensions
dependent variable	C	$\mathrm{M/L^3}$
independent variables	M/A	$\mathrm{M/L^2}$
	D	$\mathrm{L^2/T}$
	x	L
	t	T

$$C(\pm\infty, t) = 0 \tag{1.30}$$

because it is not possible for any of the tracer molecules to wander all the way out to infinity—by definition, infinity is not reachable. The initial condition is that the dye tracer is injected uniformly across the cross-section over an infinitesimally small width in the x-direction. To specify such an initial condition, we use the Dirac delta function

$$C(x, 0) = (M/A)\delta(x) \tag{1.31}$$

where $\delta(x)$ is zero everywhere accept at $x = 0$, where it is infinite, but the integral of the delta function from $-\infty$ to ∞ is 1. Thus, the total injected mass is given by

$$M = \int_V C(x,t)dV \tag{1.32}$$

$$= \int_{-\infty}^{\infty}\int_0^a (M/A)\delta(x)2\pi r dr dx. \tag{1.33}$$

$$= M \quad \text{QED.} \tag{1.34}$$

To use dimensional analysis, we must consider all the parameters that control the solution. Table 1.2 summarizes the dependent and independent variables for our problem. There are $m = 5$ parameters and $n = 3$ dimensions; thus, we can form two dimensionless groups

$$\pi_1 = \frac{C}{M/(A\sqrt{Dt})} \tag{1.35}$$

$$\pi_2 = \frac{x}{\sqrt{Dt}} \tag{1.36}$$

From dimensional analysis we have that $\pi_1 = f(\pi_2)$, which implies for the solution of C

$$C = \frac{M}{A\sqrt{Dt}} f\left(\frac{x}{\sqrt{Dt}}\right) \tag{1.37}$$

where f is a yet-unknown function with argument π_2. (1.37) is called a similarity solution because C has the same shape in x at all times t (see also Example Box 1.3). Now we need to find f in order to know what that shape is. Before we find the solution formally, compare (1.37) with the actual solution given by (1.59). Through this comparison, we see that dimensional analysis can go a long way toward finding solutions to physical problems.

The function f can be found in two primary ways. First, experiments can be conducted and then a smooth curve can be fit to the data using the coordinates π_1 and π_2. Second, (1.37) can be used as the solution to a differential equation and f solved for analytically. This is what we will do here. The power of a similarity solution is that it turns a partial differential equation (PDE) into an ordinary differential equation (ODE), which is the goal of any solution method for PDEs.

The similarity solution (1.37) is really just a coordinate transformation. We will call our new similarity variable $\eta = x/\sqrt{Dt}$. To substitute (1.37) into the diffusion equation, we will need the two derivatives

$$\frac{\partial \eta}{\partial t} = -\frac{\eta}{2t} \tag{1.38}$$

$$\frac{\partial \eta}{\partial x} = \frac{1}{\sqrt{Dt}}. \tag{1.39}$$

We first use the chain rule to compute $\partial C/\partial t$ as follows

$$\begin{aligned}
\frac{\partial C}{\partial t} &= \frac{\partial}{\partial t}\left[\frac{M}{A\sqrt{Dt}} f(\eta)\right] \\
&= \frac{\partial}{\partial t}\left[\frac{M}{A\sqrt{Dt}}\right] f(\eta) + \frac{M}{A\sqrt{Dt}} \frac{\partial f}{\partial \eta}\frac{\partial \eta}{\partial t} \\
&= \frac{M}{A\sqrt{Dt}}\left(-\frac{1}{2}\right)\frac{1}{t} f(\eta) + \frac{M}{A\sqrt{Dt}} \frac{\partial f}{\partial \eta}\left(-\frac{\eta}{2t}\right) \\
&= -\frac{M}{2At\sqrt{Dt}}\left(f + \eta \frac{\partial f}{\partial \eta}\right).
\end{aligned} \tag{1.40}$$

Similarly, we use the chain rule to compute $\partial^2 C/\partial x^2$ as follows

$$\begin{aligned}
\frac{\partial^2 C}{\partial x^2} &= \frac{\partial}{\partial x}\left[\frac{\partial}{\partial x}\left(\frac{M}{A\sqrt{Dt}} f(\eta)\right)\right] \\
&= \frac{\partial}{\partial x}\left[\frac{M}{A\sqrt{Dt}} \frac{\partial \eta}{\partial x}\frac{\partial f}{\partial \eta}\right] \\
&= \frac{M}{ADt\sqrt{Dt}} \frac{\partial^2 f}{\partial \eta^2}.
\end{aligned} \tag{1.41}$$

Upon substituting these two results into the diffusion equation, we obtain the ordinary differential equation in η

$$\frac{d^2 f}{d\eta^2} + \frac{1}{2}\left(f + \eta \frac{df}{d\eta}\right) = 0. \tag{1.42}$$

To solve (1.42), we should also convert the boundary and initial conditions to two new constraints on f. Substituting η into the boundary conditions gives

$$\begin{aligned} C(\pm\infty, t) &= 0 \\ \frac{M}{A\sqrt{Dt}} f\left(\frac{x}{\sqrt{Dt}}\right)\Big|_{x=\pm\infty} &= 0 \\ f(\pm\infty) &= 0. \end{aligned} \tag{1.43}$$

We convert the initial condition in a similar manner. Substituting η leads to

$$\begin{aligned} C(x, 0) &= \frac{M}{A}\delta x \\ \frac{M}{A\sqrt{Dt}} f\left(\frac{x}{\sqrt{Dt}}\right)\Big|_{t=0} &= \frac{M}{A}\delta x \end{aligned}$$

Rearranging the terms yields

$$f\left(\frac{x}{\sqrt{Dt}}\right)\Big|_{t=0} = \sqrt{Dt}\delta x\Big|_{t=0} \tag{1.44}$$

The left hand side will give $+\infty$ if $x > 0$ and $-\infty$ if $x < 0$. The right hand side gives zero because the $\sqrt{Dt}$ term is always zero at $t = 0$. Then, the initial condition reduces to

$$f(\pm\infty) = 0. \tag{1.45}$$

Thus, the three conditions on the original partial differential equation (two boundary conditions and an initial condition) have been reduced to two boundary conditions on the ordinary differential equation in f, given by either (1.43) or (1.45).

Another constraint is required to fix the value of M and is taken from the conservation of mass, given by (1.32). Substituting $dx = d\eta\sqrt{Dt}$ into (1.32) and simplifying, we obtain

$$\int_{-\infty}^{\infty} f(\eta) d\eta = 1. \tag{1.46}$$

Solving (1.42) requires a couple of integrations. First, we rearrange the equation using the identity

$$\frac{d(f\eta)}{d\eta} = f + \eta\frac{df}{d\eta}, \tag{1.47}$$

which gives us

$$\frac{d}{d\eta}\left[\frac{df}{d\eta} + \frac{1}{2}f\eta\right] = 0. \tag{1.48}$$

Integrating once leaves us with

$$\frac{df}{d\eta} + \frac{1}{2}f\eta = C_0. \tag{1.49}$$

It can be shown that choosing $C_0 = 0$ is required to satisfy the boundary conditions (see Appendix A for more details). For now, we will select $C_0 = 0$ and then verify that the solution we obtain does indeed obey the boundary condition $f(\pm\infty) = 0$.

With $C_0 = 0$ we have a homogeneous ordinary differential equation whose solution can readily be found. Moving the second term to the right hand side we have

$$\frac{df}{d\eta} = -\frac{1}{2}f\eta. \tag{1.50}$$

The solution is found by collecting the f- and η-terms on separate sides of the equation

$$\frac{df}{f} = -\frac{1}{2}\eta d\eta. \tag{1.51}$$

Integrating both sides gives

$$\ln(f) = -\frac{1}{2}\frac{\eta^2}{2} + C_1 \tag{1.52}$$

which after taking the exponential of both sides gives

$$f = C_1 \exp\left(-\frac{\eta^2}{4}\right). \tag{1.53}$$

To find C_1 we must use the remaining constraint given in (1.46). This is necessary since we introduce a parameter M and we would like that the integral under the concentration curve give us back the total mass. This auxiliary condition in f gives (recall (1.46))

$$\int_{-\infty}^{\infty} C_1 \exp\left(-\frac{\eta^2}{4}\right) d\eta = 1. \tag{1.54}$$

To solve this integral, we should use integral tables; therefore, we have to make one more change of variables to remove the $1/4$ from the exponential. Thus, we introduce ζ such that

$$\zeta^2 = \frac{1}{2^2}\eta^2 \tag{1.55}$$

$$2d\zeta = d\eta. \tag{1.56}$$

Substituting this coordinate transformation and solving for C_1 leaves

$$C_1 = \frac{1}{2\int_{-\infty}^{\infty} \exp(-\zeta^2) d\zeta}. \tag{1.57}$$

After looking up the integral in a table, we obtain $C_1 = 1/(2\sqrt{\pi})$. Thus,

$$f(\eta) = \frac{1}{2\sqrt{\pi}} \exp\left(\frac{\eta^2}{4}\right). \tag{1.58}$$

Replacing f in our similarity solution (1.37) gives

$$C(x,t) = \frac{M}{A\sqrt{4\pi Dt}} \exp\left(-\frac{x^2}{4Dt}\right) \tag{1.59}$$

which is a classic result in environmental fluid mechanics, and an equation that will be used thoroughly throughout this text. Generalizing to three dimensions, Fischer et al. (1979) give the the solution

$$C(x,y,z,t) = \frac{M}{4\pi t\sqrt{4\pi D_x D_y D_z t}} \exp\left(-\frac{x^2}{4D_x t} - \frac{y^2}{4D_y t} - \frac{z^2}{4D_z t}\right) \tag{1.60}$$

which they derive using the separation of variables method.

Example Box 1.2:
Maximum concentrations.

For the three-dimensional instantaneous point-source solution given in (1.60), find an expression for the maximum concentration. Where is the maximum concentration located?

The classical approach for finding maxima of functions is to look for zero-points in the derivative of the function. For many concentration distributions, it is easier to take a qualitative look at the functional form of the equation. The instantaneous point-source solution has the form

$$C(\boldsymbol{x},t) = C_1(t)\exp(-|f(\boldsymbol{x},t)|).$$

$C_1(t)$ is an amplification factor independent of space. The exponential function has a negative argument, which means it is maximum when the argument is zero. Hence, the maximum concentration is

$$C_{max}(t) = C_1(t).$$

Applying this result to (1.60) gives

$$C_{max}(t) = \frac{M}{4\pi t\sqrt{4\pi D_x D_y D_z t}}.$$

The maximum concentration occurs at the point where the exponential is zero. In this case $\boldsymbol{x}(C_{max}) = (0,0,0)$.

We can apply this same analysis to other concentration distributions as well. For example, consider the error function concentration distribution

$$C(x,t) = \frac{C_0}{2}\left(1 - \mathrm{erf}\left(\frac{x}{\sqrt{4Dt}}\right)\right).$$

The error function ranges over $[-1,1]$ as its argument ranges from $[-\infty,\infty]$. The maximum concentration occurs when erf$(\cdot)$ = -1, and gives,

$$C_{max}(t) = C_0.$$

C_{max} occurs when the argument of the error function is $-\infty$. At $t = 0$, the maximum concentration occurs for all points $x < 0$, and for $t > 0$, the maximum concentration occurs only at $x = -\infty$.

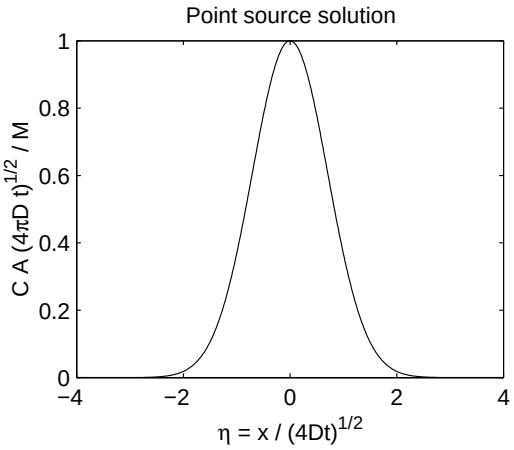

Fig. 1.8. Self-similarity solution for one-dimensional diffusion of an instantaneous point source in an infinite domain.

1.3.1 Interpretation of the similarity solution

Figure 1.8 shows the one-dimensional solution (1.59) in non-dimensional space. Comparing (1.59) with the Gaussian probability distribution reveals that (1.59) is the normal bell-shaped curve with a standard deviation σ, of width

$$\sigma^2 = 2Dt. \tag{1.61}$$

The concept of self similarity is now also evident: the concentration profile shape is always Gaussian. By plotting in non-dimensional space, the profiles also collapse into a single profile; thus, profiles for all times $t > 0$ are given by the result in the figure.

The Gaussian distribution can also be used to predict how much tracer is within a certain region. Looking at Figure 1.8 it appears that most of the tracer is between -2 and 2. Gaussian probability tables, available in any statistics book, can help make this observation more quantitative. Within $\pm\sigma$, 64.2% of the tracer is found and between $\pm 2\sigma$, 95.4% of the tracer is found. As an engineering rule-of-thumb, we will say that a diffusing tracer is distributed over a region of width 4σ, that is, $\pm 2\sigma$ in Figure 1.8.

Example Box 1.3:
Profile shape and self similarity.

For the one-dimensional, instantaneous point-source solution, show that the ratio C/C_{max} can be written as a function of the single parameter α defined such that $x = \alpha\sigma$. How might this be used to estimate the diffusion coefficient from concentration profile data?

From the previous example, we know that $C_{max} = M/\sqrt{4\pi Dt}$, and we can re-write (1.59) as

$$\frac{C(x,t)}{C_{max}(t)} = \exp\left(-\frac{x^2}{4Dt}\right).$$

We now substitute $\sigma = \sqrt{2Dt}$ and $x = \alpha\sigma$ to obtain

$$\frac{C}{C_{max}} = \exp\left(-\alpha^2/2\right).$$

Here, α is a parameter that specifies the point to calculate C based on the number of standard deviations the point is away from the center of mass. This illustrates very clearly the notion of self similarity: regardless of the time t, the amount of mass M, or the value of D, the ratio C/C_{max} is always the same value at the same position $\alpha\sigma$.

This relationship is very helpful for calculating diffusion coefficients. Often, we do not know the value of M. We can, however, always normalize a concentration profile measured at a given time t by $C_{max}(t)$. Then we pick a value of α, say 1.0. We know from the relationship above that $C/C_{max} = 0.61$ at $x = \sigma$. Next, find the locations where $C/C_{max} = 0.61$ in the experimental profile and use them to measure σ. We then use the relationship $\sigma = \sqrt{2Dt}$ and the value of t to estimate D.

1.4 Application: Diffusion in a lake

With a solid background now in diffusion, consider the following example adapted from Nepf (1995).

As shown in Figures 1.9 and 1.10, a small alpine lake is mildly stratified, with a thermocline (region of steepest density gradient) at 3 m depth, and is contaminated by arsenic. Determine the magnitude and direction of the diffusive flux of arsenic through the thermocline (cross-sectional area at the thermocline is $A = 2 \cdot 10^4$ m^2) and discuss the nature of the arsenic source. The molecular diffusion coefficient is $D_m = 1 \cdot 10^{-10}$ m^2/s.

Molecular diffusion. To compute the molecular diffusive flux through the thermocline, we use the one-dimensional version of Fick's law, given above in (1.16)

$$q_z = -D_m \frac{\partial C}{\partial z}. \tag{1.62}$$

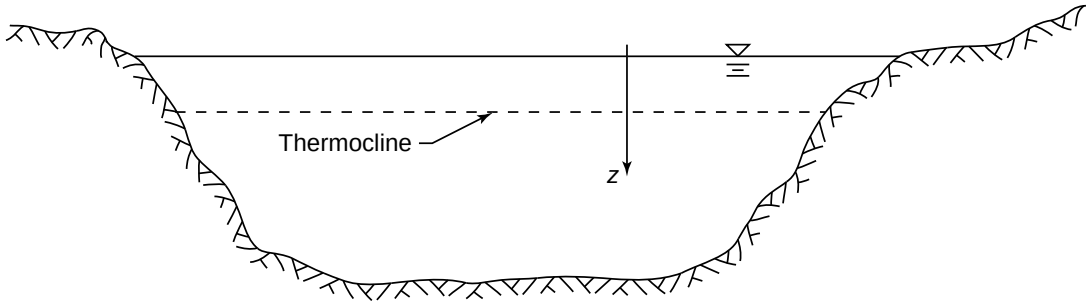

Fig. 1.9. Schematic of a stratified alpine lake.

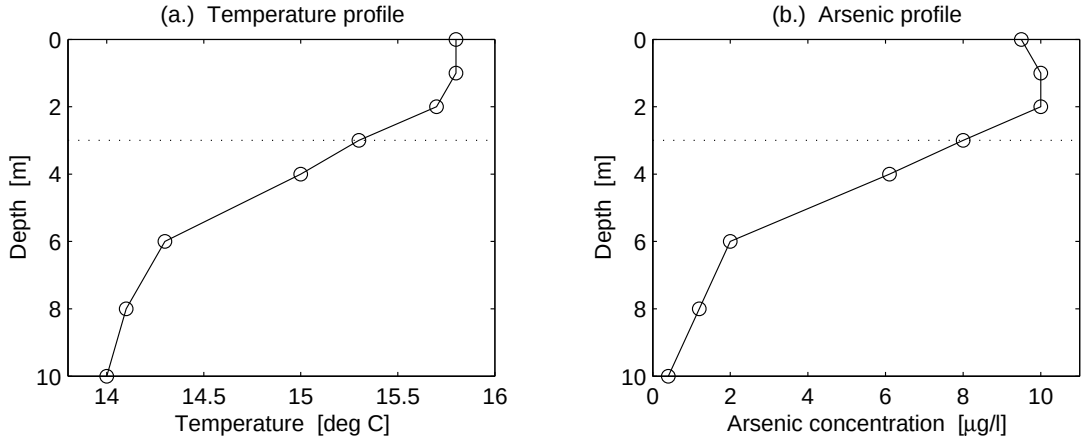

Fig. 1.10. Profiles of temperature and arsenic concentration in an alpine lake. The dotted line at 3 m indicates the location of the thermocline (region of highest density gradient).

We calculate the concentration gradient at $z = 3$ from the concentration profile using a finite difference approximation. Substituting the appropriate values, we have

$$\begin{aligned} q_z &= -D_m \frac{\partial C}{\partial z} \\ &= -(1 \cdot 10^{-10}) \frac{(10 - 6.1)}{(2 - 4)} \cdot \frac{1000 \text{ l}}{1 \text{ m}^3} \\ &= +1.95 \cdot 10^{-7} \ \mu\text{g}/(\text{m}^2 \cdot \text{s}) \end{aligned} \tag{1.63}$$

where the plus sign indicates that the flux is downward. The total mass flux is obtained by multiplying over the area: $\dot{m} = Aq_z = 0.0039 \ \mu\text{g/s}$.

Turbulent diffusion. As we pointed out in the discussion on diffusion coefficients, faster random motions lead to larger diffusion coefficients. As we will see in Chapter 3, turbulence also causes a kind of random motion that behaves asymptotically like Fickian diffusion. Because the turbulent motions are much larger than molecular motions, turbulent diffusion coefficients are much larger than molecular diffusion coefficients.

Sources of turbulence at the thermocline of a small lake can include surface inflows, wind stirring, boundary mixing, convection currents, and others. Based on studies in this lake, a turbulent diffusion coefficient can be taken as $D_t = 1.5 \cdot 10^{-6}$ m^2/s. Since turbulent diffusion obeys the same Fickian flux law, then the turbulent diffusive flux $q_{z,t}$ can be related to the molecular diffusive flux $q_{z,t} = q_z$ by the equation

$$q_{z,t} = q_{z,m} \frac{D_t}{D_m} \tag{1.64}$$

$$= +2.93 \cdot 10^{-3} \ \mu\text{g}/(\text{m}^2 \cdot \text{s}). \tag{1.65}$$

Hence, we see that turbulent diffusive transport is much greater than molecular diffusion. As a warning, however, if the concentration gradients are very high and the turbulence is low, molecular diffusion can become surprisingly significant!

Implications. Here, we have shown that the concentration gradient results in a net diffusive flux of arsenic into the hypolimnion (region below the thermocline). Assuming no other transport processes are at work, we can conclude that the arsenic source is at the surface. If the diffusive transport continues, the hypolimnion concentrations will increase. The next chapter considers how the situation might change if we include another type of transport: advection.

Summary

This chapter introduced the subject of environmental fluid mechanics and focused on the important transport process of diffusion. Fick's law was derived to represent the mass flux (transport) due to diffusion, and Fick's law was used to derive the diffusion equation, which is used to predict the time-evolution of a concentration field in space due to diffusive transport. A similarity method was used through the aid of dimensional analysis to find a one-dimensional solution to the diffusion equation for an instantaneous point source. As illustrated through an example, diffusive transport results when concentration gradients exist and plays an important role in predicting the concentrations of contaminants as they move through the environment.

Exercises

1.1 Newspaper research. Find an example of a news article that deals with fate or transport of chemicals in a situation that demonstrates concepts from Environmental Fluid Mechanics. You my chose a newspaper or web article, and the event should have occurred in the last 20 years. Attach a copy of the article and *write a short paragraph describing it's relationship to environmental fluid mechanics.*

1.2 Definitions. Write a short, qualitative definition of the following terms:

Concentration.	Partial differential equation.
Mass fraction.	Standard deviation.
Density.	Chemical fate.

Diffusion.	Chemical transport.
Brownian motion.	Transport equation.
Instantaneous point source.	Fick's law.
Similarity method.	

1.3 Concentrations in water. A student adds 1.00 mg of pure Rhodamine WT (a common fluorescent tracer used in field experiments) to 1.000 l of water at 20°C. Assuming the solution is dilute so that we can neglect the equation of state of the solution, compute the concentration of the Rhodamine WT mixture in the units of mg/l, mg/kg, ppm, and ppb.

1.4 Concentrations in air. Air consists of 21% oxygen gas (O_2). For air with a density of 1.4 kg/m^3, compute the concentration of oxygen in the units of mg/l, mg/kg, mol/l, and ppm.

1.5 Fick's law. Assume a linear concentration profile between two fixed points as depicted in the following figure:

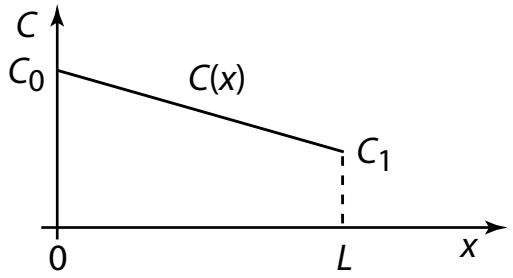

and given by the equation

$$C = bx + C_0 \tag{1.66}$$

where $b = (C_1 - C_0)/L$. Assuming the diffusion coefficient is D, find:

- The diffusive flux per unit area for any point between $x = [0, L]$.
- The total mass flux over an area A between $x = [0, L]$.

1.6 Mass fluxes. A one-dimensional concentration profile near a fixed-concentration sewage discharge is

$$C(x) = C_0 \left(1 - \text{erf}\left(\frac{x}{\sqrt{4Dt}}\right)\right) \tag{1.67}$$

where C_0 is the initial concentration near the source, erf is the error function, t is the time since the start of release, x is the distance downstream, and D is the diffusion coefficient. Compute the net mass flux vector q_x at $x = 10$ m and $t = 6$ hours. Use $D = 1 \cdot 10^{-3}$ m^2/s.

1.7 Diffusive flux in a side channel. A small fish pond located near a river bank downstream of a mine is connected to the main river through a small channel for water intake (refer to the figure below). Assume the water levels between the river and the pond are the same so that the velocity in the channel is zero. The arsenic level in the river is on average 1 ppm during the

summer, and 0 during the rest of the year. The initial level of arsenic is 0 ppm in the pond right before summer. The connecting channel is 4 m long, 2 m wide and 2 m deep. Calculate how much arsenic will diffuse into the pond over the 3 months during the summer. If the pond is approximately 100 m long, 50 m wide, and 2 m deep, what will the mean arsenic level be in the pond after the 3-month summer period? If the allowable arsenic level in the pond is 0.1 ppb, do you suggest the owner to build a gate at the connecting channel so the inflow of arsenic can be blocked?

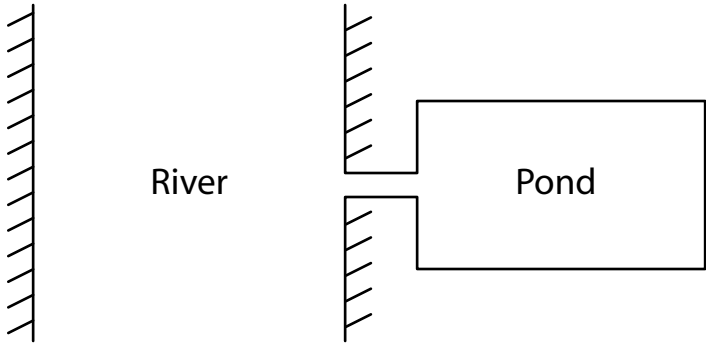

1.8 Instantaneous point source. Consider the pipe section depicted in Figure 1.7. A student injects 5 ml of 20% Rhodamine-WT solution (specific gravity 1.15) instantaneously and uniformly over the pipe cross-section ($A = 0.8$ cm^3) at the point $x = 0$ and the time $t = 0$. The pipe is filled with stagnant water. Assume the molecular diffusion coefficient is $D_m = 0.13 \cdot 10^{-4}$ cm^2/s.

- What is the concentration at $x = 0$ at the time $t = 0$?
- What is the standard deviation of the concentration distribution 1 s after injection?
- Plot the maximum concentration in the pipe, $C_{max}(t)$, as a function of time over the interval $t = [0, 24$ h$]$.
- How long does it take until the concentration over the region $x = \pm 1$ m can be treated as uniform? Define a uniform concentration distribution as one where the minimum concentration within a region is no less than 95% of the maximum concentration within that same region.

1.9 Advection versus diffusion. Rivers can often be approximated as advection dominated (downstream transport due to currents is much faster than diffusive transport) or diffusion dominated (diffusive transport is much faster than downstream transport due to currents). This property is described by a non-dimensional parameter (called the Peclet number) $Pe = f(u, D, x)$, where u is the stream velocity, D is the diffusion coefficient, and x is the distance downstream to the point of interest. Using dimensional analysis, find the form of Pe such that $Pe \ll 1$ is advection dominated and $Pe \gg 1$ is diffusion dominated. For a stream with $u = 0.3$ m/s and $D = 0.05$ m^2/s, where are diffusion and advection equally important?

1.10 Maximum concentrations. Referring to Figure 1.8, we note that the maximum concentration in space is always found at the center of the distribution ($x = 0$). For a point at $x = r$, however, the maximum concentration over time occurs at one specific time t_{max} and then decreases until an equilibrium level is reached.

- Using the one-dimensional point source solution, find an equation for the time t_{max} at which the maximum concentration occurs for an arbitrary point $x = r$.
- Write a program (MATLAB is preferred, but not required) that solves the one-dimensional point source solution at $x = r$ with r, D, M, and A as user inputs. Plot the concentration as a function of time at the location $r = 2$ with the remaining three inputs set as 1.0. Plot an adequate time period that the maximum concentration is clearly identifiable. (Please mail me your program).
- Calculate t_{max} for the case plotted in the previous step ($r = 2$, $D = M = A = 1$) and compare your value to the figure from your Matlab program.

1.11 Diffusion in a river. The Rhein river can be approximated as having a uniform depth ($h = 5$ m), width ($B = 300$ m) and mean flow velocity ($u = 0.7$ m/s). Under these conditions, 100 kg of tracer is injected as a point source (the injection is evenly distributed transversely over the cross-section). The cloud is expected to diffuse laterally as a one-dimensional point source in a moving coordinate system, moving at the mean stream velocity. The river has an enhanced mixing coefficient of $D = 10$ m^2/s. How long does it take for the center of mass of the cloud to reach a point $x = 15000$ m downstream? What is the maximum concentration that passes the point x? How wide is the cloud (take the cloud width as 4σ) when it passes this point?

1.12 Measuring diffusion coefficients 1. A chemist is trying to calculate the diffusion coefficient for a new chemical. In his experiments, he measured the concentration as a function of time at a point 5 cm away from a virtual point source diffusing in three dimensions. Select a set of coordinates such that, when plotting the data in Table 1.3, D is the slope of a best-fit line through the data. Based on this coordinate transformation, what is more important to measure precisely, concentration or time? What recommendation would you give to this scientist to improve the accuracy of his estimate for the diffusion coefficient?

1.13 Measuring diffusion coefficients 2.[1] As part of a water quality study, you have been asked to assess the diffusion of a new fluorescent dye. To accomplish this, you do a dye study in a laboratory tank (depth $h = 40$ cm). You release the dye at a depth of 20 cm (spread evenly over the area of the tank) and monitor its development over time. Vertical profiles of dye concentration in the tank are shown in Figure 1.11; the x-axis represents the reading on your fluorometer and the y-axis represents the depth.

- Estimate the molecular diffusion coefficient of the dye, D_m, based on the evolution of the dye cloud.
- Predict at what time the vertical distribution of the dye will be affected by the boundaries of the tank.

1.14 Radiative heaters. A student heats his apartment (surface area $A_r = 32$ m^2 and ceiling height $h = 3$ m) with a radiative heater. The heater has a total surface area of $A_h = 0.8$ m^2; the thickness of the heater wall separating the heater fluid from the outside air is $\delta x = 3$ mm

[1] This problem is adapted from Nepf (1995).

Table 1.3. Measured concentration and time for a point source diffusing in three-dimensions for problem number 112.

Time (days)	Concentration (μg/cm^3 ± 0.03)
0.5	0.02
1.0	0.50
1.5	2.08
2.0	3.66
2.5	4.81
3.0	5.50
3.5	5.80
4.0	5.91
4.5	5.81
5.0	5.70
5.5	5.54
6.0	5.28
6.5	5.05
7.0	4.87
7.5	4.65
8.0	4.40
8.5	4.24
9.0	4.00
9.5	3.84
10.0	3.66

(refer to Figure 1.12). The conduction of heat through the heater wall is given by the diffusion equation

$$\frac{\partial T}{\partial t} = \kappa \nabla^2 T \tag{1.68}$$

where T is the temperature in °C and $\kappa = 1.1 \cdot 10^{-2}$ kcal/(s°Cm) is the thermal conductivity of the metal for the heater wall. The heat flux $\boldsymbol{q}$ through the heater wall is given by

$$\boldsymbol{q} = -\kappa \nabla T. \tag{1.69}$$

Recall that 1 kcal = 4184 J and 1 Watt = 1 J/s.

- The conduction of heat normal to the heater wall can be treated as one-dimensional. Write (1.68) and (1.69) for the steady-state, one-dimensional case.
- Solve (1.68) for the steady-state, one-dimensional temperature profile through the heater wall with boundary conditions $T(0) = T_h$ and $T(\delta x) = T_r$ (refer to Figure 1.12).
- The water in the heater and the air in the room move past the heater wall such that $T_h = 85$°C and $T_r = 35$°C. Compute the heat flux from (1.69) using the steady-state, one-dimensional solution just obtained.

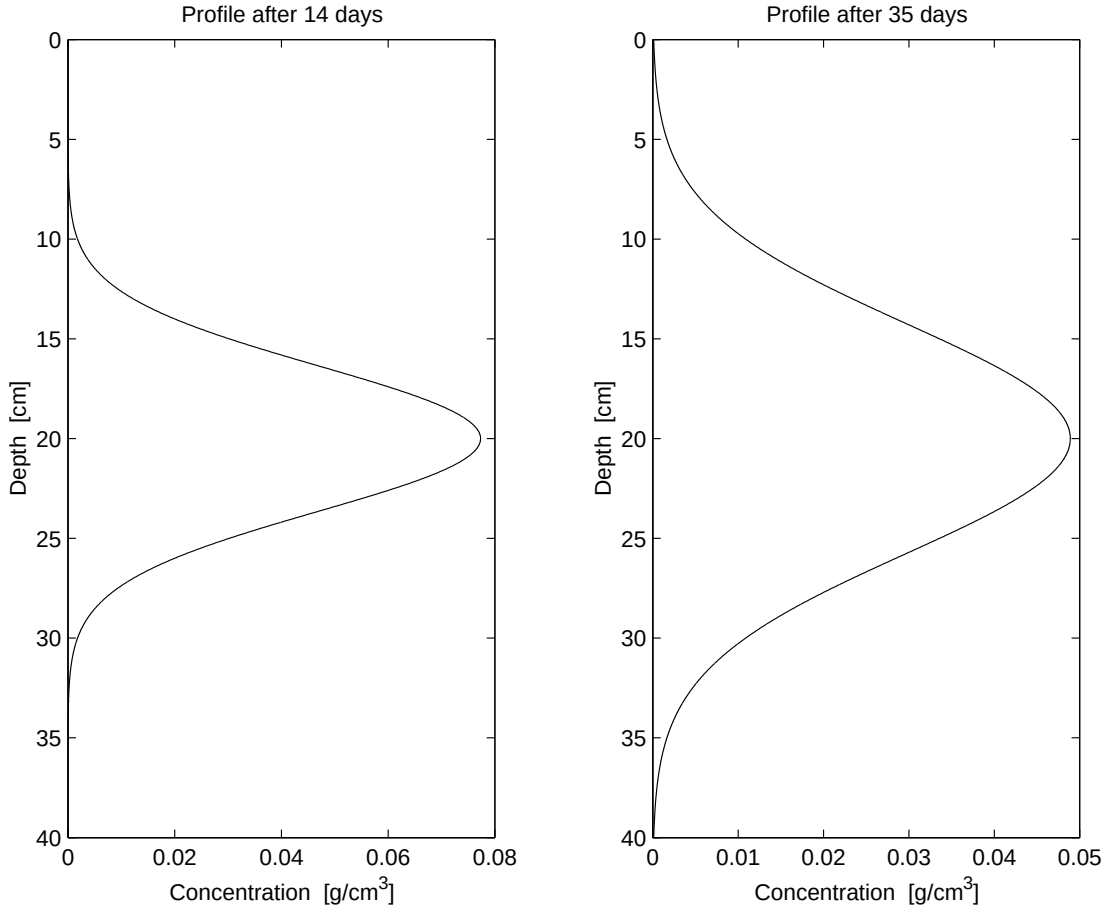

Fig. 1.11. Concentration profiles of fluorescent dye for two different measurement times. Refer to problem number 1.13.

- How many 300 Watt lamps are required to equal the heat output of the heater assuming 100% efficiency?
- Assume the specific heat capacity of the air is $c_v = 0.172$ kcal/(kg·K) and the density is $\rho_a = 1.4$ kg/m^3. How much heat is required to raise the temperature of the apartment by 5°C?
- Given the heat output of the heater and the heat needed to heat the room, how might you explain that the student is able to keep the heater turned on all the time?

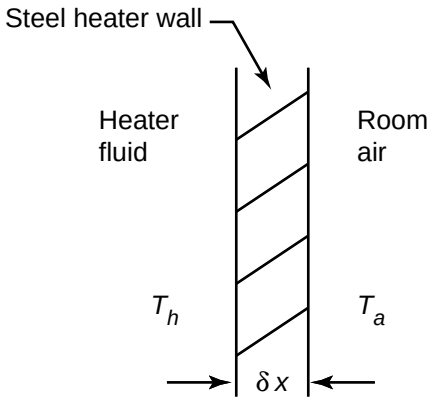

Fig. 1.12. Definitions sketch for one-dimensional thermal conduction for the heater wall in problem number 1.14.

2. Advective Diffusion Equation

In nature, transport occurs in fluids through the combination of advection and diffusion. The previous chapter introduced diffusion and derived solutions to predict diffusive transport in stagnant ambient conditions. This chapter incorporates advection into our diffusion equation (deriving the advective diffusion equation) and presents various methods to solve the resulting partial differential equation for different geometries and contaminant conditions.

2.1 Derivation of the advective diffusion equation

Before we derive the advective diffusion equation, we look at a heuristic description of the effect of advection. To conceptualize advection, consider our pipe problem from the previous chapter. Without pipe flow, the injected tracer spreads equally in both directions, describing a Gaussian distribution over time. If we open a valve and allow water to flow in the pipe, we expect the center of mass of the tracer cloud to move with the mean flow velocity in the pipe. If we move our frame of reference with that mean velocity and assume the inviscid case, then we expect the solution to look the same as before. This new reference frame is

$$\eta = x - (x_0 + ut) \tag{2.1}$$

where η is the moving reference frame spatial coordinate, x_0 is the injection point of the tracer, u is the mean flow velocity, and ut is the distance traveled by the center of mass of the cloud in time t. If we substitute η for x in our solution for a point source in stagnant conditions we obtain

$$C(x,t) = \frac{M}{A\sqrt{4\pi Dt}} \exp\left(-\frac{(x-(x_0+ut))^2}{4Dt}\right). \tag{2.2}$$

To test whether this solution is correct, we need to derive a general equation for advective diffusion and compare its solution to this one.

2.1.1 The governing equation

The derivation of the advective diffusion equation relies on the principle of superposition: advection and diffusion can be added together if they are linearly independent. How do we know if advection and diffusion are independent processes? The only way that they can be dependent is if one process feeds back on the other. From the previous chapter, diffusion was shown to be a random process due to molecular motion. Due to diffusion, each molecule in time δt will move

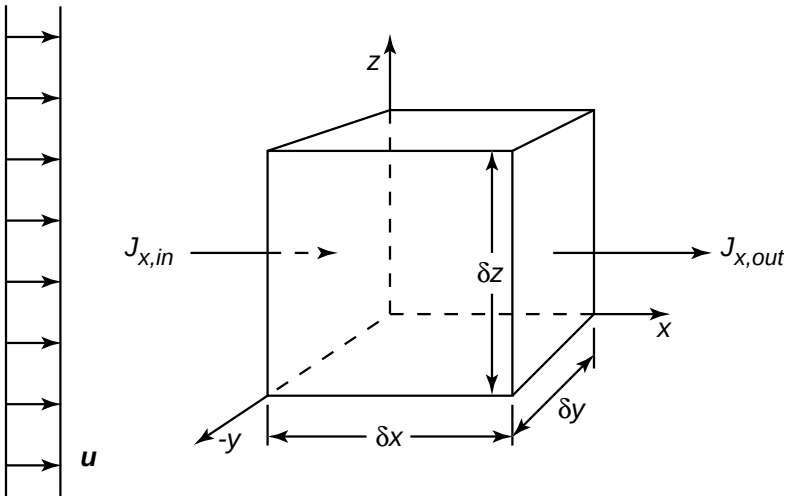

Fig. 2.1. Schematic of a control volume with crossflow.

either one step to the left or one step to the right (i.e. $\pm\delta x$). Due to advection, each molecule will also move $u\delta t$ in the cross-flow direction. These processes are clearly additive and independent; the presence of the crossflow does not bias the probability that the molecule will take a diffusive step to the right or the left, it just adds something to that step. The net movement of the molecule is $u\delta t \pm \delta x$, and thus, the total flux in the x-direction J_x, including the advective transport and a Fickian diffusion term, must be

$$\begin{aligned} J_x &= uC + q_x \\ &= uC - D\frac{\partial C}{\partial x}. \end{aligned} \tag{2.3}$$

We leave it as an exercise for the reader to prove that uC is the correct form of the advective term (hint: consider the dimensions of q_x and uC).

As we did in the previous chapter, we now use this flux law and the conservation of mass to derive the advective diffusion equation. Consider our control volume from before, but now including a crossflow velocity, $\boldsymbol{u} = (u, v, w)$, as shown in Figure 2.1. Here, we follow the derivation in Fischer et al. (1979). From the conservation of mass, the net flux through the control volume is

$$\frac{\partial M}{\partial t} = \sum \dot{m}_{in} - \sum \dot{m}_{out}, \tag{2.4}$$

and for the x-direction, we have

$$\delta\dot{m}|_x = \left(uC - D\frac{\partial C}{\partial x}\right)\Big|_1 \delta y\delta z - \left(uC - D\frac{\partial C}{\partial x}\right)\Big|_2 \delta y\delta z. \tag{2.5}$$

As before, we use linear Taylor series expansion to combine the two flux terms, giving

$$\begin{aligned} uC|_1 - uC|_2 &= uC|_1 - \left(uC|_1 + \frac{\partial(uC)}{\partial x}\Big|_1 \delta x\right) \\ &= -\frac{\partial(uC)}{\partial x}\delta x \end{aligned} \tag{2.6}$$

and

$$-D\left.\frac{\partial C}{\partial x}\right|_1 + D\left.\frac{\partial C}{\partial x}\right|_2 = -D\left.\frac{\partial C}{\partial x}\right|_1 + \left(D\left.\frac{\partial C}{\partial x}\right|_1 + \frac{\partial}{\partial x}\left(D\frac{\partial C}{\partial x}\right)\Big|_1 \delta x\right)$$
$$= D\frac{\partial^2 C}{\partial x^2}\delta x. \tag{2.7}$$

Thus, for the x-direction

$$\delta\dot{m}|_x = -\frac{\partial(uC)}{\partial x}\delta x\delta y\delta z + D\frac{\partial^2 C}{\partial x^2}\delta x\delta y\delta z. \tag{2.8}$$

The y- and z-directions are similar, but with v and w for the velocity components, giving

$$\delta\dot{m}|_y = -\frac{\partial(vC)}{\partial y}\delta y\delta x\delta z + D\frac{\partial^2 C}{\partial y^2}\delta y\delta x\delta z \tag{2.9}$$

$$\delta\dot{m}|_z = -\frac{\partial(wC)}{\partial z}\delta z\delta x\delta y + D\frac{\partial^2 C}{\partial z^2}\delta z\delta x\delta y. \tag{2.10}$$

Substituting these results into (2.4) and recalling that $M = C\delta x\delta y\delta z$, we obtain

$$\frac{\partial C}{\partial t} + \nabla\cdot(\boldsymbol{u}C) = D\nabla^2 C \tag{2.11}$$

or in Einsteinian notation

$$\frac{\partial C}{\partial t} + \frac{\partial u_i C}{\partial x_i} = D\frac{\partial^2 C}{\partial x_i^2}, \tag{2.12}$$

which is the desired advective diffusion (AD) equation. We will use this equation extensively in the remainder of this text.

Note that these equations implicitly assume that D is constant. When considering a variable D, the right-hand-side of (2.12) has the form

$$\frac{\partial}{\partial x_i}\left(D_{ij}\frac{\partial C}{\partial x_j}\right). \tag{2.13}$$

2.1.2 Point-source solution

To check whether our initial suggestion (2.2) for a solution to (2.12) was correct, we substitute the coordinate transformation for the moving reference frame into the one-dimensional version of (2.12). In the one-dimensional case, $\boldsymbol{u} = (u, 0, 0)$, and there are no concentration gradients in the y- or z-directions, leaving us with

$$\frac{\partial C}{\partial t} + \frac{\partial(uC)}{\partial x} = D\frac{\partial^2 C}{\partial x^2}. \tag{2.14}$$

Our coordinate transformation for the moving system is

$$\eta = x - (x_0 + ut) \tag{2.15}$$

$$\tau = t, \tag{2.16}$$

and this can be substituted into (2.14) using the chain rule as follows

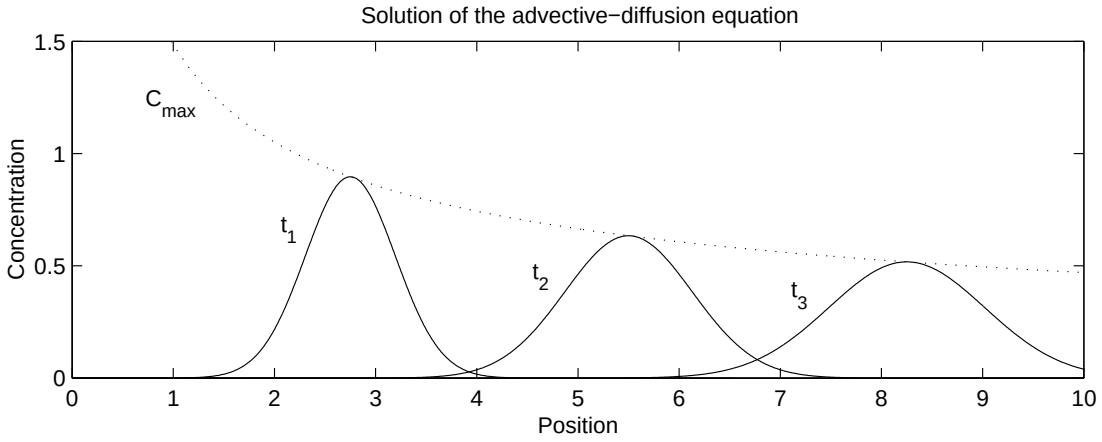

Fig. 2.2. Schematic solution of the advective diffusion equation in one dimension. The dotted line plots the maximum concentration as the cloud moves downstream.

$$\frac{\partial C}{\partial \tau}\frac{\partial \tau}{\partial t} + \frac{\partial C}{\partial \eta}\frac{\partial \eta}{\partial t} + u\left(\frac{\partial C}{\partial \eta}\frac{\partial \eta}{\partial x} + \frac{\partial C}{\partial \tau}\frac{\partial \tau}{\partial x}\right) = D\left(\frac{\partial}{\partial \eta}\frac{\partial \eta}{\partial x} + \frac{\partial}{\partial \tau}\frac{\partial \tau}{\partial x}\right)\left(\frac{\partial C}{\partial \eta}\frac{\partial \eta}{\partial x} + \frac{\partial C}{\partial \tau}\frac{\partial \tau}{\partial x}\right) \tag{2.17}$$

which reduces to

$$\frac{\partial C}{\partial \tau} = D\frac{\partial^2 C}{\partial \eta^2}. \tag{2.18}$$

This is just the one-dimensional diffusion equation (1.29) in the coordinates η and τ with solution for an instantaneous point source of

$$C(\eta, \tau) = \frac{M}{A\sqrt{4\pi D\tau}} \exp\left(-\frac{\eta^2}{4D\tau}\right). \tag{2.19}$$

Converting the solution back to x and t coordinates (by substituting (2.15) and (2.16)), we obtain (2.2); thus, our intuitive guess for the superposition solution was correct. Figure 2.2 shows the schematic behavior of this solution for three different times, t_1, t_2, and t_3.

2.1.3 Incompressible fluid

For an incompressible fluid, (2.12) can be simplified by using the conservation of mass equation for the ambient fluid. In an incompressible fluid, the density is a constant ρ_0 everywhere, and the conservation of mass equation reduces to the continuity equation

$$\nabla \cdot \boldsymbol{u} = 0 \tag{2.20}$$

(see, for example Batchelor (1967)). If we expand the advective term in (2.12), we can write

$$\nabla \cdot (\boldsymbol{u}C) = (\nabla \cdot \boldsymbol{u})C + \boldsymbol{u} \cdot \nabla C. \tag{2.21}$$

by virtue of the continuity equation (2.20) we can take the term $(\nabla \cdot \boldsymbol{u})C = 0$; thus, the advective diffusion equation for an incompressible fluid is

$$\frac{\partial C}{\partial t} + u_i \frac{\partial C}{\partial x_i} = D \frac{\partial^2 C}{\partial x_i^2}. \tag{2.22}$$

This is the form of the advective diffusion equation that we will use the most in this class.

2.1.4 Rules of thumb

We pause here to make some observations regarding the AD equation and its solutions.

First, the solution in Figure 2.2 shows an example where the diffusive and advective transport are about equally important. If the crossflow were stronger (larger u), the cloud would have less time to spread out and would be narrower at each t_i. Conversely, if the diffusion were faster (larger D), the cloud would spread out more between the different t_i and the profiles would overlap. Thus, we see that diffusion *versus* advection dominance is a function of t, D, and u, and we express this property through the non-dimensional Peclet number

$$Pe = \frac{D}{u^2 t}, \tag{2.23}$$

or for a given downstream location $L = ut$,

$$Pe = \frac{D}{uL}. \tag{2.24}$$

For $Pe \gg 1$, diffusion is dominant and the cloud spreads out faster than it moves downstream; for $Pe \ll 1$, advection is dominant and the cloud moves downstream faster than it spreads out. It is important to note that the Peclet number is dependent on our zone of interest: for "large" times or distances, the Peclet number is small and advection dominates.

Second, the maximum concentration decreases in the downstream direction due to diffusion. Figure 2.2 also plots the maximum concentration of the cloud as it moves downstream. This is obtained when the exponential term in (2.2) is 1.0. For the one-dimensional case, the maximum concentration decreases as

$$C_{max}(t) \propto \frac{1}{\sqrt{t}}. \tag{2.25}$$

In the two- and three-dimensional cases, the relationship is

$$C_{max}(t) \propto \frac{1}{t} \text{ and} \tag{2.26}$$

$$C_{max}(t) \propto \frac{1}{t\sqrt{t}}, \tag{2.27}$$

respectively.

Third, the diffusive and advective scales can be used to simplify the equations and make approximations. One of the most common questions in engineering is: when does a given equation or approximation apply? In contaminant transport, this question is usually answered by comparing characteristic advection and diffusion length and time scales to the length and time scales in the problem. For advection (subscript a) and for diffusion (subscript d), the characteristic scales are

$$L_a = ut\ ; \qquad t_a = \frac{L}{u} \tag{2.28}$$

$$L_d = \sqrt{Dt}\ ; \qquad t_d = \frac{L^2}{D}. \tag{2.29}$$

These scales can be used as a rule-of-thumb estimate for when or where certain events take place. For instance, for a point source released in the middle of a region of width L and bounded at $\pm L/2$ by impermiable boundaries, the time required before the cloud can be considered well-mixed over the region by diffusion is $t_{m,d} = L^2/(8D)$. The coefficient value 8 is derived by requiring that the concentration at $\pm L/2$ be at least 97% of the maximum concentration C_{max}. These characteristic scales (easily derivable through dimensional analysis) should be memorized and used extensively to get a rough solution to transport problems.

2.2 Solutions to the advective diffusion equation

In the previous chapter we presented a detailed solution for an instantaneous point source in a stagnant ambient. In nature, initial and boundary conditions can be much different from that idealized case, and this section presents a few techniques to deal with other general cases. Just as advection and diffusion are additive, we will also show that superpostion can be used to build up solutions to complex geometries or initial conditions from a base set of a few general solutions.

The solutions in this section parallel a similar section in Fischer et al. (1979). Appendix B presents analytical solutions for other initial and boundary conditions, primarily obtained by extending the techniques discussed in this section. Taken together, these solutions can be applied to a wide range of problems.

2.2.1 Initial spatial concentration distribution

A good example of the power of superposition is the solution for an initial spatial concentration distribution. Since advection can always be included by changing the frame of reference, we will consider the one-dimensional stagnant case. Thus, the governing equation is

$$\frac{\partial C}{\partial t} = D\frac{\partial^2 C}{\partial x^2}. \tag{2.30}$$

We will consider the homogeneous initial distribution, given by

$$C(x, t_0) = \begin{cases} C_0 \text{ if } x \le 0 \\ 0 \ \text{ if } x > 0 \end{cases} \tag{2.31}$$

where $t_0 = 0$ and C_0 is the uniform initial concentration, as depicted in Figure 2.3. At a point $x = \xi < 0$ there is an infinitesimal mass $dM = C_0 A d\xi$, where A is the cross-sectional area $\delta y \delta z$. For $t > 0$, the concentration at any point x is due to the diffusion of mass from all the differential elements dM. The contribution dC for a single element dM is just the solution of (2.30) for an instantaneous point source

$$dC(x, t) = \frac{dM}{A\sqrt{4\pi Dt}} \exp\left(-\frac{(x-\xi)^2}{4Dt}\right), \tag{2.32}$$

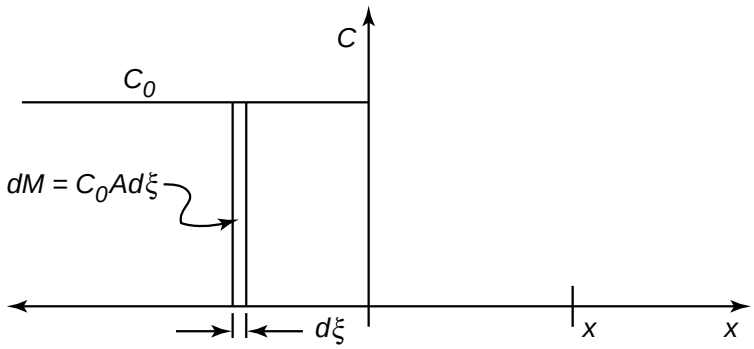

Fig. 2.3. Schematic of an instantaneous initial concentration distribution showing the differential element dM at the point $-\xi$.

and by virtue of superposition, we can sum up all the contributions dM to obtain

$$C(x,t) = \int_{-\infty}^{0} \frac{C_0 d\xi}{\sqrt{4\pi Dt}} \exp\left(-\frac{(x-\xi)^2}{4Dt}\right) \tag{2.33}$$

which is the superposition solution to our problem. To compute the integral, we must, as usual, make a change of variables. The new variable ζ is defined as follows

$$\zeta = \frac{x-\xi}{\sqrt{4Dt}} \tag{2.34}$$

$$d\zeta = -\frac{d\xi}{\sqrt{4Dt}}. \tag{2.35}$$

Substituting ζ into the integral solution gives

$$C(x,t) = \frac{C_0}{\sqrt{\pi}} \int_{\infty}^{x/\sqrt{4Dt}} -\exp(-\zeta^2) d\zeta. \tag{2.36}$$

Note that to obtain the upper bound on the integral we set $\xi = 0$ in the definition for ζ given in (2.34). Rearranging the integral gives

$$C(x,t) = \frac{C_0}{\sqrt{\pi}} \int_{x/\sqrt{4Dt}}^{\infty} \exp(-\zeta^2) d\zeta \tag{2.37}$$

$$= \frac{C_0}{\sqrt{\pi}} \left[\int_0^{\infty} \exp(-\zeta^2) d\zeta - \int_0^{x/\sqrt{4Dt}} \exp(-\zeta^2) d\zeta \right]. \tag{2.38}$$

The first of the two integrals can be solved analytically—from a table of integrals, its solution is $\sqrt{\pi}/2$. The second integral is the so called error function, defined as

$$\mathrm{erf}(\varphi) = \frac{2}{\sqrt{\pi}} \int_0^{\varphi} \exp(-\zeta^2) d\zeta. \tag{2.39}$$

Solutions to the error function are generally found in tables or as built-in functions in a spreadsheet or computer programming language. Hence, our solution can be written as

$$C(x,t) = \frac{C_0}{2} \left(1 - \mathrm{erf}\left(\frac{x}{\sqrt{4Dt}}\right)\right). \tag{2.40}$$

Figure 2.4 plots this solution for $C_0 = 1$ and for increasing times t.

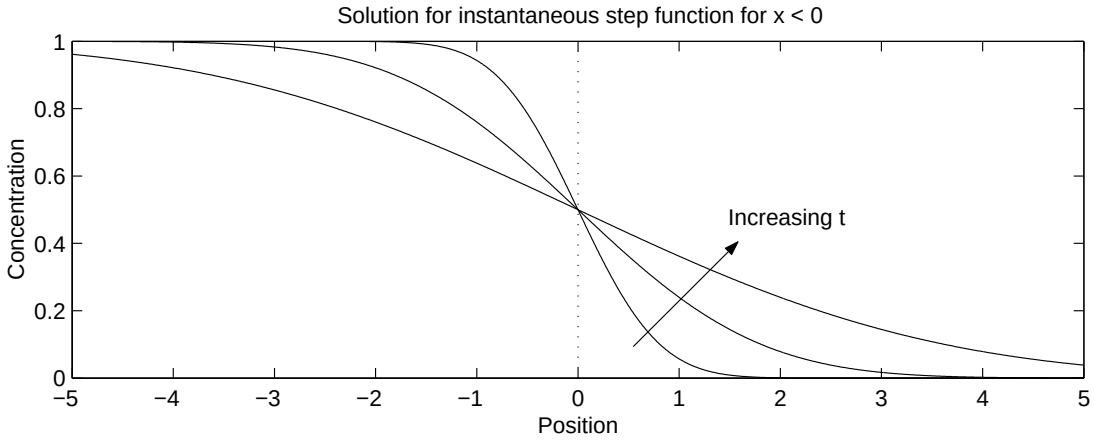

Fig. 2.4. Solution (2.40) for an instantaneous initial concentration distribution given by (2.31) with $C_0 = 1$.

Example Box 2.1:
Diffusion of an intravenous injection.

A doctor administers an intravenous injection of an allergy fighting medicine to a patient suffering from an allergic reaction. The injection takes a total time T. The blood in the vein flows with mean velocity u, such that blood over a region of length $L = uT$ contains the injected chemical; the concentration of chemical in the blood is C_0 (refer to the following sketch).

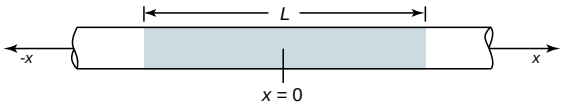

What is the distribution of chemical in the vein when it reaches the heart 75 s later?

This problem is an initial spatial concentration distribution, like the one in Section 2.2.1. Take the point $x = 0$ at the middle of the distribution and let the coordinate system move with the mean blood flow velocity u. Thus, we have the initial concentration distribution

$$C(x, t_0) = \begin{cases} C_0 \text{ if } -L/2 < x < L/2 \\ 0 \quad \text{otherwise} \end{cases}$$

where $t_0 = 0$ at the time $T/2$.

Following the solution method in Section 2.2.1, the superposition solution is

$$C(x,t) = \int_{-L/2}^{L/2} \frac{C_0 d\xi}{\sqrt{4\pi D t}} \exp\left(-\frac{(x-\xi)^2}{4Dt}\right)$$

which can be expanded to give

$$C(x,t) = \frac{C_0}{\sqrt{4\pi D t}} \cdot \left[\int_{-\infty}^{L/2} \exp\left(-\frac{(x-\xi)^2}{4Dt}\right) d\xi - \int_{-\infty}^{-L/2} \exp\left(-\frac{(x-\xi)^2}{4Dt}\right) d\xi\right].$$

After substituting the coordinate transformation in (2.34) and simplifying, the solution is found to be

$$C(x,t) = \frac{C_0}{2}\left(\text{erf}\left(\frac{x+L/2}{\sqrt{4Dt}}\right) - \text{erf}\left(\frac{x-L/2}{\sqrt{4Dt}}\right)\right).$$

Substituting $t = 75$ s gives the concentration distribution when the slug of medicine reaches the heart.

2.2.2 Fixed concentration

Another common situation is a fixed concentration at some point x_1. This could be, for example, the oxygen concentration at the air-water interface. The parameters governing the solution are the fixed concentration C_0, the diffusion coefficient D, and the coordinates $(x - x_0)$, and t. Again, we will neglect advection since we can include it through a change of variables, and we

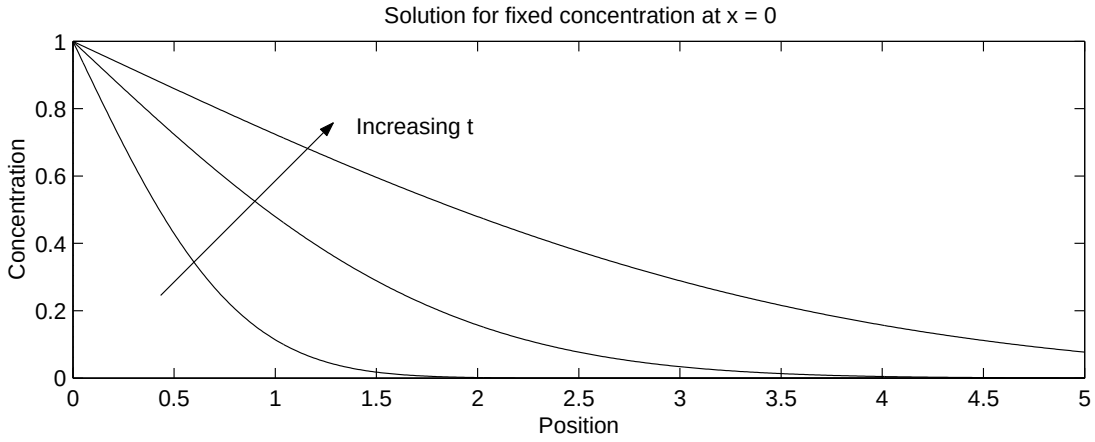

Fig. 2.5. Solution (2.43) for a fixed concentration at $x = 0$ of $C_0 = 1$.

will take $x_0 = 0$ for simplicity. As we did for a point source, we form a similarity solution from the governing variables, which gives us the solution form

$$C(x,t) = C_0 f\left(\frac{x}{\sqrt{Dt}}\right). \tag{2.41}$$

If we define the similarity variable $\eta = x/\sqrt{Dt}$ and substitute it into (2.30) we obtain, as expected, an ordinary differential equation in f and η, given by

$$\frac{d^2 f}{d\eta^2} + \frac{\eta}{2}\frac{df}{d\eta} = 0 \tag{2.42}$$

with boundary conditions $f(0) = 1$ and $f(\infty) = 0$. Unfortunately, our ordinary differential equation is non-linear. A quick look at Figure 2.4, however, might help us guess a solution. The point at $x = 0$ has a fixed concentration of $C_0/2$. If we substitute C_0 as the leading coefficient in (2.40) (instead of $C_0/2$), maybe that would be the solution. Substitution into the differential equation (2.42) and its boundary conditions proves, indeed, that the solution is correct, namely

$$C(x,t) = C_0\left(1 - \operatorname{erf}\left(\frac{x}{\sqrt{4Dt}}\right)\right) \tag{2.43}$$

is the solution we seek. Figure 2.5 plots this solution for $C_0 = 1$. Important note: this solution is *only* valid for $x > x_0$.

2.2.3 Fixed, no-flux boundaries

The final situation we examine in this section is how to incorporate no-flux boundaries. No-flux boundaries are any surface that is impermeable to the contaminant of interest. The discussion in this section assumes that no chemical reactions occur at the surface and that the surface is completely impermeable.

As you might expect, we first need to find a way to specify a no-flux boundary as a boundary condition to the governing differential equation. This is done easily using Fick's law. Since no-flux means that $\boldsymbol{q} = 0$ (and taking D as constant), the boundary conditions can be expressed

Example Box 2.2:
Dissolving sugar in coffee.

On a cold winter's day you pour a cup of coffee and add 2 g of sugar evenly distributed over the bottom of the coffee cup. The diameter of the cup is 5 cm; its height is 7 cm. If you do not stir the coffee, when does the concentration boundary layer first reach the top of the cup and when does all of the sugar dissolve? How would these answers change if you stir the coffee?

The concentration of sugar is fixed at the saturation concentration at the bottom of the cup and is initially zero everywhere else. These are the same conditions as for the fixed concentration solution; thus, the sugar distribution at height z above the bottom of the cup is

$$C(z,t) = C_0\left(1 - \text{erf}\left(\frac{z}{\sqrt{4Dt}}\right)\right).$$

The characteristic height of the concentration boundary layer is proportional to $\sigma = \sqrt{2Dt}$. Assume the concentration boundary layer first reaches the top of the cup when $2\sigma = h = 7$ cm. Solving for time gives

$$t_{mix,bl} = \frac{h^2}{8D}.$$

For an order-of-magnitude estimate, take $D \sim 10^{-9}$ m^2/s, giving

$$t_{mix,bl} \approx 6 \cdot 10^5 \text{ s}.$$

To determine how long it takes for the sugar to dissolve, we must compute the mass flux of sugar at $z = 0$. We already computed the derivative of the error function in Example Box 1.1. The mass flux of sugar at $z = 0$ is then

$$\dot{m}(0,t) = \frac{ADC_{sat}}{\sqrt{\pi Dt}}$$

where A is the cross-sectional area of the cup. The total amount of dissolved sugar M_d is the time-integral of the mass flux

$$M_d = \int_0^t \frac{ADC_{sat}}{\sqrt{\pi D\tau}} d\tau$$

Integrating and solving for time gives

$$t_d = \frac{M_d^2 \pi}{4A^2 DC_{sat}^2}$$

where t_d is the time it takes for the mass M_d to dissolve. This expression is only valid for $t < t_{mix,bl}$; for times beyond $t_{mix,bl}$, we must account for the boundary at the top of the cup. Assuming $C_{sat} = 0.58$ g/cm^3, the time needed to dissolve all the sugar is

$$t_d = 5 \cdot 10^4 \text{ s}.$$

By stirring, we effectively increase the value of D. Since D is in the denominator of each of these time estimates, we shorten the time for the sugar to dissolve and mix throughout the cup.

as

$$\begin{aligned} \boldsymbol{q}|_{S_b} \cdot \boldsymbol{n} &= 0 \\ \left(\frac{\partial C}{\partial x}, \frac{\partial C}{\partial y}, \frac{\partial C}{\partial z}\right)\Big|_{S_b} \cdot \boldsymbol{n} &= 0 \end{aligned} \tag{2.44}$$

where S_b is the function describing the boundary surface (i.e. $S_b = f(x,y)$) and $\boldsymbol{n}$ is the unit vector normal to the no-flux boundary. In the one-dimensional case, the no-flux boundary condition reduces to

$$\frac{\partial C}{\partial x}\Big|_{x_b} = 0, \tag{2.45}$$

where x_b is the boundary location. This property is very helpful in interpreting concentration measurements to determine whether a boundary, for instance, the lake bottom, is impermeable or not.

To find a solution to a bounded problem, consider an instantaneous point source injected at x_0 with a no-flux boundary a distance L to the right as shown in Figure 2.6. Our standard solution allows mass to diffuse beyond the no-flux boundary (as indicated by the dashed line in

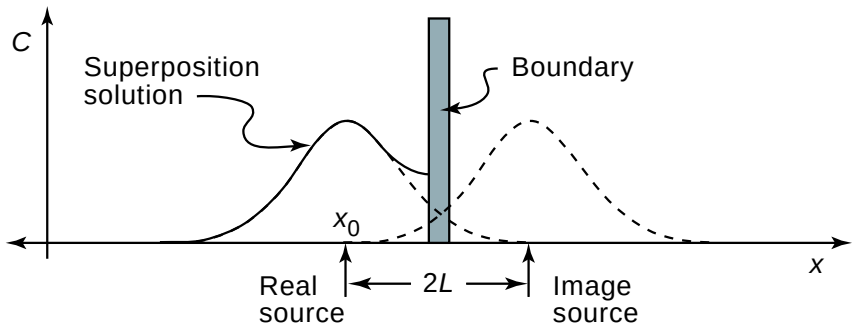

Fig. 2.6. Schematic of a no-flux boundary with real instantaneous point source to the left and an imaginary source to the right. The dotted lines indicate the individual contributions from the two sources; the solid line indicates the superposition solution.

the figure). To replace this lost mass, an image source (imaginary source) is placed to the right of the boundary, such that it leaks the same amount of mass back to left of the boundary as our standard solution leaked to the right. Superposing (adding) these two solutions gives us the desired no-flux behavior at the wall. The image source is placed L to the right of the boundary, and the solution is

$$C(x,t) = \frac{M}{A\sqrt{4\pi Dt}} \left(\exp\left(-\frac{(x-x_0)^2}{4Dt} \right) + \exp\left(-\frac{(x-x_i)^2}{4Dt} \right) \right) \tag{2.46}$$

where $x_i = x_0 + 2L$. Naturally, the solution given here is only valid to the left of the boundary. To the right of the boundary, the concentration is everywhere zero. Compute the concentration gradient $\partial C/\partial x$ at $x = 0$ to prove to yourself that the no-flux boundary condition is satisfied.

The method of images becomes more complicated when multiple boundaries are concerned. This is because the mass diffusing from the image source on the right eventually will penetrate a boundary on the left and need its own image source. In general, when there are two boundaries, an infinite number of image sources is required. In practice, the solution usually converges after only a few image sources have been included (Fischer et al. 1979). For the case of an instantaneous point source at the origin with boundaries at $\pm L$, Fischer et al. (1979) give the image source solution

$$C(x,t) = \frac{M}{A\sqrt{4\pi Dt}} \sum_{n=-\infty}^{\infty} \exp\left(-\frac{(x+2nL)^2}{4Dt} \right). \tag{2.47}$$

Obviously, the number of image sources required for the solution to converge depends on the time scale over which the solution is to be valid. These techniques will become more clear in the following examples and remaining chapters.

2.3 Application: Diffusion in a Lake

We return here to the application of arsenic contamination in a small lake presented in Chapter 1 (adapted from Nepf (1995)). After further investigation, it is determined that a freshwater spring flows into the bottom of the lake with a flow rate of 10 l/s.

Example Box 2.3:
Boundaries in a coffee cup.

In the previous example box we said that we have to account for the free surface boundary when the concentration boundary layer reaches the top of the coffee cup. Describe the image source needed to account for the free surface and state the image-source solution for the concentration distribution.

We can ignore the boundaries at the sides of the cup because sugar is evenly distributed on the bottom of the cup. This even distribution results in $\partial C/\partial x = \partial C/\partial y = 0$, which results in no net diffusive flux toward the cup walls.

To account for the free surface, though, we must add an image source with a fixed concentration of C_{sat} somewhere above the cup. Taking $z = 0$ at the bottom of the cup, the image source must be placed at $z = 2h$, where h is the depth of coffee in the cup.

Taking care that $C(z, \infty) \to C_{sat}$, the superposition solution for the sugar concentration distribution can be found to be

$$C(z,t) = C_{sat}\left(1 + \operatorname{erf}\left(\frac{2h}{\sqrt{4Dt}}\right) - \operatorname{erf}\left(\frac{z}{\sqrt{4Dt}}\right) - \operatorname{erf}\left(\frac{2h-z}{\sqrt{4Dt}}\right)\right).$$

Advection. Advection is due to the flow of spring water through the lake. Assuming the spring is not buoyant, it will spread out over the bottom of the lake and rise with a uniform vertical flux velocity (recall that z is positive downward, so the flow is in the minus z-direction)

$$\begin{aligned} v_a &= -Q/A \\ &= -5 \cdot 10^{-7} \text{ m/s}. \end{aligned} \tag{2.48}$$

The concentration of arsenic at the thermocline is 8 μg/l, which results in an advective flux of arsenic

$$\begin{aligned} q_a &= Cv_a \\ &= -4 \cdot 10^{-3} \ \mu\text{g}/(\text{m}^2\text{s}). \end{aligned} \tag{2.49}$$

Thus, advection caused by the spring results in a vertical advective flux of arsenic through the thermocline.

Discussion. Taking the turbulent and advective fluxes of arsenic together, the net vertical flux of arsenic through the thermocline is

$$\begin{aligned} J_z &= -4.00 \cdot 10^{-3} + 2.93 \cdot 10^{-3} \\ &= -1.10 \cdot 10^{-3} \ \mu\text{g}/(\text{m}^2\text{s}) \end{aligned} \tag{2.50}$$

where the minus sign indicates the net flux is upward. Thus, although the net diffusive flux is downward, the advection caused by the stream results in the net flux at the thermocline being upward. We can conclude that the arsenic source is likely at the bottom of the lake. The water above the thermocline will continue to increase in concentration until the diffusive flux at the thermocline becomes large enough to balance the advective flux through the lake, at which time the system will reach a steady state.

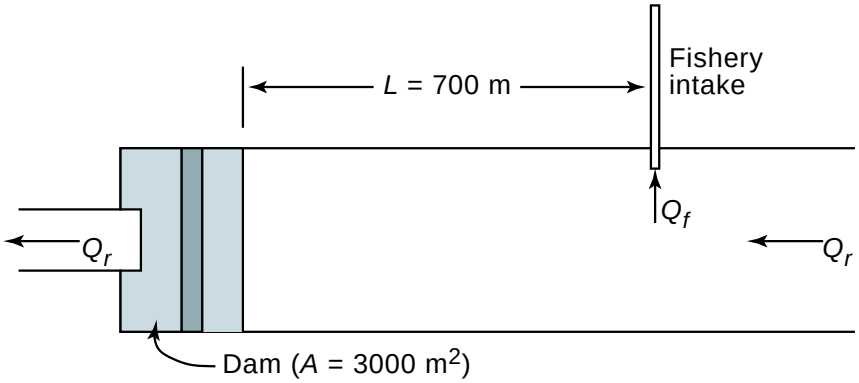

Fig. 2.7. Schematic diagram of the reservoir and fish farm intake for the copper contamination example.

2.4 Application: Fishery intake protection

As part of a renovation project, the face of a dam is to be treated with copper sulfate to remove unsightly algae build-up. A fish nursery derives its water from the reservoir upstream of the dam and has contracted you to determine if the project will affect their operations. Based on experience, the fish nursery can accept a maximum copper concentration at their intake of $1.5 \cdot 10^{-3}$ mg/l. Refer to Figure 2.7 for a schematic of the situation.

The copper sulfate is applied uniformly across the dam over a period of about one hour. Thus, we might model the copper contamination as an instantaneous source distributed evenly along the dam face. After talking with the renovation contractor, you determine that 1 kg of copper will be dissolved at the dam face. Because the project is scheduled for the spring turnover in the lake, the contaminant might be assumed to spread evenly in the vertical (dam cross-sectional area $A = 3000$ m^2). Based on a previous dye study, the turbulent diffusion coefficient was determined to be 2 m^2/s. The average flow velocity past the fishery intake is 0.01 m/s.

Advection or diffusion dominant. To evaluate the potential risks, the first step is to see how important diffusion is to the transport of copper in the lake. This is done through the Peclet number, giving

$$\begin{aligned} Pe &= \frac{D}{uL} \\ &= 0.3 \end{aligned} \tag{2.51}$$

which indicates diffusion is mildly important, and the potential for copper to migrate upstream remains.

Maximum concentration at intake. Because there is potential that copper will move upstream due to diffusion, the concentration of copper at the intake needs to be predicted. Taking the dam location at $x = 0$ and taking x positive downstream, the concentration at the intake is

$$C(x_i, t) = \frac{M}{A\sqrt{4\pi Dt}} \exp\left(-\frac{(x_i - ut)^2}{4Dt}\right). \tag{2.52}$$

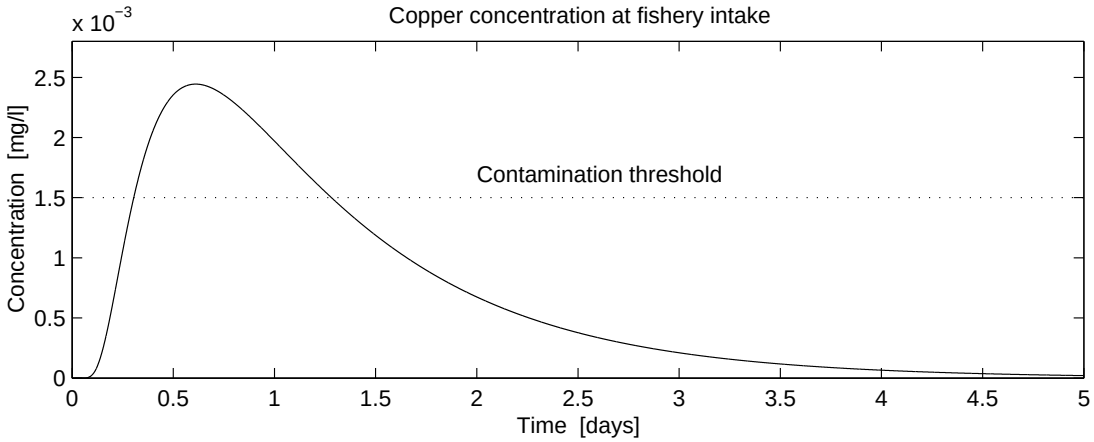

Fig. 2.8. Concentration of copper at the fishery intake as a function of time. The dotted line indicates the maximum allowable concentration of $1.5 \cdot 10^{-3}$ mg/l.

where x_i is the intake location (-700 m). Figure 2.8 shows the solution for the copper concentration at the intake from (2.52). From the figure, the maximum allowable concentration is expected to be exceeded for about 1 day between the times $t = 0.3$ and $t = 1.3$ days. The maximum copper concentration at the intake will be about $2.4 \cdot 10^{-3}$ mg/l. Thus, the fish farm will have to take precautions to prevent contamination. What other factors do you think could increase or decrease the likelihood of copper poisoning at the fish farm?

Summary

This chapter derived the advective diffusion equation using the method of superposition and demonstrated techniques to solve the resulting partial differential equation. Solutions for a stagnant ambient were shown to be easily modified to account for advection by solving in a moving reference frame. Solutions for distributed and fixed concentration distributions were presented, and the image-source method to account for no-flux boundaries was introduced. Engineering approximations should be made by evaluating the Peclet number and characteristic length and time scales of diffusion and advection.

Exercises

2.1 Superposition. If there are two point sources released simultaneously, how do you obtain the concentration field as a function of space and time? You need to prove why your particular method can be applied. If one point source is at $x = -L$ while the other is at $x = L$, what is the concentration at $x = 0$ (write the equation you would use to solve for C given D, M, A, and t)? Plot your result as a function of time with the values of D, M and A set as 1.0.

2.2 Integral evaluation. Define an appropriate coordinate transformation and show that

$$I = \frac{1}{\sqrt{\pi}} \int_{-\infty}^{4Dt+x^2/\sqrt{Dt}} 2x\sqrt{Dt} \exp\left(-\left(\frac{x^2}{\sqrt{Dt}} + 4Dt\right)^2\right) dx \tag{2.53}$$

can also be written as

$$I = \frac{Dt}{2}\left(\operatorname{erf}\left(\frac{x^2}{\sqrt{Dt}} + 4Dt\right) - 1\right) \tag{2.54}$$

2.3 Non-dimensionalization. Non-dimensionalize the three-dimensional diffusion equation and find the important parameter(s) in the equation. Use a single length scale for all three dimensions. Discuss your parameter(s) in a brief paragraph.

2.4 Peclet number. A river with cross section $A = 20$ m^2 has a flow rate of $Q = 1$ m^3/s. The effective mixing coefficient is $D = 1$ m^2/s. For what distance downstream is diffusion dominant? Where does advection become dominant? What is the length of stream where diffusion and advection have about equal influence?

2.5 Advection in a stream. To estimate the mixing characteristics of a small stream, a scientist injects 5 g of dye instantaneously and uniformly over the river cross section ($A = 5$ m^2) at the point $x = 0$. A measurement station is located 1 km downstream and records a river flow rate of $Q = 0.5$ m^3/s. In order to design the experiment, the scientist assumed that $D = 0.1$ m^2/s. Use this value to answer the following equations.

- The fluorometer used to measure the dye downstream at the measuring station has a detection limit of 0.1 μg/l. When does the measuring station first detect the dye cloud?
- When does the maximum dye concentration pass the measuring station, and what is this maximum concentration?
- After the maximum concentration passes the measuring station, the measured concentration decreases again. When is the measuring station no longer able to detect the dye?
- Why is the elapsed time between first detection and the maximum concentration different from the elapsed time between the last detection and the maximum concentration?

2.6 Fixed concentration. A beaker in a laboratory contains a solution with dissolved methane gas (CH_4). The concentration of methane in the atmosphere C_a is negligible; the concentration of methane in the uniformly-mixed portion of the beaker is C_w. The methane in the beaker dissolves out of the water and into the air, resulting in a fixed concentration at the water surface of $C_{ws} = 0$. Assume this process is limited by diffusion of methane through the water.

- Write an expression for the vertical concentration distribution of methane in the beaker. Assume the bottom boundary does not affect the profile (concentration at the bottom is C_w) and that methane is uniformly distributed in the horizontal (use the one-dimensional solution).
- Use the expression found above to find an expression for the flux of methane into the atmosphere through the water surface.

2.7 Concentration profiles. Figure 2.9 shows four concentration profiles measured very carefully at the bottom of four different lakes. For each profile, state whether the lake bottom is a no-flux or flux boundary and describe where you think the source is located and why.

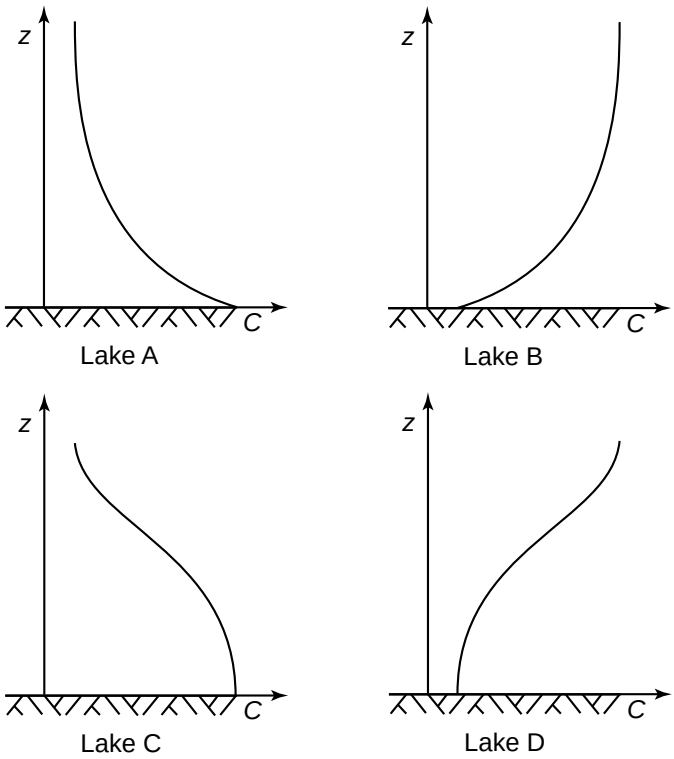

Fig. 2.9. Bottom concentration profiles for the four lakes in problem number 2.4.

2.8 Double point sources. To demonstrate the image-source method, a professor creates two instantaneous point sources of dye (three dimensional) a distance L apart and measures the concentration of dye at the point halfway between the two sources. Estimate the radius of the cloud for each point source by $r = 2\sigma$.

- Write an expression for the time t when the two sources first touch.
- Write an expression for the concentration distribution along the line connecting the two point sources.
- Differentiate this solution to show that the net flux through the measurement point along the axis of the two sources is zero.

2.9 The time-scale for a point source injected mid-way between two impermeable boundaries to become uniformly mixed across the section is given by the rule-of-thumb

$$t_m = \frac{L^2}{8D} \tag{2.55}$$

where L is the distance between the two boundaries and D is the diffusion coefficient. Referring to the sketch below, consider a line of dye released instantaneously along the centerline of a shallow river so that the problem can be treated as one-dimensional.

- Write a program applying the superposition method to calculate the relative concentration (relative to the centerline concentration of the river $C(x = 0, t)$) at the river bank $x = L/2$ as a function of time, that is, find the ratio $C(L/2, t)/C(0, t)$. The width of the river is L and the diffusion coefficient of the dye is D (please email me your final program).

- Plot your result with $C(L/2,t)/C(0,t)$ as the y-axis and $t/(L^2/D)$ as the x-axis using the values $L = 10$ m and $D = 0.01$ m^2/s.
- What is the relative concentration when $t = t_m$?

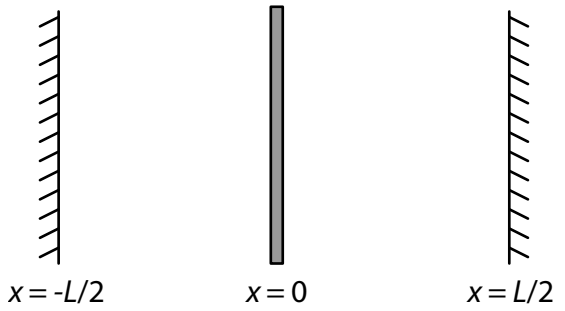

2.10 How is the three-dimensional point-source solution derived. You don't need to show the details of the derivation. Just explain the methodology with a minimum number of equations.

2.11 Smoke stack. A chemical plant has a smoke stack 75 m tall that discharges a continuous flux of carbon monoxide (CO) of 0.01 kg/s . The wind blows with a velocity of 1 m/s due east (from the west to the east) and the transverse turbulent diffusion coefficient is 4.5 m^2/s. Neglect longitudinal (downwind) diffusion.

- Write the unbounded solution for a continuous source in a cross wind.
- Add the appropriate image source(s) to account for the no-flux boundary at the ground and write the resulting image-source solution for concentration downstream of the release.
- Plot the two-dimensional concentration distribution downstream of the smoke stack for the plane 2 m above the ground.
- For radial distance r away from the smoke stack, where do the maximum concentrations occur?

2.12 Damaged smoke stack. After a massive flood, the smoke stack in the previous problem developed a leak at ground level so that all the exhaust exits at $z = 0$.

- How does this new release location change the location(s) of the image source(s)?
- Plot the maximum concentration at 2 m above the ground as a function of distance from the smoke stack for this damaged case.
- If a CO concentration of 1.0 μg/l of CO is dangerous, should the factory be closed until repairs are completed?

2.13 Boundaries in a boat arena. A boat parked in an arena has a sudden gasoline spill. The arena is enclosed on three sides, and the spill is located as shown in Figure 2.10. Find the locations of the first 11 most important image sources needed to account for the boundaries and incorporate them into the two-dimensional instantaneous point-source solution.

2.14 Image sources in a pipe. A point source is released in the center of an infinitely long round pipe. Describe the image source needed to account for the pipe walls.

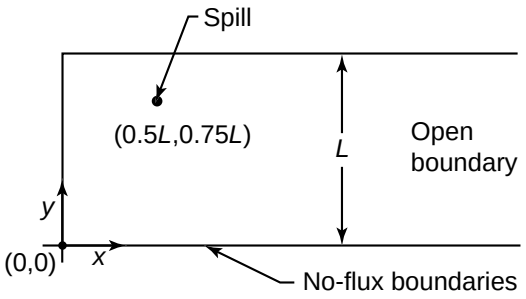

Fig. 2.10. Sketch of the boat arena and spill location for problem number 2.4.

2.15 Vertical mixing in a river. Wastewater from a chemical plant is discharged by a line diffuser perpendicular to the river flow and located at the bottom of the river. The river flow velocity is 15 cm/s and the river depth is 1 m.

- Find the locations of the first four most important image sources needed to account for the river bottom and the free surface.
- Write a spreadsheet program that computes the ratio of $C(x, z = h, t = x/u)$ to $C_{max}(t = x/u)$, where u is the flow velocity in the river and h is the water depth; $x = z = 0$ at the release location.
- Use the spreadsheet program to find the locations where the concentration ratio is 0.90, 0.95, and 0.98.
- From dimensional analysis we can write that the time needed for the injection to mix in the vertical is given by

$$t_{mix} = \frac{x_{mix}}{u} = \frac{h^2}{\alpha D} \tag{2.56}$$

  where D is the vertical diffusion coefficient. Compute the value of α for the criteria $C_{min}/C_{max} = 0.95$.
- Why is the value of α independent of D?

2.16 Mixing of joining rivers. One river (left) with a high concentration of sediment joins another river (right) with a negligible sediment concentration. The width of the low concentration river near their union is 40 m while the high concentration river is 80 m wide. Assume the river width and depth do not change much after the union, and both rivers are shallow and have the same velocity. At one particular day the mean velocity downstream of the union is 1 m/s and the diffusion coefficient is 0.1 m^2/s.

- Estimate the time required t_{mix} and the distance downstream x_{mix} until the low sediment concentration river is considered to be well-mixed with the sediment from the high concentration river. Use a relative concentration of 95% as the criteria for the well-mixed condition.
- If there is a water intake located on the low-sediment side of the river at 3 km downstream from the river union, do you expect the water taken from the intake to contain a significant amount of sediment? Justify your answer.

Table 2.1: Table of solutions to the diffusion equation

Schematic and Solution			
Instantaneous point source, infinite domain			
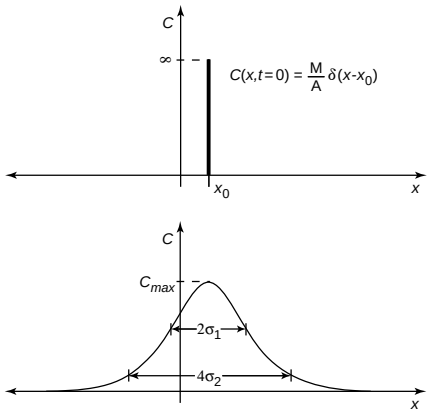	$C(x,t) = \frac{M}{A\sqrt{4\pi Dt}} \exp\left[-\frac{(x-x_0)^2}{4Dt}\right]$ $C_{max}(t) = \frac{M}{A\sqrt{4\pi Dt}}$ $q_x(x,t) = \frac{M(x-x_0)}{2At\sqrt{4\pi Dt}} \exp\left[-\frac{(x-x_0)^2}{4Dt}\right]$	Let $\sigma = \sqrt{2Dt}$ and $(2\sigma)^2 = 8Dt$. For $x_0 = 0$: $C(\pm\sigma, t) = 0.61C_{max}(t)$	Let $\sigma = \sqrt{2Dt}$ and $(4\sigma)^2 = 32Dt$. For $x_0 = 0$: $C(\pm 2\sigma, t) = 0.14C_{max}(t)$
Instantaneous distributed source, infinite domain			
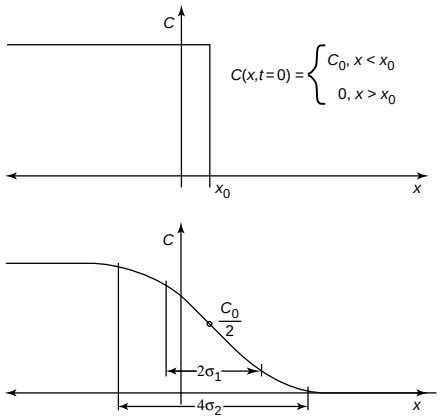	$C(x,t) = \frac{C_0}{2}\left[1 - \text{erf}\left[\frac{(x-x_0)}{\sqrt{4Dt}}\right]\right]$ $C_{max}(t) = C_0$ $q_x(x,t) = \frac{C_0\sqrt{D}}{\sqrt{4\pi t}} \exp\left[-\frac{(x-x_0)^2}{4Dt}\right]$	Let $\sigma = \sqrt{2Dt}$ and $(2\sigma)^2 = 8Dt$. For $x_0 = 0$: $C(+\sigma, t) = 0.16C_0$ $C(-\sigma, t) = 0.84C_0$	Let $\sigma = \sqrt{2Dt}$ and $(4\sigma)^2 = 32Dt$. For $x_0 = 0$: $C(+2\sigma, t) = 0.02C_0$ $C(-2\sigma, t) = 0.98C_0$

Table 2.1: (continued)

Schematic	Solution		
Fixed concentration, semi-infinite domain			
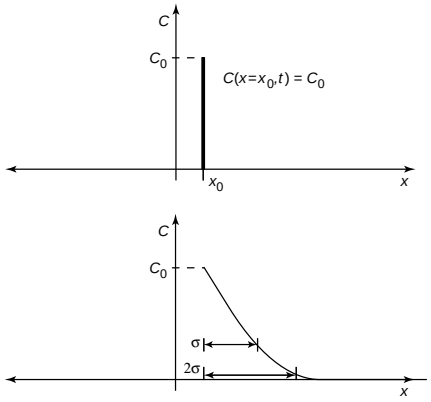	$C(x > x_0, t) = C_0 \left[1 - \text{erf}\left[\frac{(x - x_0)}{\sqrt{4Dt}}\right]\right]$ $C_{max}(t) = C_0$ $q_x(x > x_0, t) = \frac{2C_0\sqrt{D}}{\sqrt{4\pi t}} \exp\left[-\frac{(x - x_0)^2}{4Dt}\right]$	Let $\sigma = \sqrt{2Dt}$ and $\sigma^2 = 2Dt$. For $x_0 = 0$: $C(+\sigma, t) = 0.32C_0$ $C(-\sigma, t) =$ Undefined	Let $\sigma = \sqrt{2Dt}$ and $(2\sigma)^2 = 8Dt$. For $x_0 = 0$: $C(+2\sigma, t) = 0.05C_0$ $C(-2\sigma, t) =$ Undefined
Instantaneous point source, bounded domain			
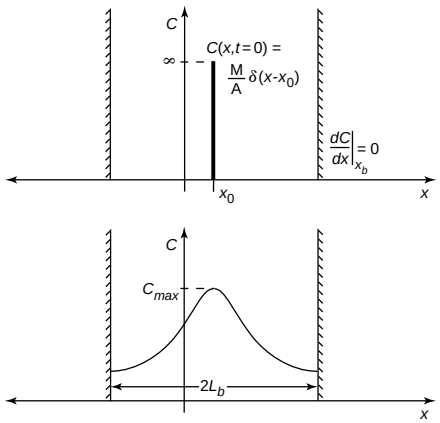	$C(x,t) = \frac{M}{A\sqrt{4\pi Dt}} \sum_{n=-\infty}^{\infty} \exp\left[-\frac{(x - x_0 + 2nL_b)^2}{4Dt}\right]$ $C_{max}(t) = \frac{M}{A\sqrt{4\pi Dt}} \sum_{n=-\infty}^{\infty} \exp\left[-\frac{(2nL_b)^2}{4Dt}\right]$ $q_x(x,t) = \frac{M}{2At\sqrt{4\pi Dt}} \sum_{n=-\infty}^{\infty} (x - x_0 + 2nL_b) \exp\left[-\frac{(x - x_0 + 2nL_b)^2}{4Dt}\right]$	Using the image-source method, the first image on the opposite side of the boundary is at $x_0 \pm 2L_b$.	

Table 2.1: (continued)

Schematic	Solution		
Instantaneous 2-D point source, infinite domain			
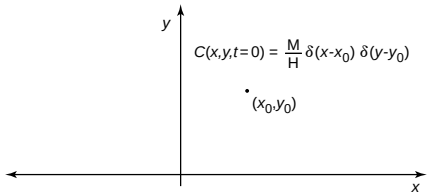 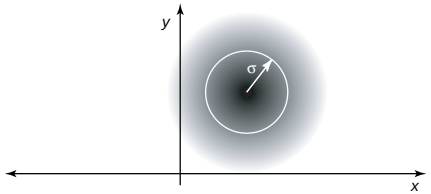	$C(x,y,t) = \frac{M}{4\pi Ht\sqrt{D_x D_y}} \exp\left[-\frac{(x-x_0)^2}{4D_x t} - \frac{(y-y_0)^2}{4D_y t}\right]$ $C_{max}(t) = \frac{M}{4\pi Ht\sqrt{D_x D_y}}$ $\boldsymbol{q}(x,y,t) = \frac{M}{8\pi Ht^2\sqrt{D_x D_y}} \exp\left[-\frac{(x-x_0)^2}{4D_x t} - \frac{(y-y_0)^2}{4D_y t}\right]((x-x_0)\boldsymbol{i} + (y-y_0)\boldsymbol{j})$	Let $D_x = D_y$,$\sigma = \sqrt{2Dt}$, $(2\sigma)^2 = 8Dt$, and $r^2 = (x-x_0)^2 + (y-y_0)^2$. For $r = \sigma$: $C(\sigma,t) = 0.61C_{max}(t)$	Let $D_x = D_y$, $\sigma = \sqrt{2Dt}$, $(4\sigma)^2 = 32Dt$, and $r^2 = (x-x_0)^2 + (y-y_0)^2$. For $r = 2\sigma$: $C(2\sigma,t) = 0.14C_{max}(t)$
Instantaneous 3-D point source, infinite domain			
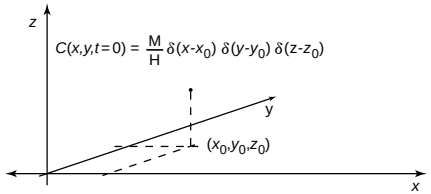 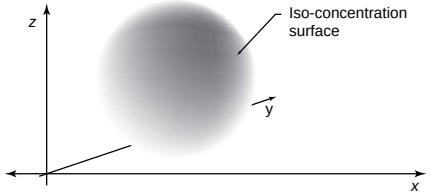	$C(x,y,z,t) = \frac{M}{4\pi t\sqrt{4\pi t D_x D_y D_z}} \exp\left[-\frac{(x-x_0)^2}{4D_x t} - \frac{(y-y_0)^2}{4D_y t} - \frac{(z-z_0)^2}{4D_z t}\right]$ $C_{max}(t) = \frac{M}{4\pi t\sqrt{4\pi t D_x D_y D_z}}$ $\boldsymbol{q}(x,y,z,t) = \frac{M}{8\pi t^2\sqrt{4\pi t D_x D_y D_z}} \exp\left[-\frac{(x-x_0)^2}{4D_x t} - \frac{(y-y_0)^2}{4D_y t} - \frac{(z-z_0)^2}{4D_z t}\right] \cdot ((x-x_0)\boldsymbol{i} + (y-y_0)\boldsymbol{j} + (z-z_0)\boldsymbol{k})$	Let $D_x = D_y = D_z$, $\sigma = \sqrt{2Dt}$, $(2\sigma)^2 = 8Dt$, and $r^2 = (x-x_0)^2 + (y-y_0)^2 + (z-z_0)^2$. For $r = \sigma$: $C(\sigma,t) = 0.61C_{max}(t)$	Let $D_x = D_y = D_z$, $\sigma = \sqrt{2Dt}$, $(4\sigma)^2 = 32Dt$, and $r^2 = (x-x_0)^2 + (y-y_0)^2 + (z-z_0)^2$. For $r = 2\sigma$: $C(2\sigma,t) = 0.14C_{max}(t)$

3. Mixing in Rivers: Turbulent Diffusion and Dispersion

In previous chapters we considered the processes of advection and molecular diffusion and have seen some example problems with so called "turbulent diffusion" coefficients, where we use the same governing equations, but with larger diffusion (mixing) coefficients. In natural rivers, a host of processes lead to a non-uniform velocity field, which allows mixing to occur much faster than by molecular diffusion alone. In this chapter, we formally derive the equations for non-uniform velocity fields to demonstrate their effects on mixing. First, we consider the effect of a random, turbulent velocity field. Second, we consider the combined effects of diffusion (molecular or turbulent) with a shear velocity profile to develop equations for dispersion. In each case, the resulting equations retain their previous form, but the mixing coefficients are orders of magnitude greater than the molecular diffusion coefficients.

We start by giving a description of turbulence and its effects on the transport of contaminants. We then derive a new advective diffusion equation for turbulent flow and show why turbulence can be described by the regular advective diffusion equation derived previously, but using larger turbulent diffusion coefficients. We then look at the effect of a shear velocity profile on the transport of contaminants and derive one-dimensional equations for longitudinal dispersion. This chapter concludes with a common dye study application to compute the effective mixing coefficients in rivers.

3.1 Turbulence and mixing

In the late 1800's, Reynolds performed a series of experiments on the transport of dye streaks in pipe flow. These were the pioneering observations of turbulence, and his analysis is what gives the Re number its name. It is interesting to realize that the first contribution to turbulence research was in the area of contaminant transport (the behavior of dye streaks); therefore, we can assume that turbulence has an important influence on transport. In his paper, Reynolds (1883) wrote (taken from Acheson (1990)):

> The experiments were made on three tubes. They were all about 4 feet 6 inches [1.37 m] long, and fitted with trumpet mouthpieces, so that water might enter without disturbance. The water was drawn through the tubes out of a large glass tank, in which the tubes were immersed, arrangements being made so that a streak or streaks of highly colored water entered the tubes with the clear water.
>
> The general results were as follows:

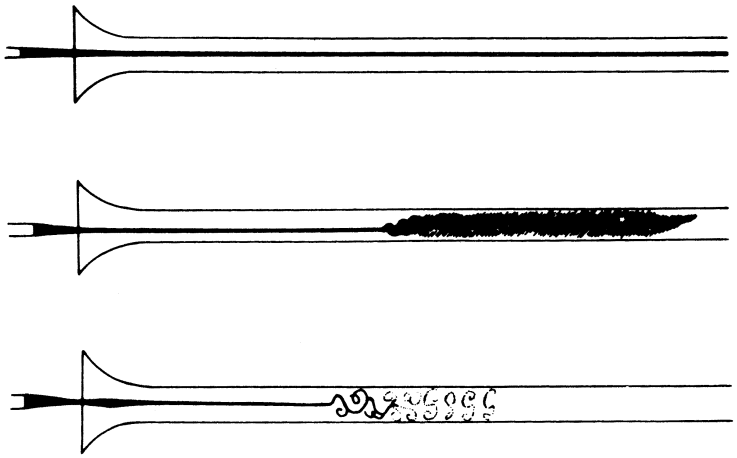

Fig. 3.1. Sketches from Reynolds (1883) showing laminar flow (top), turbulent flow (middle), and turbulent flow illuminated with an electric spark (bottom). Taken from Acheson (1990).

1. When the velocities were sufficiently low, the streak of colour extended in a beautiful straight line through the tube.
2. If the water in the tank had not quite settled to rest, at sufficiently low velocities, the streak would shift about the tube, but there was no appearance of sinuosity.
3. As the velocity was increased by small stages, at some point in the tube, always at a considerable distance from the trumpet or intake, the color band would all at once mix up with the surrounding water, and fill the rest of the tube with a mass of colored water. Any increase in the velocity caused the point of break down to approach the trumpet, but with no velocities that were tried did it reach this. On viewing the tube by the light of an electric spark, the mass of color resolved itself into a mass of more or less distinct curls, showing eddies.

Figure 3.1 shows the schematic drawings of what Reynolds saw, taken from his paper.

The first case he describes, the one with low velocities, is laminar flow: the fluid moves in parallel layers along nearly perfect lines, and disturbances are damped by viscosity. The only way that the dye streak can spread laterally in the laminar flow is through the action of molecular diffusion; thus, it would take a much longer pipe before molecular diffusion could disperse the dye uniformly across the pipe cross-section (what rule of thumb could we use to determine the required length of pipe?).

The latter case, at higher velocities, is turbulent flow: the fluid becomes suddenly unstable and develops into a spectrum of eddies, and these disturbances grow due to instability. The dye, which more or less follows the fluid passively, is quickly mixed across the cross-section as the eddies grow and fill the tube with turbulent flow. The observations with an electric spark indicate that the dye conforms to the shape of the eddies. After some time, however, the eddies will have grown and broken enough times that the dye will no longer have strong concentration gradients that outline the eddies: at that point, the dye is well mixed and the mixing is more or less random (even though it is still controlled by discrete eddies).

Reynolds summarized his results by showing that these characteristics of the flow were dependent on the non-dimensional number $Re = UL/\nu$, where U is the mean pipe flow velocity, L the pipe diameter and ν the kinematic viscosity, and that turbulence occurred at higher values of Re. The main consequence of turbulence is that it enhances momentum and mass transport.

3.1.1 Mathematical descriptions of turbulence

Much research has been conducted in the field of turbulence. The ideas summarized in the following can be found in much greater detail in the treatises by Lumley & Panofsky (1964), Pope (2000), and Mathieu & Scott (2000).

In this section we will consider a special kind of turbulence: homogeneous turbulence. The term homogeneous means that the statistical properties of the flow are steady (unchanging)—the flow can still be highly irregular. These homogeneous statistical properties are usually described by properties of the velocity experienced at a point in space in the turbulent flow (this is an Eulerian description). To understand the Eulerian properties of turbulence, though, it is useful to first consider a Lagrangian frame of reference and follow a fluid particle.

In a turbulent flow, large eddies form continuously and break down into smaller eddies so that there is always a spectrum of eddy sizes present in the flow. As a large eddy breaks down into multiple smaller eddies, very little kinetic energy is lost, and we say that energy is efficiently transferred through a cascade of eddy sizes. Eventually, the eddies become small enough that viscosity takes over, and the energy is damped out and converted into heat. This conversion of kinetic energy to heat at small scales is called dissipation and is designated by

$$\epsilon = \frac{\text{dissipated kinetic energy}}{\text{time}} \tag{3.1}$$

which has the units $[L^2/T^3]$. Since the kinetic energy is efficiently transferred down to these small scales, the dissipated kinetic energy must equal the total turbulent kinetic energy of the flow: this means that production and dissipation of kinetic energy in a homogeneous turbulent flow are balanced.

The length scale of the eddies in which turbulent kinetic energy is converted to heat is called the Kolmogorov scale L_K. How large is L_K? We use dimensional analysis to answer this question and recognize that L_K depends on the rate of dissipation (or, equivalently, production) of energy, ϵ, and on the viscosity, ν, since friction converts the kinetic energy to heat. Forming a length scale from these parameters, we have

$$L_K \propto \frac{\nu^{3/4}}{\epsilon^{1/4}}. \tag{3.2}$$

This is an important scale in turbulence.

Summarizing the Lagrangian perspective, if we follow a fluid particle, it may begin by being swept into a large eddy, and then will move from eddy to eddy as the eddies break down, conserving kinetic energy in the cascade. Eventually, the particle finds itself in a small enough eddy (one of order L_K in size), that viscosity dissipates its kinetic energy into heat. This small eddy is also a part of a larger eddy; hence, all sizes of eddies are present at all times in the flow.

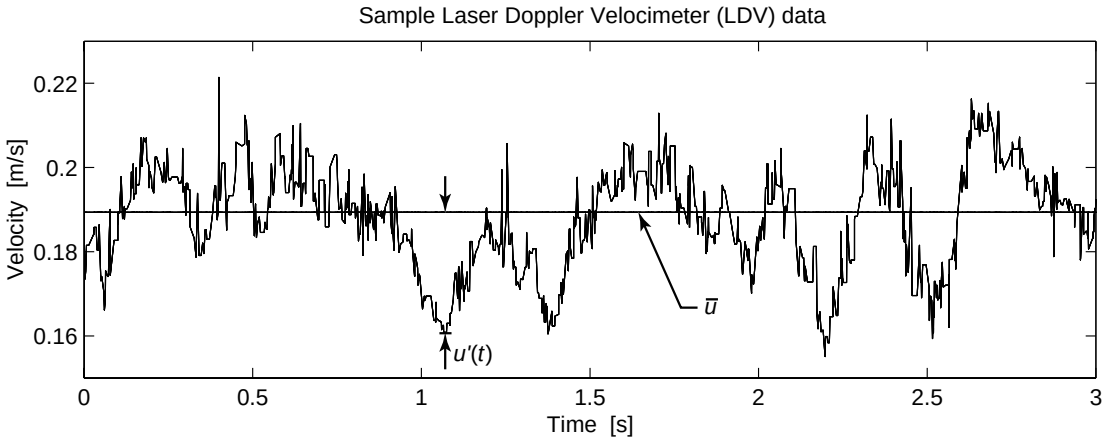

Fig. 3.2. Schematic measurement of the turbulent fluctuating velocity at a point showing the average velocity, $\overline{u}$ and the fluctuating component, $u'(t)$.

Because it is so difficult to follow a fluid particle with a velocity probe (this is what we try to do with Particle Tracking Velocimetry (PTV)), turbulent velocity measurements are usually made at a point, and turbulence is described by an Eulerian reference frame. The spectrum of eddies pass by the velocity probe, transported with the mean flow velocity. Large eddies produce long-period velocity fluctuations in the velocity measurement, and small eddies produce short-period velocity fluctuations, and all these scales are present simultaneously in the flow. Figure 3.2 shows an example of a turbulent velocity measurement for one velocity component at a point. If we consider a short portion of the velocity measurement, the velocities are highly correlated and appear deterministic. If we compare velocities further apart in the time-series, the velocities become completely uncorrelated and appear random. The time-scale at which velocities begin to appear uncorrelated and random is called the integral time scale t_I. In the Lagrangian frame, this is the time it takes a parcel of water to forget its initial velocity. This time scale can also be written as a characteristic length and velocity, giving the integral scales u_I and l_I.

Reynolds suggested that at some time longer than t_I, the velocity at a point x_i could be decomposed into a mean velocity $\overline{u_i}$ and a fluctuation u_i' such that

$$u_i(x_i, t) = \overline{u_i}(x_i) + u_i'(x_i, t), \tag{3.3}$$

and this treatment of the velocity is called Reynolds decomposition. t_I is, then, comparable to the time it takes for $\overline{u_i}$ to become steady (constant).

One other important descriptor of turbulence is the root-mean-square velocity

$$u_{rms} = \sqrt{\overline{u'u'}} \tag{3.4}$$

which, since kinetic energy is proportional to a velocity squared, is a measure of the turbulent kinetic energy of the flow (i.e. the mean flow kinetic energy is subtracted out since u' is just the fluctuation from the mean).

3.1.2 The turbulent advective diffusion equation

To derive an advective diffusion equation for turbulence, we substitute the Reynolds decomposition into the normal equation for advective diffusion and analyze the results. Before we can do that, we need a Reynolds decomposition analogy for the concentration, namely,

$$C(x_i,t) = \overline{C}(x_i) + C'(x_i,t). \tag{3.5}$$

Since we are only interested in the long-term (long compared to t_I) average behavior of a tracer cloud, after substituting the Reynolds decomposition, we will also take a time average. As an example, consider the time-average mass flux in the x-direction at our velocity probe, $\overline{uC}$:

$$\begin{aligned} q_x &= \overline{uC} \\ &= \overline{(\overline{u_i} + u_i')(\overline{C} + C')} \\ &= \overline{\overline{u_i}\overline{C}} + \overline{\overline{u_i}C'} + \overline{u_i'\overline{C}} + \overline{u_i'C'} \end{aligned} \tag{3.6}$$

where the over-bar indicates a time average

$$\overline{uC} = \frac{1}{t_I}\int_t^{t+t_I} uC\,d\tau. \tag{3.7}$$

For homogeneous turbulence, the average of the fluctuating velocities must be zero, $\overline{u_i'} = \overline{C'} = 0$, and we have

$$\overline{uC} = \overline{u_i C} + \overline{u_i' C'} \tag{3.8}$$

where we drop the double over-bar notation since the average of an average is just the average. Note that we cannot assume that the cross term $\overline{u_i' C'}$ is zero.

With these preliminary tools, we are now ready to substitute the Reynolds decomposition into the governing advective diffusion equation (with molecular diffusion coefficients) as follows

$$\begin{aligned} \frac{\partial C}{\partial t} + \frac{\partial u_i C}{\partial x_i} &= \frac{\partial}{\partial x_i}\left(D\frac{\partial C}{\partial x_i}\right) \\ \frac{\partial(\overline{C}+C')}{\partial t} + \frac{\partial(\overline{u_i}+u_i')(\overline{C}+C')}{\partial x_i} &= \frac{\partial}{\partial x_i}\left(D\frac{\partial(\overline{C}+C')}{\partial x_i}\right). \end{aligned} \tag{3.9}$$

Next, we integrate over the integral time scale t_I

$$\begin{aligned} \frac{1}{t_I}\int_t^{t+t_I}\left\{\frac{\partial(\overline{C}+C')}{\partial\tau} + \frac{\partial(\overline{u_i}+u_i')(\overline{C}+C')}{\partial x_i} = \frac{\partial}{\partial x_i}\left(D\frac{\partial(\overline{C}+C')}{\partial x_i}\right)\right\} d\tau \\ \frac{\partial(\overline{\overline{C}}+\overline{C'})}{\partial t} + \frac{\partial(\overline{\overline{u_i}\overline{C}} + \overline{\overline{u_i}C'} + \overline{u_i'\overline{C}} + \overline{u_i'C'})}{\partial x_i} = \frac{\partial}{\partial x_i}\left(D\frac{\partial(\overline{\overline{C}}+\overline{C'})}{\partial x_i}\right). \end{aligned} \tag{3.10}$$

Finally, we recognize that the terms $\overline{\overline{u_i}C'}$, $\overline{u_i'\overline{C}}$ and $\overline{C'}$ are zero, and, after moving the $\overline{u_i'C'}$-term to the right hand side, we are left with

$$\frac{\partial\overline{C}}{\partial t} + \overline{u_i}\frac{\partial\overline{C}}{\partial x_i} = -\frac{\partial\overline{u_i'C'}}{\partial x_i} + \frac{\partial}{\partial x_i}\left(D\frac{\partial\overline{C}}{\partial x_i}\right). \tag{3.11}$$

To utilize (3.11), we require a model for the term $\overline{u_i' C'}$. Since this term is of the form uC, we know that it is a mass flux. Since both components of this term are fluctuating, it must be a mass flux associated with the turbulence. Reynolds describes this turbulent component qualitatively as a form of rapid mixing; thus, we might make an analogy with molecular diffusion. Taylor (1921) derived part of this analogy by analytically tracking a cloud of tracer particles in a turbulent flow and calculating the Lagrangian autocorrelation function. His result shows that, for times greater than t_I, the cloud of tracer particles grows linearly with time. Rutherford (1994) and Fischer et al. (1979) use this result to justify an analogy with molecular diffusion, though it is worth pointing out that Taylor did not take the analogy that far. For the diffusion analogy model, the average turbulent diffusion time scale is $\Delta t = t_I$, and the average turbulent diffusion length scale is $\Delta x = u_I t_I = l_I$; hence, the model is only valid for times greater than t_I. Using a Fick's law type relationship for turbulent diffusion gives

$$\overline{u_i' C'} = D_t \frac{\partial \overline{C}}{\partial x_i} \tag{3.12}$$

with

$$\begin{aligned} D_t &= \frac{(\Delta x)^2}{\Delta t} \\ &= u_I l_I. \end{aligned} \tag{3.13}$$

Substituting this model for the average turbulent diffusive transport into (3.11) and dropping the over-bar notation gives

$$\frac{\partial C}{\partial t} + u_i \frac{\partial C}{\partial x_i} = \frac{\partial}{\partial x_i}\left(D_t \frac{\partial C}{\partial x_i}\right) + \frac{\partial}{\partial x_i}\left(D_m \frac{\partial C}{\partial x_i}\right). \tag{3.14}$$

As we will see in the next section, D_t is usually much greater than the molecular diffusion coefficient D_m; thus, the final term is typically neglected.

3.1.3 Turbulent diffusion coefficients in rivers

How big are turbulent diffusion coefficients? To answer this question, we need to determine what the coefficients depend on and use dimensional analysis.

For this purpose, consider a wide river with depth h and width $W \gg h$. An important property of three-dimensional turbulence is that the largest eddies are usually limited by the smallest spatial dimension, in this case, the depth. This means that turbulent properties in a wide river should be independent of the width, but dependent on the depth. Also, turbulence is thought to be generated in zones of high shear, which in a river would be at the bed. A parameter that captures the strength of the shear (and is also proportional to many turbulent properties) is the shear velocity u_* defined as

$$u_* = \sqrt{\frac{\tau_0}{\rho}} \tag{3.15}$$

where τ_0 is the bed shear and ρ is the fluid density. For uniform open channel flow, the shear friction is balanced by gravity, and

Example Box 3.1:
Turbulent diffusion in a room.

To demonstrate turbulent diffusion in a room, a professor sprays a point source of perfume near the front of a lecture hall. The room dimensions are 10 m by 10 m by 5 m, and there are 50 people in the room. How long does it take for the perfume to spread through the room by turbulent diffusion?

To answer this question, we need to estimate the air velocity scales in the room. Each person represents a heat source of 60 W; hence, the air flow in the room is dominated by convection. The vertical buoyant velocity w_* is, by dimensional analysis,

$$w_* = (BL)^{1/3}$$

where B is the buoyancy flux per unit area in $[L^2/T^3]$ and L is the vertical dimension of the room (here 5 m). The buoyancy of the air increases with temperature due to expansion. The net buoyancy flux per unit area is given by

$$B = \beta g \frac{H}{\rho c_v}$$

where β is the coefficient of thermal expansion (0.00024 K^{-1} for air), H is the heat flux per unit area, ρ is the density (1.25 kg/m^3 for air), and c_v is the specific heat at constant volume (1004 J/(Kg·K) for air).

For this problem,

$$H = \frac{50 \text{ pers.} \cdot 60 \text{ W/pers.}}{10^2 \text{ m}^2} = 30 \text{ W/m}^2.$$

This gives a unit area buoyancy flux of $5.6 \cdot 10^{-5}$ m^2/s^3 and a vertical velocity of $w_* = 0.07$ m/s.

We now have the necessary scales to estimate the turbulent diffusion coefficient from (3.13). Taking $u_I \propto w_*$ and $l_I \propto h$, where h is the height of the room,

$$D_t \propto w_* h \approx 0.35 \text{ m}^2/\text{s}$$

which is much greater than the molecular diffusion coefficient (compare to $D_m = 10^{-5}$ m^2/s in air). The mixing time can be taken from the standard deviation of the cloud width

$$t_{mix} \approx \frac{L^2}{D_t}.$$

For vertical mixing, $L = 5$ m, and t_{mix} is 1 minute; for horizontal mixing, $L = 10$ m, and t_{mix} is 5 minutes. Hence, it takes a few minutes (not just a couple seconds or a few hours) for the students to start to smell the perfume.

$$u_* = \sqrt{ghS} \tag{3.16}$$

where S is the channel slope. Arranging our two parameters (h and u_*) to form a diffusion coefficient gives

$$D_t \propto u_* h. \tag{3.17}$$

Because the velocity profile is much different in the vertical (z) direction as compared with the transverse (y) direction, D_t is not expected to be isotropic (i.e. it is not the same in all directions).

Vertical mixing. Vertical turbulent diffusion coefficients can be derived from the velocity profile (see Fischer et al. (1979)). For fully developed turbulent open-channel flow, it can be shown that the average turbulent log-velocity profile is given by

$$\overline{u_t}(z) = \overline{u} + \frac{u_*}{\kappa}(1 + \ln(z/h)) \tag{3.18}$$

where κ is the von Karman constant. Taking $\kappa = 0.4$, we obtain

$$D_{t,z} = 0.067 h u_*. \tag{3.19}$$

This relationship has been verified by experiments for rivers and for atmospheric boundary layers and can be considered accurate to ±25%.

Example Box 3.2:
Vertical mixing in a river.

A factory waste stream is introduced through a lateral diffuser at the bed of a river, as shown in the following sketch.

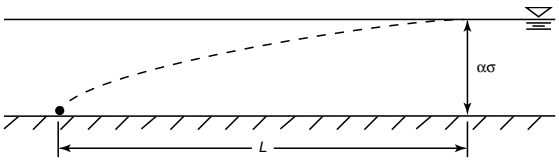

At what distance downstream can the injection be considered as fully mixed in the vertical?

The assumption of "fully mixed" can be defined as the condition where concentration variations over the cross-section are below a threshold criteria. Since the vertical domain has two boundaries, we have to use an image-source solution similar to (2.47) to compute the concentration distribution. The results can be summarized by determining the appropriate value of α in the relationship

$$h = \alpha\sigma$$

where h is the depth and σ is the standard deviation of the concentration distribution. Fischer et al. (1979) suggest $\alpha = 2.5$.

For vertical mixing, we are interested in the vertical turbulent diffusion coefficient, so we can write

$$h = 2.5\sqrt{2D_{t,z}t}$$

where t is the time required to achieve vertical mixing. Over the time t, the plume travels downstream a distance $L = \overline{u}t$. We can also make the approximation $u_* = 0.1\overline{u}$. Substituting these relationships together with (3.19) gives

$$h = 2.5\sqrt{2 \cdot 0.067h(0.1\overline{u})L/\overline{u}}.$$

Solving for L gives

$$L = 12h.$$

Thus, a bottom or surface injection in a natural stream can be treated as fully vertically mixed after a distance of approximately 12 times the channel depth.

Transverse mixing. On average there is no transverse velocity profile and mixing coefficients must be obtained from experiments. For a wealth of laboratory and field experiments reported in Fischer et al. (1979), the average transverse turbulent diffusion coefficient in a uniform straight channel can be taken as

$$D_{t,y} = 0.15hu_*. \tag{3.20}$$

The experiments indicate that the width plays some role in transverse mixing; however, it is unclear how that effect should be incorporated (Fischer et al. 1979). Transverse mixing deviates from the behavior in (3.20) primarily due to large, coherent lateral motions, which are really not properties of the turbulence in the first place. Based on the ranges reported in the experiments, (3.20) should be considered accurate to at best ±50%.

In natural streams, the cross-section is rarely of uniform depth, and the fall-line tends to meander. These two effects enhance transverse mixing, and for natural streams, Fischer et al. (1979) suggest the relationship

$$D_{t,y} = 0.6hu_*. \tag{3.21}$$

If the stream is slowly meandering and the side-wall irregularities are moderate, the coefficient in (3.21) is usually found in the range 0.4–0.8.

Longitudinal mixing. Since we assume there are no boundary effects in the lateral or longitudinal directions, longitudinal turbulent mixing should be equivalent to transverse mixing:

$$D_{t,x} = D_{t,y}. \tag{3.22}$$

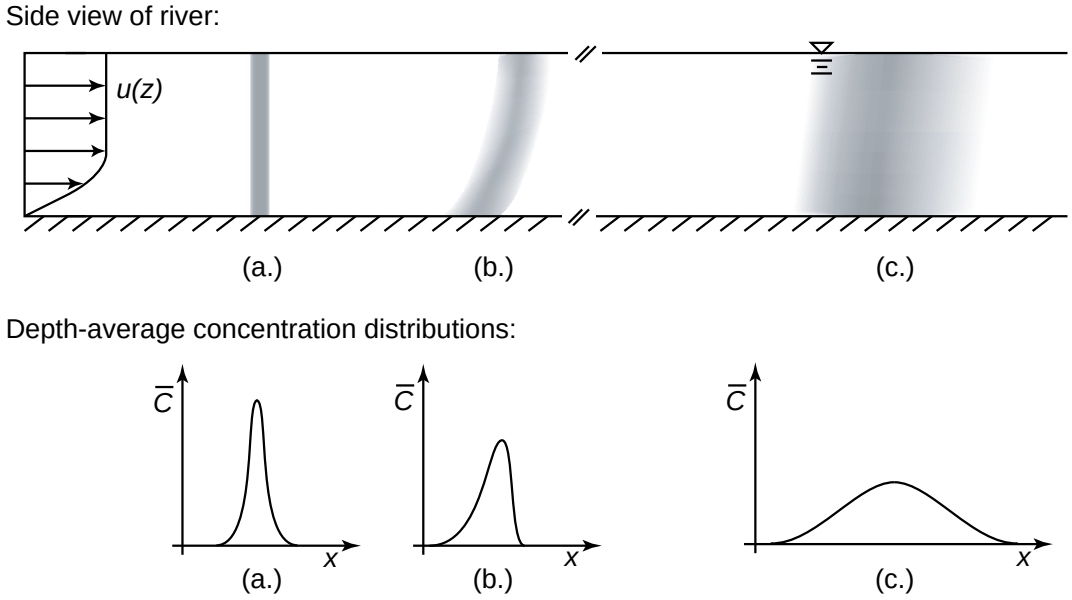

Fig. 3.3. Schematic showing the process of longitudinal dispersion. Tracer is injected uniformly at (a.) and stretched by the shear profile at (b.). At (c.) vertical diffusion has homogenized the vertical gradients and a depth-averaged Gaussian distribution is expected in the concentration profiles.

However, because of non-uniformity of the vertical velocity profile and other non-uniformities (dead zones, curves, non-uniform depth, etc.) a process called longitudinal dispersion dominates longitudinal mixing, and $D_{t,x}$ can often be neglected, with a longitudinal dispersion coefficient (derived in the next section) taking its place.

Summary. For a natural stream with width $W = 10$ m, depth $h = 0.3$ m, flow rate $Q = 1$ m^3/s, and slope $S = 0.0005$, the relationships (3.19), (3.20), and (3.22) give

$$D_{t,z} = 6.4 \cdot 10^{-4} \text{ m}^2/\text{s} \tag{3.23}$$

$$D_{t,y} = 5.7 \cdot 10^{-3} \text{ m}^2/\text{s} \tag{3.24}$$

$$D_{t,x} = 5.7 \cdot 10^{-3} \text{ m}^2/\text{s}. \tag{3.25}$$

Since these calculations show that D_t in natural streams is several orders of magnitude greater than the molecular diffusion coefficient, we can safely remove D_m from (3.14).

3.2 Longitudinal dispersion

In the previous section we saw that turbulent fluctuating velocities caused a kind of random mixing that could be described by a Fickian diffusion process with larger, turbulent diffusion coefficients. In this section we want to consider what effect velocity deviations in space, due to non-uniform velocity, or shear-flow, profiles, might have on the transport of contaminants.

Figure 3.3 depicts schematically what happens to a dye patch in a shear flow such as open-channel flow. If we inject a contaminant so that it is uniformly distributed across the cross-section at point (a.), there will be no vertical concentration gradients and, therefore, no net

diffusive flux in the vertical at that point. The patch of tracer will advect downstream and get stretched due to the different advection velocities in the shear profile. After some short distance downstream, the patch will look like that at point (b.). At that point there are strong vertical concentration gradients, and therefore, a large net diffusive flux in the vertical. As the stretched out patch continues downstream, (turbulent) diffusion will smooth out these vertical concentration gradients, and far enough downstream, the patch will look like that at point (c.). The amount that the patch has spread out in the downstream direction at point (c.) is much more than what could have been produced by just longitudinal (turbulent) diffusion. This combined process of advection and vertical diffusion is called dispersion.

If we solve the transport equation in three dimensions using the appropriate molecular or turbulent diffusion coefficients, we do not need to do anything special to capture the stretching effect of the velocity profile described above. Dispersion is implicitly included in three-dimensional models.

However, we would like to take advantage of the fact that the concentration distribution at the point (c.) is essentially one-dimensional: it is well mixed in the y- and z-directions. In addition, the concentration distribution at point (c.) is observed to be Gaussian, suggesting a Fickian-type diffusive process. Taylor's analysis for dispersion, as presented in the following, is a method to include the stretching effects of dispersion in a one-dimensional model. The result is a one-dimensional transport equation with an enhanced longitudinal mixing coefficient, called the longitudinal dispersion coefficient.

As pointed out by Fischer et al. (1979), the analysis presented by G. I. Taylor to compute the longitudinal dispersion coefficient from the shear velocity profile is a particularly impressive example of the genius of G. I. Taylor. At one point we will cancel out the terms of the equation for which we are trying to solve. Through a scale analysis we will discard terms that would be difficult to evaluate. And by thoroughly understanding the physics of the problem, we will use a steady-state assumption that will make the problem tractable. Hence, just about all of our mathematical tools will be used.

3.2.1 Derivation of the advective dispersion equation

To derive an equation for longitudinal dispersion, we will follow a modified version of the Reynolds decomposition introduced in the previous section to handle turbulence. Referring to Figure 3.4, we see that for one component of the turbulent decomposition, we have a mean velocity that is constant at a point x_i in three dimensional space and fluctuating velocities that are variable in time so that

$$u(x_i, t) = \overline{u}(x_i) + u'(x_i, t). \tag{3.26}$$

For shear-flow decomposition (here, we show the log-velocity profile in a river), we have a mean velocity that is constant over the depth and deviating velocities that are variable over the depth such that

$$u(z) = \overline{u} + u'(z) \tag{3.27}$$

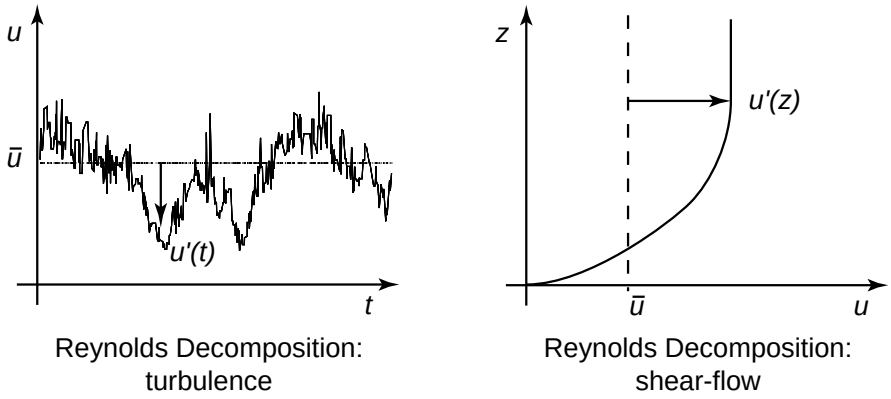

Fig. 3.4. Comparison of the Reynolds decomposition for turbulent flow (left) and shear flow (right).

where the over-bar represents a depth average, not an average o turbulent fluctuations. We explicitly assume that $\overline{u}$ and $u'(z)$ are independent of x. A main difference between these two equations is that (3.26) has a random fluctuating component $u'(x_i, t)$; whereas, (3.27) has a deterministic, non-random (and fully known!) fluctuating component $u'(z)$, which we rather call a deviation than a fluctuation. As for turbulent diffusion above, we also have a Reynold's decomposition for the concentrations

$$C(x, z) = \overline{C}(x) + C'(x, z) \tag{3.28}$$

which is dependent on x, and for which $C'(x, z)$ is unknown.

Armed with these concepts, we are ready to follow Taylor's analysis and apply it to longitudinal dispersion in an open channel. For this derivation we will assume laminar flow and an infinitely wide channel with no-flux boundaries at the top and bottom, so that $v = w = 0$. The dye patch is introduced as a plane so that we can neglect lateral diffusion ($\partial C/\partial y = 0$). The governing advective diffusion equation is

$$\frac{\partial C}{\partial t} + u\frac{\partial C}{\partial x} = D_x\frac{\partial^2 C}{\partial x^2} + D_z\frac{\partial^2 C}{\partial z^2}. \tag{3.29}$$

This equation is valid in three dimensions and contains the effect of dispersion. The diffusion coefficients would either be molecular or turbulent, depending on whether the flow is laminar or turbulent. Substituting the Reynolds decomposition for the shear velocity profile, we obtain

$$\frac{\partial(\overline{C} + C')}{\partial t} + (\overline{u} + u')\frac{\partial(\overline{C} + C')}{\partial x} = D_x\frac{\partial^2(\overline{C} + C')}{\partial x^2} + D_z\frac{\partial^2(\overline{C} + C')}{\partial z^2}. \tag{3.30}$$

Since we already argued that longitudinal dispersion will be much greater than longitudinal diffusion, we will neglect the D_x-term for brevity (it can always be added back later as an additive diffusion term). Also, note that $\overline{C}$ is not a function of z; thus, it drops out of the final D_z-term.

As usual, it is easier to deal with this equation in a frame of reference that moves with the mean advection velocity; thus, we introduce the coordinate transformation

$$\xi = x - \overline{u}t \tag{3.31}$$

$$\tau = t \tag{3.32}$$

$$z = z, \tag{3.33}$$

and using the chain rule, the differential operators become

$$\begin{aligned}\frac{\partial}{\partial x} &= \frac{\partial}{\partial \xi}\frac{\partial \xi}{\partial x} + \frac{\partial}{\partial \tau}\frac{\partial \tau}{\partial x} + \frac{\partial}{\partial z}\frac{\partial z}{\partial x} \\ &= \frac{\partial}{\partial \xi}\end{aligned} \tag{3.34}$$

$$\begin{aligned}\frac{\partial}{\partial t} &= \frac{\partial}{\partial \xi}\frac{\partial \xi}{\partial t} + \frac{\partial}{\partial \tau}\frac{\partial \tau}{\partial t} + \frac{\partial}{\partial z}\frac{\partial z}{\partial t} \\ &= \frac{\partial}{\partial \tau} - \overline{u}\frac{\partial}{\partial \xi}\end{aligned} \tag{3.35}$$

$$\begin{aligned}\frac{\partial}{\partial z} &= \frac{\partial}{\partial \xi}\frac{\partial \xi}{\partial z} + \frac{\partial}{\partial \tau}\frac{\partial \tau}{\partial z} + \frac{\partial}{\partial z}\frac{\partial z}{\partial z} \\ &= \frac{\partial}{\partial z}.\end{aligned} \tag{3.36}$$

Substituting this transformation and combining like terms (and dropping the terms discussed above) we obtain

$$\frac{\partial(\overline{C} + C')}{\partial \tau} + \frac{\partial u'(\overline{C} + C')}{\partial \xi} = D_z \frac{\partial^2 C'}{\partial z^2}, \tag{3.37}$$

which is effectively our starting point for Taylor's analysis.

The discussion above indicates that it is the gradients of concentration and velocity in the vertical that are responsible for the increased longitudinal dispersion. Thus, we would like, at this point, to remove the non-fluctuating terms (terms without a prime) from (3.37). This step takes great courage and profound foresight, since that means getting rid of $\partial\overline{C}/\partial t$, which is the quantity we would ultimately like to predict (Fischer et al. 1979). As we will see, however, this is precisely what enables us to obtain an equation for the dispersion coefficient.

To remove the constant components from (3.37), we will take the depth average of (3.37) and then subtract that result from (3.37). The depth-average operator is

$$\frac{1}{h}\int_0^h dz. \tag{3.38}$$

Applying the depth average to (3.37) leaves

$$\frac{\partial \overline{C}}{\partial \tau} + \frac{\partial \overline{u'C'}}{\partial \xi} = 0, \tag{3.39}$$

since the depth average of C' is zero, but the cross-term, $\overline{u'C'}$, may not be zero. This equation is the one-dimensional governing equation we are looking for. We will come back to this equation once we have found a relationship for $\overline{u'C'}$. Subtracting this result from (3.37), we obtain

$$\frac{\partial C'}{\partial \tau} + u'\frac{\partial \overline{C}}{\partial \xi} + u'\frac{\partial C'}{\partial \xi} = \frac{\partial \overline{u'C'}}{\partial \xi} + D_z \frac{\partial^2 C'}{\partial z^2}, \tag{3.40}$$

which gives us a governing equation for the concentration deviations C'. If we can solve this equation for C', then we can substitute the solution into (3.39) to obtain the desired equation for $\overline{C}$.

Before we solve (3.40), let us consider the scale of each term and decide whether it is necessary to keep all the terms. This is called a scale-analysis. We are seeking solutions for the point (c.) in Figure 3.3. At that point, a particle in the cloud has thoroughly sampled the velocity profile, and $C' \ll \overline{C}$. Thus,

$$u' \frac{\partial C'}{\partial \xi} \ll u' \frac{\partial \overline{C}}{\partial \xi} \text{ and} \tag{3.41}$$

$$\frac{\partial \overline{u'C'}}{\partial \xi} \ll u' \frac{\partial \overline{C}}{\partial \xi}. \tag{3.42}$$

We can neglect the two terms on the left-hand-side of the inequalities above, leaving us with

$$\frac{\partial C'}{\partial \tau} + u' \frac{\partial \overline{C}}{\partial \xi} = D_z \frac{\partial^2 C'}{\partial z^2}. \tag{3.43}$$

This might be another surprise. In the turbulent diffusion case, it was the cross-term $\overline{u'C'}$ that became our turbulent diffusion term. Here, we have just discarded this term. In turbulence (as will also be the case here for dispersion), that cross-term represents mass transport due to the fluctuating velocities. But let us, also, take a closer look at the middle term of (3.43). This term is an advection term working on the mean concentration, $\overline{C}$, but due to the non-random deviating velocity, $u'(z)$. Thus, it is the transport term that represents the action of the shear velocity profile.

Next, we see another insightful simplification that Taylor made. In the beginning stages of dispersion ((a.) and (b.) in Figure 3.3) the concentration fluctuations are unsteady, but downstream (at point (c.)), after the velocity profile has been thoroughly sampled, the vertical concentration fluctuations will reach a steady state (there will be a balanced vertical transport of contaminant), which represents the case of a constant (time-invariant) dispersion coefficient. At steady state, (3.43) becomes

$$u' \frac{\partial \overline{C}}{\partial \xi} = \frac{\partial}{\partial z} \left(D_z \frac{\partial C'}{\partial z} \right) \tag{3.44}$$

where we have written the form for a non-constant D_z. Solving for C' by integrating twice gives

$$C'(z) = \frac{\partial \overline{C}}{\partial \xi} \int_0^z \frac{1}{D_z} \int_0^z u' dz dz, \tag{3.45}$$

which looks promising, but still contains the unknown $\overline{C}$-term.

Step back for a moment and consider what the mass flux in the longitudinal direction is. In our moving coordinate system, we only have one velocity; thus, the advective mass flux must be

$$q_a = u'(\overline{C} + C'). \tag{3.46}$$

To obtain the total mass flux, we take the depth average

$$\begin{aligned}\overline{q_a} &= \frac{1}{h}\int_0^h u'(\overline{C}+C')dz \\ &= \frac{1}{h}\int_0^h u'C'dz \\ &= \overline{u'C'}.\end{aligned} \tag{3.47}$$

Recall that the depth average of $u'\overline{C}$ is zero. Substituting the solution for C' from (3.45), the depth-average mass flux becomes

$$\overline{q_a} = \frac{1}{h}\int_0^h u'\frac{\partial \overline{C}}{\partial \xi}\int_0^z \frac{1}{D_z}\int_0^z u'dzdzdz. \tag{3.48}$$

We can take $\partial\overline{C}/\partial\xi$ outside of the integral since it is independent of z, leaving us with

$$\overline{q_a} = -D_L\frac{\partial \overline{C}}{\partial \xi} \tag{3.49}$$

where

$$D_L = -\frac{1}{h}\int_0^h u'\int_0^z \frac{1}{D_z}\int_0^z u'dzdzdz, \tag{3.50}$$

and we have a Fick's law-type mass flux relationship in (3.49). Since the equation for D_L is just a function of the depth and the velocity profile, we can calculate D_L for any velocity profile by integrating; thus, we have an analytical solution for the longitudinal dispersion coefficient.

The final step is to introduce this result into the depth-average governing equation (3.39) to obtain

$$\frac{\partial \overline{C}}{\partial \tau} = \frac{\partial}{\partial \xi}\left(D_L\frac{\partial \overline{C}}{\partial \xi}\right), \tag{3.51}$$

which, in the original coordinate system, gives the one-dimensional advective dispersion equation

$$\frac{\partial \overline{C}}{\partial t} + \overline{u}\frac{\partial \overline{C}}{\partial x} = \frac{\partial}{\partial x}\left(D_L\frac{\partial \overline{C}}{\partial x}\right) \tag{3.52}$$

with D_L as defined by (3.50).

3.2.2 Calculating longitudinal dispersion coefficients

All the brilliant mathematics in the previous section really paid off since we ended up with an analytical solution for the dispersion coefficient

$$D_L = -\frac{1}{h}\int_0^h u'\int_0^z \frac{1}{D_z}\int_0^z u'dzdzdz.$$

In real streams, it is usually the lateral shear (in the y-direction) rather than the vertical shear that plays the more important role. For lateral shear, Fischer et al. (1979) derive by a similar analysis the relationship

$$D_L = -\frac{1}{A}\int_0^W u'h\int_0^y \frac{1}{D_y h}\int_0^y u'hdydydy \tag{3.53}$$

where A is the cross-sectional area of the stream and W is the width. Irrespective of which relationship we choose, the question that remains is, how do we best calculate these integrals.

Example Box 3.3:
River mixing processes.

As part of a dye study to estimate the mixing coefficients in a river, a student injects a slug (point source) of dye at the surface of a stream in the middle of the cross-section. Discuss the mixing processes and the length scales affecting the injected tracer.

Although the initial vertical momentum of the dye injection generally results in good vertical mixing, assume here that the student carefully injects the dye just at the stream surface. Vertical turbulent diffusion will mix the dye over the depth, and from Example Box 3.2 above, the injection can be treated as mixed in the vertical after the point

$$L_z = 12h$$

where h is the stream depth.

As the dye continues to move downstream, lateral turbulent diffusion mixes the dye in the transverse direction. Based on the discussion in Example Box 3.2, the tracer can be considered well mixed laterally after

$$L_y = \frac{W^2}{3h}$$

where W is the stream width.

For the region between the injection and L_z, the dye cloud is fully three-dimensional, and no simplifications can be made to the transport equation. Beyond L_z, the cloud is vertically mixed, and longitudinal dispersion can be applied. For distances less than L_y, a two-dimensional model with lateral turbulent diffusion and longitudinal dispersion is required. For distances beyond L_y, a one-dimensional longitudinal dispersion model is acceptable.

Analytical solutions. For laminar flows, analytical velocity profiles may sometimes exist and (3.50) can be calculated analytically. Following examples in Fischer et al. (1979), the simplest flow is the flow between two infinite plates, where the top plate is moving at U relative to the bottom plate. For that case

$$D_L = \frac{U^2 d^2}{120 D_z} \tag{3.54}$$

where d is the distance between the two plates. Similarly, for laminar pipe flow, the solution is

$$D_L = \frac{a^2 U_0^2}{192 D_r} \tag{3.55}$$

where a is the pipe radius, U_0 is the pipe centerline velocity and D_r is the radial diffusion coefficient.

For turbulent flow, an analysis similar to the section on turbulent diffusion can be carried out and the result is that (3.50) keeps the same form, and we substitute the turbulent diffusion coefficient and the mean turbulent shear velocity profile for D_z and u'. The result for turbulent flow in a pipe becomes

$$D_L = 10.1 a u_*. \tag{3.56}$$

One result of particular importance is that for an infinitely wide open channel of depth h. Using the log-velocity profile (3.18) with von Karman constant $\kappa = 0.4$ and the relationship (3.50), the dispersion coefficient is

$$D_L = 5.93 h u_*. \tag{3.57}$$

Comparing this equation to the prediction for longitudinal turbulent diffusion from the previous section ($D_{t,x} = 0.15 h u_*$) we see that D_L has the same form ($\propto h u_*$) and that D_L is indeed much greater than longitudinal turbulent diffusion. For real open channels, the lateral shear velocity profile between the two banks becomes dominant and the leading coefficient for D_L can range

from 5 to 7000 (Fischer et al. 1979). For further discussion of analytical solutions, see Fischer et al. (1979).

Numerical integration. In many practical engineering applications, the variable channel geometry makes it impossible to assume an analytical shear velocity profile. In that case, one alternative is to break the river cross-section into a series of bins, measure the mean velocity in each bin, and then compute the second relationship (3.53) by numerical integration. Fischer et al. (1979) give a thorough discussion of how to do this.

Engineering estimates. When only very rough measurements are available, it is necessary to come up with a reasonably accurate engineering estimate for D_L. To do this, we first write (3.53) in non-dimensional form using the dimensionless variables (denoted by *) defined by

$$y = Wy^*; \quad u' = \sqrt{\overline{u'^2}}u'^*; \quad D_y = \overline{D_y}D_y^*; \quad h = \overline{h}h^*$$

where the over-bar indicates a cross-sectional average. As we already said, longitudinal dispersion in streams is dominated by the lateral shear velocity profile, which is why we are using y and D_y. Substituting this non-dimensionalization into (3.53) we obtain

$$D_L = \frac{W^2\overline{u'^2}}{\overline{D_y}}I \tag{3.58}$$

where

$$I = -\int_0^1 u'^* h^* \int_0^{y^*} \frac{1}{D_y^* h^*} \int_0^{y^*} u'^* h^* dy^* dy^* dy^*. \tag{3.59}$$

As Fischer et al. (1979) point out, in most practical cases it may suffice to take $I \approx 0.01 to 0.1$.

To go one step further, we introduce some further scales measured by Fischer et al. (1979). From experiments and comparisons with the field, the ratio $\overline{u'^2}/\overline{u}^2$ can be taken as 0.2 ± 0.03. For irregular streams, we can take $\overline{D_y} = 0.6du^*$. Substituting these values into (3.58) with $I = 0.033$ gives the estimate

$$D_L = 0.011\frac{\overline{u}^2 W^2}{du_*} \tag{3.60}$$

which has been found to agree with observations within a factor of 4 or so. Deviations are primarily due to factors not included in our analysis, such as recirculation and dead zones.

Geomorphological estimates. Deng et al. (2001) present a similar approach for an engineering estimate of the dispersion coefficient in straight rivers based on characteristic geomorphological parameters. The expression they obtain is

$$\frac{D_L}{hu_*} = \frac{0.15}{8\epsilon_{t0}}\left(\frac{W}{h}\right)^{5/3}\left(\frac{\overline{u}}{u_*}\right)^2 \tag{3.61}$$

where ϵ_{t0} is a dimensionless number given by:

$$\epsilon_{t0} = 0.145 + \left(\frac{1}{3520}\right)\left(\frac{\overline{u}}{u_*}\right)\left(\frac{W}{h}\right)^{1.38}. \tag{3.62}$$

These equations are based on the hydraulic geometry relationship for stable rivers and on the assumption that the uniform-flow formula is valid for local depth-averaged variables. Deng et al.

(2001) compare predictions for this relationship and predictions from (3.60) with measurements from 73 sets of field data. More than 64% of the predictions by (3.61) fall within the range of $0.5 \leq D_L|_{prediction}/D_L|_{measurement} \leq 2$. This accuracy is on average better than that for (3.60); however, in some individual cases, (3.60) provides the better estimate.

Dye studies. One of the most reliable means of computing a dispersion coefficient is through a dye study, as illustrated in the applications of the next sections. It is important to keep in mind that since D_L is dependent on the velocity profile, it is, in general, a function of the flow rate. Hence, a D_L computed by a dye study for one flow rate does not necessarily apply to a situation at a much different flow rate. In such cases, it is probably best to perform a series of dye studies over a range of flow rates, or to compare estimates such as (3.60) to the results of one dye study to aid predictions under different conditions.

3.3 Application: Dye studies

The purpose of a dye tracer study is to determine a river's flow and transport properties; in particular, the mean advective velocity and the effective longitudinal dispersion coefficient. To estimate these quantities, we inject dye upstream, measure the concentration distribution downstream, and compare the results to analytical solutions. The two major types of dye injections are instantaneous injections and continuous injections. The following sections discuss typical results for these two injection scenarios.

3.3.1 Preparations

To prepare a dye injection study, we use engineering estimates for the expected transport properties to determine the location of the measurement station(s), the duration of the experiment, the needed amount of dye, and the type of dye injection.

For illustration purposes, assume in the following discussion that you measure a river cross-section to have depth $h = 0.35$ m and width $W = 10$ m. The last time you visited the site, you measured the surface current by timing leaves floating at the surface and found $U_s = 53$ cm/s. A rule-of-thumb for the mean stream velocity is $\overline{U} = 0.85U_s = 0.45$ cm/s. You estimate the river slope from topographic maps as $S = 0.0005$. The channel is uniform but has some meandering.

Measurement stations. A critical part of a dye study is that you measure far enough downstream that the dye is well mixed across the cross-section. If you measure too close to the source, you might obtain a curve for $C(t)$ that looks Gaussian, but the concentrations will not be uniform across the cross-section, and dilution estimates will be biased. We use our mixing length rules of thumb to compute the necessary downstream distance.

Assuming the injection is at a point (conservative case), it must mix both vertically and transversely. The two relevant turbulent diffusion coefficients are

$$\begin{aligned} D_{t,z} &= 0.067 d\sqrt{gdS} \\ &= 9.7 \cdot 10^{-4} \text{ m}^2/\text{s} \end{aligned} \tag{3.63}$$

$$D_{t,y} = 0.6d\sqrt{gdS}$$
$$= 8.7 \cdot 10^{-3} \text{ m}^2/\text{s}. \tag{3.64}$$

The time it takes for diffusion to spread a tracer over a distance l is $l^2/(12.5D)$; thus, the distance the tracer would move downstream in this time is

$$L_x = \frac{l^2}{12.5D}U. \tag{3.65}$$

There are several injection possibilities. If you inject at the bottom or surface, the dye must spread over the whole depth; if you inject at middle depth, the dye must only spread over half the depth. Similarly, if you inject at either bank, the dye must spread across the whole river; if you inject at the stream centerline, the dye must only spread over half the width. Often it is possible to inject the dye in the middle of the river and at the water surface. For such an injection, we compute in our example that $L_{m,z}$ for spreading over the full depth is 4.2 m, whereas, $L_{m,y}$ for spreading over half the width is 95 m. Thus, the measuring station must be at least $L_m = 100$ m downstream of the injection.

The longitudinal spreading of the cloud is controlled by the dispersion coefficient. Using the estimate from Fischer et al. (1979) given in (3.60), we have

$$D_L = 0.011\frac{U^2W^2}{d\sqrt{gdS}}$$
$$= 15.4 \text{ m}^2/\text{s}. \tag{3.66}$$

We would like the longitudinal width of the cloud at the measuring station to be less than the distance from the injection to the measuring station; thus, we would like a Peclet number, Pe, at the measuring station of 0.1 or less. This criteria gives us

$$L_m = \frac{D}{UPe}$$
$$= 342 \text{ m}. \tag{3.67}$$

Since for this stream the Peclet criteria is more stringent than that for lateral mixing, we chose a measurement location of $L_m = 350$ m.

Experiment duration. We must measure downstream long enough in time to capture all of the cloud or dye front as it passes. The center of the dye front reaches the measuring station with the mean river flow: $t_c = L_c/U$. Dispersion causes some of the dye to arrive earlier and some of the dye to arrive later. An estimate for the length of the dye cloud that passes after the center of mass is

$$L_\sigma = 3\sqrt{2D_L L_m/U}$$
$$= 525 \text{ m} \tag{3.68}$$

or in time coordinates, $t_\sigma = 1170$ s. Thus, we should start measuring immediately after the dye is injected and continue taking measurements until $t = t_c + t_\sigma = 30$ min. To be conservative, we select a duration of 35 min.

Amount of injected dye tracer. The general public does not like to see red or orange water in their rivers, so when we do a tracer study, we like to keep the concentration of dye low enough that the water does not appear colored to the naked eye. This is possible using fluorescent dyes because they remain visible to measurement devices at concentrations not noticeable to casual observation. The most common fluorescent dye used in river studies is Rhodamine WT. Many other dyes can also be used, including other types of Rhodamine (B, 6G, etc.) or Fluorescein. Smart & Laidlay (1977) discuss the properties of many common fluorescent dyes.

In preparing a dye study, it is necessary to determine the amount (mass) of dye to inject. A common field fluorometer by Turner Designs has a measurement range for Rhodamine WT of $(0.04 \text{ to } 40)\cdot 10^{-2}$ mg/l. To have good sensitivity and also leave room for a wide range of river flow rates, you should design for a maximum concentration at the measurement station near the upper range of the fluorometer, for instance $C_{max} = 4$ mg/l.

The amount of dye to inject depends on whether the injection is a point source or a continuous injection. For a point source injection, we use the instantaneous point source solution with the longitudinal dispersion coefficient estimated above

$$\begin{aligned} M &= C_{max} A \sqrt{4\pi D_L L_m / U} \\ &= 5.4 \text{ g}. \end{aligned} \tag{3.69}$$

For a continuous injection, we estimate the dye mass flow rate from the expected dilution

$$\begin{aligned} \dot{m} &= U_0 A_r C_{max} \\ &= 6.3 \text{ g/s}. \end{aligned} \tag{3.70}$$

These calculations show that a continuous release uses much more dye than a point release. These estimates are for the pure (usually a powder) form of the dye.

Type of injection. To get the best injection characteristics, we dissolve the powder form of the dye in a solution of water and alcohol before injecting it in the river. The alcohol is used to obtain a neutrally buoyant mixture of dye. For a point release, we usually spill a bottle of dye mixture containing the desired initial mass of dye in the center of the river and record the time when the injection occurs. For a continuous release, we require some tubing to direct the dye into the river, a reservoir containing dye at a known concentration, and a means of regulating the flow rate of dye.

The easiest way to get a constant dye flow rate is to use a peristaltic pump. Another means is to construct a Marriot bottle as described in Fischer et al. (1979) and shown in Figure 3.5. The idea of the Marriot bottle is to create a constant head tank where you can assume the pressure is equal to atmospheric pressure at the bottom of the vertical tube. As long as the bottle has enough dye in it that the bottom of the vertical tube is submerged, a constant flow rate Q_0 will result by virtue of the constant pressure head between the tank and the injection. We must calibrate the flow rate in the laboratory for a given head drop prior to conducting the field experiment.

The concentration of the dye C_0 for the continuous release is calculated according to the equation

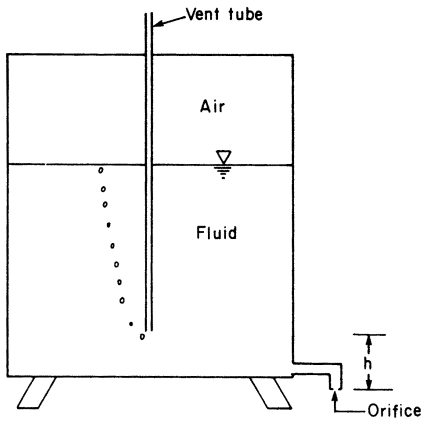

Fig. 3.5. Schematic of a Marriot bottle taken from Fischer et al. (1979).

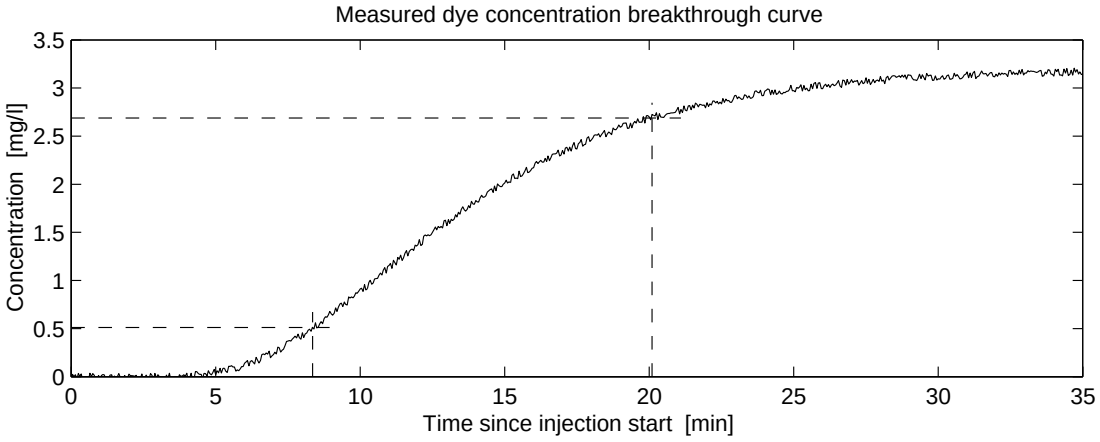

Fig. 3.6. Measured dye concentration for example dye study. Dye fluctuations are due to instrument uncertainty, not due to turbulent fluctuations.

$$\dot{m} = Q_0 C_0 \tag{3.71}$$

where Q_0 is the flow rate from the pump or Marriot bottle. With these design issues complete, a dye study is ready to be conducted.

3.3.2 River flow rates

Figure 3.6 shows a breakthrough curve for a continuous injection, based on the design in the previous section. The river flow rate can be estimated from the measured steady-state concentration in the river C_r at $t = 35$ min. Reading from the graph, we have $C_r = 3.15$ mg/l. Thus, the actual flow rate measured in the dye study was

$$\begin{aligned} Q_r &= \frac{\dot{m}}{C_r} \\ &= 2.0 \text{ m}^3/\text{s}. \end{aligned} \tag{3.72}$$

Notice that this estimate for the river flow rate is independent of the cross-sectional area.

To estimate the error in this measurement, we use the error-propagation equation

$$\delta\gamma = \sqrt{\sum_{i=1}^{n} \left(\frac{\partial \gamma}{\partial m_i} \delta m_i \right)^2} \tag{3.73}$$

where $\delta\gamma$ is the error in some quantity γ, estimated from n measurements m_i. Computing the error for our river flow rate estimate, we have

$$\delta Q_r = \sqrt{\left(\frac{C_0}{C_r} \delta Q_0 \right)^2 + \left(\frac{Q_0}{C_r} \delta C_0 \right)^2 + \left(\frac{Q_0 C_0}{C_r^2} \delta C_r \right)^2}. \tag{3.74}$$

If the uncertainties in the measurements were $C_r = (3.15 \pm 0.04)$ mg/l, $C_0 = 32 \pm 0.01$ g/l and $Q_0 = 0.2 \pm 0.01$ l/s, then our estimate should be $Q_r = 2.0 \pm 0.1$ m^3/s. The error propagation formula is helpful for determining which sources of error contribute the most to the overall error in our estimate.

3.3.3 River dispersion coefficients

The breakthrough curve in Figure 3.6 also contains all the information we need to estimate an *in situ* longitudinal dispersion coefficient. To do that, we will use the relationship

$$\sigma^2 = 2D_L t. \tag{3.75}$$

Since our measurements of σ are in time, we must convert them to space in order to use this equation. One problem is that the dye cloud continues to grow as it passes the site, so the width measured at the beginning of the front is less than the width measured after most of the front has passed; thus, we must take an average.

The center of the dye front can be taken at $C = 0.5C_0$, which passed the station at $t = 12.94$ min and represents the mean stream velocity. One standard deviation to the left of this point is at $C = 0.16C_0$, as shown in the figure. This concentration passed the measurement station at $t = 8.35$ min. One standard deviation to the right is at $C = 0.84C_0$, and this concentration passed the station at $t = 20.12$ min. From this information, the average velocity is $\overline{u} = 0.45$ m/s and the average width of the front is $2\sigma_t = 20.12 - 8.35 = 11.77$ min. The time associated with this average sigma is $t = 8.35 + 11.77/2 = 14.24$ min.

To compute D_L from (3.75), we must convert our time estimate of σ_t to a spatial estimate using $\sigma = \overline{u}\sigma_t$. Solving for D_L gives

$$\begin{aligned} D_L &= \frac{\overline{u}^2 \sigma_t^2}{2t} \\ &= 14.8 \text{ m}^2/\text{s}. \end{aligned} \tag{3.76}$$

This value compares favorably with our initial estimate from (3.50) of 15.4 m^2/s.

3.4 Application: Dye study in Cowaselon Creek

In 1981, students at Cornell University performed a dye study in Cowaselon Creek using an instantaneous point source of Rhodamine WT dye. The section of Cowaselon Creek tested has

a very uniform cross-section and a straight fall line from the injection point through the measurement stations. At the injection site, the students measured the cross-section and flow rate, obtaining

$$Q = 0.6 \text{ m}^3/\text{s} \qquad W = 10.7 \text{ m}$$
$$\overline{u} = 0.17 \text{ m/s} \qquad h = 0.3 \text{ m}.$$

From topographic maps, they measured the creek slope over the study area to be $S = 4.3 \cdot 10^{-4}$.

The concentration profiles were measured at three stations downstream. The first station was 670 m downstream of the injection, the second station was 2800 m downstream of the injection, and the final station was 5230 m downstream of the injection. At each location, samples were taken in the center of the river and near the right and left banks. Figure 3.7 shows the measured concentration profiles.

For turbulent mixing in the vertical direction, the downstream distance would be $L_{m,z} = 12d = 17$ m. This location is well upstream of our measurements; thus, we expect the plume to be well-mixed in the vertical by the time it reaches the measurement stations.

For mixing in the lateral direction, the method in Example Box 3.3 (using $D_{t,y} = 0.15du_*$ for straight channels) gives a downstream distance of $L_{m,y} = 2500$ m. Since the first measurement station is at $L = 670$ m we clearly see that there are still lateral gradients in the concentration cloud. At the second measurement station, 2800 m downstream, the lateral gradients have diffused, and the lateral distribution is independent of the lateral coordinate. Likewise, at the third measurement station, 5230 m downstream, the plume is mixed laterally; however, due to dispersion, the plume has also spread more in the longitudinal direction.

To estimate the dispersion coefficient, we can take the travel time between the stations two and three and the growth of the cloud. The travel time between stations is $\delta t = 3.97$ hr. The width at station one is $\sigma_1 = 236$ m, and the width at station two is $\sigma_2 = 448$ m. The dispersion coefficient is

$$\begin{aligned} D_L &= \frac{\sigma_2^2 - \sigma_1^2}{2\delta t} \\ &= 5.1 \text{ m}^2/\text{s}. \end{aligned} \tag{3.77}$$

Comparing to (3.60) and (3.61), we compute

$$D_L|_{Fischer} = 3.4 \text{ m}^2/\text{s} \tag{3.78}$$
$$D_L|_{Deng} = 5.4 \text{ m}^2/\text{s}. \tag{3.79}$$

Although the geomorphological estimate of 5.4 m^2/s is closer to the true value than is 3.3 m^2/s, for practical purposes, both methods give good results. Dye studies, however, are always helpful for determining the true mixing characteristics of rivers.

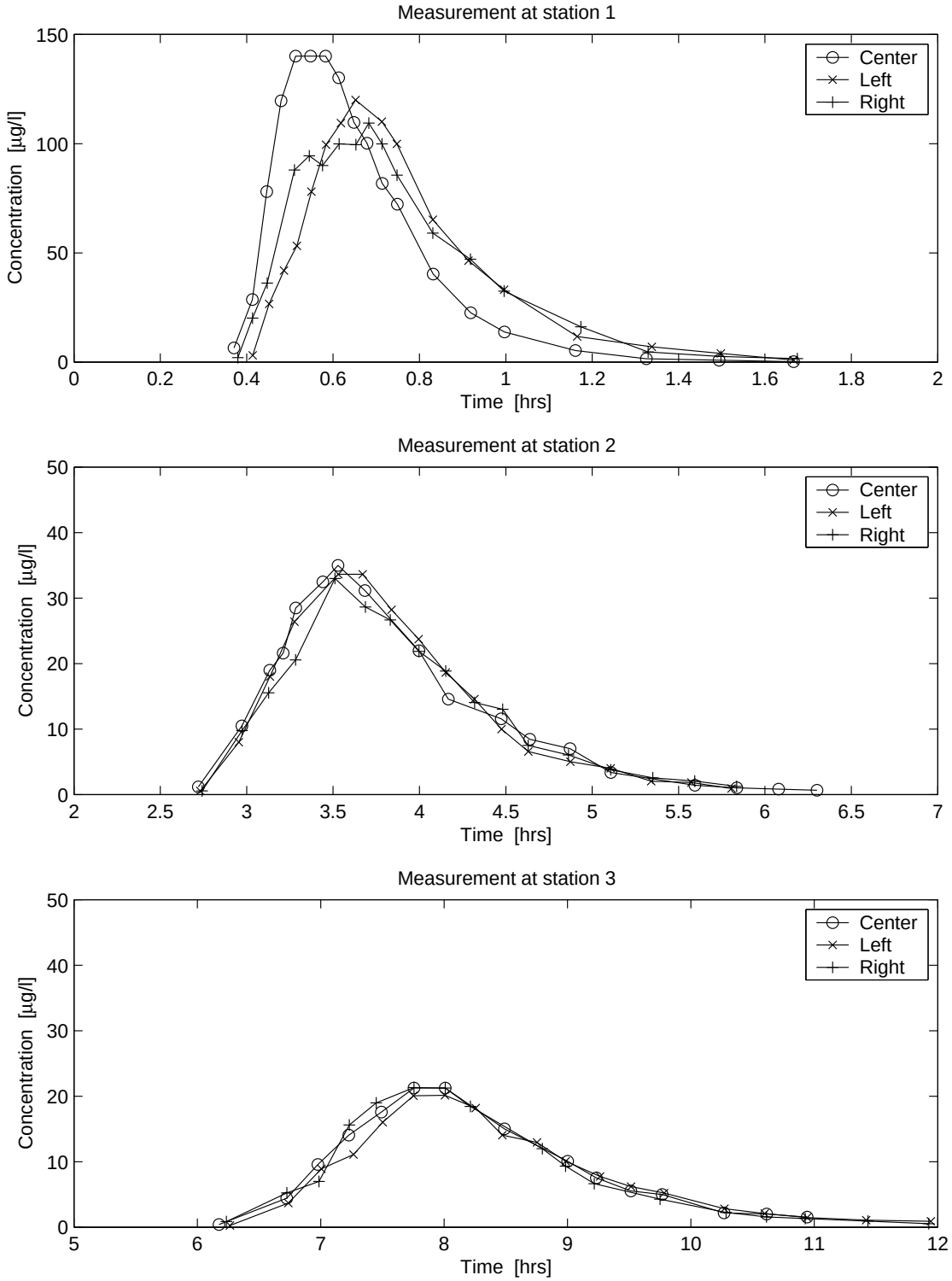

Fig. 3.7. Measured dye concentrations at two stations in Cowaselon Creek for a point injection. Measurements at each station are presented for the stream centerline and for locations near the right and left banks.

Summary

This chapter presented the effects of contaminant transport due to variability in the ambient velocity. In the first section, turbulence was discussed and shown to be composed of a mean velocity and a random, fluctuating turbulent velocity. By introducing the Reynolds decomposition of the turbulent velocity into the advective diffusion equation, a new equation for turbulent diffusion was derived that has the same form as that for molecular diffusion, but with larger, turbulent diffusion coefficients. The second type of variable velocity was a shear velocity profile, described by a mean stream velocity and deterministic deviations from that velocity. Substituting a modified type of Reynolds decomposition for the shear profile into the advective diffusion equation and depth averaging led to a new equation for longitudinal dispersion and an integral relationship for calculating the longitudinal dispersion coefficient. To demonstrate how to use these equations and obtain field measurements of these properties, the chapter closed with an example of a simple dye study to obtain stream flow rate and longitudinal dispersion coefficient.

Exercises

3.1 Properties of turbulence. The axial velocity u of a turbulent jet can be measured using a laser Doppler velocimetry (LDV) system. Obtain a data file that contains only one column (the u component velocity) with a unit of m/s; the sampling rate is 100 Hz. Do the following:

- Plot the velocity and examine whether the flow is turbulent by checking the randomness in your plot. Comment on your observations.
- Use Matlab to calculate the mean velocity and create a variable that contains just the fluctuating velocity (you do not have to turn in anything for this step).
- Plot the fluctuating velocity.
- Calculate the mean value of the fluctuating velocity .
- Write a program to compute the correlation function (normalized so the maximum correlation is 1.0) and plot the function.
- Calculate the integral time scale (integrate between 0 to 0.3 s only).
- Estimate the "typical" size of the eddies (find the integral length scale).

3.2 Turbulent diffusion coefficients. The Rhine river in the vicinity of Karlsruhe has width $B = 300$ m and Manning's friction factor 0.02. The slope is $1 \cdot 10^{-4}$. Assume the river is always at normal depth and that the width is constant for all flow rates.

- For each flow rate in Table 3.1, compute the dispersion coefficient from the equation from Fischer *et al.* (1977)

$$D_L = 0.011 \frac{\overline{u}^2 B^2}{h u_*} \tag{3.80}$$

where $\overline{u}$ is the mean velocity and u_* is the shear velocity.

Table 3.1. Flow rates in the Rhine river near Karlsruhe.

Flow rate [m^3/s]
120
240
500
800
1200

- For each flow rate in Table 3.1, compute the dispersion coefficient from the equation from Deng et al. (2001)

$$\frac{D_L}{hu_*} = \frac{0.15}{8\epsilon_{t0}} \left(\frac{B}{h}\right)^{5/3} \left(\frac{\overline{u}}{u_*}\right)^2 \tag{3.81}$$

with

$$\epsilon_{t0} = 0.145 + \left(\frac{1}{3520}\right) \left(\frac{\overline{u}}{u_*}\right) \left(\frac{B}{h}\right)^{1.38}. \tag{3.82}$$

where h is the water depth and B is the channel width.
- Plot the dispersion coefficient for each method as a function of flow rate and comment on the trends. Do you think it is adequate to do one dye study to evaluate D_L? Why or why not?

3.3 Numerical integration. Using the velocity profile data in Table 3.2 (from Nepf (1995)), perform a numerical integration of (3.53) to estimate a longitudinal dispersion coefficient. You should obtain a value of $D_L = 1.5$ m^2/s.

3.4 Dye study. This problem is adapted from Nepf (1995). A small stream has been found to be contaminated with Lindane, a pesticide known to cause convulsions and liver damage. Groundwater wells in the same region have also been found to contain Lindane, and so you suspect that the river contamination is due to groundwater inflow. To test your theory, you conduct a dye study using a continuous release of dye. Based on the information given in Figure 3.8, what is the groundwater volume flux and the concentration of Lindane in the groundwater between Stations 2 and 3? The variables in the figure are Q_d the volume flow rate of the dye at the injection, C_d the concentration of the dye at the injection and at downstream stations, C_l the concentration of Lindane in the river at each station, W the width of the river, and d the depth in the river. (Hint: this is a steady-state problem, so you do not need to use diffusion coefficients to solve the problem other than to determine whether the dye is well-mixed when it reaches Station 2.)

Due to problems with the pump, the dye flow rate has an error of $Q_d = 100 \pm 5$ cm^3/s. Assume this is the only error in your measurement and report your measurement uncertainty.

Table 3.2. Stream velocity data for calculating a longitudinal dispersion coefficient.

Station number	Distance from bank [cm]	Total depth d [cm]	Measurement depth, z/d [–]	Velocity u [cm/s]
1	0.0	0	0	0.0
2	30.0	14	0.6	3.0
3	58.4	42	0.2	6.0
			0.8	6.4
4	81.3	41	0.2	16.8
			0.8	17.6
5	104.1	43	0.2	13.4
			0.8	13.6
6	137.2	41	0.2	13.6
			0.8	14.2
7	170.2	34	0.2	9.0
			0.8	9.6
8	203.2	30	0.2	5.0
			0.8	5.4
9	236.2	15	0.2	1.0
			0.8	1.4
10	269.2	15	0.2	0.8
			0.8	1.2
11	315.0	14	0.6	0.0
12	360.7	0	0	0.0

3.5 Accidental kerosene spill. A tanker truck has an accident and spills 100 kg of kerosene into a river. The spill occurs over a span of 3 minutes and can be approximated as uniformly distributed across the lateral cross-section of the river. A fish farm has its water intake 2.5 km downstream of the spill location. Refer to Figure 3.9.

- Use the following relationship to compute the longitudinal dispersion coefficient, D_L:

$$\frac{D_L}{Hu_*} = \frac{0.15}{8\epsilon_{t0}} \left(\frac{B}{H}\right)^{5/3} \left(\frac{U}{u_*}\right)^2 \tag{3.83}$$

  B and H are the river width and depth, U is the average flow velocity, u_* is the shear velocity, and ϵ_{t0} is a non-dimensional number given by:

$$\begin{aligned} \epsilon_{t0} &= 0.145 + \left(\frac{1}{3520}\right) \left(\frac{U}{u_*}\right) \left(\frac{B}{H}\right)^{1.38} \\ &= 0.229 \end{aligned} \tag{3.84}$$

- What is the length in the downstream direction that the spill occupies due to its 3 minute duration? At what point downstream of the spill do you think it would be reasonable to approximate the spill using an instantaneous point source release?

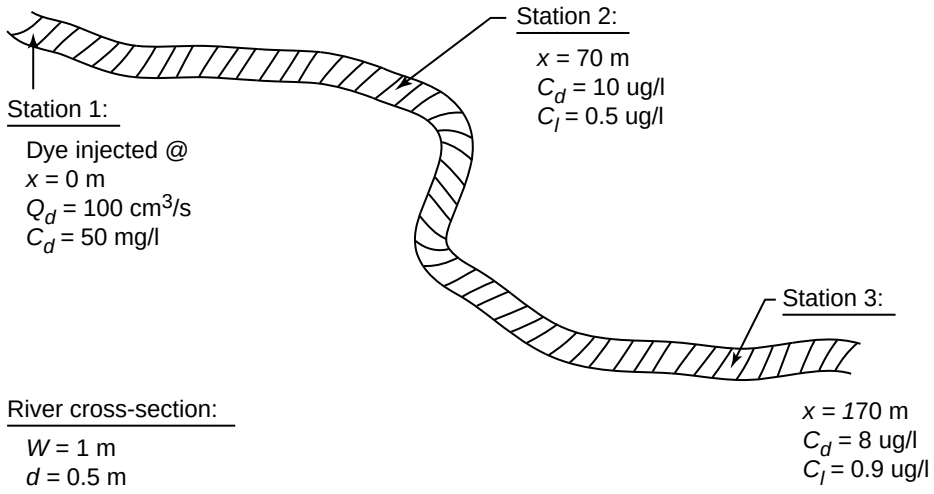

Fig. 3.8. Dye study to determine the source of Lindane contamination in a small stream.

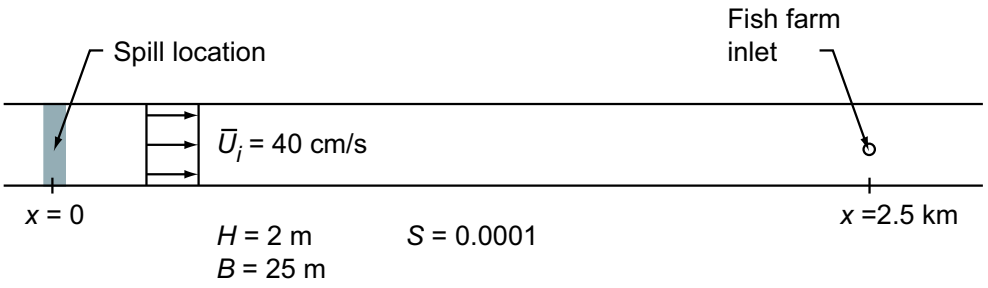

Fig. 3.9. Schematic of the accidental spill with the important measurement values. B and H are the width and depth of the river, $\overline{U_i}$ is the average river flow velocity at the accident location, and S is the channel slope.

- Plot the concentration in the river as a function of downstream distance at $t = 2$ hr after the accident. From the figure, determine the location of the center of mass of the kerosene cloud, the maximum concentration in the river, and the characteristic width of the cloud in the x-direction (approximate the cloud using one standard deviation of the concentration distribution).
- Write the equation for the concentration as a function of time at the inlet to the fish farm. Plot your equation and determine at what time the maximum concentration passes the fish farm.
- A dye study was conducted in the river at an earlier time and concluded that there is a flow of groundwater into the river along the stretch between the accident and the fish farm. How would this information influence the results reported in the previous steps of this problem?

3.6 Ocean mixing. This problem is adapted from Nepf (1995). Ten surface drogues are released into a coastal region at local coordinates $(x, y) = (0, 0)$. The drogues move passively with the surface currents and are tracked using radio signals. Their locations at the end of $t_1 = 1$ and $t_2 = 20$ days are given in the following table.

Table 3.3. Drogue position data.

Drogue Number	$x(t_1)$ [km]	$y(t_1)$ [km]	$x(t_2)$ [km]	$y(t_2)$ [km]
1	2.5	0.2	5.3	8.1
2	4.6	1.4	2.3	1.0
3	2.3	-1.2	6.6	3.9
4	3.1	-0.4	6.7	-2.8
5	1.5	0.8	0.5	4.2
6	1.4	2.1	10.1	3.6
7	4.7	2.1	6.6	-1.4
8	2.7	0.2	6.0	-2.9
9	1.5	2.6	3.2	2.1
10	4.9	2.3	-4.0	1.7

1. Estimate the advection velocity and the lateral coefficients of diffusion (D_x and D_y) for this coastal region.
2. Using the radio links, the positions of all ten drogues can be collected within ten minutes. Suppose the radio link were to break down and the positions were instead determined through visual observation. Even using a helicopter, it requires nearly four hours to locate all ten drogues. How does this change the accuracy of your data? Can you still consider the measurements to be synoptic?
3. Later, a freight ship is caught in a winter storm off the coast where this drogue study was conducted. High winds and rough seas cause several shipping containers to be washed overboard. One of the containers breaks open, releasing its contents: 29,000 children's bathtub toys. Estimate how long it will take for the toys to begin to wash up on shore assuming the same transport characteristics as during the drogue study and that the spill occurs 1 km off the coast. (This really happened in the Pacific Ocean, and the trajectory of the bathtub toys, plastic turtles and ducks, were subsequently used to gain information about the current system.)

3.7 Mixing of a continuous point source in a river. Many dye studies are conducted by injecting a continuous point source of dye at one station and measuring the dilution at downstream stations, where the dye is assumed to be well-mixed across the cross-section. The continuous point source solution in an infinite domain with constant, uniform advection current in the x-direction, U, is

$$C(x,y,z) = \frac{\dot{m}}{4\pi x\sqrt{D_z D_y}} \exp\left(-\frac{(z-z_0)^2 U}{4D_z x} - \frac{(y-y_0)^2 U}{4D_y x}\right) \tag{3.85}$$

where $\dot{m}$ is the mass flux of dye at the injection, x is the downstream distance, D_z is the vertical diffusion coefficient, D_y is the lateral diffusion coefficient, z_0 is the vertical position of the injection, and y_0 is the lateral position of the injection. To derive this solution, we have assumed that longitudinal diffusion is negligible (called the slender-plume approximation).

In a river there are four boundaries that must be accounted for. In the vertical direction, there are boundaries at the channel bed and at the free-water surface. In the lateral direction, there are boundaries at each channel bank. Write a Matlab function that solves this problem for an arbitrary injection point at $(0, y_0, z_0)$. It should take the vertical coordinate as positive upward with origin at the channel bed and the lateral coordinate as positive toward the right-hand bank with origin at the channel center-line.

Dimensional analysis can be used to estimate the distance L_m downstream of an injection at $x = 0$ at which the injection may be considered well-mixed in the vertical or lateral direction. This relationship is

$$L_m \propto \frac{L^2 U}{D} \tag{3.86}$$

where L is the distance over which the dye must spread (for vertical mixing, this would be the water depth), L_m is the downstream distance to the point where the cloud can be considered well-mixed, and D is the pertinent diffusion coefficient (for vertical mixing, this would be D_z). To calibrate this relationship, we define "well-mixed" as the point at which the ratio of the minimum dye concentration C_{min} to the maximum dye concentration C_{max} across the cross-section reaches a threshold value. Common practice is to define well-mixed as $C_{min}/C_{max} = 0.95$. Using this criteria, we can calculate L_m, and a proportionality constant α can be determined, giving the relationship

$$L_m = \alpha \frac{L^2 U}{D}. \tag{3.87}$$

Use this information to study a river with the following characteristics:

- Width $B = 10.7$ m
- Depth $H = 0.3$ m
- Slope $S = 4.3 \cdot 10^{-4}$
- Mean flow velocity $\overline{u} = 0.17$ m/s
- Dye injection rate $\dot{m} = 1$ g/s;

Use enough image sources that your solution is independent of the number of images you are using and answer the following questions:

1. What is the value of Manning's roughness coefficient n that corresponds to the given flow depth and channel slope? Do you think that this value is reasonable? If it seems too high or too low, do you expect that the estimate for the shear velocity of $u_* = \sqrt{gHS}$ is an over-prediction or under-prediction for this stream? Use your calibrated value of n for the remaining questions.
2. Plot the relative concentration $C(x, 0, H)/C(x, 0, 0.5H)$ for an injection at $(0, 0, 0.5H)$ versus downstream distance for x between $x = 1$ m and $x = 45$ m.
3. Calibrate the coefficient α in (3.87) for vertical mixing for an injection at $y_0 = 0$ and $z_0 = [0, 0.25H, 0.5H, 0.75H, H]$ for the criteria $C(z)_{min}/C(z)_{max} = 0.95$.
4. Repeat your calculations in the previous step, but move the injection to $y_0 = B/2$. Does this affect your results? Why or why not?

5. Calibrate the coefficient α in (3.87) for lateral mixing for an injection at $z_0 = 0.5H$ and $y_0 = [B/2, B/4, 0, -B/4, -B/2]$ for the criteria $C(y)_{min}/C(y)_{max} = 0.95$. Do you think your results would change if you moved the injection at z_0 to a different elevation? Why or why not?
6. Repeat your calculations in the previous step, but using a lateral diffusion coefficient of $D_y = 0.6u_*H$. Did this change your value of α?
7. Based on these results, what value of α would you recommend for an arbitrary injection location (you must pick a single value of α that best represents your data).

(Hint: it would probably be a good idea to do your calculations by writing a second Matlab program that solves the questions above. You can plot the relative concentration downstream and use `ginput` to pick the point where $C_{min}/C_{max} = 0.95$).

4. Physical, Chemical, and Biological Transformations

In the previous chapters, concentrations change in response to transport processes, such as diffusion, advection, and dispersion, and we have considered these processes in mass conserving systems. Now, we would like to look at systems where the mass of a given species of interest is not conserving. Processes that remove mass can be physical, chemical or biological in nature. Since the total mass of the system must be conserved, these processes generally change the species of interest into another species; thus, we will call these processes transformation.

This chapter begins by describing the common types of transformation reactions. Since we are interested in concentration changes, we review reaction kinetics and derive rate laws for first- and second-order systems. The methods are then generalized to higher-order reactions. Transformation is then added to our transport equation for two types of reactions. In the first case, the reaction becomes a source or sink term in the governing differential equation; in the second case, the reaction occurs at the boundary and becomes a boundary constraint on the governing transport equation. The chapter closes with an engineering application to bacteria die-off downstream of a wastewater treatment plant.

4.1 Concepts and definitions

Transformation is defined as production (or loss) of a given species of interest through physical, chemical, or biological processes. When no transformation occurs, the system is said to be conservative, and we represent this characteristic mathematically with the conservation of mass equation

$$\frac{dM_i}{dt} = 0 \tag{4.1}$$

where M_i is the total mass of species i. When transformation does occur, the system is called reactive, and, for a given species of interest, the system is no longer conservative. We represent this characteristic mathematically as

$$\frac{dM_i}{dt} = S_i \tag{4.2}$$

where S_i is a source or sink term. For reactive systems, we must supply these reaction equations that describe the production or loss of the species of interest. Since the total system mass must be conserved, these reactions are often represented by a system of transformation equations.

Transformation reactions are broadly categorized as either homogeneous or heterogeneous. Homogeneous reactions occur everywhere within the fluid of interest. This means that they are

distributed throughout the control volume; hence, they are represented as a source or sink term in the governing differential equation. By contrast, heterogeneous reactions occur only at fluid boundaries. They are not distributed throughout the control volume; hence, they are specified by source or sink boundary conditions constraining the governing differential equation.

Some reactions have properties of both homogeneous and heterogeneous reactions. As an example, consider a reaction that occurs on the surface of suspended sediment particles. Because the reaction occurs only at the sediment/water interface, the reaction is heterogeneous. But, because the sediment is suspended throughout the water column, the effect of the reaction is homogeneous in nature. Models that represent the reaction through boundary conditions (i.e. they treat the reaction as heterogeneous) are sometimes called two-phase, or multi-phase, models. Models that simplify the reaction to treat it as a homogeneous reaction are called single-phase, or mixture, models. To obtain analytical solutions, we often must use the single-phase approach.

4.1.1 Physical transformation

Physical transformations result from processes governed by the laws of physics. The classical example, which comes from the field of nuclear physics, is radioactive decay. Radioactive decay is the process by which an atomic nucleus emits particles or electromagnetic radiation to become either a different isotope of the same element or an atom of a different element. The three radioactive decay paths are alpha decay (the emission of a helium nucleus), beta decay (the emission of an electron or positron), and gamma decay (the emission of a photon). Gamma decay alone does not result in transformation, but it is generally accompanied by beta emission, which does.

A common radioactive element encountered in civil engineering is radon, a species in the uranium decay chain. Radon decays to polonium by alpha decay according to the equation

$$^{222}\mathrm{Rn} \rightarrow {}^{218}\mathrm{Po} + \alpha \tag{4.3}$$

where α represents the ejected helium nucleus, $^{4}_{2}\mathrm{He}$. As we will see in the section on kinetics, this single-step reaction is first order, and the concentration of radon decreases exponentially with time. The time it takes for half the initial mass of radon to be transformed is called the half-life.

Another common example that we will treat as a physical transformation is the settling of suspended sediment particles. Although settling does not actually transform the sediment into something else, it does remove sediment from our control volume by depositing it on the river bed. This process can be expressed mathematically by heterogeneous transformation equations at the river bed; hence, we will discuss it as a transformation.

4.1.2 Chemical transformation

Chemical transformation refers to the broad range of physical and organic chemical reactions that do not involve transformations at the atomic level. Thus, the periodic table of the elements contains all the building blocks of chemical transformations.

A classic example from aqueous phase chemistry is the dissolution of carbon dioxide (CO_2) in water (H_2O), given by the equilibrium equation

$$CO_2 + H_2O \rightleftharpoons HCO_3^- + H^+ \tag{4.4}$$

where HCO_3^- is called bicarbonate and H^+ is the hydrogen ion. The terms on the left-hand-side of the equation are called the reactants; the terms on the right-hand-side of the equation are called the products. Equilibrium refers to the state in which the formation of products occurs at the same rate as the reverse process that re-forms the reactants from the products. This give-and-take balance between reactants and products is indicated by the $\rightleftharpoons$ symbol.

4.1.3 Biological transformation

Biological transformation refers to that sub-set of chemical reactions mediated by living organisms through the processes of photosynthesis and respiration. These reactions involve the consumption of a nutritive substance to produce biomass, and are accompanied by an input or output of energy.

The classical photosynthesis equation shows the production of glucose, $C_6H_{12}O_6$, from CO_2 through the input of solar radiation, h_ν:

$$6CO_2 + 6H_2O \underset{h_\nu}{\rightarrow} C_6H_{12}O_6 + 6O_2. \tag{4.5}$$

Photosynthesis and respiration (particularly in the form of biodegradation) are of particular interest in environmental engineering because they affect the concentration of oxygen, a component essential for most aquatic life.

4.2 Reaction kinetics

Reaction kinetics is the study of the rate of formation of products from reactants in a transformation reaction. All reactions occur at a characteristic rate Δt_k. A common measure of this characteristic rate is the half-life, the time for half of the reactants to be converted into products. The other physical processes of interest in our problems (i.e. diffusion and advection) also occur with characteristic time scales, Δt_p. Comparing these characteristic time-scales, three cases can be identified:

- $\Delta t_k \ll \Delta t_p$: For these reactions we can assume the products are formed as soon as reactants become available, and we can neglect the reaction kinetics. Such reactions are called instantaneous and are reactant-limited; that is, the rate of formation of products is controlled by the rate of formation of reactants and not by the reaction rate of the tranformation equation.
- $\Delta t_k \gg \Delta t_p$: For these reactions the reaction can be ignored altogether, and we have a conservative (non-reacting) system.
- $\Delta t_k \approx \Delta t_p$: For these reactions neither the reaction nor the reaction kinetics can be ignored. Assuming the products are readily available, such reactions are called rate-limited, and the rate of formation of products is controlled by the reaction kinetics of the chemical transformation.

This last case, where the reactions are rate-limited, is the case of interest in this chapter, and in this section we discuss the rate laws of chemical kinetics.

To formulate the rate laws for a generic reaction, consider the mixed chemical reaction

$$aA + bB \rightarrow cC + dD, \tag{4.6}$$

where the lower-case letters are the stoichiometric coefficients of the reaction and the upper-case letters are the reactants (A and B) and products (C and D). The general form of the rate law for species A can be written as

$$\frac{d[A]}{dt} = R_A, \tag{4.7}$$

where R_A is a function describing the rate law for species A. We use the $[A]$-notation to designate concentration of species A (we will also use the equivalent notation C_A). From the stoichiometry of the reaction, the following ratios can also be inferred:

$$\frac{d[A]/dt}{d[B]/dt} = \frac{a}{b}, \text{ and}$$
$$\frac{d[A]/dt}{-d[C]/dt} = \frac{a}{c}.$$

Substituting the rate laws gives the relationships

$$R_A = +\frac{a}{b}R_B, \text{ and} \tag{4.8}$$
$$R_A = -\frac{a}{c}R_C. \tag{4.9}$$

We still require a means of writing the rate law for species i, R_i.

The general form of the rate law for product i formed from j reactants is

$$R_i = k_i C_1^{n_1} C_2^{n_2} ... \, C_j^{n_j}, \tag{4.10}$$

where k is the rate constant of the reaction, n_j is the order of the reaction with respect to constituent j, and $K = \sum_{i=1}^{j} n_i$ is the overall reaction order (note that the units of k depend on K). In general, reaction order cannot be predicted (except for simple, single-step, elementary reactions, where reaction order is the stoichiometric coefficient). Hence, reaction rate laws are determined on an experimental basis.

As one might expect, the reaction rate k is temperature dependent. One way to find a relationship for $k(T)$ is to use Arrhenius equation for an ideal gas

$$k = A \exp(-E_a/(RT)), \tag{4.11}$$

where A is a constant, E_a is the activation energy, R is the ideal gas constant, and T is the absolute temperature. Defining $k_1 = k(T_1)$ we can rearrange this equation to obtain

$$k(T) = k_1 \exp\left(\frac{E_a(T - T_1)}{RTT_1}\right). \tag{4.12}$$

for small temperature changes, this equation can be linearized by defining the constant

$$\theta = \frac{E_a}{RT_2T_1}. \tag{4.13}$$

Then, for $T_1 \leq T \leq T_2$,

$$k(T) = k_1 \exp(\theta(T - T_1)). \tag{4.14}$$

This form of the temperature dependence is often applied to non-gaseous systems as well.

4.2.1 First-order reactions

The general equation for a first-order reaction is

$$\frac{dC}{dt} = \pm kC, \tag{4.15}$$

where k has units $[1/T]$. Common examples are radioactive decay and the die-off of bacteria in a river. Whether mass increases or decreases in our control volume depends on our perspective: it depends on which species we are interested in, since one species will decrease as the other is created. To avoid confusion, we will always report the rate constant for the reaction using an absolute value. In this way, k is always positive. We then must chose the positive or negative sign in (4.15) depending on whether the species of interest is increasing (positive sign) or decreasing (negative sign) in our control volume.

This is a standard initial-value problem, whose solution can be found subject to the initial condition

$$C(t = 0) = C_0. \tag{4.16}$$

First, rearrange the governing equation to obtain

$$\frac{dC}{C} = \pm k dt. \tag{4.17}$$

Next, integrate both sides, yielding

$$\begin{aligned} \int \frac{dC}{C} &= \int \pm k dt \\ \ln(C) &= \pm kt + C_1, \end{aligned} \tag{4.18}$$

where C_1 is an integration constant. Solving for C we obtain

$$C = C_1' \exp(\pm kt), \tag{4.19}$$

where C_1' is another constant (given by $\exp(C_1)$). After applying the initial condition, we obtain

$$C(t) = C_0 \exp(\pm kt). \tag{4.20}$$

Figure 4.1 plots this solution for a decreasing concentration (negative sign in solution) for $C_0 = 1$ and $k = 1$.

As already discussed above, the characteristic reaction time is given by the time it takes for the ratio $C(t)/C_0$ to reach a specified value. For radioactive decay, k is negative, and two common characteristic times are the half-life and the e-folding time. The half-life, $T_{1/2}$, is the time required for the concentration ratio to reach $1/2$. From (4.20), the half-life is

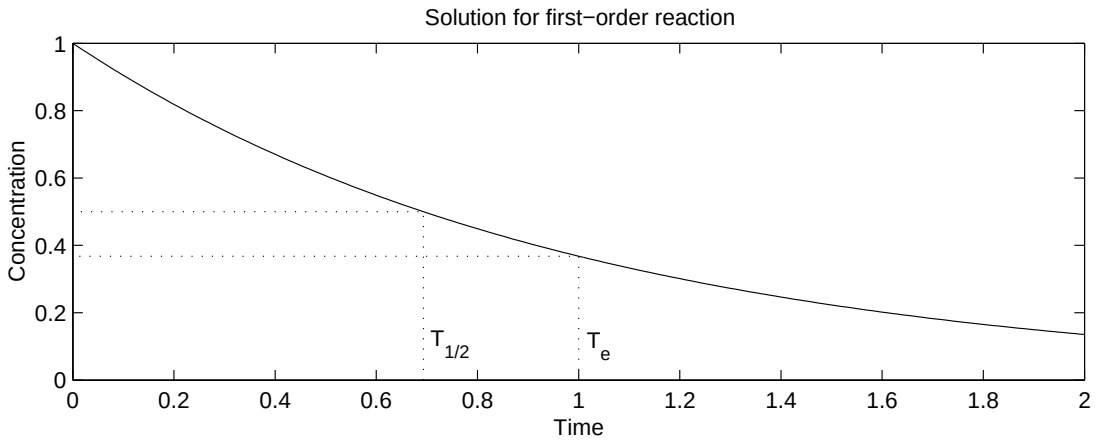

Fig. 4.1. Solution for a first-order transformation reaction. The reaction rate is $k = -1$.

$$T_{1/2} = \frac{\ln(1/2)}{k} \approx -\frac{0.69}{k}. \tag{4.21}$$

The e-folding time is the time required for the concentration ratio to reach $1/e$, given by

$$T_e = -\frac{1}{k}. \tag{4.22}$$

Hence, the characteristic times for first-order reactions are independent of the initial concentration (or mass).

Example Box 4.1:
Radioactive decay.

A radioactive disposal site receives a sample of high-grade plutonium containing 1 g of ^{239}Pu and a sample of low-grade plutonium containing 1 g of ^{242}Pu. The half-lives of the two samples are 24,100 yrs for ^{239}Pu and 379,000 yrs for ^{242}Pu. On average, how many atoms transform per second for each sample of plutonium?

The instantaneous disintegration rate is given by

$$\frac{\partial C}{\partial t} = -kC = \frac{\ln(0.5)}{T_{1/2}} C.$$

The molar weight of plutonium is 244.0642 g/mol; hence, we have $N_0 = 2.467 \cdot 10^{21}$ atoms per sample. For ^{239}Pu, we have

$$\frac{\partial N}{\partial t} = -2.876 \cdot 10^{-5} N_0 = -2.248 \cdot 10^{9} \text{ atoms/s}$$

and for ^{239}Pu, we have

$$\frac{\partial N}{\partial t} = -1.829 \cdot 10^{-6} N_0 = -1.430 \cdot 10^{8} \text{ atoms/s}.$$

Hence, even though the half-lives are very long, we still have a tremendous number of transformations per second in these two samples of plutonium.

4.2.2 Second-order reactions

The general equation for a second-order reaction is

Example Box 4.2:
Radio-carbon dating.

Radio-carbon dating can be used to estimate the age of things that once lived. The principle of radio-carbon dating is to compare the ^{14}C ratio in something when it was alive to the ^{14}C ratio in the artifact now and use (4.20) to estimate how long the artifact has been dead. The main assumption is that all living things absorb the same ratio of radioactive carbon, ^{14}C, to stable carbon, ^{12}C, as has the atmosphere. For this method, scientists require an accurate estimate of the half-life of ^{14}C, which is 5730±40 yrs. Use the error-propogation equation (3.73) to estimate the accuracy of this method.

Currently, the radioactive carbon in the atmosphere is about $1 \cdot 10^{-10}$ % of the total carbon. Thus, per mole of C, there would be $6.022 \cdot 10^{11}$ atoms of ^{14}C. If we assume the atmosphere has historically had the same ^{14}C ratio, then we can use this number for C_0. A student carefully measures the ^{14}C content of a sample to have $C = 7.528 \cdot 10^{10}$ atoms of ^{14}C per mole. Thus, the age of the sample is

$$\begin{aligned} t &= -\frac{1}{k} \ln\left(\frac{C}{C_0}\right) \\ &= 17190 \text{ yrs old.} \end{aligned}$$

We can estimate the accuracy as follows. First, re-write the estimate equation as

$$t = -\frac{1}{k} \left(\ln(C) - \ln(C_0)\right).$$

Second, we calculate the necessary derivatives

$$\begin{aligned} \frac{\partial t}{\partial k} &= \frac{1}{k^2} \ln\left(\frac{C}{C_0}\right) \\ \frac{\partial t}{\partial C} &= -\frac{1}{kC} \\ \frac{\partial t}{\partial C_0} &= -\frac{1}{kC_0}. \end{aligned}$$

Finally, we incorporate these derivatives into the error-propagation equation

$$\begin{aligned} \delta t = \Bigg[&\left(\frac{1}{k^2} \ln\left(\frac{C}{C_0}\right) \delta k\right)^2 + \left(\frac{1}{kC} \delta C\right)^2 \\ &+ \left(\frac{1}{kC_0} \delta C_0\right)^2 \Bigg]^{1/2}. \end{aligned}$$

Assuming an accuracy of ±0.1% for the ^{14}C concentrations, the accuracy of our estimate is

$$\begin{aligned} \delta t &= \sqrt{119.4^2 + 8.2^2 + 8.3^2} \\ &= \pm 120 \text{ yrs.} \end{aligned}$$

Hence, the error in the half-life is the most important error, and leads of an error of ±120 yrs for this sample.

$$\frac{dC}{dt} = \pm k C^2, \tag{4.23}$$

where k has units $[L^3/M/T]$. An example is the reaction of iodine gas given by the reaction

$$2\text{I(g)} \rightarrow \text{I}_2\text{(g)}, \tag{4.24}$$

which has rate constant $k = 7 \cdot 10^9$ l/(mol·s).

This is another initial-value problem, which can be solved subject to the initial condition

$$C(t = 0) = C_0. \tag{4.25}$$

We begin by rearranging the governing equation to obtain

$$\frac{dC}{C^2} = \pm k t. \tag{4.26}$$

This time we integrate using definite integrals and our initial condition, giving

$$\begin{aligned} \int_{C_0}^{C} \frac{dC'}{C'^2} &= \int_0^t \pm k dt \\ -\left(\frac{1}{C} - \frac{1}{C_0}\right) &= \pm k t. \end{aligned} \tag{4.27}$$

Solving for $C(t)$ gives

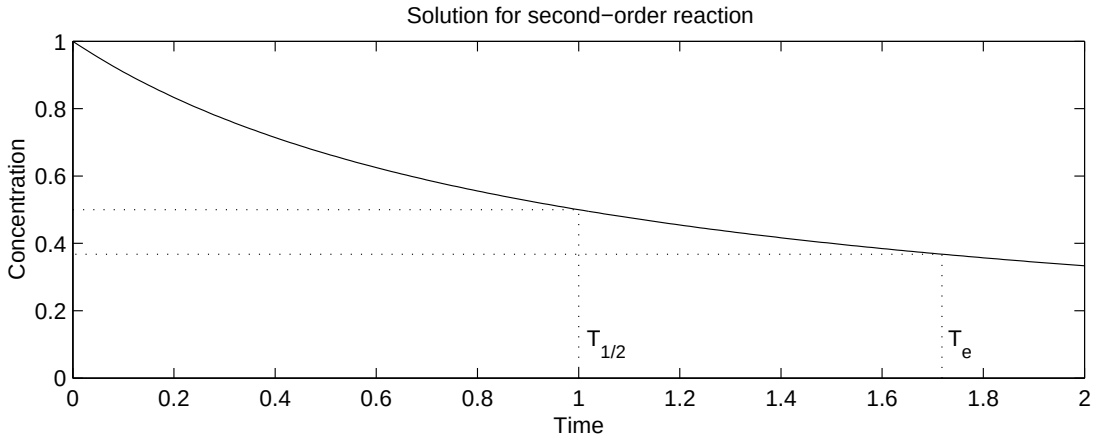

Fig. 4.2. Solution for a second-order transformation reaction. The reaction rate is $k = -1$.

$$C(t) = \frac{1}{\mp kt + 1/C_0}. \tag{4.28}$$

Figure 4.2 plots this solution for decreasing concentration (positive sign in the equation) with $C_0 = 1$ and $k = 1$.

The characteristic times for a second-order reaction are given by

$$T_{1/2} = -\frac{1}{kC_0}, \text{ and} \tag{4.29}$$

$$T_e = -\frac{(e-1)}{kC_0}. \tag{4.30}$$

Hence, for second- and higher-order reactions, the characteristic times depend on the initial concentration!

4.2.3 Higher-order reactions

The general equation for an nth-order reaction is

$$\frac{dC}{dt} = \pm kC^n, \tag{4.31}$$

where k has units $[L^{3(n-1)}/M^{(n-1)}/T]$. The general solution subject to the initial condition $C(t = 0) = C_0$ is

$$\left(\frac{1}{(n-1)}\right)\left[\frac{1}{C^{n-1}} - \frac{1}{C_0^{(n-1)}}\right] = kt \tag{4.32}$$

for $n \geq 2$. Such reactions are rare, and one generally tries different values of n to find the best fit to experimental data.

A common means of dealing with higher-order reaction rates is to linearize the reaction in the vicinity of the concentration of interest, C_I. The linearized reaction rate equation is

$$R = k^*C - kC_I^2, \tag{4.33}$$

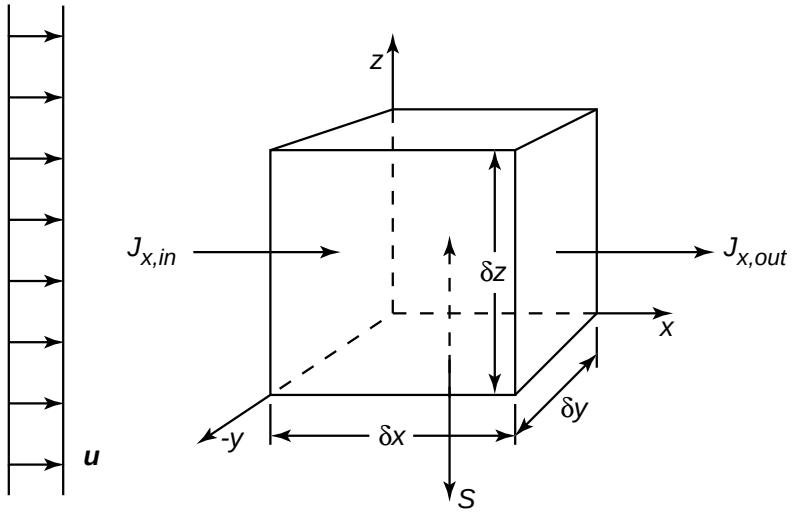

Fig. 4.3. Schematic of a control volume with crossflow and reaction.

where k is the real rate constant and k^* is the linearized rate constant; note that kC_I^2 is also a constant. Thus, higher-order reactions can be treated as first-order reactions in the vicinity of a known concentration C_I.

4.3 Incorporating transformation with the advective-diffusion equation

Having a thorough understanding of transformations and reaction kinetics, we are ready to incorporate transformations into our transport equation, the advective diffusion equation. As we pointed out earlier, reactions are treated differently, depending on whether they are homogeneous or heterogeneous. Homogeneous reactions add a term to the governing differential equation; whereas, heterogeneous reactions are enforced with special boundary conditions.

4.3.1 Homogeneous reactions: The advective-reacting diffusion equation

Homogeneous reactions add a new term to the governing transport equation because they occur everywhere within our system; hence, they provide another flux to our law of conservation of mass. Referring to the control volume in Figure 4.3, the mass conservation equation is

$$\frac{\partial M}{\partial t} = \sum \dot{m}_{in} - \sum \dot{m}_{out} \pm S, \tag{4.34}$$

where S is a source or sink reaction term. We have already seen in the derivation of the advective diffusion equation that

$$\delta \dot{m} = \left(D \frac{\partial^2 C}{\partial x_i^2} - u_i \frac{\partial C}{\partial x_i} \right) \delta x \delta y \delta z. \tag{4.35}$$

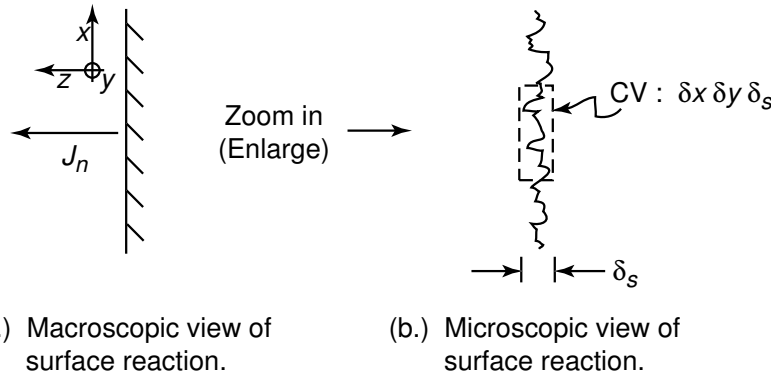

Fig. 4.4. Schematic representation of the reaction boundary condition. S represents the source or sink term, δ_s is the reaction sublayer, and $\delta x \delta y$ is the surface area into the page of the boundary control volume.

The reaction term is just the kinetic rate law integrated over the volume, giving

$$S = \pm R \delta x \delta y \delta z. \tag{4.36}$$

Combining these results in an equation for the concentration, we obtain

$$\frac{\partial C}{\partial t} + \frac{\partial u_i C}{\partial x_i} = D \frac{\partial^2 C}{\partial x_i^2} \pm R, \tag{4.37}$$

where R has the same form as in the sections discussed above. Appendix B presents solutions for a wide range of cases.

As an example, consider the solution for an instantaneous point source of a first-order reacting substance in one dimension. The solution for $C(t)$ can be found using Fourier transformation to be

$$C(x,t) = \frac{M}{A\sqrt{4\pi D t}} \exp\left(-\frac{(x-ut)^2}{4Dt}\right) \exp(\pm kt), \tag{4.38}$$

where M is the total mass of substance injected, A is the cross-sectional area, D is the diffusion coefficient, u is the flow velocity, and k is the reaction rate constant. If we compare this solution to the solution for a first-order reaction given in (4.20), we see that the initial concentration C_0 is replaced by the time-varying solution in the absence of transformation. This observation is helpful for deriving solutions to cases not presented in Appendix B.

4.3.2 Heterogeneous reactions: Reaction boundary conditions

Heterogeneous reactions occur only at the boundaries; hence, they provide new flux boundary conditions as constraints on the governing transport equation. Examples include corrosion, where there is an oxygen sink at the boundary, and also catalyst reactions, where the presence of other-phase boundaries is needed to facilitate or speed up the reaction. Figure 4.4 shows a macroscopic and microscopic view of the solid boundary. To define the boundary condition, we require an expression for the source/sink flux, J_n.

Writing the conservation of mass for the control volume in the microscopic view, we have

$$\frac{dM}{dt} = \pm S, \tag{4.39}$$

where S is the source or sink mass flux over the control volume. We can expand this expression to obtain

$$\delta x \delta y \delta_s \frac{dC_s}{dt} = \pm \delta x \delta y \delta_s R, \tag{4.40}$$

where δ_s is the reaction sublayer depth and C_s is the mean surface concentration within the reaction sublayer. Since we are looking for a flux, $\boldsymbol{J}_n$, with units [M/(L^{2}T)], we must write the above equation on a per unit area basis, that is

$$\delta_s \frac{dC_s}{dt} = \pm \delta_s R = \pm J_n. \tag{4.41}$$

Thus, the general form of a reaction boundary condition is

$$J_n = \delta_s R. \tag{4.42}$$

As an example, consider the one-dimensional case for a first-order reacting boundary condition. For first order reactions, $R = kC_s$, and for the one-dimensional case, $J_n = -D(dC/dn)|_s$. Substituting into the general case, we obtain

$$-D\frac{dC}{dn}\bigg|_s = \pm \delta_s k C_s. \tag{4.43}$$

The reaction constant, k, is controlled by the boundary geometry, the possible presence of a catalyst, and by the kinetics for the species of interest; hence, k is a property of both the species and the boundary surface. The reaction rate is often given as a reaction velocity, $k_s = k\delta_s$. These types of boundary conditions will be handled in greater detail in the chapter on sediment- and air/water interfaces.

4.4 Application: Wastewater treatment plant

A wastewater treatment plant (WWTP) discharges a constant flux of bacteria, $\dot{m}$ into a stream. How does the concentration of bacteria change downstream of the WWTP due to the die-off of bacteria? The river is $h = 20$ cm deep, $L = 20$ m wide and has a flow rate of $Q = 1$ m^3/s. The bacterial discharge is $\dot{m} = 5 \cdot 10^{10}$ bacteria/s, and the bacteria can be modeled with a first-order transformation equation with a rate constant of 0.8 day^{-1}. The bacteria are discharged through a line-source diffuser so that the discharge can be considered well-mixed both vertically and horizontally at the discharge location. Refer to Figure 4.5 for a schematic of the situation.

The solution for a first-order reaction was derived above and is given by

$$C(t) = C_0 \exp(-kt). \tag{4.44}$$

The initial concentration C_0 is the concentration at the discharge, which we can derive through the relationship

$$\dot{m}_0 = QC_0. \tag{4.45}$$

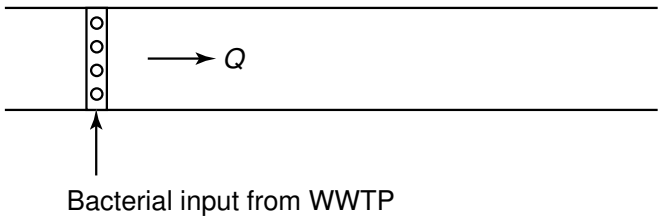

Fig. 4.5. Schematic of bacterial discharge at WWTP.

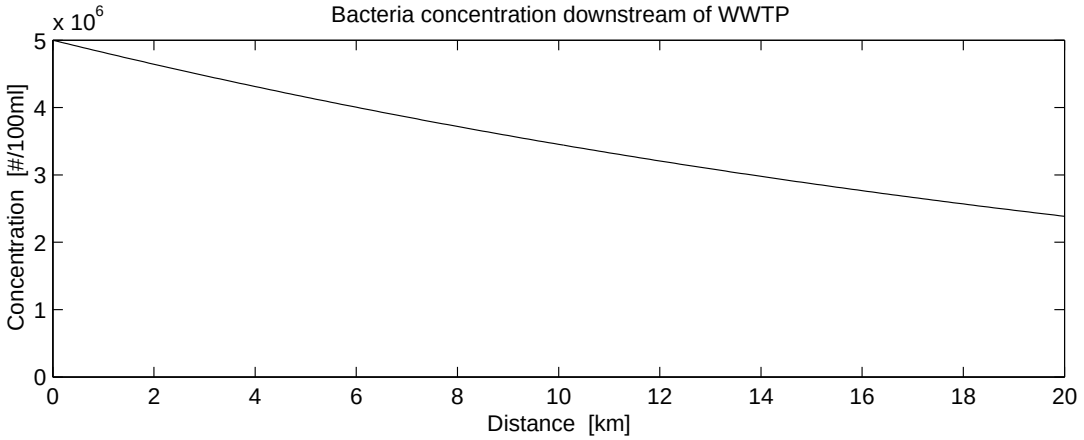

Fig. 4.6. Bacteria concentration downstream of WWTP.

Substituting the values given above, $C_0 = 5 \cdot 10^6$ #/100ml. The next step is to convert the time t in our general solution to space x through the relationship

$$x = ut. \tag{4.46}$$

Substituting, we have

$$\begin{aligned} C(x) &= C_0 \exp\left(-k\frac{x}{u}\right) \\ &= 5 \cdot 10^6 \exp(-3.7 \cdot 10^{-5} x) \ \#/100\text{ml}. \end{aligned} \tag{4.47}$$

The half-life for this case can be given in terms of downstream distance. From (4.21), we have

$$\begin{aligned} x_{1/2} &= -\frac{0.69}{k} \\ &= -\frac{0.69}{-3.7 \cdot 10^{-5}} \\ &= 18.6 \text{ km}. \end{aligned} \tag{4.48}$$

Figure 4.6 plots the solution for the first 20 km of downstream distance.

Summary

This chapter introduced the treatment of transformation processes. Three classes of transformations were considered: physical, chemical and biological. The rate laws governing the transformations were derived from chemical reaction kinetics. Solutions for first and second order reactions were derived, and methods for dealing with higher-order reactions and temperature dependence of rate constants were presented. These rate laws were then combined with the transport equation for two types of reactions: for homogeneous reactions, the rate law becomes a source or sink term in the governing differential transport equation; for heterogeneous reactions, a modified rate law becomes a boundary condition constraining the governing differential equation. An example of bacterial die-off downstream of a WWTP closed the chapter.

Exercises

4.1 Reaction order. A chemical reaction is of order 1.5. What are the units of the rate constant? What is the solution to the rate equation (i.e. what is $C(t)$)? Write an expression for the half-life.

4.2 Clean disposal. A chemical tanker runs aground near the shore of a wide river. The company declares the load on the tanker a complete loss, due to contamination by river water, and decides to slowly discharge the hazardous material into the river to dispose of it. The material (an industrial acid) reacts with the river water (the material is buffered by the river alkalinity) and is converted to harmless products with a rate constant of $k = 5 \cdot 10^{-5}$ s^{-1}. Calculate the maximum discharge rate such that a concentration standard of 0.01 mg/l is not exceeded at a distance of 1.5 km downstream. The river flow rate is $Q = 15$ m^3/s, the depth is $h = 2$ m, the width is $B = 75$ m, and the concentration of acid in the grounded tanker is 1200 mg/l. If the tanker contains 10000 m^3, how long will it take to safely empty the tanker?

4.3 Water treatment. In part of a water treatment plant, a mixing tank is used to remove heavy metals. Untreated water flows into the tank where is it rigorously mixed (instantaneously mixed) and brought into contact with other chemicals that remove the metals. A single outlet is installed in the tank. Assume the inflow and outflow rates are identical, and assume metals are removed in a first-order reaction with a rate constant of $k = 0.06$ s^{-1}. The tank volume is 15 m^3. What is the allowable flow rate such that the exit stream contains 10% of the metals in the input stream? How high can the flow rate be if the reaction rate constant is doubled?

5. Boundary Exchange: Air-Water and Sediment-Water Interfaces

In the previous chapter we introduced transformation and described both homogeneous and heterogeneous reactions. Now, we would like to look in more detail at heterogeneous reactions and discuss the chemical and physical processes at interfaces that lead to boundary fluxes of chemical species. The two major boundary types in environmental fluid mechanics are the air-water and sediment-water interfaces. Because the processes at both boundaries are very similar, we treat them together in this chapter under the heading of boundary exchange.

This chapter is divided into three main sections. First, the boundary layer in the vicinity of the interface is described, and two common models for treating the boundary dynamics are introduced without specifying what type of boundary is involved. Second, the air-water interface is introduced, and methods are described for treating gas exchange across the interface. As an example, the Streeter-Phelps equation for predicting oxygen concentrations downstream of an organic waste stream is introduced. Third, the sediment-water interface is described, including the complex physical and transformation processes that bring sediment and water into contact, and a short description of the chemistry that occurs at the sediment-water interface is provided.

5.1 Boundary exchange

Under the concept of boundary exchange, we are primarily interested in the transfer of substances that can be dissolved in the water phase. Examples at the air-water interface include chemicals present in both phases (the air and the water), such as oxygen and carbon dioxide, as well as volatile chemicals that off-gas from the water into the atmosphere, where the concentration is negligible, such as mercuric compounds (e.g. $(CH_3)_2Hg$), chlorinated hydrocarbons (e.g. CH_2Cl), and a host of other organic compounds. Examples at the sediment-water interface include metals, salts, nutrients, and organic compounds.

The transfer of these substances at an interface leads to a net mass flux, $\boldsymbol{J}$, which can have diffusive and advective components. Diffusive transfer is often assumed to be controlled by equilibrium chemistry. Advective transfer results from a host of processes, such as the ejection of sea spray from waves or the flow of groundwater. In general, this net mass flux becomes a boundary condition that is imposed on the governing transport equation that is then solved either numerically or analytically.

The challenge in describing boundary exchange is in predicting the magnitude of $\boldsymbol{J}$. Unfortunately, the dynamics that control the magnitude of the exchange flux are often microscopic in nature and must be predicted by sub-models. If we consider the example of sugar dissolving in a

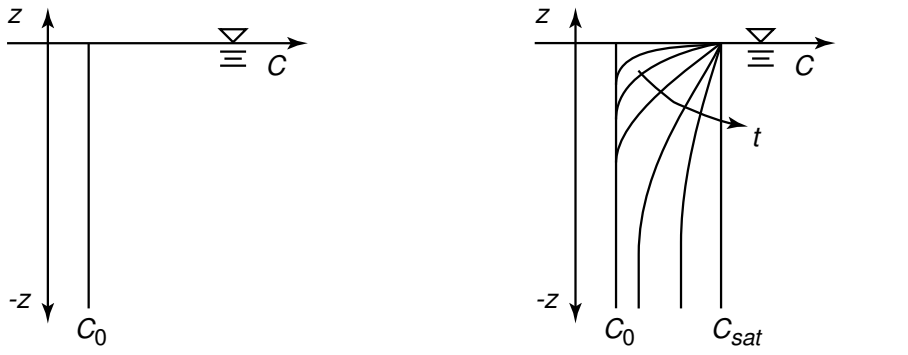

Fig. 5.1. Schematic for the boundary exchange for a dissolving substance into a stagnant water body. Figure (a.) shows the initial condition, and Figure (b.) shows the time-response of the concentration profiles. C_{sat} is the saturation concentration of the dissolving substance.

cup of tea, we know from experience that the sugar dissolves much faster if we stir the tea than if we let the system remain stagnant. But, if we add sand to a cup of tea and stir for a few years, the sand will still not completely dissolve. Hence, we expect $\boldsymbol{J}$ to depend on the physico-chemical properties of the species in the exchange process, as well as on the hydrodynamic conditions in each phase.

5.1.1 Exchange into a stagnant water body

As a simple introduction, consider a completely stagnant case, where the hydrodynamic effects on transfer are negligible. Figure 5.1 describes such a situation. The initial condition is that a semi-infinite body of water has a uniform initial concentration $C(z,t) = C_0$ that is less than the saturation concentration of the substance, C_{sat}. The surface interface is then instantaneously exposed to an infinite source of the substance. Because the concentration in the water body is below C_{sat}, the substance will want to dissolve into the water until the water body reaches a uniform concentration of C_{sat}. The dissolution reaction is a very fast reaction; hence, the concentration at the surface becomes C_{sat} as soon as the source is applied. However, the movement of C into the water body is limited by diffusion away from the surface. This process is illustrated schematically in Figure 5.1(b.).

To treat this stagnant case quantitatively, consider the governing transport equation and its solution. Because $\partial C/\partial x = \partial C/\partial y = 0$, we can use the one-dimensional equation, and because the fluid is stagnant, we can neglect advection, leaving us with

$$\frac{\partial C}{\partial t} = D\frac{\partial^2 C}{\partial z^2}. \tag{5.1}$$

The boundary and initial conditions are:

$$C(-\infty, t) = C_0 \tag{5.2}$$

$$C(0, t) = C_{sat} \tag{5.3}$$

$$C(z, 0) = C_0. \tag{5.4}$$

The solution for this case was found in Section 2.2.2 for the case of $C_0 = 0$. The modified solution for this case is

$$\frac{C(z,t) - C_0}{C_{sat} - C_0} = 1 - \text{erf}\left(\frac{-z}{\sqrt{4Dt}}\right) \tag{5.5}$$

where the minus sign inside the error function is needed since z is negative downward. Recall also that (5.5) is only valid for $z \leq 0$.

From this solution we can derive an expression for the boundary flux at $z = 0$ using Fick's law. Writing the flux law for the stagnant case in one-dimension, we have

$$\begin{aligned} J_z &= uC - D \left.\frac{\partial C}{\partial z}\right|_{z=0} \\ &= -D \left.\frac{\partial C}{\partial z}\right|_{z=0} \end{aligned} \tag{5.6}$$

since $u = 0$. Substituting the solution above, we can compute J_z as

$$J_z(t) = -(C_{sat} - C_0)\sqrt{\frac{D}{\pi t}}. \tag{5.7}$$

We can also compute the characteristic thickness, δ, of the mixing layer, or the concentration boundary layer, over which the concentrations change from C_{sat} to C_0:

$$\delta = \sigma_z = \sqrt{2Dt}. \tag{5.8}$$

Hence, for the stagnant case, the mixing layer grows deeper in time and the boundary flux can be written as

$$J_z = -k_l(C_{sat} - C_0) \tag{5.9}$$

where k_l is the transfer velocity, given in this stagnant case by $k_l = \sqrt{D/(\pi t)}$, with units $[L/T]$.

5.1.2 Exchange into a turbulent water body

When the water body present below (or above) the interface is turbulent, large-scale motion within the fluid body will interact with the mixing layer, defined by the concentration boundary layer δ.

This turbulent motion has two major effects. First, the turbulence in the bulk fluid erodes the boundary layer, thereby, limiting the growth of the layer thickness δ. Since the bulk fluid and interface concentrations C_0 and C_i are independent of δ, this effect will increase the concentration gradient; hence, J_z will be larger than in the stagnant case. Second, the turbulence in the bulk fluid will cause motion within the boundary layer, thereby, increasing the effective diffusivity. Hence, J_z will again be larger than the stagnant case. However, molecular diffusion is still expected to be a rate-limiting process since turbulence (three-dimensional motion) cannot exist directly at the surface. For the case of a large groundwater flux, this last statement may have to be relaxed, but for now we will assume the actual interface is laminar.

These effects of turbulence can be summarized in the following list of expectations regarding the concentration boundary layer for a turbulent flow:

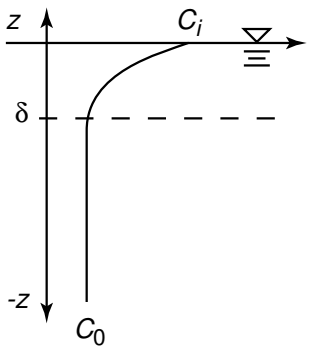

Fig. 5.2. Schematic of the interface exchange for a turbulent water body.

1. We expect an average film thickness, δ. That is, turbulence will prevent δ from growing arbitrarily large.
2. We expect an average boundary layer flux (transfer velocity). This is a consequence of the previous expectation.
3. The transfer rate can be limited on either side of the interface by the chemical or hydrodynamic conditions in that phase.

The following two sections introduce models which seek expressions for k_l that satisfy the three expectations listed above.

5.1.3 Lewis-Whitman model

The simplest type of model is the Lewis-Whitman model, which says that the mixing layer is a constant thickness, δ, which leads to k_l given by

$$k_l = \frac{D}{\delta} \tag{5.10}$$

(refer to Figure 5.2). Note that for this model k_l is linearly proportional to D, as compared to the square-root dependence derived in the stagnant case. Also, the mixing depth δ is a pure function of the hydrodynamic condition. Thus, once one has an expression for δ, the transfer velocity for different substances can be computed using the various respective molecular diffusivities D_m. The weakness of this model is that is does not provide any physical insight into how to predict δ; hence, δ must be determined empirically.

5.1.4 Film-renewal model

The film-renewal model improves on the Lewis-Whitman model by providing a physical mechanism that controls the boundary layer thickness; hence, we can use this mechanism to formulate a predictive model for δ. In the film renewal model, the boundary layer is allowed to grow as in the stagnant case until at some point the turbulence suddenly replaces the water in the boundary layer, and the mixing layer growth starts over from the beginning. This mixing layer exchange,

or film-renewal, occurs periodically with a renewal frequency that is a function of the turbulent characteristics of the flow.

Under the idealized case that the boundary layer grows undisturbed until it is suddenly completely replaced by water from the bulk turbulent flow, the net flux at the boundary can be determined analytically. The governing transport equation and the initial and boundary conditions are exactly the same as in the stagnant case (see (5.1) to (5.4)). The solution is given by (5.5), and the net flux at the boundary is given by (5.7). These solutions are only valid, however, from $t = 0$ to $t = t_r$, the time between renewal events. The mean boundary flux over one cycle can be found easily by taking the time average

$$\begin{aligned}\overline{J}_z &= \frac{1}{t_r}\int_t^{t+t_r} J_z(t)dt \\ &= \frac{1}{t_r}\int_t^{t+t_r} -(C_i - C_0)\sqrt{\frac{D}{\pi t}}dt \\ &= -(C_i - C_0)\sqrt{\frac{4D}{\pi t_r}}\end{aligned} \tag{5.11}$$

or, since the renewal frequency, r, is just $1/t_r$,

$$\overline{J}_z = -(C_i - C_0)\sqrt{\frac{4Dr}{\pi}}. \tag{5.12}$$

Thus, the average transfer velocity is independent of time and is given by

$$k_l = \sqrt{\frac{4Dr}{\pi}} \tag{5.13}$$

which leaves us with the need to predict r.

The renewal frequency r is a characteristic of the turbulence. Recall that a turbulent flow is a spectrum of eddy sizes, from the integral scale down to the Kolmogorov scale, and is driven, for homogeneous turbulence, by the dissipation rate

$$\epsilon = \frac{u_I^3}{l_I} \tag{5.14}$$

where u_I and l_I are the integral velocity and length scales of the flow, respectively. For a shear flow, the approximations $u_I = u_*$ and $l_I = h$ are generally valid, where u_* is the shear velocity and h is the depth of the shear layer. We can derive two extreme estimates for r: one for the case that the concentration boundary layer is renewed by Kolmogorov-scale eddies (called the small-eddy estimate), and another for the case that the concentration boundary layer is renewed by integral-scale eddies (called the large-eddy estimate).

Small-eddy estimate of r. Since the smallest eddies are dissipated by viscosity ν, an estimate for the Kolmogorov time scale t_K can be written as

$$t_K = \sqrt{\frac{\nu}{\epsilon}}. \tag{5.15}$$

Taking r as $1/t_K$ and substituting approximations for u_I and l_I for a shear flow, we can obtain

$$r = \sqrt{\frac{u_*^3}{h\nu}}. \tag{5.16}$$

If we further substitute the shear velocity as $u_* = \overline{u}\sqrt{f/8}$, where $\overline{u}$ is the mean flow velocity and f is a friction coefficient, then an estimate for k_l can be written as

$$k_l = K\frac{\overline{u}^{3/4}}{h^{1/4}} \tag{5.17}$$

where K is a constant that depends on the fluid properties (i.e. ν) , the physico-chemical properties of the substance (i.e. D), and on the boundary type (i.e. f). For k_l at the air-water interface with units cm/s, K is of order 10^{-1} to 10^0.

Large-eddy estimate of r. The time scale of the largest eddies is given by the integral time scale t_I, which for a shear flow is

$$t_I = \frac{u_*}{h}. \tag{5.18}$$

Taking $r = 1/t_I$, and substituting $u_* = \overline{u}\sqrt{f/8}$ leads the the expression for k_l given by

$$k_l = K\frac{\overline{u}^{1/2}}{h^{1/2}} \tag{5.19}$$

where K is another constant which depends on the the physico-chemical properties of the substance (i.e. D), and on the boundary type (i.e. f).

Experimental data are sparse, but tend to agree better with the relationship $k_l \propto \overline{u}^{3/4}$; hence, it is most likely the small-scale eddies that are responsible for the film renewal.

5.2 Air/water interface

At the air-water interface we are primarily concerned with the transfer of gases that can be dissolved in the water. The substance may, or may not, be measurable in the gas phase. Figure 5.3 demonstrates the general case for a substance with measurable concentrations in both the gas and liquid phase. As the figure demonstrates, there is a concentration boundary layer in the vicinity of the water surface for both the phases. Because there cannot be a build-up of concentration at the interface, the flux from the gas into the water, $\dot{m}_a$, must equal the flux at the interface into the water, $\dot{m}_w$. Hence, only one of the phases contains the rate-limiting step.

The rate of transfer at the interface is controlled by the transfer velocity k_l; thus, the rate-limiting phase will have the lowest value of k_l. Consider first the Lewis-Whitman model. The transfer velocity increases as the diffusion coefficient increases and as the concentration boundary layer gets thinner. Both of these conditions are higher in the gas phase than in the liquid phase. The more complex film-renewal model gives the same conclusion: the flux at the interface can be higher in the air than in the water. Therefore, we generally assume the substance is immediately available at the gas side of the interface, and we must only consider the concentration boundary layer in the water phase in order to compute the net flux at the boundary.

Because the air-water interface is a moving boundary, two further complications can arise that are not addressed in either of our boundary transfer models. First, wind generates shear

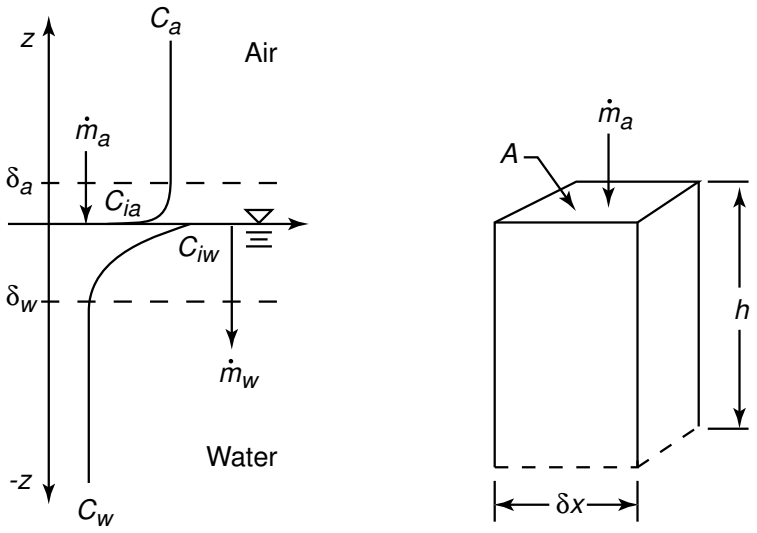

Fig. 5.3. Schematic of the air-water interface for a substance with measurable concentrations in both the air and the water.

directly at the interface. We considered shear at the channel bed as the generation mechanism for turbulence in the film-renewal model. However, shear at the air-water interface generates motion at the interface that can strongly affect (and greatly increase) the transfer velocity from the case of a stagnant wind. These effects are particularly important in the ocean and in lakes. Second, surface waviness, breaking and instabilities, greatly increases gas transfer by disturbing the exchange boundary layer. For example, breaking waves entrain air and carry air bubbles deep into the fluid, that then dissolve as they rise back to the water surface. Such dynamic situations must be handled by more complicated techniques.

5.2.1 General gas transfer

Assuming the rate-limiting step is on the liquid side of the interface, we can now derive a general expression for gas transfer into a well-mixed medium, such as at the surface layer of a lake in summer. We will consider the control volume in Figure 5.3(b.). The conservation of mass equation is

$$\frac{dM}{dt} = \dot{m}_{in} - \dot{m}_{out} \tag{5.20}$$

$$= \dot{m}_w. \tag{5.21}$$

To write M as a concentration, we must define the size of the control volume. A common assumption is to use the depth of the well-mixed water body, h, and a non-specified surface area, A. Then, substituting from (5.9)

$$Ah\frac{dC_w}{dt} = Ak_l(C_{iw} - C_w) \tag{5.22}$$

which is rearranged to give

Example Box 5.1:
Volatilization.

As an example, consider the off-gassing of the volatile compound benzyl chloride (CH_2Cl) from a stream with velocity $\overline{u} = 1$ m/s and initial concentration of CH_2Cl of $C_0 = 0.1$ mg/l. The gas transfer coefficient is $K_l = 1 \cdot 10^{-4}$ s^{-1}. Because CH_2Cl is not present in the atmosphere, C_{iw} can be taken as zero. Then (5.23) becomes

$$\frac{dC_w}{dt} = -K_l C_w$$

which, after substituting $t = x/\overline{u}$, has solution

$$C_w(x) = C_0 \exp\left(-K_l \frac{x}{\overline{u}}\right).$$

Thus, CH_2Cl concentration decreases exponentially downstream from the source due to volatilization.

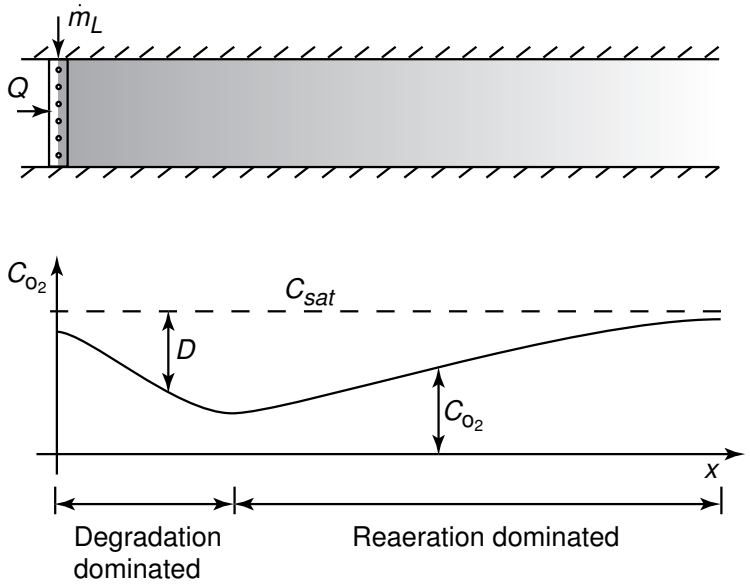

Fig. 5.4. Schematic of the dissolved oxygen sag curve downstream of a biodegradable waste stream. The upper figure illustrates the receiving stream; the lower diagram shows the downstream dissolved oxygen concentration.

$$\frac{dC_w}{dt} = K_l(C_{iw} - C_w) \tag{5.23}$$

where $K_l = k_l/h$ is the gas transfer coefficient with units [T^{-1}].

5.2.2 Aeration: The Streeter-Phelps equation

A common problem that requires modeling the exchange of oxygen through the air-water interface is that of predicting the oxygen dynamics in a river downstream of a biodegradable waste stream. As the waste is advected downstream, it degrades, thereby consuming oxygen. The oxygen deficit, however, drives the counteracting aeration process, so that the situation is similar to that shown in Figure 5.4.

Biodegradation is a reaction that consumes oxygen. A general biodegradation equation can be written as

$$\mathrm{OM} + \mathrm{O_2} \underset{\text{microorganisms}}{\rightarrow} \mathrm{CO_2} + \mathrm{H_2O} + \text{new cells} + \text{stable products}$$

where OM stands for organic matter (the biodegradable waste). It can be shown in the laboratory that the consumption of OM is a first-order reaction. Thus, the rate-law for the consumption of OM is given by

$$\frac{d[\mathrm{OM}]}{dt} = -k_d[\mathrm{OM}] \tag{5.24}$$

where k_d is the rate constant for biodegradation. In the classical literature on this subject, the concentration of OM is called the oxygen demand and is given the symbol L. Substituting L for [OM] in the above equation and imposing the initial condition $L(t = 0) = L_0$, the solution for the consumption of oxygen demand becomes

$$L(t) = L_0 \exp(-k_d t) \tag{5.25}$$

where L_0 is called the ultimate carbonaceous oxygen demand. The word carbonaceous refers to the fact that the oxygen consumption is due to conversion of carbon-based organic matter as opposed to any other chemical reaction that might consume oxygen. Because $\mathrm{O_2}$ is consumed at the same rate as OM, we can write the following relationship:

$$\begin{aligned}\frac{d[\mathrm{O_2}]}{dt} &= \frac{d[\mathrm{OM}]}{dt} \\ &= -k_d L_0 \exp(-k_d t).\end{aligned} \tag{5.26}$$

If we define the oxygen deficit, $D = ([\mathrm{O_2}]_{sat} - [\mathrm{O_2}])$, then the production of oxygen deficit is given by

$$\frac{dD}{dt} = k_d L_0 \exp(-k_d t). \tag{5.27}$$

This equation represents a sink term for oxygen due to biodegradation of the waste stream.

At the same time the waste is being degraded the river is being aerated by exchange at the air-water interface. The mass flux of oxygen, $\dot{m}_{\mathrm{O_2}}$, is derived from the boundary exchange flux in (5.9)

$$\begin{aligned}\dot{m}_{\mathrm{O_2}} &= -Ak_r([\mathrm{O_2}]_{sat} - [\mathrm{O_2}]) \\ &= -Ak_r D\end{aligned} \tag{5.28}$$

where k_r is the river aeration transfer velocity for oxygen and the negative sign indicates a flux of oxygen goes into the river.

We can now use the control volume in Figure 5.3(b.) to derive the oxygen balance downstream of the waste source. If we make the one-dimensional assumption and move our control volume with the mean flow velocity in the river, then the mass balance for our control volume is

$$\frac{dM_{\mathrm{O_2}}}{dt} = \dot{m}_{\mathrm{O_2}} - S \tag{5.29}$$

where S is a sink term representing the biodegradation process. Taking the width of the river as W and the depth as h, we can write the equation for the concentration of $\mathrm{O_2}$ as

$$W\delta x h\frac{d[\mathrm{O}_2]}{dt} = \dot{m}_{\mathrm{O}_2} - S$$
$$= W\delta x k_r([\mathrm{O}_2]_{sat} - [\mathrm{O}_2]) - W\delta x h R_{\mathrm{O}_2} \tag{5.30}$$

where R_{O_2} is the reaction rate law for the consumption of O_2. Rewriting this equation for the oxygen deficit D, we have

$$\frac{dD}{dt} = R_D - K_r D \tag{5.31}$$

where R_D is the rate law for the production of D and $K_r = k_r/h$ is the oxygen transfer coefficient. Substituting (5.27) R_D, we obtain the inhomogeneous ordinary differential equation

$$\frac{dD}{dt} = k_d L_0 \exp(-k_d t) - K_r D \tag{5.32}$$

subject to the initial condition $D(t = 0) = D_0$, which is the initial oxygen deficit just upstream of the point where the waste stream is introduced. The solution to this equation is the classic Streeter-Phelps equation:

$$D(t) = \frac{k_d L_0}{K_r - k_d}(\exp(-k_d t) - \exp(-K_r t)) + D_0 \exp(-K_r t). \tag{5.33}$$

The derivation of this solution is given in Appendix C.

5.3 Sediment/water interface

Unlike the air-water interface, where the interface is generally confined to an abrupt transition at the water surface, the sediment-water interface is very difficult to define and is controlled by a number of complicated physical and chemical processes. The real difficulty of the sediment-water interface lies in the multi-phase (dispersive) nature of the interface. At an individual sediment grain, the interface may be clearly defined. However, since we cannot treat every sediment grain individually, a continuum description of the system is necessary. Two important quantities are used to describe dispersed systems. The porosity, n, is the volume of water contained in a unit volume of mixture

$$n = \frac{V_w}{V}. \tag{5.34}$$

This parameter can vary widely, but is generally between 0.1 and 0.9 within a porous media (groundwater system) and is 0.99 and higher within the water column (suspended sediment system). For suspended sediments, the second parameter is also important: the slip velocity, or settling velocity, u_s. The settling velocity is generally taken as the terminal fall velocity of the sediment in a quiescent system. The porous media/water column interface can then be defined as the point where n becomes small enough that u_s goes to zero due to contact with other sediment particles, forming a (relatively) fixed matrix.

As shown in Figure 5.5 many processes lead to the transport of chemical species in the water column and through the sediment bed. These processes are organized in the figure into two categories. On the left are physical processes that do not involve chemical transformation; on the right are chemical and biological processes.

Example Box 5.2:
Dissolved-oxygen sag curve.

As an example of the application of the Streeter-Phelps equation, consider the following waste stream. A wastewater treatment plant discharges an oxygen demanding waste stream at a rate of $\dot{m} = 295$ g/s of BOD (biochemical oxygen demand) into a stream $h = 3$ m deep, $W = 30$ m wide, and with a flow rate $Q = 27$ m^3/s. The waste stream is introduced through a longitudinal diffuser so that the we can assume complete lateral and vertical mixing at the source. The initial concentration of BOD in the river L_0 is then

$$\begin{aligned} L_0 &= \frac{\dot{m}}{Q} \\ &= \frac{295}{27} \\ &= 10.9 \text{ mg/l}. \end{aligned}$$

Based on regular experiments conducted by the facility operator, the decay rate of the waste is known to be $k_d = 0.2$ day^{-1}.

A rule of thumb often used for computing the aeration rate is

$$K_r = \frac{3.9\overline{u}^{1/2}}{h^{3/2}}$$

where K_r is in day^{-1}, $\overline{u}$ is the mean stream velocity in m/s, and h is the depth in m. For this stream $K_r = 0.4$ day^{-1}. The initial oxygen deficit was measured to be $D_0 = 1.5$ mg/l (the saturation oxygen concentration is 9.1 mg/l). The plot below shows the solution (5.33) for the oxygen concentration ($[O_2]_{sat} - D$) downstream of the mixing zone. The critical time to reach the minimum oxygen concentration is

$$t_c = \frac{1}{K_r - k_d} \ln \left[\frac{K_r}{k_d} \left(1 - \frac{D_0(K_r - k_d)}{k_d L_0} \right) \right]$$

which for this case is 2.67 days, or 69 km. This example illustrates how slow the aeration process can be in the absence of aeration devices, such as cascades and water falls.

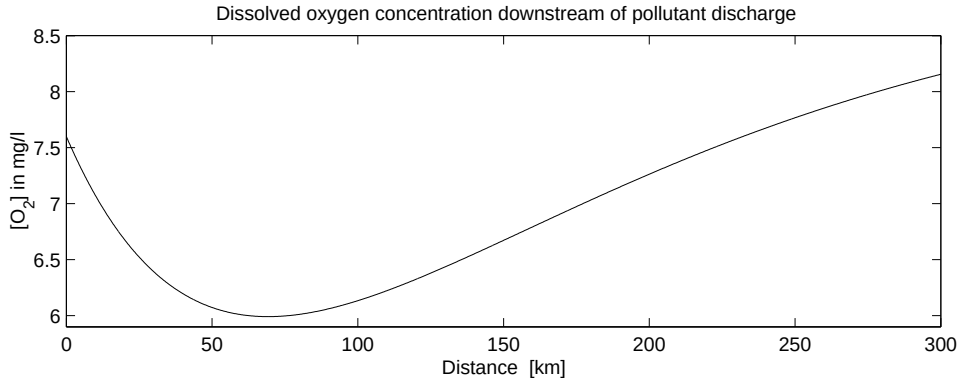

The physical processes are responsible for transport. Within the water column, chemicals can move with either the solid or liquid phase. Of the transport processes listed in the figure, we have already discussed advection and diffusion (both turbulent and molecular) in detail. The other transport processes in the water column (which are specific to the sediment phase) are:

- **Flocculation and settling**: flocculation is the sticking together of several sediment particles to form larger particles. Settling is the downward fall of sediment particles due to their negative buoyancy. Accept for very small particles (colloids), sediment particles always have a negative vertical velocity component relative to the water column motion.
- **Sedimentation**: sedimentation is the process whereby sediment is lost from the water column and gained by the sediment bed. This occurs once the settling sediment particles reach the channel, lake or ocean bottom and rejoin the sediment bed.

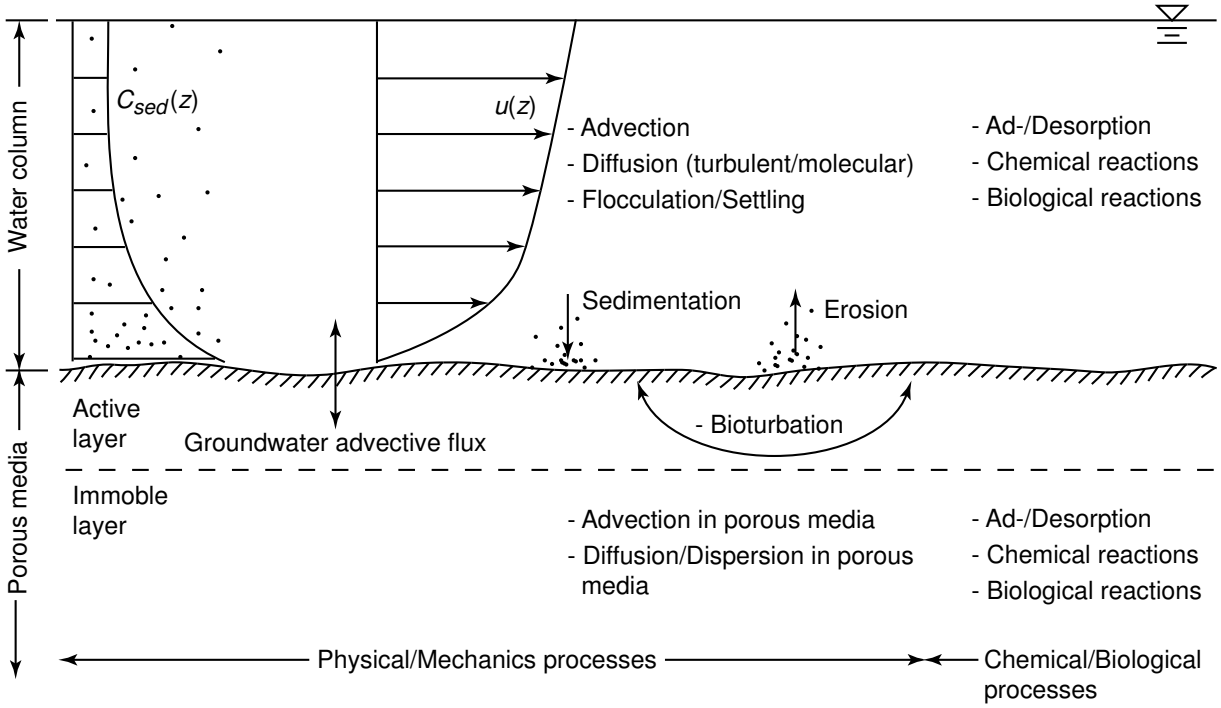

Fig. 5.5. Schematic of processes occurring at the sediment-water interface, in the water column and in the sediment bed (porous media).

- **Erosion**: erosion is the process by which sediment is lost from the sediment bed and entrained into the water column.

Within the sediment bed, or porous media, further transport processes are at work. For species in the liquid phase, the processes of advection, diffusion, and dispersion are active throughout the porous media. For the sediment particles, physical transport occurs only in the upper active layer due to the process of bioturbation:

- **Bioturbation**: bioturbation is the name given to the mixing of sediment caused by animals living in the sediment (mostly worms). These animals move sediment as they dig. Two important classes of worms mix the sediment differently. In the one case, sediment is eaten at the base of the active layer and moved up to the surface. In the other case, sediment is removed from the surface and carried down to the bottom of the active layer. The net movement of sediment is often modeled by an enhanced diffusion process, where we use bioturbation diffusion coefficients.

Through the combination of all these transport processes, chemical species move in and out of the water column and the porous media.

Through transformation processes, chemical species move in and out of the solid and liquid phases and, also, change to other species. We have already discussed chemical and biological transformation reactions. These reactions occur both in the water column and in the porous media. They can also occur in either the liquid phase, the solid phase or at the interface.

Processes at the sediment interface are particularly important for the transport of chemicals through these multi-phase systems:

- **Adsorption/desorption**: the chemical processes of adsorption and desorption control the distribution of certain chemicals between the solid and liquid phases. Due to complex chemical/physical processes, some molecules have an affinity for sticking to the solid phase (often due to electrical charge interaction). That is, some molecules would rather stick to a sediment particle than remain dissolved in the surrounding fluid. The behavior of most organic compounds and heavy metals is controlled by sorption chemistry.

Because sorption is a dominant process occurring at the sediment-water interface, it is discussed in more detail at the end of this section.

As discussed in Gschwend (1987), the processes at the sediment-water interface (at the bottom of a lake or channel) depend on the energetic state of the water body. Beginning with laminar conditions (as in a deep lake) and progressing to increasingly energetic, turbulent conditions (as in reservoirs, estuaries, and streams), the progression is as follows. With no motion, exchange occurs due to direct sorption exchange and diffusion of dissolved species from the pore water. Next, the system begins to flow, allowing the advective and dispersive flux of groundwater flow. Bioturbation, which may always be present, adds energy by actively mixing the sediments. As the water column begins to flow, sediments can be pushed along the top layer of sediments in a process called bed-load transport. Finally, with an energetic water column, erosion begins, sediment is carried up into the water column, and suspended transport (advection of sediment in the water column) becomes important. Hence, the transport of species associated with sediment is a complex problem dependent on the chemistry of the species and the mobility of the sediment.

5.3.1 Adsorption/desorption in disperse aqueous systems

Ignoring the complex problems that lead to the transport of sediment, we focus in this section on the exchange at the solid/liquid interface of a mixed solution of suspended sediment particles in a dispersed (large n) system. An important process controlling the distribution of many toxins in sediment-laden solutions is adsorption/desorption. Defined above, this process causes a large fraction of the sorbing compound to attach to the sediment particles. Hence, sorption controls the concentration of dissolved contaminant, and causes much of the contaminant to be transported with the sediment.

Figure 5.6 illustrates the situation. Sorbing compounds include most polar and non-polar organic compounds and heavy metal ions. To describe the situation quantitatively, we define two concentrations. First, the concentration of substance A that is dissolved in solution is designated C and is defined as

$$C = \frac{M_{\text{dissolved}}}{V_w} \tag{5.35}$$

having normal concentration units. Second, the non-dimensional sorbed-fraction concentration, C_s^*, is defined as

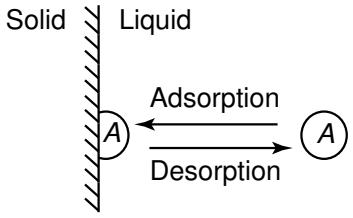

Fig. 5.6. Schematic of the adsorption/desorption process for the molecule A.

$$\begin{aligned} C_s^* &= \frac{M_{\text{adsorbed}}/V_w}{M_{\text{sediment}}/V_w} \\ &= \frac{M_{\text{adsorbed}}}{M_{\text{sediment}}}. \end{aligned} \tag{5.36}$$

These equations are valid only for highly dispersed systems, where $nV \approx V$.

Because sorption kinetics are very fast, we can usually assume that equilibrium exists between the adsorbed and desorbed fractions. Based on experiments, the following simple type of equilibrium relationship has been proposed:

$$C_s^* = \frac{\Gamma C}{K + C} \tag{5.37}$$

which is called the Langmuir equation. The coefficient K is a constant with units of concentration; the coefficient Γ is a non-dimensional constant, called the Langmuir isotherm, which gives the asymptotic value of C_s^* as C becomes large. Figure 5.7 plots the Langmuir equation for $\Gamma = 1$ and $K = 1$. For most toxins in the environment, $C \ll K$, and we can simplify the Langmuir equation to

$$C_s^* = \mathcal{P} C \tag{5.38}$$

where $\mathcal{P}$ is the partition coefficient with units [L^3/M]. Typical values of $\mathcal{P}$ are between 10^3 to 10^6 l/kg.

In order to avoid the confusion caused by C_s^* being non-dimensional, a dimensional concentration of adsorbed contaminant is convenient to define. From the density of the sediment ρ_s and the porosity, the dimensional adsorbed concentration is

$$\begin{aligned} C_s &= C_s^* \rho_s \left(\frac{1-n}{n} \right) \\ &= K_D C \end{aligned} \tag{5.39}$$

where K_D is a non-dimensional distribution coefficient. It is important to note that $\mathcal{P}$ is a purely physico-chemical parameter; whereas, K_D also depends on the sediment concentration and physical characteristics (through the porosity and density, respectively).

Summary

This chapter introduced the processes that result in boundary exchange of chemical species. The general issue in describing boundary exchange is in determining the net boundary flux $\boldsymbol{J}$. Once

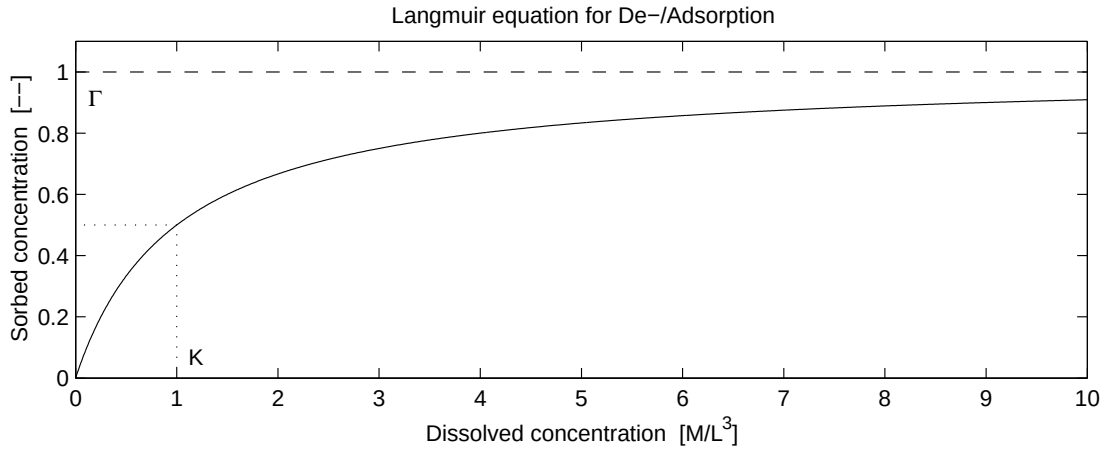

Fig. 5.7. Langmuir equation for de-/adsorption with $\Gamma = 1$ and $K = 1$. Note that C_s^* is $1/2$ at $C = K$.

Example Box 5.3:
Naphthalene partitioning.

Consider the partitioning of the organic toxin naphthalene, the smallest of the polynuclear aromatic hydrocarbons (PAHs). We wish to find the fraction of dissolved to adsorbed naphthalene, f_d. Using (5.38), this fraction is given by

$$f_d = \frac{C}{C + C_s} = \frac{1}{1 + \rho_s \left(\frac{1-n}{n}\right) \mathcal{P}}.$$

For naphthalene $\mathcal{P} = 10^3$ l/kg. Typical sediment has a density of 2600 kg/m^3. For a mixture with $n = 0.99$, $f_d = 4\%$.

We can see that f_d is always large for low concentrations C by looking at the range of expected K_D. From above

$$K_D = \rho_s \left(\frac{1-n}{n}\right) \mathcal{P}.$$

Making the following order-or-magnitude estimates

$$\rho_s = 10^3$$
$$(1-n)/n = 10^{-3}$$
$$\mathcal{P} = 10^3 \text{ to } 10^6$$

K_D ranges from 10^3 to 10^6; f_d ranges from 10^{-3} to 10^{-6}. Therefore, we can assume that a large fraction of the contaminant is present in the sorbed state.

If we manage to eliminate the source of a toxic contaminant that is also sorbed to the sediments, then the sediment bed itself will start to release its sediment load into the water column water, creating a new source (see Exercise 5.3). Unfortunately, because f_d is so large, the sediment load is large, and it takes a long time before the water column is free from this sediment source of the contaminant.

that flux is know, boundary exchange becomes a boundary condition on the governing transport equation. The solution for $\boldsymbol{J}$ in a stagnant water body was used to develop two descriptions of exchange in turbulent water bodies. The Lewis-Whitman model, the simplest model, assumes the concentration boundary layer between phases has a constant depth. The film-renewal model assumes that turbulence constantly refreshes the fluid in the concentration boundary layer, and that the renewal rate derives from turbulent eddy characteristics. The exchange at the air-water interface was discussed in more detail, with examples for volatile chemicals and oxygen aeration. The sediment-water interface was described qualitatively, and the sorption chemistry at the sediment water interface was described in more detail.

Table 5.1. Measurements of time and oxygen concentration for a BOD test. (Data taken from Nepf (1995))

Time [days]	$[O_2]$ [mg/l]
0	9.00
2	5.21
4	3.81
6	3.30
8	3.11
10	3.04
12	3.01
14	3.01
16	3.00
18	3.00
20	3.00

Exercises

5.1 BOD test. To determine the biodegradation rate coefficient of a particular waste, the waste is placed in solution in a closed bottle, where the oxygen concentration in monitored over time. Table 5.1 gives the results of a typical test. Based on all the data in the table, estimate the value of the rate coefficient, k_d.

5.2 Gas exchange rates. A river has the following characteristics: water depth $h = 1.0$ m, width $B = 100$ m, bottom slope $S = 9 \cdot 10^{-4}$, and Manning coefficient $n = 0.01$. The turbulent intensity is 15%.

- Use the Lewis-Whitman model to estimate the transfer velocity k_l. A typical layer thickness δ is of order $O(0.1\text{mm})$ to $O(1\text{mm})$.
- Use the small-eddy film renewal model to estimate k_l.
- Use the large-eddy film renewal model to estimate k_l.
- Compare and discuss the three k_l's you obtained.
- Calculate the flux of dissolved oxygen (DO) into the river using the most reasonable k_l (use your own judgment with justification) among the three above. The saturated concentration $[\text{DO}]_{\text{sat}}$ is 8.0 mg/L while the measured [DO] near the bottom of the river is 4.0 mg/L.
- What is the total mass transfer of DO into the river for every kilometer of length?

5.3 PCB contamination. An industrial plant releases PCBs (polychlorinated biphenols) through a diffuser into a river. The river moves swiftly, with a modest sediment load. PCB is volatile (will off-gas into the atmosphere) and can be adsorbed by the sediment in the river. Describe the network of complex interactions that must be investigated to predict the fate of PCBs from this disposal source.

5.4 Sediment source of phosphorus. Phosphorus, in the form of phosphate (PO_4^{3-}), is often a limiting nutrient for algae production in lakes. Because the uncontrolled growth of algae is undesirable, the discharge of phosphorus into the environment should be minimized (this is why you cannot buy laundry detergent any more that contains phosphorus). The U.S. Environmental Protection Agency recommends a limit of 0.05 mg/l PO_4^{3-} for streams that flow into freshwater lakes.

An old chemical plant recently shut off their phosphorus discharge; however, high concentrations of phosphorus are still being measured downstream of the chemical plant. After further investigation, the following facts were collected:

- The concentration of phosphate in the stream water upstream of the plant is $C_0 = 0.003$ mg/l.
- The sediments in the stream are saturated with sorbed phosphorus for a distance of 2 km downstream of the plant.
- The phosphate concentration at the sediment bed is kept constant by desorption at a value of $C_b = 0.1$ mg/l.
- The design conditions in the stream are $h = 2$ m deep and $u = 0.2$ m/s.
- The phosphate transfer velocity at the sediment bed is given approximately by the relationship (film-renewal model):

$$k_l = 0.002 \frac{u^{3/4}}{h^{1/4}} \text{ in m/s.} \tag{5.40}$$

Based on the above data: What is the concentration of phosphate in the stream just after passing the region of contaminated sediments? If the stream carries a suspended sediment load, how would that affect the concentration of phosphate in the stream?

6. Atmospheric Mixing

Previous chapters have dealt solely with transport in various water bodies and have presented examples of one-dimensional solutions to the transport equations. We now turn our attention to transport and mixing in the atmosphere, and by necessity, we will have to give more attention to three-dimensional solutions. Because of the atmosphere's unique composition and boundary and forcing conditions, atmospheric turbulence is more complicated than the idealized homogeneous, stationary, isotropic case. Moreover, these complications impact transport and mixing because they determine the values of the turbulent diffusion and dispersion coefficients. Hence, a concise discussion of atmospheric mixing requires also studying atmospheric turbulence and the resulting modifications in the behaviour of mixing coefficients from the idealized case.

This chapter begins with an introduction to atmospheric turbulence and a review of turbulent boundary layer structure. The log-velocity profile for a turbulent shear flow is introduced, and the behaviour of turbulence throughout a neutrally stable atmospheric boundary layer is described. Because of their importance to turbulence characteristics, the buoyancy effects of heating and cooling within the boundary layer are discussed qualitatively. The discussion on mixing begins with a review of turbulent mixing in three-dimensional, homogeneous, stationary turbulence. The solution for a continuous point source is derived and used to illustrate mixing in the remaining section. The chapter closes by adapting the idealized solution in homogeneous, stationary turbulence to the turbulence present in the atmosphere.

Much of the material in this chapter was taken from Csanady (1973) and from Fedorovich (1999). For further reading, those two sources are highly recommended, along with the classic books by Lumley & Panofsky (1964) and Pasquill (1962) and more recent contributions by Garratt (1992) and Kaimal & Finnigan (1994).

6.1 Atmospheric turbulence

In Environmental Fluid Mechanics, we are concerned with local mixing processes in fluids that interact with living organisms. For the atmosphere, this means that we are interested in mixing processes near the earth's surface. Because of the no-slip boundary condition at the surface, wind in the upper atmosphere generates a near-surface boundary layer, defined by variations in velocity and often accompanied by variations in temperature (and density). Figure 6.1 shows this situation schematically. Because of its dominant role in mixing near the earth's surface, we present here a short introduction to turbulence in the atmospheric boundary layer.

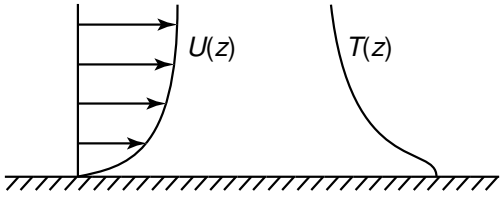

Fig. 6.1. Schematic of the velocity and temperature variation within the atmosphere near the earth's surface. The region of high velocity shear is called a boundary layer.

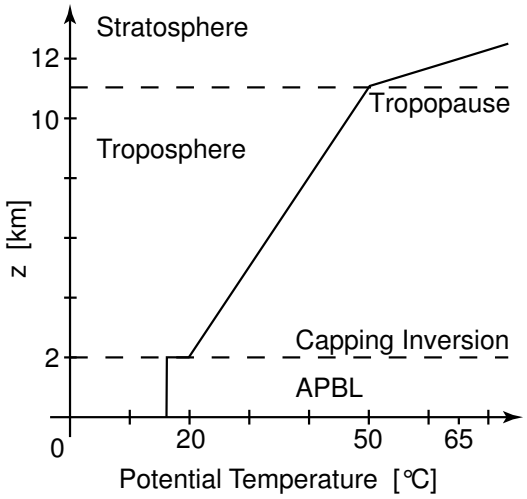

Fig. 6.2. Schematic of the potential temperature profile in the earth's troposphere and lower stratosphere showing the atmospheric planetary boundary layer (APBL).

6.1.1 Atmospheric planetary boundary layer (APBL)

Fedorovich (1999) defines the atmospheric planetary boundary layer (APBL) as the subdomain of the lower portion of the earth's planetary atmosphere (troposphere) which is in contact with the bottom boundary (earth's surface) and which varies in depth from several meters to a few kilometers. Figure 6.2 provides a schematic of this definition. The figure depicts the APBL as the lower part of the troposphere and shows that it is separated from the linearly stratified region of the troposphere by a strong density gradient, called the capping inversion. The capping inversion arises due to strong mixing that occurs at the earth's surface which results in a weaker density gradient within the APBL than in the upper troposphere. Although the density gradient shown in the figure is for a neutral APBL (no density gradient), heating and cooling processes within the APBL can lead to both unstable and stable conditions, discussed below under buoyancy effects. Above the APBL, the wind has an approximately constant velocity; hence, the APBL encompasses the full near-surface boundary layer.

6.1.2 Turbulent properties of a neutral APBL

Figure 6.3 shows the development of a general turbulent boundary layer over a flat surface. In the upper figure, the boundary layer is tripped at $x = 0$ and begins to grow in height downstream as an increasing function of $x^{1/2}$. In the idealized case, the boundary layer is tripped by the edge of

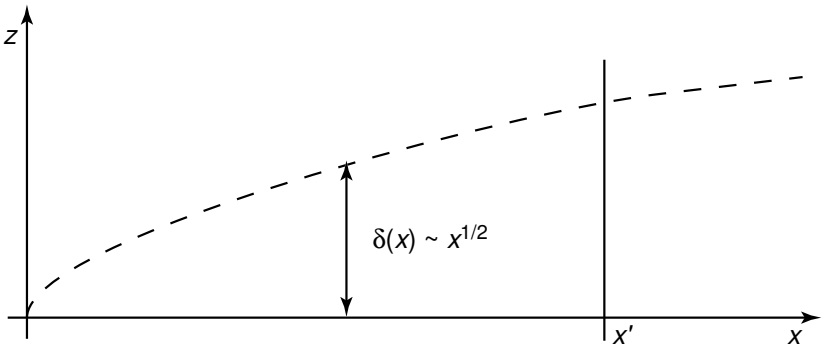

(a.) Growth of a boundary layer with increasing fetch.

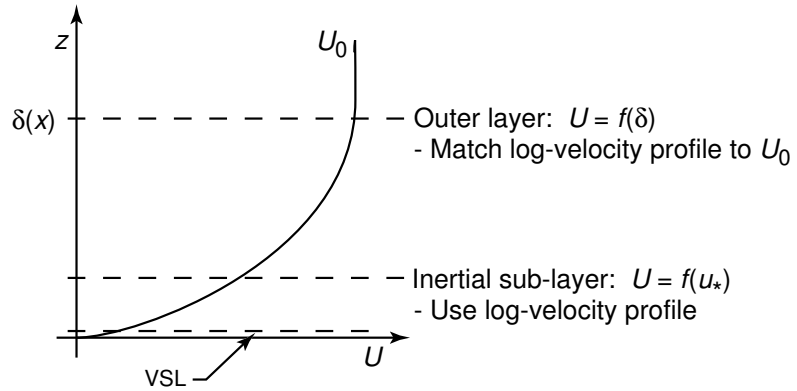

(b.) Boundary layer structure at the section x'.

Fig. 6.3. Schematic of the development of a turbulent boundary layer over a flat surface.

a flat plate extending into a free turbulent flow. In nature, boundary layers start in response to changes in friction (roughness), as when the wind blows over a long, smooth lake and suddenly encounters a forest on the other side. The distance the wind has blown downstream of a major change in surface properties is called the fetch.

A turbulent boundary layer at any point x contains three major zones that differ in their turbulence characteristics (refer to Figure 6.3(b.)). The lowest layer, directly in contact with the surface, is the viscous sub-layer (VSL). It has a depth of about $5\nu/u_*$ (of order millimeter in the atmosphere). The VSL thickness is independent of the total boundary layer depth $\delta(x)$, and velocities in the VSL are low so that the flow is laminar. A transition to turbulence occurs between $5\nu/u_*$ and $50\nu/u_*$. Above this transition zone, and to a height of about 10-20% of the total boundary layer depth (of order 100 m in the atmosphere), lies the inertial sub-layer (ISL), also called the Prandtl layer in the atmosphere. The inertial sub-layer is fully turbulent, and turbulent properties are functions of the friction velocity only (i.e. they are independent of the total boundary layer depth). The mean longitudinal velocity profile in the ISL is given by the well-known log-velocity profile

$$\frac{U(z)}{u_*} = \frac{1}{\kappa} \ln\left(\frac{u_* z}{\nu}\right) + C \tag{6.1}$$

where $\kappa \approx 0.4$ is the von Karman constant and C is an integration constant about equal to five. It is important to note that within this layer $U(z)$ is independent of $\delta(x)$. The remaining region of the boundary layer is called the outer layer, or Ekman layer in the atmosphere, and extends up to where the velocity becomes U_0. Within the atmosphere, the Ekman layer is deep enough that it experiences Coriolis effects due to the earth's rotation. In the outer layer, turbulence properties and the velocity profile are dependent on the total layer depth, and we use a technique called matching to adjust the log-velocity profile in this layer so that it reaches U_0 at $z = \delta(x)$.

In general, turbulence measurements in the APBL depend on the height of the measurement, the roughness of the ground, and the stability (Csanady 1973). Measurements near the surface (within the ISL) demonstrate that

$$u_{rms} \propto u_* \tag{6.2}$$

where $u_{rms} = (\overline{u'^2})^{1/2}$. Above this surface layer, u_{rms} tends to decay with height. Because the land surface is quite rough in comparison to an idealized flat plate, the log-velocity profile cited above is adjusted in the ISL to give

$$U(z) = \frac{u_*}{\kappa} \ln\left(\frac{z}{z_0}\right) \tag{6.3}$$

where z_0 is the roughness height (valid for $z \gg z_0$).

Because the mean wind-speed increases with height and the turbulent fluctuation velocities are constant with height within the neutral APBL, turbulence intensity decreases with height. Turbulence intensity is defined as

$$i_x = \frac{(\overline{u'^2})^{1/2}}{U(z)} \tag{6.4}$$

$$i_y = \frac{(\overline{v'^2})^{1/2}}{U(z)} \tag{6.5}$$

$$i_z = \frac{(\overline{w'^2})^{1/2}}{U(z)} \tag{6.6}$$

where i_y and i_z are the turbulence intensities (non-dimensional), u' is the longitudinal fluctuation velocity, v' is the transverse fluctuation velocity, and w' is the vertical fluctuation velocity. Measurements by Panofsky (1967) revealed for a neutral surface layer that

$$(\overline{u'^2})^{1/2} = 2.2u_* \tag{6.7}$$

$$(\overline{v'^2})^{1/2} = 2.2u_* \tag{6.8}$$

$$(\overline{w'^2})^{1/2} = 1.25u_*. \tag{6.9}$$

Combining these relationships with the log velocity profile yields

$$i_x = i_y = \frac{0.88}{\ln(z/z_0)} \tag{6.10}$$

$$i_z = \frac{0.50}{\ln(z/z_0)}. \tag{6.11}$$

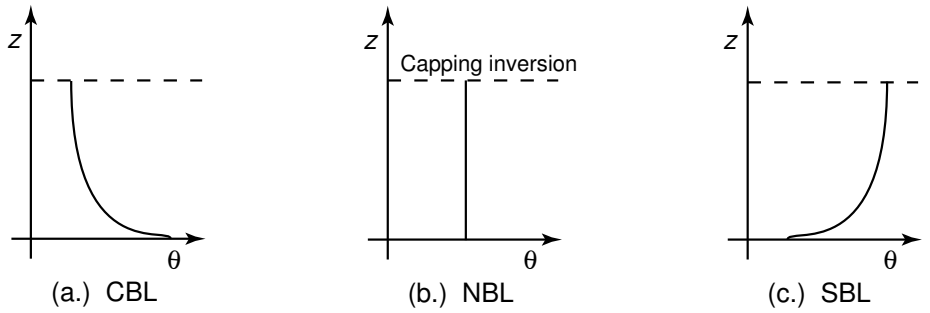

Fig. 6.4. Potential temperature, θ, profiles in the APBL for the three main stability classes: (a.) the convective boundary layer (CBL), (b.) the neutral boundary layer (NBL), and (c.) the stable boundary layer (SBL).

It is important to note that these data were collected under idealized conditions: large fetch, flat ground, and uniform roughness (often prairie grass).

6.1.3 Effects of buoyancy

Unfortunately, the idealized neutral conditions described above are rarely strictly valid. Heating and cooling within the boundary layer result in temperature differences, which equate to density differences; thus, buoyancy effects and stability/instability are important processes in the APBL.

Shown in Figure 6.4, three general stability types are possible. We have already discussed the neutral case, where the density is constant throughout the boundary layer (refer to Figure 6.4(b.)). During the day, solar radiation heats the bottom air, creating an unstable density profile as shown in Figure 6.4(a.). This case is called a convective boundary layer (CBL). The warm air at the bottom rises, due to its buoyancy, creating enhanced vertical velocities. Because of its special kind of instability, convective instabilities are cellular in shape. That is, circular regions of warm upward-moving air, called thermals, are surrounded by layers of cooler downward moving air. This kind of instability can be seen in a pot of water heated on the stove. The third stability type is show in Figure 6.4(c.). At night, the bottom layer cools rapidly, and the boundary layer develops a stable density profile (heavy air below lighter air). This stable density profile damps the turbulence, in particular the vertical turbulent fluctuation velocities, and encourages internal wave motion. Because of the cellular instability structure of the CBL, and internal wave fields of the SBL, these boundary layers have spatially heterogeneous properties.

Despite these complicated and inter-related effects, generalized quantitative results can be obtained for natural boundary layers. Pasquill (1962) suggested a means of predicting the stability type as a function of wind speed, time of day, and radiative conditions (in particular, cloud cover, which provides insulation). Table 6.1 provides this stability categorization. Cramer (1959) suggested the associated typical turbulent intensities near the ground level as shown in Table 6.2. As demonstrated in the tables, turbulence intensities are indeed higher in unstable conditions than for stable conditions, and both the vertical and horizontal turbulence intensities are affected.

Combining all these processes, Fedorovich (1999) summarizes the processes affecting mixing as follows:

Table 6.1. Pasquill stability categories taken from Csanady (1973).

Surface wind speed in [m/s]	Solar insolation			Night conditions	
	Strong	Moderate	Slight	mainly overcast or $\geq 4/8$ low cloud	$\leq 3/8$ Low cloud
2	A	A–B	B	–	–
2-3	A–B	B	C	E	F
3-5	B	B–C	C	D	E
5-6	C	C–D	D	D	D
6	C	D	D	D	D

A - Extremely unstable, B - Moderately unstable, C - Slightly unstable, D - Neutral, E - Slightly stable, F - Moderately stable.

Table 6.2. Typical turbulence intensities near the ground level, taken from Csanady (1973)

Thermal stratification	i_y	i_z
Extremely unstable	0.40–0.55	0.15–0.55
Moderately unstable	0.25–0.40	0.10–0.15
Near neutral	0.10–0.25	0.05–0.08
Moderately stable	0.08–0.25	0.03–0.07
Extremely stable	0.03–0.25	0.00–0.03

- large-scale meteorologic forcing (U_0).
- earth's rotation (Coriolis)
- external and internal heating/cooling ($T(z)$)
- physical properties of the surface (z_0)
- physical properties of air (u_*)

The remaining sections incorporate these processes in a description of atmospheric mixing.

6.2 Turbulent mixing in three dimensions

Before we discuss mixing in the atmospheric boundary layer, we should review the turbulent transport equation in a simpler turbulent flow. In Chapter 3 we derived the turbulent advective diffusion equation for homogeneous and stationary turbulence. The transport equation for the mean concentration field C was found to be

$$\frac{\partial C}{\partial t} + \frac{\partial u_i C}{\partial x_i} = D_{x,t}\frac{\partial^2 C}{\partial x^2} + D_{y,t}\frac{\partial^2 C}{\partial y^2} + D_{z,t}\frac{\partial^2 C}{\partial z^2} \tag{6.12}$$

where $D_{i,t}$ are the turbulent diffusion coefficients.

In Chapter 3 we only presented the solutions for times greater than the integral time scale of the turbulence t_I, where we could assume the turbulent diffusion coefficients were constant in time. In general, the turbulent diffusion coefficient in the x direction is given by

$$D_{x,t} = \frac{1}{2}\frac{d\sigma_x^2}{dt} \tag{6.13}$$

where σ_x is the standard deviation of the concentration field in the x-direction (Csanady 1973). Similar relationships are valid for the y- and z-directions. From Taylor's theorem it follows that

$$D_{x,t} = \overline{u'^2}\int_0^t R(\tau)d\tau \tag{6.14}$$

where R is the velocity correlation function of the turbulent flow (Csanady 1973). Generally, we consider two limiting solutions to this equation: at short times for $t \to 0$, and at large times for $t \to \infty$. These solutions are

$$D_{x,t} = \frac{(\overline{u'^2})^2}{\overline{u}}x \quad (x \to 0) \tag{6.15}$$

$$D_{i,t} = (\overline{u'^2})^2 t_L \quad (x \to \infty). \tag{6.16}$$

Thus, the turbulent diffusion coefficients grow linearly at short times until they reach a constant value at times greater than t_L.

Example: Continuous point release. As an example, consider the classical problem of a continuous release at a height h above the ground level. We set the coordinate system so that the mean wind is in the x-direction. The source strength is $\dot{m}$ in [M/T]. To enforce the solid boundary condition at $z = 0$ we use an image source. The solution for the slender plume assumption (diffusion in the x-direction is negligible) is given in Csanady (1973) as

$$C(x,y,z) = \frac{\dot{m}}{2\pi\overline{u}\sigma_y\sigma_z}\left[\exp\left\{-\frac{y^2}{2\sigma_y^2} - \frac{(z-h)^2}{2\sigma_z^2}\right\} + \exp\left\{-\frac{y^2}{2\sigma_y^2} - \frac{(z+h)^2}{2\sigma_z^2}\right\}\right]. \tag{6.17}$$

The solution for the concentration at ground level is given by setting $z = 0$:

$$C(x,y,0) = \frac{\dot{m}}{\pi\overline{u}\sigma_y\sigma_z}\exp\left[-\frac{y^2}{2\sigma_y^2} - \frac{h^2}{2\sigma_z^2}\right] \tag{6.18}$$

and the solution for the centerline of the plume at ground level is given by setting $z = y = 0$:

$$C(x,0,0) = \frac{\dot{m}}{\pi\overline{u}\sigma_y\sigma_z}\exp\left[-\frac{h^2}{2\sigma_z^2}\right]. \tag{6.19}$$

Figure 6.5 shows the solutions of the latter two equations at short times ($t \to 0$) in non-dimensional form.

6.3 Atmospheric mixing models

The results for homogeneous, stationary turbulence are extended in this section to applications in the atmosphere. An underlying assumption for the derivation of (6.12) is that the Eulerian and Lagrangian descriptions of the velocity field are identical. Csanady (1973) points out that this is only true for homogeneous and stationary turbulence if the system is unbounded or bounded by

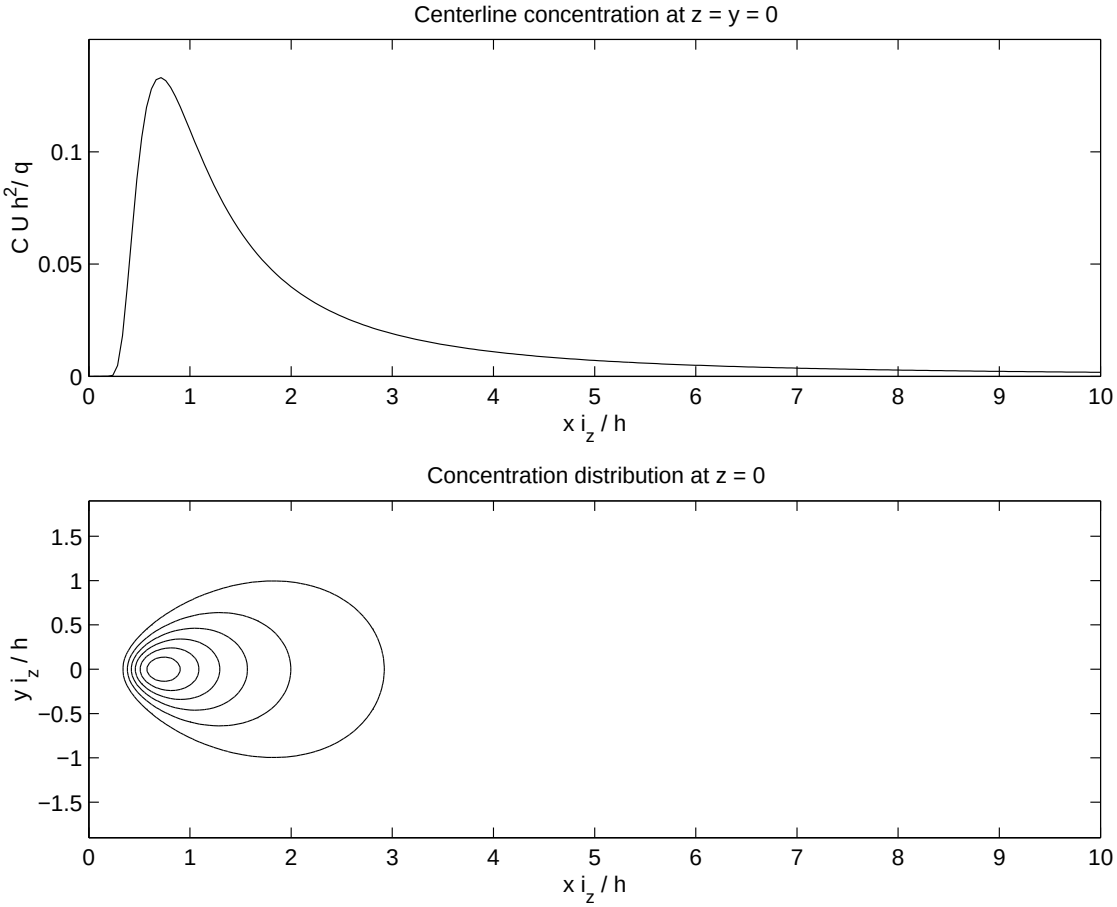

Fig. 6.5. Concentration distributions for a continuous release at a height h into a homogeneous and stationary turbulent flow.

rigid, impermeable walls. The atmospheric boundary layer is indeed bounded from below by a solid boundary, but the top boundary (the capping inversion in Figure 6.2) is permeable. That is, fluid parcels moving in the APBL can move through the capping inversion, bringing high velocity fluctuations with them, and these parcels are replaced by fluid with lower turbulence intensities from above the capping layer. This departure from the idealized case of a solid or semi-infinite boundary results in changes to the velocity correlation function, R, in the APBL. Csanady (1973) shows, however, that because the solution for the transport equation is insensitive to the shape of the velocity correlation function, this limitation is not dramatic and we will continue to use solutions similar to those in the previous section.

Based on (6.15) and (6.16), we expect different results for short and long times. The processes at short times occur near the source and are called near-field processes. Similarly, the processes at long times occur far from the source and are called far-field processes.

6.3.1 Near-field solution

In the near-field of a release, it is reasonable to assume that the results given above are valid without modification. This is because, at short times, the release has not fully sampled the velocity field and does not know that the turbulence field is bounded by a permeable capping inversion. Hence, the cloud width grows in the near field as

$$\sigma_y = \frac{(\overline{v'^2})}{\overline{v}} x = i_y x \tag{6.20}$$

$$\sigma_z = \frac{(\overline{w'^2})}{\overline{w}} x = i_z x. \tag{6.21}$$

The relationships for the turbulent intensities at a height z were given above. For a release at $z = h$, it is reasonable to use average turbulence intensities. Taking the average from $z = 0$ to $z = h$ gives

$$i_y = \frac{0.88}{\ln(h/z_0) - 1} \tag{6.22}$$

$$i_z = \frac{0.5}{\ln(h/z_0) - 1}. \tag{6.23}$$

Csanady (1973) shows that the near-field solution is valid for a considerable range, often up to the distance where the plume grows so large that is touches the ground, in which vicinity also the maximum ground level concentrations are observed. This is because the Lagrangian time scale is very large, given approximately by

$$t_L = \frac{z_i}{\overline{u}} \tag{6.24}$$

where z_i is the height of the capping inversion.

6.3.2 Far-field solution

Far from the source, the growth of the cloud should depend on the Lagrangian time scale and, due to the shear velocity profile, should be affected by dispersion. Sutton (1932) and Sutton (1953) propose power law formulas for the standard deviations

$$2\sigma_y^2 = C_y^2 x^{2-n} \tag{6.25}$$

$$2\sigma_z^2 = C_z^2 x^{2-n} \tag{6.26}$$

where C_y, C_z, and n are constants, their value depending on atmospheric stability and source height h (Csanady 1973). Under neutral conditions Sutton found the values $n = 0.25$, while over flat grass-land near ground level he proposed $C_y = 0.4\ \mathrm{cm}^{1/8}$ and $C_z = 0.2\ \mathrm{cm}^{1/8}$ (Csanady 1973). Though this formula is rarely used today, it is important because it represents observed facts.

Under non-neutral conditions, the coefficients introduced above are functions of the stability. Looking first at the *horizontal* growth of the cloud, n has been found to be roughly constant for all stability regimes; C_y is sufficient to adjust σ_y to unstable and stable conditions; and, higher values of C_y are observed in CBLs, and lower values of C_y are observed in SBLs. For *vertical*

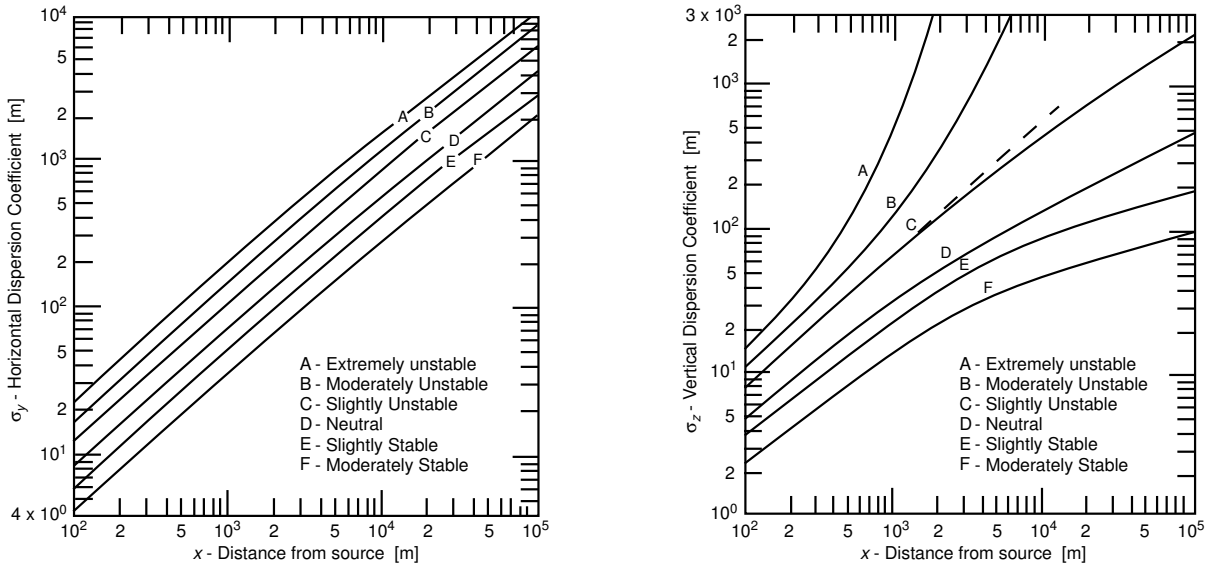

(a.) Horizontal dispersion coefficient. (b.) Vertical dispersion coefficient.

Fig. 6.6. Horizontal (a.) and vertical (b.) atmospheric mixing coefficients. Taken from Csanady (1973).

cloud growth, both parameters are functions of the stability. Figure 6.6 shows the values of σ_y and σ_z for the range of stability classes introduced above. In CBLs, the vertical growth of the cloud becomes vary large due to the large upward velocities of the convective currents. In SBLs, the vertical growth of the cloud is damped due buoyancy effects.

Summary

This chapter introduced mixing in the lower part of the atmosphere, the planetary atmospheric boundary layer (APBL). Turbulence properties in idealized boundary layers were discussed first and then extended to the APBL. The effects of heating and cooling in the APBL result in a range of stability classes, from convectively unstable when heating is from below to stable when cooling is from below. Turbulent mixing in homogeneous stationary turbulence was reviewed and solutions for a continuous source at a height h above a solid boundary were introduced. The results in idealized turbulence were extended in the final section to turbulence in the atmosphere. Simplified atmospheric mixing models were introduced for the near- and far-field cases.

Exercises

6.1 Boundary influence. The effects of a solid boundary are only felt after a plume grows large enough to touch the boundary. Assuming a total plume depth of $4\sigma_z$, find the distance downstream of the release point to where a continuous source release at a height h above a solid boundary first touches the boundary.

6.2 Smoke-stack exhaust. A power company releases 1 kg/s of CO_2 from a height of 30 m into a wind with average velocity 4 m/s. The sky is partly cloudy and the terrain down-wind of the release is pasture land. Estimate the turbulence intensities and find the maximum concentration at ground level downstream of the release. How do the results change if the release point is lowered by 15 m?

6.3 Urban roughness. The results presented in this chapter were for surfaces with uniform roughness and elevations much greater than the roughness height z_0. How do you expect relationships for turbulence intensity to change near the street level in an urban setting (where the roughness is largely due to buildings and houses)?

7. Water Quality Modeling

Until now we have derived governing equations for and sought solutions to idealized cases where analytical solutions could be found. Many problems in the natural world, however, are complex enough that simplified analytical solutions are inadequate to predict the transport and mixing behavior. In these situations, approximations of the governing transport equations (such as finite difference) must be made so that numerical solutions can be found. These approximations can be simple or complex, but often result in a large number of equations that must be solved to predict the concentration distribution. Hence, computer algorithms are used to make the numerical solutions tractable.

In this chapter, we introduce the field of water quality modeling based on computerized (numerical or digital) tools. This chapter begins by outlining how to select an appropriate numerical tool. The next two section describe common computer approximations. First, simple numerical models based on plug-flow and continuously-stirred tank reactors are introduced. Second, an overview of numerical approximations to the governing equations is presented. Because we are now dealing with approximate solutions, new procedures are needed to assure that our results are acceptable. The final section outlines the crucial steps necessary to test the accuracy of a numerical result. Although computer power is rapidly growing, it remains important to use simple tools and thorough testing in order to understand and synthesize the meaning of numerical results.

7.1 Systematic approach to modeling

A model is any analysis tool that reduces a physical system to a set of equations or a reduced-scale physical model. Moreover, all of the solutions in previous chapters are analytical models of natural systems. Whether analytical or numerical, the main question the modeler must answer is: which model should I use?

7.1.1 Modeling methodology

The ASCE & WPCF (1992) design manual *Design and Construction of Urban Stormwater Management Systems* outlines a four-step selection processes for choosing a water quality analysis tool. These steps are discussed in detail in the following and include (1) defining project goals, (2) describing an acceptable modeling tool, (3) listing the available tools that could satisfy the goals and model description, and (4) selecting the model to be used based on an optimal compromise between goals and available tools.

1. Define project goals. It may sound like an obvious first step, but it is essential and, regrettably, often overlooked: define the project goals before even choosing the model. Fischer et al. (1979) emphasize this step as well, saying that the choice of a model depends crucially on what the model is to do. Modeling goals are quite variable, ranging from the practical (provide the analysis necessary to get the client his discharge permit) to the research oriented (develop a new tool that overcomes some current modeling shortfall).

During this step, as much as possible should be learned about the system to be modeled. Fischer et al. (1979) suggest that if possible, the investigator should become personally familiar with the water body by going out on it in the smallest boat that is safe. Then, before venturing near a computer or a model basin, he or she should make all possible computations, being approximate where necessary, but seeking a feel for what the model will predict. Only after we understand our system can we formulate appropriate project goals. In the words of the famous landscape photographer Ansel Adams, "Visualization is of utmost importance; many failures occur because of our uncertainty about the final image" (quoted in Fischer et al. (1979)). During this stage one begins to formulate the necessary attributes of the model. This leads naturally the next step.

2. Describe an acceptable modeling tool. Before selecting the model for the analysis, formulate a list of abilities and characteristics that the model must have. These can include things like input/output flexibility, common usage in the regulatory community, and physical mixing processes the model must include. Our simplified predictions from step 1 of how the system behaves are used in this step to formulate the model requirements. For instance, if we expect rapid near-field mixing, we may suggest using a one-dimensional model. This step should keep in mind what models are available, but not limit the analysis to known tools if they would be inadequate to meet the project goals. In this stage the project goals may also need to be revised. If the only acceptable modeling tool to meet a particular goal is too costly in terms of computation time and project resources, perhaps that goal can be reformulated within a reasonable project scope. The purpose, therefore, of this step is to optimize the modeling goals by describing practical requirements of the modeling tool.

3. List applicable tools. Once the analysis tool has been adequately described, one must formulate a list of available tools that meet these requirements. In engineering practice, we must often choose an existing model with a broad user base. Appendix D lists several public-domain models. Most of them are available free of charge from government sponsor agencies, but some are also commercial. The purpose of choosing an existing model is that it has been thoroughly tested by many previous users and that the regulatory agencies are accustomed to seeing and interpreting its output. However, available tools may not always be adequate to meet the project goals.

If existing tools are inadequate, then a new tools must be developed, and a list of existing methods is an important step. Methods are the building blocks of models. A one-dimensional finite difference model employs two methods: a one-dimensional approximation and a finite difference numerical scheme. Going a step deeper, the finite-difference method can have many attributes, such as forward, central, or backward differencing, implicit or explicit formulation,

and first-, second-, or higher-order solution algorithms. Section 7.3 describes what some of these terms mean. The point is that, when designing a new tool, there are many existing building blocks from which to choose, and these can be quite helpful. It may turn out that simply adding an unsteady algorithm to an existing steady-state model will meet the project goals. Hence, knowing as much as possible about existing models and methods is essential to implementing and/or designing an analysis tool.

4. Make an optimal compromise between goals and available tools. In the final step of choosing a modeling tool, we seek an optimal compromise between the project goals and the available tools. This is where the decision to proceed with a given modeling tool is made. The project goals are the guide to choosing the model. It sounds simple, but choose the best model to meet the project goals, not just the best available model. As computers become faster, the tendency is to just pick the biggest, boldest model and to force it to meet your needs. However, the enormous amount of output from such a model may be overwhelming and costly and unnecessary in the light of certain project goals. Therefore, choose the most appropriate, simplest model that also satisfies the scientific rigor of the project goals, and when necessary, develop new tools.

7.1.2 Issues of scale and complexity

Throughout the process of choosing a modeling tool one is confronted with issues of system scale and complexity. The world is inherently three-dimensional and turbulent, but with current computer resources, we must often limit our analysis to one- and two-dimensional approximations with turbulence closure schemes that approximate the real world. Hence, we must make trade offs between prototype complexity and model ability.

We can evaluate these trade offs by doing a scale analysis to determine the important scales in our problem. This is the essence of steps one and two, above, where we try to predict what the model will tell us and use this information to characterize the needed tool. For transport problems, we must consider the advective, diffusing reaction equation. For illustration, consider a first-order reaction

$$\frac{\partial C}{\partial t} + \frac{\partial (uC)}{\partial x} + \frac{\partial (vC)}{\partial y} + \frac{\partial (wC)}{\partial z} = D_x \frac{\partial^2 C}{\partial x^2} + D_y \frac{\partial^2 C}{\partial y^2} + D_z \frac{\partial^2 C}{\partial z^2} \pm kC. \tag{7.1}$$

This equation has three unit scales: mass, time, and length. It also has three processes: advection, diffusion, and reaction. We would like to formulate typical scales of these three processes from the typical units in the problem. For example, the advection time scale is the time it takes for fluid to move through our system. If we are modeling a river reach of length L with mean velocity U, then the advective time scale is

$$T_a = L/U. \tag{7.2}$$

Processes that occur on time scales much shorter than T_a can neglect advection. We can use these scales to non-dimensionalize the governing equation. To do this, we define the non-dimensional variables using primes as follows

$$
\begin{aligned}
x &= L_x x'; \qquad y = L_y y' \\
z &= L_z z'; \qquad u = U u' \\
v &= V v'; \qquad w = W w' \\
C &= C_0 C'; \qquad t = T_0 t' \\
k &= 1/T_r k'
\end{aligned} \tag{7.3}
$$

where the upper-case variables are typical scales in the problem. For example T_0 is an external time scale, such as a discharge protocol or the diurnal cycle and T_r is the reaction time scale, such as the half-life for a dye-off reaction. The L's are system dimensions and U, V, and W are average velocities. Substituting into (7.1) gives

$$
\begin{aligned}
\frac{1}{T_0}\frac{\partial C'}{\partial t'} + \frac{U}{L_x}\frac{\partial (u'C')}{\partial x'} + \frac{V}{L_y}\frac{\partial (v'C')}{\partial y'} + \frac{W}{L_z}\frac{\partial (w'C')}{\partial z'} = \\
\frac{D_x}{L_x^2}\frac{\partial^2 C'}{\partial x'^2} + \frac{D_y}{L_y^2}\frac{\partial^2 C'}{\partial y'^2} + \frac{D_z}{L_z^2}\frac{\partial^2 C'}{\partial z'^2} \pm \frac{1}{T_{1/2}} k' C'.
\end{aligned} \tag{7.4}
$$

Note that to make this equation fully non-dimensional, we must multiple each term by a time scale, for example T_0. We can now determine the relative importance of each term by considering their leading coefficients. Comparing the convective terms

$$
\frac{\text{Longitudinal advection}}{\text{Lateral advection}} = \frac{U}{V} \cdot \frac{L_y}{L_x} \tag{7.5}
$$

$$
\frac{\text{Longitudinal advection}}{\text{Vertical advection}} = \frac{U}{W} \cdot \frac{L_z}{L_x} \tag{7.6}
$$

If these ratios are much greater than one, then longitudinal advection is the only advection term that we must keep in the equation. Thus, the importance of a given convection term depends on the velocity scales in our problem and the length of river we are considering. In many river problems, these ratios are much greater than one, and we only keep the longitudinal advection term. Likewise, we can compare the diffusion terms to the advection term. For longitudinal diffusion we have

$$
\frac{\text{Longitudinal diffusion}}{\text{Longitudinal advection}} = \frac{D_x}{L_x^2 T_a} \tag{7.7}
$$

which is our familiar Peclet number. For large Peclet numbers, we only consider diffusion, and for small Peclet numbers, we only consider advection. Hence, the important terms in the equation again depend on the length of river we are considering.

As an example, when might a one-dimensional steady-state model with dye-off be an acceptable model for a given river reach? The governing model equation would be

$$
u\frac{\partial C}{\partial x} = D_x \frac{\partial^2 C}{\partial x^2} - kC. \tag{7.8}
$$

By comparing with the non-dimensional equation above, this equation implies several constraints on the river. Consider first the external time-scale. This model implies

$$
\frac{UT_0}{L_x} \gg 1. \tag{7.9}
$$

For the convective terms, this model implies that

$$\frac{UL_y}{VL_x} \gg 1 \tag{7.10}$$

$$\frac{UL_z}{WL_x} \gg 1 \tag{7.11}$$

or alternatively

$$\frac{\partial C}{\partial y} = \frac{\partial C}{\partial z} = 0. \tag{7.12}$$

Similarly, for diffusion this model implies that

$$\frac{UL_y^2}{L_x D_y} \gg 1 \tag{7.13}$$

$$\frac{UL_z^2}{L_x D_z} \gg 1 \tag{7.14}$$

or, again, alternatively

$$\frac{\partial C}{\partial y} = \frac{\partial C}{\partial z} = 0. \tag{7.15}$$

Finally, for the reaction, this model implies that

$$\frac{UT_{1/2}}{L_x} \approx 1. \tag{7.16}$$

Therefore, by comparing the relevant scales in our problem to the approximations made by models, we can determine just how complex the model must be to approximate our system adequately.

7.1.3 Data availability

As a final comment on the selection and implementation of an analysis tool, we discuss a few points regarding the data that are used to validate the model (Section 7.4 below discusses how to test a model in more detail). The only test available to determine whether the model adequately reproduces our natural system is to compare model output to data (measurements) taken from the prototype system. In general, as the model complexity increases, the number of parameters we can use to adjust the model results to match the prototype also increases, giving us more degrees of freedom. The more degrees of freedom we have, the more data we need to calibrate our model. Hence, the data requirements of a model are directly proportional to the model complexity. If very limited data are available, then complex models should be avoided because they cannot be adequately calibrated or validated.

7.2 Simple water quality models

Some simple water quality models can be developed for special cases where advection or diffusion is dominant. As introduced in Chapter 2, the Peclet number is a measure of diffusion to advection dominance. The Peclet number, Pe, is defined as

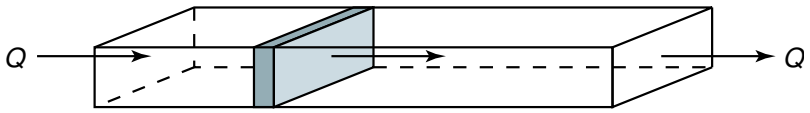

Fig. 7.1. Schematic of a plug-flow reactor.

$$Pe = \frac{D}{uL} \tag{7.17}$$

$$= \frac{D}{u^2 t} \tag{7.18}$$

where the two definitions are equivalent. The Peclet number is small when advection is dominant and large when diffusion is dominant. Two simple models can be developed for the limiting cases of $Pe \to 0$ and $Pe \to \infty$. A third hybrid model is also introduced in this section for simplified application to arbitrary Pe.

7.2.1 Advection dominance: Plug-flow reactors

For $Pe \to 0$ we can neglect longitudinal diffusion and dispersion, and we have the so-called plug-flow reactor. Shown in Figure 7.1, a slab of marked fluid is advected with the mean flow, perhaps undergoing reactions, but not spreading in the lateral. Taking $D = 0$, the governing reactive transport equation becomes

$$\frac{\partial C}{\partial t} + u\frac{\partial C}{\partial x} = \pm R. \tag{7.19}$$

To solve this equation, we make the familiar coordinate transformation to move our coordinate system with the mean flow. That is,

$$\xi = x - ut \tag{7.20}$$

$$\tau = t. \tag{7.21}$$

As demonstrated in Chapter 2, using the chain rule to substitute this coordinate transformation into (7.19) gives

$$\frac{\partial C}{\partial \tau} = \pm R \tag{7.22}$$

which is easily solved after defining an initial condition and the transformation reaction R.

For example, consider a first-order die-off reaction for a slab with initial concentration C_0. The solution to (7.22) is

$$C(\tau) = C_0 \exp(-k\tau) \tag{7.23}$$

or in the original coordinate system, we have the interchangeable solutions

$$C(t) = C_0 \exp(-kt) \tag{7.24}$$

$$C(x) = C_0 \exp(-kx/u). \tag{7.25}$$

The residence time for a plug-flow reactor depends on the distance of interest L_0. From the definition of residence time

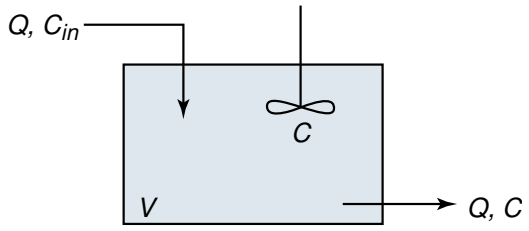

Fig. 7.2. Schematic of a continuously-stirred tank reactor (CSTR).

$$\begin{aligned} t_{res} &= \frac{V}{Q} \\ &= \frac{L_0 A}{Q} \end{aligned} \tag{7.26}$$

where A is the cross-sectional area of the channel and Q is the steady flow rate. The fluid residence time, the travel time for a slab to move the distance L_0, can also be expressed using the same variables

$$\begin{aligned} t_{slab} &= \frac{L_0}{u} \\ &= \frac{L_0 A}{Q} \\ &= t_{res}. \end{aligned} \tag{7.27}$$

Hence, the fluid and species residence times are equal.

7.2.2 Diffusion dominance: Continuously-stirred tank reactors

For $Pe \to \infty$ we can neglect advection and we have the so-called continuously-stirred tank reactor (CSTR). Shown in Figure 7.2, fluid that enters the reactor is assumed to instantaneously mix throughout the full reactor volume. To write the governing equation, consider mass conservation in the tank

$$\frac{dM}{dt} = \dot{m}_{in} - \dot{m}_{out}. \tag{7.28}$$

The inflow provides the mass flux into the control volume, $\dot{m}_{in}$. Loss of mass, $\dot{m}_{out}$ is given by the outflow and possible die-off reactions. Writing the conservation of mass in concentrations and flow rates yields

$$\frac{d(CV)}{dt} = Q(C_{in} - C_{out}) \pm S \tag{7.29}$$

where V is the volume of the tank and $S = VR$ is a source or sink reaction term. Because the tank is well mixed, we can assume that C_{out} is equal to the concentration in the tank C. Taking V as constant, we can move it outside the derivative, and the governing equation becomes

$$\frac{dC}{dt} = \frac{Q}{V}(C_{in} - C) \pm R. \tag{7.30}$$

Substituting the definition of the residence time, we have finally

$$\frac{dC}{dt} = \frac{1}{t_{res}}(C_{in} - C) \pm R \tag{7.31}$$

which is the governing equation for a CSTR.

Consider first the conserving case, where $R = 0$. Taking the initial condition as a clean tank $C_0 = 0$, the solution to (7.31) is

$$C(t) = C_{in}\left[1 - exp\left(-\frac{t}{t_{res}}\right)\right]. \tag{7.32}$$

Thus, the concentration in the tank increases exponentially with a rate constant $k = 1/t_{res}$. The concentration in the tank reaches steady state asymptotically. If we define steady state as the time, t_{ss}, until $C = 0.99C_0$, then

$$t_{ss} = 4.6t_{res}. \tag{7.33}$$

Therefore, without reactions, steady state is reached in about 4.6 residence times.

The solution for the reacting case is slightly more complicated because (7.31) is an inhomogeneous differential equation with forcing function $\pm R$. Consider the case of a first-order die-off reaction and an initial tank concentration of $C_0 = 0$. Assuming a particular solution (refer to Appendix C for an example of solving an inhomogeneous equation) of the form $C_p = AC_{in}$, the solution is found to be

$$C(t) = \frac{C_{in}}{1 + kt_{res}}\left[1 - \exp\left[-\left(\frac{1 + kt_{res}}{t_{res}}\right)t\right]\right]. \tag{7.34}$$

Because of the reaction, the steady state concentration in the tank is no longer the inflow concentration, but rather

$$C_{ss} = \frac{C_{in}}{1 + kt_{res}} \tag{7.35}$$

and the coefficient $1/(1 + kt_{res})$ is one minus the removal rate. The time to reach steady state, t_{ss}, is the time to reach $0.99C_{ss}$ or

$$t_{ss} = \frac{4.6t_{res}}{1 + kt_{res}}. \tag{7.36}$$

7.2.3 Tanks-in-series models

The simplest type of river-flow model that incorporates some form of diffusion or dispersion is the tanks-in-series model, which is a chain of linked CSTRs. An example tanks-in-series model is shown in Figure 7.3. In the example each tank has the same dimensions, and the flow rate is constant. The method also works for variable volume tanks, and under gradually-varied flow conditions, stage-discharge relationships can be used to route variable flows through the tanks. To see why the tanks-in-series model produces diffusion, consider an instantaneous pulse injection in the first tank. The outflow from that tank would be the solution to the CSTR given by (7.32). The outflow from the first tank is, therefore, exponential, clearly not the expected Gaussian distribution. But, this outflow goes into the next tank. At first, that tank is clean, and the little bit of tracer entering the tank in the beginning is quickly diluted; hence, the outflow concentration starts at zero and increases slowly. Eventually, a large amount of the

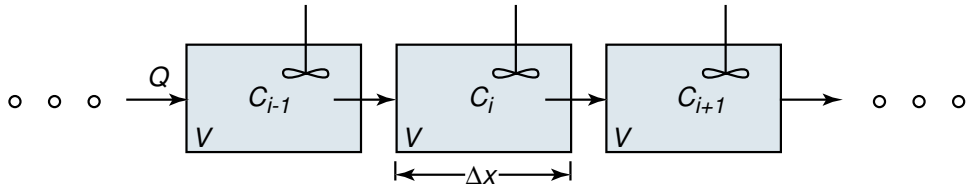

Fig. 7.3. Schematic of a tanks-in-series model. The model is made up of several CSTR linked in series.

tracer in the first tank has moved on to the second tank and the outflow from the second tank reaches a maximum concentration. The inflow from the first tank becomes increasingly cleaner, and the outflow from the second tank also decreases in concentration. Eventually, all the tracer has flowed through both tanks and the concentration is zero at the outlet of the second tank. The concentration curve over time for the second tank started at zero, increased smoothly to a maximum concentration, then decreased slowly back down to zero. These characteristics are very similar to the Gaussian distribution; hence, we expect that by dimensioning the tanks properly, we should be able to reproduce the behavior of advective diffusion in the downstream tanks.

To find the proper tank dimensions, consider the mass conservation equation for a central tank. Inflow comes from the upstream tank, and outflow goes to the downstream tank; thus, we have

$$\frac{dM_i}{dt} = Q(C_{i-1} - C_i) \pm VR. \tag{7.37}$$

For the remaining analysis we will neglect the reaction term. Assuming each tank has the same length, the tank volume can be written as $V = A\Delta x = A(x_i - x_{i-1})$. Using this definition to write M_i in concentration units gives

$$\frac{dC_i}{dt} = u\frac{C_{i-1} - C_i}{x_i - x_{i-1}} \tag{7.38}$$

which is the discrete equation describing the tanks-in-series model.

The difference term on the right-hand-side of (7.38) is very close to the backward difference approximation to $\partial C/\partial x$:

$$\frac{\partial C}{\partial x} = \frac{C_i - C_{i-1}}{x_i - x_{i-1}} \tag{7.39}$$

which has no error for $\Delta x \to 0$. For finite grid size, the Taylor-series expansion provides an estimate of the error. The second-order Taylor-series expansion of C_{i-1} about C_i is

$$C_{i-1} = C_i + \left.\frac{\partial C_i}{\partial x}\right|_i (x_{i-1} - x_i) + \frac{1}{2}\left.\frac{\partial^2 C_i}{\partial x^2}\right|_i (x_{i-1} - x_i)^2 + \cdots \tag{7.40}$$

as given in Thomann & Mueller (1987). Rearranging this equation, we can obtain

$$\frac{C_i - C_{i-1}}{x_i - x_{i-1}} = \frac{\partial C_i}{\partial x} - \frac{1}{2}\frac{\partial^2 C_i}{\partial x^2}(x_i - x_{i-1}). \tag{7.41}$$

Multiplying this result by -1 gives

$$\frac{C_{i-1} - C_i}{x_i - x_{i-1}} = -\frac{\partial C_i}{\partial x} + \frac{1}{2}\frac{\partial^2 C_i}{\partial x^2}(x_i - x_{i-1}) \tag{7.42}$$

which can be substituted immediately for the right-hand-side of (7.38) leaving

$$\frac{dC_i}{dt} = -u\frac{\partial C_i}{\partial x} + \frac{u(x_i - x_{i-1})}{2}\frac{\partial^2 C_i}{\partial x^2}. \tag{7.43}$$

Dropping the subscripts and recognizing $\Delta x = (x_i - x_{i-1})$ gives the governing equation

$$\frac{dC}{dt} + u\frac{\partial C}{\partial x} = \frac{u\Delta x}{2}\frac{\partial^2 C}{\partial x^2}. \tag{7.44}$$

Thus, our derived governing equation for a tanks-in-series model has the same form as the advective diffusion equation with a diffusion coefficient of $D_n = u\Delta x/2$.

The effective diffusion coefficient, D_n, for a tanks-in-series model is actually a numerical error due to the discretization. As the discretization becomes more course, the numerical error increases and the numerical diffusion goes up. For $\Delta x \to 0$, the numerical diffusion vanishes, and we have the plug-flow reactor. Hence, for a tanks-in-series model, we choose the tank size such that D_n is equal to the physical longitudinal diffusion and dispersion in the river reach.

7.3 Numerical models

Although the tank-in-series model was shown to be a special discretization of the advective diffusion equation, other numerical techniques specifically set out to discretize the governing equation. For our purposes, a numerical model is any model that seeks to solve a differential equation by discretizing that equation on a numerical grid.

7.3.1 Coupling hydraulics and transport

To simulate chemical transport, the velocity field, represented by $\boldsymbol{u}$ in the transport equation must also be computed. The model that calculates $\boldsymbol{u}$ is called the hydrodynamic or hydraulic model. Thus, to simulate transport, the hydrodynamic and transport models must be properly coupled.

Whether the hydrodynamic and transport models must be implicitly coupled or whether they can be run in series depends on the importance of buoyancy effects. If the system is free from buoyancy effects, the hydrodynamics are independent of the transport; hence, they can be run first and their output stored. Then, many transport simulations can be run using the hydrodynamic data without re-running the hydrodynamic code. If buoyancy effects are present in the water body, then the transport of buoyancy (heat or salinity or both) must be coupled with the hydrodynamics, and both models must be run together. Once the output from the coupled model is stored, further transport simulations can be run for constituents that do not influence the buoyancy (these are called passive constituents). Because the hydrodynamic portion of the model is computationally expensive, the goal in transport modeling is to de-couple the two models as much as possible.

7.3.2 Numerical methods

There are probably as many numerical methods available to solve the coupled hydrodynamic and advective transport equations as there are models; however, most models can be classified by a few key words.

There are three main groups of numerical methods: finite difference, finite volume, and finite element. For special selections of basis functions and geometries, the three methods can all be made equivalent, but in their standard applications, the methods are all slightly different. The finite difference method is built up from a series of nodes, the finite volume method is built up from a group of cells, and the finite element method is made up of a group of elements, where each element is comprised of two or more grid points. In the finite difference case, the differential equation is discretized over the numerical grid, and derivatives become difference equations that are functions of the surrounding cells. In the finite volume case, the fluxes through the cell network are tracked and the differential equations are integrated over the cell volume. For finite elements, a basis function is chosen to describe the variation of an unknown over the element and the coefficients of the basis functions are found by substituting the basis functions as solutions into the governing equations. Because finite difference methods are easier to implement and understand, these methods are more widely used.

A numerical method may further be explicit or implicit. An explicit scheme is the easiest to solve because the unknowns are written as functions of known quantities. For instance, the concentration at the new time is dependent on concentrations at the previous time step and at upstream (known) locations. In an implicit scheme, the equations for the unknowns are functions of other unknown quantities. For instance, the concentration at the new time may depend on other concentrations at the new time or on downstream locations not yet computed. In the implicit case, the equations represent a system of simultaneous equations that must be solved using matrix algebra. The advantage of an implicit scheme is that it generally has greater accuracy.

Finally, numerical methods can be broadly categorized as Eulerian or Lagrangian. Eulerian schemes compute the unknown quantities on a fixed grid based on functions of other grid quantities. Lagrangian methods use the method of characteristics to track unknown quantities along lines of known value. For instance, in a Lagrangian transport model, the new concentration at a point could be found by tracking the hydrodynamic solution backward in time to find the point where the water parcel originated and then simply advecting that concentration forward to the new time. Because the Lagrangian method relies heavily on the velocity field, small errors in the velocity field (particularly for fields with divergence) can lead to large errors in the conservation of mass. The advantage of the Lagrangian method is that it can backtrack over several hydrodynamic time steps; hence, there is no theoretical limitation on the size of the time step in a Lagrangian transport model. An example of a one-dimensional Lagrangian scheme is the Holly-Preissman method. By contrast, for the Eulerian model, the time step is limited by a so-called Courant number restriction, that says that the time step cannot be so large that fluid in one cell advects beyond the next adjacent cell over one time step. Mathematically, this can be written as

$$\Delta t \leq \frac{\Delta x}{u} \tag{7.45}$$

where Δt is the time step and Δx is the grid size.

7.3.3 Role of matrices

In the case of explicit models, matrices are not a necessity, but for implicit models and models simulating many contaminant, matrices provide a comfortable (and often necessary) means of solving the governing equations. For an implicit scheme, the equations for a given node at the new time are dependent on the solutions at other nodes at the same time. This means that implicit schemes are inherently a system of equations (sometimes non-linear), which are best solves with matrices. The general matrix equation is

$$\underline{A}\boldsymbol{x} = \boldsymbol{b} \tag{7.46}$$

where $\underline{A}$ is an n x n matrix of equation coefficients, x is an n x 1 vector of unknowns (for example, flow rates), and b is an n x 1 vector of forcing functions. Writing the equations in such a way makes derivation of the model equations manageable and implementation in the computer algorithm straightforward. The solution of (7.46) is

$$\boldsymbol{x} = \underline{A}^{-1}\boldsymbol{b} \tag{7.47}$$

where $\underline{A}^{-1}$ is the matrix inverse. Most computer languages have built-in methods for solving matrices. For the non-linear case, an iteration technique must be employed. A common method is the Newton-Raphson method.

7.3.4 Stability problems

One limitation already mentioned for an Eulerian transport scheme is the Courant number restriction. In general, all schemes have a range of similar restrictions that limit the allowable spatial grid size and time step such that the scheme remains stable. If the time step is set longer than such a constraint, the model is unstable and will give results with large errors that eventually blow up. The full hydrodynamic equations are hyperbolic and generally have more stringent limitations than the parabolic transport equation. Before implementing a model, it is advised to seek out the published stability criteria for the model; this can save a lot of time in getting the model to run smoothly.

7.4 Model testing

An unfortunate fact of numerical modeling is that implementation and calibration is very time consuming, and little time is available for a thorough suite of model tests. This does not excuse the fact that model testing is necessary, but rather explains why it is often neglected. Even when using well-known tools, the following suite of tests is imperative to ensure that the model is working properly for your application. The following tests are specific to transport models, but apply in a generalized sense to all models.

7.4.1 Conservation of mass

All transport (water quality models) must conserve mass! This is a zeroth-order test that confirms whether the zeroth-moment of the concentration distribution is accurately reproduced in the solution. Clearly, when reactions are present, a given species may be loosing or gaining mass due to the reaction. This test must confirm, then, that the total system mass remains constant and that a species only gains mass at the rate allowed by the reaction equation. This test is often conducted in conjunction with the next test. However, it should always also be conducted for the complex real-world case being simulated, where analytical solutions are not available.

7.4.2 Comparison with analytical solutions

The model should be tested in idealized conditions to compare its results to known analytical solutions. This test confirms whether the model actually solves the governing equation that it was designed to solve. Deviations may be caused by many sources, most notably programming errors and numerical inaccuracy. Although most widely used models are free from programming errors, this cannot be tacitly assumed. In this author's experience, programming errors have been found in well-known, government-supported models by running this test. The issue of numerical inaccuracy arises due to the discretization, as in the case of numerical diffusion mentioned for the tanks-in-series model described above. Hence, the idealized case should have length and time scales as close to the prototype as possible in order to accurately assess the importance of numerical inaccuracy arising from the numerical method and the discretization.

This step can save a lot of time in applying the model to the prototype because the source of errors can often be identified faster in idealized systems. First, the analytical solution is a known result. If the model gives another result, the model must be wrong. Second, the complexity of the real-world case makes it difficult to assess the importance of deviations from measured results. Once the model has been thoroughly tested against analytical results, deviations can be explained by physical phenomena in the prototype not present or falsely implemented in the model. Third, this test helps determine the stability requirements for complex models.

7.4.3 Comparison with field data

Only after it is certain that the model is solving the equations properly and within a known level of error can the model be compared to field or laboratory measurements of the prototype. The comparison of model results with these date serves two purposes. First, the model must be calibrated; that is, its parameters must be adjusted to match the behavior of the prototype. Second the model must be validated. This means that a calibrated model must be compared to data *not* used in the calibration to determine whether the model is applicable to cases outside the calibration data set. These prototype measurements fall into two categories: tracer studies and data collection of natural events.

Tracer studies. In a tracer study, dye is injected into the natural system, and concentrations are measured in time and space to record how the dye is transported and diluted. The advantage of a tracer study is that the source injection rate and location are known with certainty and that reactions can (often) be neglected. Tracer studies help calibrate the model parameters (such as diffusion and dispersion coefficients and turbulent closure schemes) to the real-world case. These studies also help to confirm whether the model assumptions are met (such as the one-dimensional approximation) and are good tests of both the hydrodynamic and water quality models.

Water quality data. The final set of data available for model testing is actual measurements of the modeled constituents in the prototype under natural conditions. These measurements represent true values, but are difficult to interpret because of our incomplete description of the prototype itself. We often do not know the total loading of constituent, and all the model equations are approximations of the actual physical processes in the prototype. These measurements further help to confirm whether the model assumptions are valid and to calibrate model parameters. Once the tests listed above are completed, the modeler should have a good understanding of how the complex physical processes in the model combine to give the model results. Deviations between the model and the field measurements should then be explained through the physical insight available in the model.

It is important to point out that the water quality measurement campaign should compliment the output available from the model. That is, the data should be collected such that they can be used to calibrate and test the model. If the model only outputs daily predictions, then the measurements should be able to predict daily values; instantaneous point measurements are only useful for a parameter that does not vary much over the diurnal cycle. In summary, the model is only as good as the data that support it, and the data must be compatible with the model and flex the parts of the model that are the most uncertain.

Summary

This chapter introduced the concept of water quality modeling. A model is defined as any analysis tool that reduces a physical system to a set of equations or a reduced-scale physical model. A four-step procedure was suggested to help select the appropriate model: (1) define project goals, (2) describe an acceptable modeling tool, (3) list the available tools that could satisfy the goals and model description, and (4) select the model to be used based on an optimal compromise between goals and available tools. Because analytical solutions are not always adequate, numerical techniques were introduced. These included tank reactor models and numerical solution methods for differential equations, such as finite difference and finite element. Because numerical solutions result in a large number of calculations, a rigorous procedure for testing a numerical model was also suggested. These steps include (1) confirming that model conserves mass, (2) testing the model in idealized cases against analytical solutions, and (3) comparing the model to field data in the form of dye studies and the collection of water quality data. Good modeling projects should follow all of these suggested procedures.

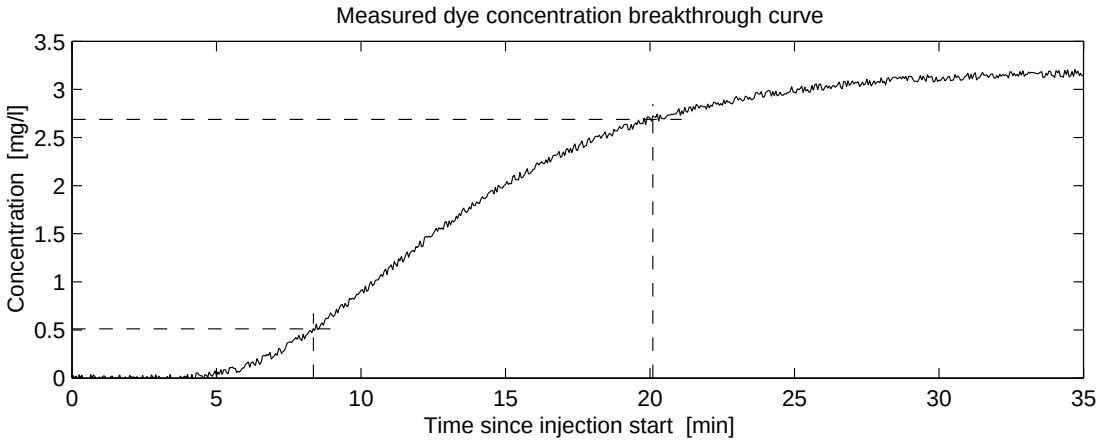

Fig. 7.4. Measured dye concentration for example dye study. Dye fluctuations are due to instrument uncertainty, not due to turbulent fluctuations.

Exercises

7.1 Equation scaling. Non-dimensionalize the one-dimensional momentum equation

$$\frac{\partial u}{\partial t} + u\frac{\partial u}{\partial x} = \frac{1}{\rho}\frac{\partial p}{\partial x} + \nu\frac{\partial^2 u}{\partial x^2} \tag{7.48}$$

using the non-dimensional variable definitions

$$u = U_0 u' \; ; \qquad x = Lx' \tag{7.49}$$

$$t = (L/U_0)t' \; ; \qquad p = \rho U_0^2 p' \tag{7.50}$$

Divide the equation by the coefficient in front of $\partial u'/\partial t'$. What familiar non-dimensional number becomes the leading coefficient of the viscous term? When is the viscous term negligible?

7.2 Finite difference. Write the explicit backward-difference approximation to the reaction equation

$$\frac{dC}{dt} = kC. \tag{7.51}$$

Program this solution in a computer and suggest a criteria for selecting the appropriate time step Δt by comparing to the analytical solution

$$C(t) = C_0 \exp(kt). \tag{7.52}$$

7.3 Tanks-in-series model. A river has a cross-section of $h = 1$ m deep and $B = 10$ m wide. The mean stream velocity is 22.5 cm/s. A dye study was conducted my injecting 2.25 g/s of dye uniformly across the cross-section 150 m upstream of a measurement point. The measurements of dye concentration at $L = 150$ m are given in Figure 7.4. From the figure, determine the value of the dispersion coefficient. Based on this value, how many tanks in a tanks-in-series model would be needed to reproduce this level of dispersion in the numerical model?

A. Point-source Diffusion in an Infinite Domain: Boundary and Initial Conditions

In this appendix we discuss how the boundary and initial conditions for a point source in an infinite, one-dimensional domain are applied to find the solution of the diffusion equation. The governing equation is

$$\frac{\partial C}{\partial t} = D\frac{\partial^2 C}{\partial x^2} \tag{A.1}$$

with boundary conditions $C(\pm\infty, t) = 0$ and initial condition $C(x, 0) = (M/A)\delta(x)$ (for more detail, refer to Chapter 1).

In this case we will use the Fourier exponential transform instead of the similary method to obtain our result. Although each method is equally valid, it is easier to see how the boundary conditions are applied using the Fourier transform. Since the governing equations that is obtained after applying the boundary conditions will be the same using either method, applying the Fourier transform method here is the better approach. For this method we use the Fourier exponential transformation defined by

$$\mathcal{F}(\alpha, t) = \int_{-\infty}^{\infty} F(x, t)e^{-i\alpha x}dx \tag{A.2}$$

where $\mathcal{F}(\alpha, t)$ is the Fourier transformation of $F(x, t)$, α is a transformation variable, and i is the imaginary number. This method implicitly satisfies the boundary conditions at $\pm\infty$. This is called a behavioral boundary condition (see e.g. Boyd 1989), and it is not necessary to apply the boundary to fix the values of integration constants—the solution implicitely obeys the boundary conditions because of our use of the Fourier transform. The following application of this method to the diffusion equation is taken from Mei (1997).

The Fourier transform of the governing diffusion equation gives

$$\frac{d\mathcal{C}}{dt} + D\alpha^2\mathcal{C} = 0. \tag{A.3}$$

The power of the Fourier transform is that it converts partial differential equations into ordinary differential equations, this time a simple, first-order ODE with solution

$$\mathcal{C}(\alpha, t) = \mathcal{F}(\alpha)\exp(-D\alpha^2 t). \tag{A.4}$$

$\mathcal{F}(\alpha)$ is found by applying the initial condition. Applying the Fourier transform to the initial condition gives

$$\begin{aligned}\mathcal{F}(\alpha) &= \mathcal{C}(\alpha, 0)\\ &= \int_{-\infty}^{\infty} (M/A)\delta(x)e^{-i\alpha x}dx\end{aligned}$$

$$= M/A. \tag{A.5}$$

The drawback of the Fourier transform method is that the inverse transform to get back to our desired dimensional space is sometimes a difficult integral.

We stop here to take a look at what we have done so far. The Fourier transform method implicitly satisfies the boundary conditions; therefore, we do not have to think about them anymore. Further, the initial condition was used to find the solution to the ODE obtained after the Fourier transform. Thus, our solution

$$\mathcal{C}(\alpha, t) = (M/A)\exp(-D\alpha^2 t) \tag{A.6}$$

satisfies all our boundary and initial conditions. The remaining task is to perform a Fourier inverse transform on this solution.

The Fourier inverse transform is defined in general as

$$F(x,t) = \frac{1}{2\pi}\int_{-\infty}^{\infty} \mathcal{F}(\alpha, t)e^{i\alpha x}d\alpha. \tag{A.7}$$

For our problem, the inverse transform becomes

$$C(x,t) = \frac{1}{2\pi}\int_{-\infty}^{\infty} (M/A)\exp(-D\alpha^2 t)e^{i\alpha x}d\alpha. \tag{A.8}$$

We can simplify a little by recognizing that $e^{i\alpha x} = \cos(\alpha x) + i\sin(\alpha x)$. Since $e^{-D\alpha^2 t}$ is an even function and $i\sin(\alpha x)$ is an odd function, we can neglect the sin-contribution, leaving us with the integral

$$C(x,t) = \frac{M}{2\pi A}\left(2\int_0^{\infty} e^{-D\alpha^2 t}\cos(\alpha x)d\alpha\right) \tag{A.9}$$

which we still must solve.

The first step in solving (A.9) is to simplify the exponential using the change of variable

$$\alpha = \frac{x}{\sqrt{Dt}} \tag{A.10}$$

$$d\alpha = \frac{dx}{\sqrt{Dt}} \tag{A.11}$$

(note, this in an arbitrary change of variable that puts the integral in a form more likely to be found in integral tables). Further, we define a new variable

$$\eta = \frac{x}{\sqrt{Dt}} \tag{A.12}$$

(note, this is also an arbitrary decision). Substituting these definitions leaves us with

$$C(x,t) = \frac{M}{\pi A\sqrt{Dt}}\int_0^{\infty} e^{-x^2}\cos(\eta x)dx. \tag{A.13}$$

Thus, our solution simplifies to having to solve the integral

$$I(\eta) = \int_0^{\infty} e^{-x^2}\cos(\eta x)dx. \tag{A.14}$$

The integral in (A.14) is not a trivial integral, but can be solved by employing the following tricks. Basically, we need to find the derivative of I with respect to η and then put it in a useful form. We begin with

$$\frac{dI}{d\eta} = \int_0^\infty -xe^{-x^2}\sin(\eta x)dx. \tag{A.15}$$

Next, recognize that $xdx = (1/2)d(x^2)$, giving

$$\frac{dI}{d\eta} = -\frac{1}{2}\int_0^\infty e^{-x^2}\sin(\eta x)d(x^2). \tag{A.16}$$

Similarly, we make use of the identity $e^{-x^2}d(x^2) = -d(e^{-x^2})$, which lets us write

$$\frac{dI}{d\eta} = \frac{1}{2}\int_0^\infty \sin(\eta x)d(e^{-x^2}). \tag{A.17}$$

Now, we integrate by parts (where $u = \sin(\eta x)$ and $dv = d(e^{-x^2})$) yielding

$$\begin{aligned}\frac{dI}{d\eta} &= \frac{1}{2}(e^{-x^2}\sin(\eta x))\Big|_0^\infty - \frac{1}{2}\int_0^\infty e^{-x^2}d(\sin(\eta x)) \\ &= 0 - \frac{\eta}{2}\int_0^\infty e^{-x^2}\cos(\eta x)dx \\ &= -\frac{\eta}{2}I(\eta).\end{aligned} \tag{A.18}$$

We can rearrange the last line as follows

$$\frac{dI}{d\eta} + \frac{\eta}{2}I(\eta) = 0 \tag{A.19}$$

which looks remarkably like (1.49) if C_0 is taken as zero. The initial condition necessary to solve the above ODE is given by

$$I(0) = \int_0^\infty e^{-x^2}dx. \tag{A.20}$$

If we convert I in the previous two equations to our variables used in the similarity solution, we obtain

$$\frac{df}{d\eta} + \frac{\eta}{2}f(\eta) = 0 \tag{A.21}$$

with initial condition

$$\int_{-\infty}^\infty f(\eta)d\eta = 1. \tag{A.22}$$

Therefore, we have shown through a rigorous application of the Fourier transform method, that the above two equations give the solution to the diffusion equation that we seek in an infinite domain for an instantaneous point source *after* having applied the appropriate boundary and initial conditions.

B. Solutions to the Advective Reacting Diffusion Equation

This appendix presents solutions to the advective reacting diffusion equation given by

$$\frac{\partial C}{\partial t} + u\frac{\partial C}{\partial x} + v\frac{\partial C}{\partial y} + w\frac{\partial C}{\partial z} = E_x\frac{\partial^2 C}{\partial x^2} + E_y\frac{\partial^2 C}{\partial y^2} + E_z\frac{\partial^2 C}{\partial z^2} - kC \tag{B.1}$$

for homogeneous, anisotropic turbulence with the steady velocity $\boldsymbol{u} = (u, v, w)$. The E_i's are the anisotropic turbulent diffusion coefficients, and k is a constant first-order decay rate. In previous chapters we denoted the turbulent diffusion coefficient by D_t. We use $D_t = E$ here so that the subscripts do not get too complicate and to expose the reader to another notation for the turbulent diffusion coefficient common in the literature.

B.1 Instantaneous point source

An instantaneous point source has an injection of mass, M, at the point $\boldsymbol{x} = (x_1, y_1, z_1)$ at time $t = 0$. The following solutions cover different ambient conditions.

B.1.1 Steady, uni-directional velocity field

For a steady velocity field $\boldsymbol{u} = (U, 0, 0)$, the solutions is

$$C(x,y,z,t) = \frac{M}{4\pi t\sqrt{4\pi E_x E_y E_z t}} \exp\left(-\frac{((x-x_1)-Ut)^2}{4E_x t} - \frac{(y-y_1)^2}{4E_y t} - \frac{(z-z_1)^2}{4E_z t} - kt\right). \tag{B.2}$$

B.1.2 Fluid at rest with isotropic diffusion

For isotropic diffusion, $E_x = E_y = E_z = E$, and, in a stagnant ambient without decay, (B.2) simplifies to

$$C(x,y,z,t) = \frac{M}{(4\pi E t)^{3/2}} \exp\left(-\frac{r^2}{4Et}\right) \tag{B.3}$$

where $r = \sqrt{x^2 + y^2 + z^2}$ and $x_1 = y_1 = z_1 = 0$.

B.1.3 No-flux boundary at $z = 0$

The no-flux boundary condition at $z = 0$ is enforced by an image source at $\boldsymbol{x} = (x_1, y_1, -z_1)$, giving the solution for $z > 0$ neglecting decay and crossflow as

$$\begin{aligned} C(x,y,z,t) = & \frac{M}{4\pi t\sqrt{4\pi E_x E_y E_z t}} \cdot \\ & \exp\left(-\frac{(x-x_1)^2}{4E_x t} - \frac{(y-y_1)^2}{4E_y t} - \frac{(z-z_1)^2}{4E_z t}\right) \\ & + \frac{M}{4\pi t\sqrt{4\pi E_x E_y E_z t}} \cdot \\ & \exp\left(-\frac{(x-x_1)^2}{4E_x t} - \frac{(y-y_1)^2}{4E_y t} - \frac{(z+z_1)^2}{4E_z t}\right). \end{aligned} \tag{B.4}$$

B.1.4 Steady shear flow

The following solution, presented in Okubo & Karweit (1969), is for the special shear flow given by $\boldsymbol{u} = (u_0(t) + \lambda_y y + \lambda_z z, 0, 0)$, where λ_y and λ_z are the velocity gradients defined by

$$\lambda_y = \frac{\partial u}{\partial y} \tag{B.5}$$

$$\lambda_z = \frac{\partial u}{\partial z}. \tag{B.6}$$

The solution is

$$\begin{aligned} C(x,y,z,t) = & \frac{M}{4\pi t\sqrt{4\pi E_x E_y E_z t}\sqrt{1+\phi^2 t^2}} \cdot \\ & \exp\left(-\frac{\left(x - \int_0^t u_0(t')dt' - \frac{1}{2}(\lambda_y y + \lambda_z z)t\right)^2}{4E_x t(1+\phi^2 t^2)}\right. \\ & \left. -\frac{y^2}{4E_y t} - \frac{z^2}{4E_z t} - kt\right), \end{aligned} \tag{B.7}$$

where the injection is at $(0,0,0)$ and ϕ^2 is given by

$$\phi^2 = \frac{1}{12}\left(\lambda_y^2 \frac{E_y}{E_x} + \lambda_z^2 \frac{E_z}{E_x}\right). \tag{B.8}$$

B.2 Instantaneous line source

An instantaneous line source has an injection of mass, m', per unit length along the line through $\boldsymbol{x} = (x_1, y_1)$ for $z = \pm\infty$ at time $t = 0$. The following solutions cover different ambient conditions.

B.2.1 Steady, uni-directional velocity field

For a steady velocity field $\boldsymbol{u} = (U, 0, 0)$, the solutions is

$$C(x,y,z,t) = \frac{m'}{4\pi t\sqrt{E_x E_y}} \cdot \exp\left(-\frac{((x-x_1)-Ut)^2}{4E_x t} - \frac{(y-y_1)^2}{4E_y t} - kt\right). \tag{B.9}$$

B.2.2 Truncated line source

For the line source along the line $\boldsymbol{x} = (0,0)$ for $z = \pm z_2$, the solution is

$$C(x,y,z,t) = \frac{m'}{8\pi t\sqrt{E_x E_y}} \left(\operatorname{erf}\left(\frac{z+z_2}{\sqrt{4E_z t}}\right) - \operatorname{erf}\left(\frac{z-z_2}{\sqrt{4E_z t}}\right)\right) \cdot \exp\left(-\frac{(x-Ut)^2}{4E_x t} - \frac{y^2}{4E_y t} - kt\right). \tag{B.10}$$

B.3 Instantaneous plane source

An instantaneous plane source has an injection of mass, m'', per unit area distributed uniformly on the y-z plane passing through x_1. The solution for the uni-directional velocity field given by $\boldsymbol{u} = (U,0,0)$ is

$$C(x,y,z,t) = \frac{m''}{\sqrt{4\pi E_x t}} \exp\left(-\frac{((x-x_1)-Ut)^2}{4E_x t} - kt\right). \tag{B.11}$$

B.4 Continuous point source

The solution for a *continuous* point source is obtained by the time-integration of the solution for an *instantaneous* point source. The injection duration is t_1, and the general form of the solution is

$$C(x,y,z,t) = \gamma \int_0^{t_1} \frac{1}{(t-\tau)^{3/2}} \exp\left(-\frac{\alpha}{(t-\tau)} - \beta(t-\tau)\right) d\tau \tag{B.12}$$

where

$$\alpha = \frac{(x-x_1)^2}{4E_x} + \frac{(y-y_1)^2}{4E_y} + \frac{(z-z_1)^2}{4E_z} \tag{B.13}$$

$$\beta = \frac{U^2}{4E_x} + k \tag{B.14}$$

$$\gamma = \frac{\dot{m}\exp\left(\frac{(x-x_1)U}{2E_x}\right)}{4\pi\sqrt{4\pi E_x E_y E_z}} \tag{B.15}$$

and $\dot{m}$ is the time rate of mass injection $\partial M/\partial t$.

B.4.1 Times after injection stops

Assuming an injection period from $t = 0$ to $t = t_1$, the solution for times greater than t_1 (i.e. after injection stops) is

$$\begin{aligned} C(x,y,z,t) = \frac{\gamma\sqrt{\pi}}{2\sqrt{\alpha}} \Bigg\{ & \exp(2\sqrt{\alpha\beta}) \left(\operatorname{erf}\left(\sqrt{\frac{\alpha}{(t-t_1)}} + \sqrt{\beta(t-t_1)} \right) \right. \\ & \left. - \operatorname{erf}\left(\sqrt{\frac{\alpha}{t}} + \sqrt{\beta t} \right) \right) \\ & + \exp(-2\sqrt{\alpha\beta}) \left(\operatorname{erf}\left(\sqrt{\frac{\alpha}{(t-t_1)}} - \sqrt{\beta(t-t_1)} \right) \right. \\ & \left. \left. - \operatorname{erf}\left(\sqrt{\frac{\alpha}{t}} - \sqrt{\beta t} \right) \right) \right\} \end{aligned} \tag{B.16}$$

B.4.2 Continuous injection

A continuous injection in an injection from time $t = 0$ to the current time t, and the solution is

$$\begin{aligned} C(x,y,z,t) = \frac{\gamma\sqrt{\pi}}{2\sqrt{\alpha}} \Bigg\{ & \exp(2\sqrt{\alpha\beta}) \operatorname{erfc}\left(\sqrt{\frac{\alpha}{t}} + \sqrt{\beta t} \right) + \\ & \exp(-2\sqrt{\alpha\beta}) \operatorname{erfc}\left(\sqrt{\frac{\alpha}{t}} - \sqrt{\beta t} \right) \Bigg\}. \end{aligned} \tag{B.17}$$

The steady-state solution is found for $t \to \infty$ to be

$$C(x,y,z) = \frac{\gamma\sqrt{\pi}}{\sqrt{\alpha}} \exp(-2\sqrt{\alpha\beta}). \tag{B.18}$$

For the special case of a homogeneous, isotropic diffusion at steady state, we have

$$C(x,y,z) = \frac{\dot{m}}{4\pi E r} \exp\left(-\frac{r\sqrt{U^2 + 4Ek} - xU}{2E} \right) \tag{B.19}$$

where $r = \sqrt{x^2 + y^2 + z^2}$.

B.4.3 Continuous point source neglecting longitudinal diffusion

The steady-state solution for homogeneous turbulence and neglecting longitudinal diffusion is found from the governing equation

$$U\frac{\partial C}{\partial x} = E_y\frac{\partial^2 C}{\partial y^2} + E_z\frac{\partial^2 C}{\partial z^2} - kC. \tag{B.20}$$

For an infinite domain, the solution is

$$C(x,y,z) = \frac{\dot{m}}{4\pi x\sqrt{E_y E_z}} \exp\left(-\frac{y^2 U}{4xE_y} - \frac{z^2 U}{4xE_z} - \frac{kx}{U} \right). \tag{B.21}$$

B.4.4 Continuous point source in uniform flow with anisotropic, non-homogeneous turbulence

Here, we treat a special type of non-homogeneous turbulence, where the turbulent diffusion coefficients are functions of x, only, and where we will neglect longitudinal diffusion. The governing equation at steady state is

$$U\frac{\partial C}{\partial x} = E_y(x)\frac{\partial^2 C}{\partial y^2} + E_z(x)\frac{\partial^2 C}{\partial z^2}. \tag{B.22}$$

where the diffusivities are taken from Walters (1962) as

$$E_y = a_y x^{\alpha} \tag{B.23}$$

$$E_z = a_z x^{\beta}. \tag{B.24}$$

The solution for this special case is

$$C(x,y,z) = \frac{\dot{m}}{2\pi}\sqrt{\frac{(1+\alpha)(1+\beta)}{a_y a_z}}x^{-\left(1+\frac{\alpha+\beta}{2}\right)} \cdot \exp\left(-\frac{(1+\alpha)U}{4x^{1+\alpha}}\frac{y^2}{a_y} - \frac{(1+\beta)U}{4x^{1+\beta}}\frac{z^2}{a_z}\right). \tag{B.25}$$

B.4.5 Continuous point source in shear flow with non-homogeneous, isotropic turbulence

Smith (1957) investigated the specific case of a shear flow of the from

$$u(z) = a_0 z^{\mu} \tag{B.26}$$

where a_0 is a constant and $\mu = 1/2$. For this case the turbulent diffusion coefficient can be taken as

$$E_z(z) = b_0 z^{1-\mu} \tag{B.27}$$

where b_0 is another constant. The governing equation at steady state is

$$u(z)\frac{\partial C}{\partial x} = E_z(z)\frac{\partial^2 C}{\partial y^2} + \frac{\partial}{\partial z}\left(E_z(z)\frac{\partial C}{\partial z}\right), \tag{B.28}$$

and the solution is found to be

$$C(x,y,z) = \frac{\dot{m}a_0^{1/4}}{2(b_0 x)^{5/4}\sqrt{3\pi}}\exp\left(-\frac{a_0(y^2+z^2)}{4b_0 x}\right). \tag{B.29}$$

B.5 Continuous line source

The solution for a continuous line-source injection is obtained by integrating the solution of an instantaneous line-source (B.9). Taking the line source along the z-axis and assuming a uniform crossflow in the x-direction, the solution is derived by integrating

$$C(x,y,t) = \int_0^t \frac{\dot{m}'}{4\pi(t-\tau)\sqrt{E_x E_y}} \cdot \exp\left(-\frac{(x-U(t-\tau))^2}{4E_x(t-\tau)} - \frac{y^2}{4E_y(t-\tau)} - k(t-\tau)\right) d\tau \tag{B.30}$$

where $\dot{m}'$ is the time rate of mass injection per unit length.

B.5.1 Steady state solution

The solution to (B.30) for $t \to \infty$ is given by

$$C(x,y) = \frac{\dot{m}'}{2\pi\sqrt{E_x E_y}} \exp\left(\frac{Ux}{2E_x}\right) K_0(2\beta_2) \tag{B.31}$$

where K_0 is the modified Bessel function of second kind of order zero and

$$\beta_2 = \frac{\sqrt{(E_y x^2 + E_x y^2)(U^2 E_y + 4E_x E_y k)}}{4E_x E_y}. \tag{B.32}$$

B.5.2 Continuous line source neglecting longitudinal diffusion

For the special case where we can neglect longitudinal diffusion, E_x, the solution becomes

$$C(x,y) = \frac{\dot{m}'}{\sqrt{4\pi x U E_y}} \exp\left(-\frac{Uy^2}{4E_y x} - \frac{kx}{U}\right). \tag{B.33}$$

B.6 Continuous plane source

The time integral solution for a continuous infinite (in the y- and z-directions) plane source is given by integrating the solution for an instantaneous plane, namely:

$$C(x,t) = \int_0^{t_1} \frac{\dot{m}''}{\sqrt{4\pi E_x(t-\tau)}} \cdot \exp\left(-\frac{(x-U(t-\tau))^2}{4E_x(t-\tau)} - k(t-\tau)\right) d\tau, \tag{B.34}$$

where $\dot{m}''$ is the time rate of mass injection per unit area.

B.6.1 Times after injection stops

Assuming an injection period from $t = 0$ to $t = t_1$, the solution for times greater than t_1 is

$$C(x,t) = \frac{\dot{m}'' e^{Ux/(2E_x)}}{2\Omega}\left(\exp\left(\frac{x\Omega}{2E_x}\right)\left\{\operatorname{erf}\left(\frac{x+\Omega t}{\sqrt{4E_x t}}\right) - \operatorname{erf}\left(\frac{x+\Omega(t-t_1)}{\sqrt{4E_x(t-t_1)}}\right)\right\} - \exp\left(\frac{-x\Omega}{2E_x}\right)\cdot \left\{\operatorname{erf}\left(\frac{x-\Omega t}{\sqrt{4E_x t}}\right) - \operatorname{erf}\left(\frac{x-\Omega(t-t_1)}{\sqrt{4E_x(t-t_1)}}\right)\right\}\right), \tag{B.35}$$

where $\Omega = \sqrt{U^2 + 4kE_x}$.

B.6.2 Continuous injection

For an injection from time $t = 0$ to the current time t, the solution is

$$C(x,t) = \frac{\dot{m}'' e^{Ux/(2E_x)}}{2\Omega}\left(\exp\left(\frac{x\Omega}{2E_x}\right)\left\{\operatorname{erf}\left(\frac{x+\Omega t}{\sqrt{4E_x t}}\right) \mp 1\right\} - \exp\left(\frac{-x\Omega}{2E_x}\right)\left\{\operatorname{erf}\left(\frac{x-\Omega t}{\sqrt{4E_x t}}\right) \mp 1\right\}\right). \tag{B.36}$$

For the location $x = 0$, the solution simplifies to

$$C(0,t) = \frac{\dot{m}''}{\Omega}\operatorname{erf}\left(\frac{\Omega t}{\sqrt{4E_x t}}\right). \tag{B.37}$$

For the limiting case where the system reaches steady state ($t \to \infty$), the solution becomes

$$C(x) = \frac{\dot{m}''}{\Omega}\exp\left(\frac{x}{2E_x}(U \mp \Omega)\right). \tag{B.38}$$

B.6.3 Continuous plane source neglecting longitudinal diffusion in downstream section

If we neglect longitudinal diffusion (diffusion in the flow direction) downstream of the injection plane, then the solution at steady state for $x > 0$ simplifies to

$$C(x) = \frac{\dot{m}''}{U}\exp\left(-\frac{kx}{U}\right). \tag{B.39}$$

B.6.4 Continuous plane source neglecting decay in upstream section

If we neglect decay upstream of the injection plane, then the solution at steady state for $x < 0$ simplifies to

$$C(x) = \frac{\dot{m}''}{U}\exp\left(\frac{Ux}{E_x}\right). \tag{B.40}$$

B.7 Continuous plane source of limited extent

B.7.1 Semi-infinite continuous plane source

For a source over the region $-\infty < y < 0$, $-\infty < z < \infty$, the governing differential equation for steady state is

$$U\frac{\partial C}{\partial x} = E_y\frac{\partial^2 C}{\partial y^2} - kC, \tag{B.41}$$

and the solution is

$$C(x,y) = \frac{\dot{m}'' e^{kx/U}}{2U}\text{erfc}\left(\frac{y}{2}\sqrt{\frac{U}{E_y x}}\right). \tag{B.42}$$

B.7.2 Rectangular continuous plane source

For a continuous plane source over the domain $-b/2 < y < b/2$, $-\infty < z < \infty$, Brooks (1960) gives the steady-state solution for a series of cases.

Homogeneous turbulence. For homogeneous turbulence (E_y = constant), the solution is

$$\frac{C(x,y)}{C_0} = \frac{e^{kx/U}}{2}\left(\text{erf}\left(\frac{y+b/2}{2}\sqrt{\frac{U}{E_y x}}\right) - \text{erf}\left(\frac{y-b/2}{2}\sqrt{\frac{U}{E_y x}}\right)\right), \tag{B.43}$$

where C_0 is the concentration at the source. The solution for $y = 0$ simplifies to

$$\frac{C(x,0)}{C_0} = e^{kx/U}\text{erf}\left(\frac{b}{4}\sqrt{\frac{U}{E_y x}}\right). \tag{B.44}$$

The relationship for the plume width, defined by $L(x) = 2\sqrt{3}\sigma_y(x)$ is given by

$$\frac{L}{b} = \sqrt{1 + \frac{24E_y x}{Ub^2}}. \tag{B.45}$$

Non-homogeneous turbulence. For non-homogeneous turbulence of the form $E_y = E_{y0}(L/b)$, the center-line solution and plume width are given by

$$\frac{C(x,0)}{C_0} = e^{kx/U}\text{erf}\sqrt{\frac{3/2}{\left(1+\frac{12E_{y0}x}{Ub^2}\right)^2 - 1}} \tag{B.46}$$

and

$$\frac{L}{b} = 1 + \frac{12E_{y0}x}{Ub^2}, \tag{B.47}$$

respectively.

For non-homogeneous turbulence of the form $E_y = E_{y0}(L/b)^{4/3}$ (the so-called 4/3-power law), the center-line solution and plume width are given by

$$\frac{C(x,0)}{C_0} = e^{kx/U}\text{erf}\sqrt{\frac{3/2}{\left(1+\frac{8E_{y0}x}{Ub^2}\right)^3 - 1}} \tag{B.48}$$

and

$$\frac{L}{b} = \left(1 + \frac{8E_{y0}x}{Ub^2}\right)^{3/2}, \tag{B.49}$$

respectively.

B.8 Instantaneous volume source

For the one-dimensional case of an instantaneous injection of mass M over the range $L_1 < x < L_2$, producing the initial concentration C_i given by

$$C_i = \frac{M}{A(L_2 - L_1)}, \tag{B.50}$$

where A is a cross-sectional area perpendicular to the x-axis, the solution is

$$\frac{C(x,t)}{C_i} = \frac{e^{-kt}}{2}\left(\operatorname{erf}\left(\frac{(x - L_1) - Ut}{\sqrt{4E_x t}}\right) - \operatorname{erf}\left(\frac{(x - L_2) - Ut}{\sqrt{4E_x t}}\right)\right). \tag{B.51}$$

For the special case of $L_1 = -\infty$ and $L_2 = 0$, the solution is

$$\frac{C(x,t)}{C_i} = \frac{1}{2}\left(1 - \operatorname{erf}\left(\frac{x - Ut}{\sqrt{4E_x t}}\right)\right). \tag{B.52}$$

C. Streeter-Phelps Equation

The Streeter-Phelps equation is the solution to the differential equation

$$\frac{dD}{dt} = k_d L_0 \exp(-k_d t) - K_r D, \tag{C.1}$$

derived in Section 5.2.2. The oxygen deficit is $D = [O_2]_{sat} - [O_2]$, k_d is the degradation rate of organic matter, L_0 is the total carbonaceous oxygen demand, and K_r is the river oxygen aeration coefficient. The solution is subject to the initial condition $D(t = 0) = D_0$.

Since this is an inhomogeneous equation, we first find the complimentary solution, which is the solution to the homogeneous equation

$$\frac{dD}{dt} = -K_r D, \tag{C.2}$$

which has the solution

$$D_c(t) = C_1 \exp(-K_r t), \tag{C.3}$$

where C_1 is a constant that must satisfy the initial condition in the final solution.

To find a particular solution, we assume the solution has the same form as the forcing function ($k_d L_0 \exp(-k_d t)$). Thus, we assume the solution

$$D_p(t) = A \exp(-k_d t). \tag{C.4}$$

Substituting into (C.1) and solving for A, we obtain

$$A = \frac{k_d L_0}{K_r - k_d}. \tag{C.5}$$

The general solution is the sum of the complimentary and particular solutions:

$$D(t) = \frac{k_d L_0}{K_r - k_d} \exp(-k_d t) + C_1 \exp(-K_r t). \tag{C.6}$$

Setting $t = 0$ and equating with the initial condition, leads to

$$C_1 = D_0 - \frac{k_d L_0}{K_r - k_d}. \tag{C.7}$$

Substituting this result into the general solution yields the classic Streeter-Phelps equation:

$$D(t) = \frac{k_d L_0}{K_r - k_d}(\exp(-k_d t) - \exp(-K_r t)) + D_0 \exp(-K_r t). \tag{C.8}$$

D. Common Water Quality Models

In this appendix we introduce a few of the common models used in water quality analysis. This is by no means a complete list, but does provide a starting point from which to work. Much of the text in this appendix was copied from the internet home pages describing each of the models. The web page[1] for this course provides links to each of these models in the web.

D.1 One-dimensional models

One-dimensional models are most commonly used in rivers, but can also be used in special cases in estuaries and lakes with large length-to-width ratios. Accept for the ATV model, these models are publicly available free of charge, and most can be downloaded over the internet. The list of models below progresses from steady-state models, to dynamic tanks-in-series models, to fully-dynamic numerical models. Refer to Chapter 7 for an introduction to water quality modeling and its methodology.

D.1.1 QUAL2E: Enhanced stream water quality model

The QUAL2E series of models has a long history in stream water quality modeling. It was primarily developed by the U.S. Environmental Protection Agency (EPA) in the early 1970s. Since, it has gained a broad user base, including applications outside the U.S. in Europe, Asia, and South and Central America.

The Enhanced Stream Water Quality Model (QUAL2E) is applicable to well mixed, dendritic streams. It simulates the major reactions of nutrient cycles, algal production, benthic and carbonaceous demand, atmospheric reaeration and their effects on the dissolved oxygen balance. It can predict up to 15 water quality constituent concentrations. It is intended as a water quality planning tool for developing total maximum daily loads (TMDLs) and can also be used in conjunction with field sampling for identifying the magnitude and quality characteristics of non-point sources. By operating the model dynamically, the user can study diurnal dissolved oxygen variations and algal growth. However, the effects of dynamic forcing functions, such as headwater flows or point source loads, cannot be modeled with QUAL2E. QUAL2E-U is an enhancement allowing users to perform three types of uncertainty analyses: sensitivity analysis, first-order error analysis, and Monte Carlo simulation.

[1] `http://ceprofs.tamu.edu/ssocolofsky/CVEN489/Book/Book.htm`

The model only simulates steady-state streamflow and contaminant loading conditions; the reference to dynamic modeling above refers only to water quality forcing functions of climatologic variables (air temperature, solar radiation, among others). The transport scheme in the model is the implicit backward-difference finite difference method.

D.1.2 HSPF: Hydrological Simulation Program–FORTRAN

Developed in the late 1970s by the EPA, HSPF is a union between the Stanford Watershed Model, an advanced, continuous-simulation, process-oriented hydrologic model, and several water quality models developed by the EPA, including the Agricultural Runoff Model (ARM) and the NonPoint Source model (NPS). The model is intended for both conventional and toxic organic pollutants. Contaminant loads are either user-input point sources or nonpoint sources modeled by build-up and wash-off parameterizations. It is the only comprehensive model of watershed hydrology and water quality that allows the integrated simulation of land and soil contaminant runoff processes with in-stream hydraulic and sediment-chemical interactions. However, make no mistake: it is not a three-dimensional model.

An advantage of HSPF is in its software development, which resulted in a complete data-management tool. A disadvantage of HSPF is its large data requirements, which include physical data such as watershed data, river network discretization, soil types, geologic setting, vegetative cover, towns, and other regional data, meteorologic data such as hourly data for precipitation, solar radiation, air temperature, dew-point temperature, and wind speed and daily evapotranspiration. In addition, the model has a wealth of empirical calibration parameters that must be determined from handbook values and by calibrating to field measurements.

The river transport model is a tanks-in-series model that uses flood routing *via* stage-discharge relationships (which must be input by the user from external knowledge).

D.1.3 SWMM: Stormwater Management Model

In urban settings, where pressurized pipe flow in sewer systems is to be modeled, the EPA model SWMM is recommended. The SWMM model is actually a package of models. In one mode, it can function as a design model which undertakes detailed simulations of storm events, using relatively short time steps and as much catchment and drainage system detail as necessary. In another mode it can be used as a routine planning model for an overall assessment of the urban runoff problems and proposed abatement options. The planning mode is typified by continuous simulation for several years using long (e.g. hourly) time steps and minimum detail in the catchment scheme. Like HSPF, the model requires a great deal of input data (both physical and meteorological).

The modular nature of SWMM allows it to simulate diverse situations. Both single-event and continuous simulation can be performed on catchments having storm sewers, or combined sewers and natural drainage, for prediction of flows, stages and pollutant concentrations. The Extran Block solves complete dynamic flow routing equations (St. Venant equations) for accurate simulation of backwater, looped connections, surcharging, and pressure flow. The modeler

can simulate all aspects of the urban hydrologic and quality cycles, including rainfall, snowmelt, surface and subsurface runoff, flow routing through drainage networks, storage and treatment. Statistical analyses can be performed on long-term precipitation data and on output from continuous simulation.

The strength of this model is in its hydrodynamics. The transport modules, which are also quite flexible, use simple tanks-in-series formulation, and are not available in the Extran Block (where the complete dynamic flow equations are solved).

D.1.4 DYRESM-WQ: Dynamic reservoir water quality model

The model DYRESM-WQ is a one-dimensional hydrodynamics model for predicting the vertical distribution of temperature, salinity and density in lakes and reservoirs. It is assumed that the water bodies comply with the one-dimensional approximation in that the destabilizing forcing variables (wind, surface cooling, and plunging inflows) do not act over prolonged periods of time. DYRESM-WQ has been used for simulation periods extending from weeks to decades. Thus, the model provides a means of predicting seasonal and inter-annual variation in lakes and reservoirs, as well as sensitivity testing to long term changes in environmental factors or watershed properties.

DYRESM-WQ can be run either in isolation, for hydrodynamic studies, or coupled to CAEDYM for investigations involving biological and chemical processes. The computational demands of DYRESM-WQ are quite modest and multi-year simulations can be performed on PC platforms under Windows operating systems. The code is written in modular fashion to support future updates and improvements.

D.1.5 CE-QUAL-RIV1: A one-dimensional, dynamic flow and water quality model for streams

Administered and developed by the U.S. Army Corps of Engineers, CE-QUAL-RIV1, or more commonly just RIV1, is a fully dynamic (flow and water quality) one-dimensional model. The hydrodynamic portion is computed first, solving the St. Venant equations using the four-point implicit finite difference scheme. The hydrodynamic model does not allow for super-critical flow. This can lead to problems for natural streams under low flow where steep river sections form cataracts. Following the hydrodynamics, the transport equation is solved using an explicit two-point, fourth-order accurate Holly-Preissman scheme. The Holly-Preissman scheme is a backward method of characteristics; however, because the search routine in RIV1 for finding the feet of the characteristic lines only searches the upstream segment, the Courant number restriction still applies. The water quality model can predict variations in each of 12 state variables: temperature, carbonaceous biochemical oxygen demand (CBOD), organic nitrogen, ammonia nitrogen, nitrate + nitrite nitrogen, dissolved oxygen, organic phosphorus, dissolved phosphates, algae, dissolved iron, dissolved manganese, and coliform bacteria. In addition, the impacts of macrophytes can be simulated. Because of the use of the characteristic method, numerical accuracy for the advection of sharp gradients is preserved.

D.1.6 ATV Gewässergütemodell

The ATV Gewässergütemodell, also called the AVG (allgemein verfügbares Gewässergütemodell) or in English the ATV water quality model, was developed in Germany as a new model to bridge the problems (limitations) inherent in some of the models listed above. It is designed as a series of building blocks, each building block to be implemented as needed. The first building block is the hydrodynamic model, which solves the St. Venant equations for either the steady or unsteady case. The remaining building blocks can be added to the hydraulics as needed, including water temperature, conservative tracers, (C)BOD, phosphorus, nitrogen cycle, silicon, algae, zooplankton, sediment/water exchange, suspended sediment transport, oxygen dynamics, pH dynamics, heavy metals, and organic chemicals. The solution to the transport equation uses the method of characteristics and does not have a Courant number constraint. Because of the model's modular design, simulations can be made as simple or as complicated as desired; however, the numerical expense of the hydrodynamic routine should not be underestimated.

D.2 Two- and three-dimensional models

Two- and three-dimensional models are typically used in reservoirs, lakes, and estuaries. They are almost exclusively finite element, finite volume, or finite difference. Because large water bodies are generally stratified, they must simulate buoyancy effects; thus, the hydrodynamic and transport equations are coupled. Because buoyancy effects are a major complication in these models (and the subject of next semester) this section briefly summarizes each model without discussing the details.

D.2.1 CORMIX: Cornell Mixing-Zone Model

Begun at Cornell and currently under continued development at the Oregon Graduate Institute, the CORMIX system is a near-field model for the analysis, prediction, and design of aqueous toxic or conventional pollutant discharges into diverse water bodies. Major emphasis is on computation of plume geometry and dilution characteristics within a receiving water's initial mixing zone so that compliance with regulatory constraints can be judged. It also computes discharge plume behavior at larger distances. The model has three modules: CORMIX1 for submerged single-point discharges, CORMIX2 for submerged multi-port diffuser discharges, and CORMIX3 for buoyant surface discharges. As implied by the title, the model predicts mixing (dilution) of the input chemicals, but does not allow for interaction among multiple chemicals (though first-order decay of a single species is implemented).

The model equations are based on jets and plumes, which traditionally are modeled using integral equations. Integral equations rely on self-similarity to reduce the three-dimensional equations to a one-dimensional ODE. The model then solves for the three-dimensional trajectory of the plume centerline using the one-dimensional integral equations. Hydrodynamic conditions (though allowed to be unsteady) must be supplied as input to the model.

D.2.2 WASP: Water Quality Analysis Simulation Program

The WASP system is a generalized framework for modeling contaminant fate and transport in surface waters. The model does not solve a set of multi-dimensional dynamical equations, but rather is based on the flexible compartment modeling approach. WASP can be applied in one, two, or three dimensions. Problems that have been studied using the WASP framework include biochemical oxygen demand and dissolved oxygen dynamics, nutrients and eutrophication, bacterial contamination, and organic chemical and heavy metal contamination.

Because WASP in an EPA model, input and output linkages also have been provided to other stand-alone models. Flows and volumes predicted by the link-node hydrodynamic model DYNHYD can be read and used by WASP. Loading files from PRZM and HSPF can be reformatted and read by WASP. Toxicant concentrations predicted by TOXI can be read and used by both the WASP Food Chain Model and the fish bioaccumulation model FGETS.

A body of water is represented in WASP as a series of computational elements or segments. Environmental properties and chemical concentrations are modeled as spatially constant within segments. Segment volumes and type (surface water, subsurface water, surface benthic, subsurface benthic) must be specified, along with hydraulic coefficients for riverine networks.

D.2.3 POM: Princeton ocean model

POM is the precursor to ECOM-si (see the next section), and was developed in the late 1970s. It is a fully three-dimensional hydrodynamic numerical model, designed to predict ocean circulation. The POM model is freely available to non-commercial applications.

The POM model contains an imbedded second moment turbulence closure sub-model to provide vertical mixing coefficients. It is a sigma coordinate model in that the vertical coordinate is scaled on the water column depth. The horizontal grid uses curvilinear orthogonal coordinates. The horizontal time differencing is explicit whereas the vertical differencing is implicit. The latter eliminates time constraints for the vertical coordinate and permits the use of fine vertical resolution in the surface and bottom boundary layers. The model has a free surface and a split time step. The external mode portion of the model is two-dimensional and uses a short time step. The internal mode is three-dimensional and uses a long time step. Complete thermodynamics have been implemented.

D.2.4 ECOM-si: Estuarine, coastal and ocean model

ECOM-si is a three-dimensional ocean circulation model developed principally by Alan Blumberg of HydroQual. It is similar to the POM model, but incorporates a semi-implicit scheme for solving the gravity wave so that the need for separate barotropic (external) and baroclinic (internal) time steps is eliminated. The ECOM-si model is not freely available, but must be obtained through HydroQual.

ECOM-si includes a free surface, nonlinear advective terms, coupled density and velocity fields, river runoff, heating and cooling of the sea surface, a 2.5 level turbulence closure scheme to

represent vertical mixing, and is designed to easily allow "realistic" simulations. In addition, the combination of orthogonal curvilinear coordinates in the horizontal plane and sigma-coordinates in the vertical dimension allows grid refinement in regions of interest without sacrificing the well-known characteristics of Cartesian grid schemes. For water quality modeling, both POM and ECOM-si must be combined with a transport model.

Glossary

adjacent [*angrenzend o. benachbart*]:
Next to, nearby, or having a common endpoint or border.

advection [*Advection*]:
Transported by an imposed ambient current, as in a river or coastal waters.

ambient (fluid) [*umgebend(es Fluid)*]:
Ambient means "existing or present on all sides." Ambient fluid is the fluid surrounding the region of interest.

application [*Anwendung*]:
An act of putting to use new techniques. A use to which something is put.

approach [*Vorgehensweise*]:
In science: a methodology applied to solve a problem.

assumption [*Annahme*]:
A fact or statement (as in a propostition, axiom, postulate, or notion) that is taken for granted (assumed).

average [*Durchschnitt*]:
A single value (as a mean, mode, or median) that summarizes or represents the general significance of a set of unequal values.

boundary condition [*Randbedingung*]:
A constraint applied to a differential equation at a physical location (boundary) in space.

buoyancy [*Auftrieb*]:
The tendency of a body to float or to rise when submerged in a fluid; the power of a fluid to exert an upward force on a body placed in it, also, the upward force exerted on the body.

coherent [*zusammenhängend o. kohrent*]:
Ordered of integrated in way that produces an interdependence.

control volume [*Kontrollvolumen*]:
The three-dimensional region defined by the boundaries of a system. Usually, a differential element used to derive conservation laws.

convection [*Konvektion*]:
Vertical transport induced by hydrostatic instability, such as the flow over a heated plate, or below a chilled water surface in a lake.

current [*Strömung*]:
The part of a fluid body (such as air or water) moving continuously in a certain direction.

decay [*Abbau o. Zerfall*]:
To decrease gradually in quantity, activity, or force.

density [*Dichte*]:
The mass of a unit volume.

derivation [*Ableitung o. Herleitung*]:
The act or processes of forming a physical relationship from basic, accepted relationships.

diffusion (molecular) [*Diffusion (molekulare)*]:
The scattering of particles by random molecular motions, which may be described by Fick's law and the classical diffusion equation.

diffusion (turbulent) [*Diffusion (turbulente)*]:
The random scattering of particles by turbulent motion, considered roughly analogous to molecular diffusion, but with eddy diffusion coefficients (which are much larger than molecular diffusion coefficients).

dilution [*Verdünnung*]:
The act of reducing the strength, or concentration by adding more liquid.

discharge [*Abfluß*]:
A flow, generally of contaminants, that is emitted into the environment, usually from a localized source.

dispersion [*Dispersion*]:
The scattering of particles or a cloud of contaminants by the combined effects of shear and transverse diffusion.

dissolve [*lösen*]:
To cause to pass into solution.

droplets [*Tröpfchen*]:
Small drops (as of a liquid), such as rain drops, drops of oil, and others. The liquid-phase version of a gas bubble.

dye [*Farbstoff*]:
A soluble or insoluble coloring matter.

eddy [*Wirbel*]:
A current of water or air running contrary to the main current. In turbulent flow, especially, a circular current or current with vorticity.

effluent [*Ausfluß o. ausfließend*]:
The fluid flowing out from a discharge.

entrainment [*Einmischung*]:
To draw in and transport (as solid particles or ambient fluid) by the flow of a fluid.

environmental impact statement [*Umweltverträglichkeitsstudie*]:
Legal document reporting the projected positive and negative results to the environment of a proposed engineering project.

equation [*Gleichung*]:
A mathematical statement of equality or inequality.

estuary [*Flußmündung o. Meeresbucht o. Ästuar*]:
The a tidal region where fresh water (from continental sources) mixes with ocean water. The estuary is generally defined up to the point where salt concentrations equal the ambient ocean salinity.

evaporation [*Evaporation*]:
The transport of water vapor from a water or soil surface to the atmosphere.

fluctuation [*Schwankung*]:
A shirt back and forth uncertainly, or to ebb and flow in waves.

gauge (water gauge) [*Meßgerät (Wasserstandsanzeiger)*]:
An instrument with a graduated scale or dial for measuring or indicating quantity.

impact [*Auswirkung o. Einfluß*]:
The changes, both positive and negative, on a natural system due to an external influence (as an engineering project).

inertia [*Trägheit*]:
a property of matter by which it remains at rest or in uniform motion in the same straight line unless acted upon by some external force

initial condition [*Anfangsbedingung*]:
A constraint applied to a differential equation at a physical moment in time (generally at $t = 0$).

interface [*Grenzfläche*]:
The boundary between two fluids.

jet [*Strahl*]:
A momentum-driven boundary-layer flow. A usually forceful stream of fluid (as water or gas) discharged from a narrow opening or a nozzle.

manifold [*Verteiler- bzw. Sammelrohr*]:
A pipe fitting with several lateral outlets.

mean [*Mittel*]:
See *average*.

mixing [*Mischung*]:
Diffusion or dispersion as described above; turbulent diffusion in buoyant jets and plumes; any process which causes one parcel of water to be mingled with or diluted by another.

momentum [*Impuls*]:
A property of a moving body that the body has by virtue of its mass and motion and that is equal to the product of the body's mass and velocity.

nozzle [*Düse*]:
A short tube with a taper or constriction used (as on a hose) to speed up or direct a flow of fluid.

order of magnitude [*Größenordnung*]:
A range of magnitude extending from some value to ten times that value.

orifice [*Düse o. Öffnung o. Mündung*]:
An opening (as a vent, mouth, or hole) through which something may pass.

particle entrainment [*Teilcheneinmischen*]:
The picking up of particles, such as sand or organic detritus, from the bed of a water body by turbulent flow past the bed.

particle settling [*Teilchenabsetzen*]:
The sinking (or rising) of particles having densities different from the ambient fluid, such

as sand grains or dead plankton. (In lakes and oceans the latter may be the dominant mechanism for downward transport of nutrients, often all the way to the bottom.)

persistent [*beständig*]:
Existing for a long or longer than usual time or continuously; continuing without change in function or structure. Also, degraded only slowly by the environment (as persistent contaminants).

plume [*Fahne*]:
A buoyancy-driven boundary-layer flow. A stream of fluid (as water or gas) with density different from the ambient, recieving fluid, discharged from a narrow opening or nozzle, or the fluid flow resultant from a discharge of heat.

plunge [*eintauchen*]:
To cause to penetrate or enter quickly and forcibly into something. To descend or dip suddenly.

pollutant [*Schmutzstoff*]:
A substance that makes physically impure or unclean. To contaminant especially with manmade waste.

porous media flow [*Strömung in porösem Medium*]:
Groundwater flow. Flow through a solid matrix containing many interconnected pores or cavities (voids).

port [*Öffnung*]:
An opening (as in a diffuser manifold) for intake or exhaust of a fluid. See also *orifice*.

precipitation [*Niederschlag*]:
A deposit on the earth of hail, mist, rain, sleet, or snow. Also refers to the quantity of water deposited.

probability [*Wahrscheinlichkeit*]:
The chance that a given event will occur. The branch of mathematics concerned with the study of probabilities.

radiation [*Strahlung*]:
The flux of radiant energy, such as at a water surface.

random [*Zufall*]:
Without a definite aim, direction, rule, or method; lacking a definite plan, purpose, or pattern.

residual [*Rest*]:
The remaining product or substance.

salinity [*Salzgehalt*]:
A measure of the salt content of seawater, specifically, the ratio of the mass of dissolved salts to the total mass of water and salt.

saturated [*gesättigt*]:
Being a solution that is unable to absorb or dissolve any more of a solute at a given temperature and pressure.

sewage [*Abwasser*]:
The raw refuse liquids or waste matter carried off by sewers.

sewage treatment plant [*Klärwerk o. Kläranlage*]:
The facility where sewage is prepared (cleaned) before releasing it into the environment as effluent.

shear flow [*Scherströmung*]:
The advection of fluid at different velocities at different positions; this may be simply the normal velocity profile for a turbulent flow where the water flows faster with increasing elevation above the bed of the stream; or shear may be the changes in both magnitude and direction of the velocity vector with depth in complex flows such as in estuaries or coastal waters.

shear stress [*Scherspannung*]:
A force exerted from one fluid layer to another, due to differences in their velocity, that tends to pull on, push against, or compress or twist the fluid body.

soluble [*löslich*]:
The property of being able to be dissolved in a fluid (the dissolving fluid is referred to as the solute).

source [*Quelle*]:
The location and flux of a flow (usually of a contaminant or substance of interest).

spatial [*räumlich*]:
Relating to, occupying, or having the character of space. A spatial distribution is the description of the variation of a quantity in space. Compare with *temporal*.

standard deviation [*Standardabweichung*]:
A statistical quantity describing the degree of spread of a distribution. Defined as the square root of the variance. The variance is the mean of the squared deviations from the mean.

steady [*stationär*]:
In steady state, or unchanging. The mathematical representation is that the time derivative is zero.

stratification [*Schichtung*]:
The property of being stratified. An organization of a fluid body based on density. The most common form of density stratification is the stable form, where density decreases as height increases.

submerged [*abgetaucht*]:
The state of being emersed within a fluid (as being underwater).

temporal [*zeitlich*]:
Relating to, occupying, or having the character of time. A temporal distribution is the description of the variation of a quantity in time. Compare with *spatial*.

tracer [*Tracer*]:
Any conservative (non-transforming) substance that moves exactly with the fluid (i.e. does not move relative to the fluid).

transformation [*Transformation*]:
The changing of a chemical substance into another chemical substance, usually accompanied by the loss of the original substance (i.e. carbon dioxide transformed into oxygen by photosynthesis).

transport [*Transport*]:
The movement of a parcel of water or tracer by advection, diffusion, or mixing.

unsteady [*instationär*]:
Changing, or developing in time. The mathematical representation is that the time derivative is not zero. See also steady.

volatile [*flüchtig*]:
Readily vaporizable at a relatively low temperature.

vortex [*Wirbel*]:
See *eddy*.

vorticity [*Wirbelstärke*]:
A vector measure of the local rotation in a fluid flow.

wake [*Nachlaufwirbel*]:
The region of velocity deficit behind an object held stationary relative to an ambient fluid flow.

wastewater [*Abwasser*]:
An effluent flow of fluid no longer of use. See also *sewage*.

References

Acheson, D. J. (1990), *Elementary Fluid Dynamics*, Clarendon Press, Oxford.

ASCE & WPCF (1992), 'Design and construction of urban stormwater management systems'.

Batchelor, G. K. (1967), *An introduction to fluid dynamics*, Cambridge University Press, Cambridge, England.

Boyd, J. P. (1989), *Lecture Notes in Engineering 49: Chebyshev and Fourier Spectral Methods*, Springer Verlag, Heidelberg, Germany.

Brooks, N. H. (1960), Diffusion of sewage effluent in an ocean current, *in* 'Proc. 1st Int. Conf. Waste Disposal Mar. Environ.', Pergamon Press, Oxford, pp. 246–267.

Cramer, H. E. (1959), *Am. Ind. Hyg. Assoc. J.* **20**, 183.

Csanady, G. T. (1973), *Turbulent Diffusion in the Environment*, Geophysical and Astrophysics Monographs, D. Reidel Publishing Company, Dordrecht, Holland.

Deng, Z.-Q., Singh, V. P. & Bengtsson, L. (2001), 'Longitudinal dispersion coefficient in straight rivers', *J. Hydr. Engrg.* **127**(11), 919–927.

Fedorovich, E. (1999), Course notes: Atmospheric diffusion and dispersion, Technical report, European Graduate School of Hydraulics, Short course on Environmental Fluid Mechanics: Theory, Experiments, Applications, IAHR-EGH, Karlsruhe, Germany.

Fischer, H. B., List, E. G., Koh, R. C. Y., Imberger, J. & Brooks, N. H. (1979), *Mixing in Inland and Coastal Waters*, Academic Press, New York, NY.

Garratt, J. R. (1992), *The atmospheric boundary layer*, Cambridge Atmospheric and Space Science Series, Cambridge University Press, Cambridge, England.

Gschwend, P. S. (1987), Modeling the benthos-water column exchange of hydrophobic chemicals, Technical Report unkn., USEPA, Environmental Research Lab., Wash., D.C.

Kaimal, J. C. & Finnigan, J. J. (1994), *Atmospheric Boundary Layer flows: Their structure and measurement*, Oxford University Press, Inc., New York.

Lumley, J. L. & Panofsky, H. A. (1964), *The Structure of Atmospheric Turbulence*, Interscience Publishers, New York.

Mathieu, J. & Scott, J. (2000), *An introduction to turbulent flow*, Cambridge University Press, Cambridge.

Mei, C. C. (1997), *Mathematical Analysis in Engineering*, Cambridge University Press, Cambridge, England.

Nepf, H. M. (1995), 'Course notes and problem sets', *MIT Course 1.77: Water Quality Control* .

Okubo & Karweit (1969), 'Title', *Journal* p. Pages.

Panofsky, H. A. (1967), A survey of current throught on wind properties relevant for diffusion in the lowest 100 m, *in* 'Symp. Atm. Turb. Diffusion', Sandia Laboratories, Albuquerque, NM, pp. 47–58.

Pasquill, F. (1962), *Atmospheric Diffusion*, D. van Nostrand Co. Ltd., New York.

Pope, S. B. (2000), *Turbulent Flows*, Cambridge University Press, Cambridge.

Reynolds, O. (1883), *Phil. Trans. R. Soc. Lond.* **174**, 935–982.

Rutherford, J. C. (1994), *River Mixing*, John Wiley & Sons, Chichester, England.

Smart, P. L. & Laidlay, I. M. S. (1977), 'An evaluation of some fluorescent dyes for water tracing', *Wat. Res. Res.* **13**(1), 15–33.

Smith (1957), 'Title', *Journal* p. Pages.

Sutton, O. G. (1932), *Proc. Roy. Soc. London A* **135**, 143.

Sutton, O. G. (1953), *Micrometeorology*, McGraw-Hill Book Co., New York.

Taylor, G. I. (1921), 'Diffusion by continuous movements', *Proc. London Math. Soc., Ser. 2* **20**, 196–212.

Thomann, R. V. & Mueller, J. A. (1987), *Principles of Surface Water Quality Modeling and Control*, Harper & Row, Publishers, New York.

Walters (1962), 'Title', *Journal* p. Pages.

Index